Site-directed mutagenesis of charged amino acid residues on the $CpxA_{SD}$ and CpxP in *E. coli*, potentially important for signaling and direct interaction

by

Rodrigo Margain Quevedo

A thesis submitted in partial fulfillment of the requirements for the degree of

Master of Science

in

Microbiology and Biotechnology

Department of Biological Sciences

University of Alberta

Abstract

Bacterial pathogens must endure diverse environmental stresses that they encounter while colonizing and infecting a host. Two-component signal transduction systems (TCSTs) are the most widespread regulatory systems in bacteria, but importantly absent in mammals. In general, TCSTs sense and interpret stimuli, then use such information to respond by modulating the repertoire of genes expressed, allowing to ultimately mediate adaptations for survival. The CpxRA TCST envelope stress response (ESR) system in *Escherichia coli* and other Gram-negatives has been linked to virulence factors, antibiotic resistance and envelope stress. The CpxRA system is made up of the sensor histidine kinase (HK) CpxA, the cytosolic response regulator (RR) CpxR, and the periplasmic accessory inhibitor CpxP. In the absence of inducers, the periplasmic sensor domain of CpxA has been proposed to interact with CpxP, inhibiting CpxA autokinase activity and causing it to act as a phosphatase for CpxR~P dephosphorylation, maintaining the pathway in an off state. Intriguingly, the mechanism by which CpxA detects and transduces signals, as well as the one allowing for it to directly interact with CpxP, are still not completely understood. In the present study, I sought to determine whether some of the recently identified surface-exposed amino acid residues comprising large negatively charged patches in the $CpxA_{SD}$ of *E. coli* are important for pathway activation and partner interaction (specifically with CpxP). Experimental analyses were performed by following a site-directed specific mutational approach, based on structural and electrostatic analysis of the $CpxA_{SD}$. The effects of *cpxA* lysine and alanine mutations were analyzed by transforming them into a *ΔcpxA E. coli* strain. Such strains were grown in either acid, neutral or alkaline pH, or in the presence of *nlpE* or *cpxP* overexpression. Cpx activity levels were then determined using a Cpx-regulated *lacZ* reporter gene (*cpxP'-lacZ*$^{+}$) to indirectly measure pathway activation through β-galactosidase assays. The *cpxA* strains harboring the $E_{91}K$, $D_{113}K$ or $E_{91}K+D_{113}K$ mutated alleles displayed constitutive pathway hyperactivation activities and lost

sensitivity toward overproduction of CpxP and NlpE. Protein levels however did not seem to be affected by the introduced mutations. I also investigated the potential for specific positively charged residues in CpxP to be direct interaction points of the previosuly characterized negatively charged residues in $CpxA_{SD}$, using complementary charge mutations. I determined that a specific direct-contact site could be located between the D_{113} negatively charged amino acid residue in the $CpxA_{SD}$ and the R_{139} positively charged residue in the CpxP concave surface. This represents the first time in which a specific localized interaction site between two amino acid residues of the CpxA and CpxP components has been described. A better understanding and characterization of such interaction could open the path for targeted inhibition of the pathway in the future, leading to alternative therapeutic treatments for diseases such as infectious diarrhea.

Preface

This thesis is an original work by Rodrigo Margain Quevedo. A portion of this thesis is currently in preparation to be included in a research publication. Some of the experimental work conducted for this thesis forms part of a research collaboration, led by Dr. Tracy Raivio at the University of Alberta, with Dr. Mark Glover and Dr. Jun Lu being the lead collaborators also at the University of Alberta. Plasmid construction, cloning and the site-directed mutagenesis by overlap extension PCR for the generation of the first set of mutated strains referred to in chapter 2 were performed by myself, with the assistance and guidance of Dr. Jun Lu.

Dedication

This work is dedicated to my mother, my father, my brother and my late grandparents ("mis avis"), who have always supported me in every step of my life.

Acknowledgements

I would first like to thank my supervisor Dr. Tracy Raivio, who never stopped supporting and believing in me throughout my graduate degree. Tracy did an amazing job in motivating me and reminding me that I had the necessary skills to successfully complete my research project, even through some really difficult times filled with frustration and uncertainty in my life. Tracy was always there to listen and talk about science and life, and I will forever be grateful for the fact that she gave me an opportunity to be part of her research group and fulfill one of my dreams of living in Canada. I would also like to thank Dr. Mark Glover for the enormously useful insights and feedback during my committee meetings and through electronic correspondence, and Dr. Amit Bhavsar for being my arm's length examiner during my thesis defense.

I would also like to thank all the members of the Raivio lab who constantly supported me and shared their discoveries, knowledge, drinks and laughs with me. Thanks Randi for always being willing to share your expertise and passion for science. Special thanks to Sam and Joseph, who made this experience very enjoyable and gave me their lasting friendship since the day we started in the lab together. Thank you Junshu, Laude and Yun for all the encouragement and help.

Very special thanks to my parents, my grandparents and my brother for always believing in me, challenging me to be a better person, for supporting me, keeping in contact with me so the distance does not feel so bad, and all the encouragement to not give up during difficult times. Very special thanks as well to my fiancée Paola for being there for me through good and bad, and for all the incredible life experiences we have shared. I am extremely excited for our next adventures together. I would also like to thank the rest of my family, loved ones and friends in Canada and Mexico. I could not have overcome these years without all of you. Lastly, I would like to thank CONACYT for the funding provided to complete this research project and graduate degree.

Table of contents

Heading **Page number**

List of Tables

List of Figures

List of Symbols and Abbreviations

A_{420}: absorbance at 420 nm

A_{600}: absorbance at 600 nm

Ac~CoA: acetyl coenzyme A

Ac~P: acetyl phosphate

AckA: acetate kinase

AE: attaching and effacing

AGAs: aminoglycoside antibiotics

Amp: ampicillin

ATP: adenosine triphosphate

Asp: aspartate

Bae: Bacterial adaptive response

CA: catalytic and ATP-binding domains

Cam: chloramphenicol

Cpx: Conjugative plasmid expression

DHp: Dimerization and Histidine phosphorylation domain

DNA: deoxyribonucleic acid

ECA: enterobacterial common antigen

EHEC: enterohemorrhagic *E. coli*

EPEC: enteropathogenic *Escherichia coli*

ESR: envelope stress response

ETEC: enterotoxigenic *E. coli*

GI: gastrointestinal

HK: histidine kinase

His: histidine

HU: hydroxyurea

HUS: haemolytic uremic syndrome

IM: inner membrane

IPTG: isopropyl β-D-thiogalactopyranoside

Kan: kanamycin

LB: Luria Bertani broth – Lennox

LEE: locus of enterocyte effacement

LPS: lipopolysaccharide

MBP: maltose-binding protein

NlpE: new lipoprotein E

NMR: nuclear magnetic resonance

OD_{600}: optical density at 600 nm

OM: outer membrane

OMP: outer membrane protein

ONP: ortho-nitrophenol

ONPG: ortho-nitrophenyl-β-D-galactopyranoside

ORS: oral rehydration solution

OX: overexpression

PAS: Per/ARNT/Sim motif

PBS: phosphate buffer saline

PCR: polymerase chain reaction

PDC: PhoQ-DcuS-CitA domain

PE: phosphatidylethanolamine

PG: peptidoglycan

PMF: proton motive force

PP: periplasm

PsP: phage-shock protein

Pta: phosphotransacetylase

Rcs: Regulator of capsular synthesis

RNA: ribonucleic acid

RNAP: RNA polymerase

RNase: ribonuclease

Rpm: rotations per minute

RR: response regulator

SD: sensor domain

SDS-PAGE: sodium dodecyl sulfate-polyacrylamide gel electrophoresis

T3SSs: type III secretion systems

TBS: tris-buffered saline

TCSTs: Two-Component Signal Transduction systems

UNICEF: United Nations Children's Emergency Fund

VC: vector control

WHO: World Health Organization

WT: wild-type

Chapter 1: Introduction

1.1 General overview

Pathogens responsible for causing diarrhea, including Gram-negative bacteria such as *Escherichia coli* and *Vibrio cholerae*, represent a current global problem since the greater impact they have on the human health occurs in children inhabiting underdeveloped countries (Aggarwal, Uppal, Ghosh, Prakash, & Rajeshwari, 2013). These bacteria must endure diverse environmental stresses that they encounter while colonizing and infecting a host, including extreme pH conditions, osmolarity modifications, temperature changes, nutrient availability, antimicrobial components and antibiotics, among others (Buelow & Raivio, 2010; Runkel, Wells, & Rowley, 2013). To be able to sense and adequately mount a response to these stimuli so they can ultimately adapt and survive by means of controlling cellular functions, bacteria utilize widespread regulatory systems called Two-Component Signal Transduction systems (TCSTs) (Buelow & Raivio, 2010; Bury-Moné et al., 2009; Eguchi & Utsumi, 2008; MacRitchie, Buelow, Price, & Raivio, 2008). These include the Conjugative Plasmid Expression (Cpx) Envelope Stress Response (ESR) system, which functions through a conserved set of phospho-transfer reactions. This response is needed to detect and counter external perturbations that result in the misfolding of proteins, which could potentially be detrimental to the bacterial cell envelope (MacRitchie et al., 2008; McEwen & Silverman, 1980; Vogt & Raivio, 2012).

The TCSTs allow bacteria to selectively modulate gene expression, regulating protein production and activity, so that only the proteins and mechanisms that provide the major physiological advantages are utilized under inducing or stressful conditions. This ultimately enables bacteria to change cellular physiology to adapt to the surroundings, while preserving energy and enhancing their fitness for survival and persistence (Beier & Gross, 2006). Since TCSTs are the most prevalent means of signal transduction in bacteria, but importantly absent in

mammals, our understanding on how they operate is crucial, so we can eventually combat these defense mechanisms in a more effective and targeted manner, to better treat diseases in human populations, including the infectious diarrhea (Buelow & Raivio, 2010; Gotoh et al., 2010; Stephenson & Hoch, 2002, 2004). However, the information we possess to date regarding exactly how the sensor element of the Cpx system detects and transduces signals to the rest of the pathway is limited, as well as the information on how the specific interaction between the elements that constitute the system occurs, which could be valuable for better comprehension of this defense mechanism and the potential future elaboration of specific compounds that could target these components and complement antibiotic therapies (Fleischer, Heermann, Jung & Hunke, 2007; Raivio, Laird, Joly & Silhavy, 2000; Thede et al., 2011; Zhou et al., 2011).

1.2 Infectious diarrhea in humans

Human diarrhea caused by enteric pathogens, commonly known as infectious diarrhea, is a notable global health problem that impacts morbidity in developed countries and results in a high degree of mortality in the underdeveloped ones, primarily affecting 5-year old or younger children and ranking as the second-most common cause of death within this population by The United Nations Children's Emergency Fund (UNICEF) and the World Health Organization (WHO) (Aggarwal et al., 2013; Hodges & Gill, 2010; Kosek, Bern, & Guerrant, 2003; Viswanathan, Hodges, & Hecht, 2009).

Similar to other infectious illnesses, communities located in non-developed countries are the most vulnerable ones to diarrheal pathogens, where an average of 25% of the young population is not properly provided with food or appropriate health care, more than a billion people cannot utilize or drink clean or potable water, and more than 2 billion are not able to take adequate hygiene

measures to prevent the spread of such diseases. Furthermore, diarrhea is linked to both cognitive and physical disabilities in children living under such circumstances (Cheng, McDonald, & Thielman, 2005; Hodges & Gill, 2010). An average of seven annual episodes per child in underdeveloped countries occurs versus only two episodes per child per year in developed countries, and fatal cases (including severe sequelae) are practically nonexistent in the first-world nations (Cheng et al., 2005). The overall incidence of pediatric diarrhea has not been significantly modified since the 1980s, comprising a yearly average of 3.2 diarrheal episodes per child, worldwide. Treatments including oral rehydration therapy in the form of oral electrolyte solutions (an effective and simple, but underutilized treatment) have helped to decrease fatal cases since 1982, when 4.6 million deceased were registered, compared to 2.5 million cases in 2000 (Kosek et al., 2003; Thapar & Sanderson, 2004; Viswanathan et al., 2009).

Water comprises approximately 75% of what is considered by physicians and health care professionals as a "healthy human stool mass". However, an increase of over 85% water along with a higher than normal frequency of intestinal motility (averaging over 3 bowel movements per minute, and the excretion of stool with excess water more than 3 times in a day) is medically defined as diarrhea by the WHO (Guttman & Finlay, 2008; Thapar & Sanderson, 2004).

While colonizing the human gut, bacterial pathogens generate effector proteins and secrete toxins that disturb the organization of the epithelium, resulting in infectious diarrhea. Such effector proteins disrupt both secretion and absorption of ions and solutes, after which water movement occurs as a mechanism of the intestine to try to re-establish adequate concentrations (Guttman & Finlay, 2008; Viswanathan et al., 2009). The direct disruption to water regulation in the gastrointestinal (GI) tract that takes place during this process enables the bacterial manipulation of the gut microenvironment. This happens through alterations in the GI motility, epithelial barrier,

ion and water channels, so that pathogens can outcompete the residing host microbiota, and also aids them in the rapid propagation into the environment. The latter may result in infection of new hosts and has been found to increase the virulence in some of these bacteria, resulting in even more severe health problems in humans (Guttman & Finlay, 2008; Viswanathan et al., 2009).

Even though diarrhea benefits the host by working as a defense mechanism to reduce bacterial load, it is important to mention that it impacts humans in a negative manner likewise, due to the simultaneous loss of liquid and electrolytes, especially in vulnerable populations (Viswanathan et al., 2009).

Oral rehydration solutions (ORS) for the prevention and treatment of dehydration linked to infectious diarrhea in pediatric patients is recommended by the UNICEF and WHO (Aggarwal et al., 2013). Antibiotics have reformed the therapy for infections in the human gut caused by bacteria and have been correlated with an important role in reduction of fatalities. For example, severe cases in children, 20-60% of travellers affected by diarrhea in underdeveloped countries, or those patients who do not respond to rehydration therapy as expected, are frequently treated with antibiotics to alleviate symptoms related to the disease. Multiple studies have determined that the treatment of patients using a course of antibiotics that includes tetracycline, trimethoprim/sulfamethoxazole and fluoroquinolones, generally decreases the disease duration from an average of 3 days to approximately 1 day in patients suffering from infectious diarrhea (Cheng et al., 2005; Hill & Beeching, 2010; Nguyen, Le, Le, & Weintraub, 2005).

Antimicrobial resistance in enteric pathogens has rapidly become an international concern, specifically due to overuse and misuse of drugs in third world countries for diarrheal treatment, leaving the physicians with limited antimicrobial options for therapy. Multi-drug resistance has been recently increased and worsened since an indiscriminate use of antibiotics and acquisition of

resistance genes permitted bacteria to generate and utilize extended-spectrum beta-lactamase enzymes, propitiating resistance mainly against penicillins, up to third-generation cephalosporins and aztreonam (Aggarwal et al., 2013; Nguyen et al., 2005).

1.3 Characteristics of bacterial pathogens responsible for infectious diarrhea

The most common bacterial causes of infectious diarrhea are members of the gamma proteobacteria of the Enterobacteriales order and other associated Gram-negative bacteria, including pathogenic *Escherichia coli*, *Campylobacter* spp, *Yersinia* spp, *Shigella* spp and *Salmonella* spp. *Shigella* spp has been determined to be the most common cause of bacterial dysentery or acute bloody diarrhea, accounting for 15% of deceases related to diarrhea in children. *V. cholerae* is similarly a major cause of diarrheal outbreaks, especially after natural disasters compromise sanitation in human communities (Cheng et al., 2005; Thapar & Sanderson, 2004).

1.3.1 Characteristics of pathogenic *Escherichia coli*

E. coli strains are present in the human intestine as either commensals or pathogens. A classification has been made based on their somatic (O) and flagellar (H) antigens, and the strains responsible for infectious diarrhea have been categorized into six different groups: diffusely adherent *E. coli* (DAEC); enteroaggregative *E. coli* (EAggEC); enterohemorrhagic *E. coli* (EHEC); enteroinvasive *E. coli* (EIEC); enteropathogenic *E. coli* (EPEC); and enterotoxigenic *E. coli* (ETEC) (Croxen & Finlay, 2010; Thapar & Sanderson, 2004).

Pathogenic *E. coli* strains have many common strategies of virulence, as well as the need for adherence to host cells (excluding EIEC) through fimbriae or pili, the capacity to subvert processes carried out by host cells via secreted toxins so they can invade such cells and resist the

responses by the host immune system. However, each pathovar also possesses specific characteristics for attaching and exploiting host cells, and the ability to produce and secrete diverse virulence factors. Their genome is diverse and larger than that of commensal populations, due to the acquisition and loss of pathogenicity islands and accessory genetic material, consisting of a core of 2,200 genes and a pan-genome of 13,000 genes (Croxen & Finlay, 2010; Debnath et al., 2013).

EPEC is an important cause of deadly diarrhea in children living in the underdeveloped world. It belongs to a group of infectious bacteria that form attaching and effacing lesions (A/E lesions) on epithelial cells in the gut. These bacteria attach and then efface the microvilli to manipulate actin in the host cells, so it can form the characteristic pedestal-like structure underneath the attachment site. EPEC can form such structures by expressing the genes encoded in the locus of enterocyte effacement (LEE) pathogenicity island that sets up the production of a type III secretion system that injects bacterial effector proteins into the host cells (Croxen & Finlay, 2010; MacRitchie, Acosta, & Raivio, 2012).

Enterohemorrhagic *Escherichia coli* (EHEC) is a highly infectious pathogen that has the ability to produce A/E lesions likewise. It colonizes the large intestine in humans and causes diarrheal and gastroenteritis outbreaks in developed regions, including hemorrhagic colitis and hemolytic uremic syndrome (HUS) in both children and adults. Its main virulence factor is the phage-encoded Shiga toxin, responsible for HUS, and is able to attach due to the production of a similar T3SS to the one observed in EPEC (Croxen & Finlay, 2010). In comparison, enterotoxigenic *Escherichia coli* (ETEC) is the principal cause of traveller's diarrhea and can kill infected children that are under 5 years old. ETEC mediates adhesion to epithelial cells in the small intestine via colonization factors (CFs) that can be either fimbrial, non-fimbrial, helical or fibrillar.

Diarrhea caused by ETEC has been related to the secretion of heat-stable enterotoxins, heat-labile enterotoxins or a combination of both (Croxen & Finlay, 2010; Thapar & Sanderson, 2004).

1.3.2 Cell envelope in Gram-negative bacteria

The cell envelope found in Gram-negative bacteria is a complex structure that acts as the point of interaction and contact with the surrounding environments. It serves the purpose of protecting bacteria from adverse conditions and is responsible for mediating many of the cellular functions that allow them to colonize, survive and infect their hosts. These functions include transport of nutrients and waste, cell integrity surveillance, motility regulation and attachment to surfaces for colonization, among others (Silhavy, Kahne, & Walker, 2010). The envelope is formed by three different layers: the externally-located outer membrane (OM), the inner membrane encompassing the cytoplasm (IM, also known as the cytoplasmic membrane), and the periplasmic space (or periplasm, PP) containing a layer of peptidoglycan (PG) localized in between the two mentioned membranes (Figure 1-1) (Runkel et al., 2013; Schwechheimer & Kuehn, 2015; Silhavy et al., 2010). The OM serves as the barrier that protects bacteria from external perturbations or toxic compounds including antibiotics, and is formed by proteins, phospholipids and lipopolysaccharide (LPS) (Runkel et al., 2013; Schwechheimer & Kuehn, 2015). The IM is made up of a phospholipid bilayer in which many proteins are embedded or associated with electrochemical functions. The PP is an oxidative setting where protein folding occurs, and its PG layer provides the cell both with its characteristic shape, and with protection against osmotic changes and sheer stress (Schwechheimer & Kuehn, 2015; Silhavy et al., 2010).

1.3.2.1 The outer membrane (OM)

The OM is the external, atypical and asymmetrical lipid bilayer that constitutes the main trait of Gram-negative bacteria. It contains phospholipids on the interior leaflet facing the periplasm, and glycolipids on the exterior side facing the environment (particularly LPS), although it is important to highlight that this is not a phospholipid bilayer (Flores-Kim & Darwin, 2014; Kamio & Nikaido, 1976; MacRitchie et al., 2008; Schwechheimer & Kuehn, 2015; Silhavy et al., 2010). Besides lipids, some proteins are present in this membrane and they can be classified into either lipoproteins (harboring lipid moieties connected to an amino-terminal residue of cysteine) or β-barrel proteins (including porin proteins). The OM is the principal site where lipoproteins can be found in *E. coli*. (Flores-Kim & Darwin, 2014; Okuda & Tokuda, 2011; Ruiz, Kahne & Silhavy, 2006; Silhavy et al., 2010). Approximately 100 OM lipoproteins in *E. coli* have been identified, but the functions of the majority of these are still unknown or not completely understood. It is generally accepted that they are involved in processes such as the insertion of the different components into the OM (Okuda & Tokuda, 2011; Silhavy et al., 2010). The transmembrane proteins embedded in the OM that usually exhibit a trimeric β-barrel configuration are known as integral outer membrane proteins (OMPs) (Bos, Robert, & Tommassen, 2007; Silhavy et al., 2010). Examples of these include the porins OmpF and OmpC, that work by allowing small molecules (such as monosaccharides, disaccharides and amino acids) to passively diffuse across the membrane (Schwechheimer & Kuehn, 2015; Silhavy et al., 2010).

The active site of the enzymes present within the OM is placed facing the cell environment, and mutated strains that have undergone deletion of non-essential enzymes do not exhibit any noticeable phenotype. LPS, a crucial OM component that permits it to function as a barrier, exhibits a glucosamine disaccharide with six or seven acyl chains (lipid A), an extended

polysaccharide repeating chain (the "O-antigen") and a core made of oligosaccharides (Raetz & Whitfield, 2002; Ruiz et al., 2006; Silhavy et al., 2010). The facts that LPS molecules form a nonfluid wall against hydrophobic molecules and that porins limit the passage of hydrophilic particles make the OM a selective and highly effective permeability barrier (Silhavy et al., 2010).

1.3.2.2 The inner membrane (IM)

Since bacteria do not possess intracellular organelles, the processes associated with membranes that would comparatively occur in eukaryotes are carried on in the inner membrane in prokaryotes, including regulation of small-molecule transport by the proteins present in this section of the bacterial envelope (Ruiz et al., 2006; Silhavy et al., 2010). The IM is a phospholipid bilayer with symmetric constitution, that contains a conserved set of proteins necessary for the production of energy, secretion of proteins, regulation of signal transduction and biosynthesis of lipids, among others (Flores-Kim & Darwin, 2014; Ruiz et al., 2006). The main phospholipids found in *E. coli* are phosphatidyl-glycerol (a negatively charged phospholipid that accounts for 15-20% of the membrane) and phosphatidylethanolamine (PE, a zwitterionic phospholipid comprising most of the IM, between 70-80% of the total), as well as cardiolipin and phosphatidyl-serine in lower quantities (5% or less) (Ruiz et al., 2006; Silhavy et al., 2010; Van Dalen & De Kruijff, 2004). Examples of other minor lipids present are polyisoprenoid carriers involved in the translocation of activated sugar-intermediates needed for biogenesis of the envelope (Raetz & Dowhan, 1990).

The specific proteins located in the inner membrane comprise up to 25% of the *E. coli* encoded genes and reflect the context that bacteria experience at any given time period, and the composition can change accordingly in order to secure available energy required for the fulfillment of different cell functions under diverse conditions (Luirink, von Heijne, Houben, & de Gier, 2005;

Schwechheimer & Kuehn, 2015; Silhavy et al., 2010). These proteins can be catalogued into either lipoproteins, integral proteins or peripheral membrane proteins (Ruiz et al., 2006). The first type mentioned are attached to the outer side of the membrane by changes in the N-terminal cysteine amino acid residue of their mature structure and face the periplasmic space; integral proteins span the IM and are formed by transmembrane domains with α-helices (Dalbey, Wang, & Kuhn, 2011); and lastly the peripheral proteins are found solubilized in the cytoplasm or periplasm, in association with the membrane, but do not traverse the phospholipid bilayer (Luirink et al., 2005; Ruiz et al., 2006; Tokuda & Matsuyama, 2004).

1.3.2.3 The periplasmic space or periplasm (PP) and the peptidoglycan (PG) cell wall

The periplasmic space is an aqueous cellular section of the envelope, located in between the OM and IM. It is characterized by both the peptidoglycan (PG) layer and the dense amount of soluble proteins present in it, conferring a higher grade of viscosity as compared to the cytoplasm (Mullineaux, Nenninger, Ray, & Robinson, 2006; Van Wielink & Duine, 1990). Proteins within the periplasm include chaperone-like molecules important in the role they play during biogenesis of the envelope, and periplasmic binding proteins required during the processes of the transport of carbohydrates and amino acids (Ruiz et al., 2006; Ehrmann, 2007). Some of the proteins found in the PP function under the oxidizing conditions that this compartment presents. They work by monitoring the proper folding or degrading of proteins depending on each situation or growth cycle that the bacteria face and allowing for disulfide bonds (S-S) to form. Specifically, these molecular bonds are formed by disulfide-dithiol oxidoreductases, important for enabling an adequate folding of the proteins present in the envelope and stabilizing their structure (Ito & Inaba, 2008). Examples of these enzymes include DsbA, which recognizes cysteine amino acid residues in the protein

substrates to catalyze the proper formation of the S-S bonds, after which the reduced DsbA is reverted to its oxidized state by DsbB. The periplasmic oxidoreductase DsbC and the inner membrane DsbD enzymes rearrange any incorrect cysteine isomers that are detected (Sevier & Kaiser, 2002). Additional examples of proteins present in this compartment include the ones responsible for monitoring the quality of the folding in the proteins synthesized by either degrading or repairing them, such as proteases that do not depend on ATP, peptidyl-prolyl *cis-trans* isomerases, and other chaperone molecules (Merdanovic, Clausen, Kaiser, Huber, & Ehrmann, 2011).

The PG layer contained within the PP is formed by repetitive disaccharide units of the N-acetyl glucosamine-N-acetyl muramic acid that are cross-linked by pentapeptide side chains. Its importance resides in that it determines the cell shape and confers physical protection against changes in osmolarity due to its rigidity (Ehrmann, 2007; Merdanovic et al., 2011; Silhavy et al., 2010).

1.3.3 Protein complexes elaborated in the envelope for adherence and secretion

The cell surface in Gram-negative bacteria is the location where multiproteinaceous structures are situated, some either anchored to the OM and others extending through the entirety of the IM, PP and OM. These organelles can be classified into either essential structures for motility (flagella), those used in adhesion (fimbriae and pili) and the ones utilized in secretion and required to inject effector proteins into host cells (needle complexes and secretion systems) (Allen, Phan, & Waksman, 2012; Giltner, Nguyen, & Burrows, 2012; Ruiz et al., 2006; Thanassi, Bliska, & Christie, 2012).

Flagella are elongated filaments that expand to the outside of the cell, required for movement. These filaments are formed by 3 principal subunits: an engine, a propeller, and a joint or "hook". The engine, also known as the basal body, harbors a rotor and stator that traverse the IM, a rod located from the PG layer to the OM, and a complex formed on the periphery of the rod that in turn forms a pore in the OM. The propeller is a long, helical filament formed by thousands of flagellin protein subunits that are connected to the basal body. The hook confers selectable articulation depending on the angular rotation of the filament or the rod (Büttner, 2012; Chevance & Hughes, 2008; Erhardt, Namba, & Hughes, 2010).

Pili are non-flagellar appendages important in pathogenic bacterial strains since they are critical virulence factors responsible for adhering to and infecting target cells. Pili also allow the bacteria to escape from the host immune response and form biofilms, hence they have been targeted in studies researching the development of potential new drugs (Allen et al., 2012; Thanassi et al., 2012). Pili can be classified into five major groups, depending on the biosynthetic pathway through which each is formed: chaperone/usher (CU) pili, curli, type IV pili, type III secretion injectisome and type IV secretion pili (Fronzes, Remaut, & Waksman, 2008). The chaperone/usher pili make up the most prominent group encountered in bacteria. These consist of non-covalent polymers of pilus subunits, anchored to the OM at their base. The CU pathway is made up of a dedicated chaperone in the periplasmic space that is responsible for guiding the subunits across the PP into the OM and the usher assembly platform integrated to the OM that is required for the polymerization step of the assembly. The CU pathway is responsible for the formation of linear and unbranched aggregates of hundreds of subunits of pilin on the cell surface. CU pili have been linked to functions that include biofilm formation, interactions with other bacterial cells and abiotic surface adhesion (Allen et al., 2012; Fronzes et al., 2008; Thanassi et al., 2012). Curli are a related

class of OM filaments that were identified recently. They play a role in pathogenesis by facilitating adherence and invasion, causing an inflammatory response, and bleeding in humans during sepsis. These filaments are formed by two subunits (minor and major) capable of being translocated to the surface of the OM via a specific pore, through a complex that is related to that responsible for CU pili translocation (Sec) (Fronzes et al., 2008).

Type IV pili and the type III injectisomes are made by large assembly machineries that span both the IM and OM within the cell envelope, and include ATPases in the IM to power the system (Allen, Phan, & Waksman, 2012; Giltner, Nguyen, & Burrows, 2012; Thanassi, Bliska, & Christie, 2012). Type IV pili are long pilin polymers that work by adhering to host cells and other surfaces, forming microcolonies and biofilms, and play an important role in cellular invasion and electron transfer. They are usually described as thin fibres able to bend, characterized by being 6-9 nm in diameter and can reach several micrometers in length (Allen et al., 2012; Fronzes et al., 2008; Thanassi et al., 2012; Xicohtencatl-Cortes et al., 2007). *V. cholera* and other pathogens including EPEC synthesize type IV pili in bundles, primordial for numerous procedures involved in virulence, amongst which cellular invasion, auto-aggregation, twitching locomotion and adhesion are found (Fronzes et al., 2008). The type III secretion systems (T3SSs), importantly produced in EPEC and other Gram-negatives, but not in non-pathogenic strains of *E. coli*, allow bacteria to alter the target cells by means of directly delivering effector proteins into them. These are formed by conserved products from genes that display homology to those involved in the export and assembly of flagella. It is thought that the T3 injectisome components cross the membranes and periplasm in a similar fashion to flagellin subunits, and are subsequently assembled into their correct location (the nanosyringe-type structures or injectisomes have been considered as an evolutionarily related surface structures similar to flagella) (Büttner, 2012; Notti

& Stebbins, 2016). The assembly is mediated by signals conferred by the surroundings the bacteria face, in a coordinated and regulated manner. T3SSs encompass three primary components: core transmembrane proteins, a basal body, and flagella or injectisomes exposed on the bacterial cell surface. Both the basal body and flagella/injectisomes elements are different at the primary and tertiary structural levels due to their differences in functions, whereas core transmembrane proteins remain highly similar (Büttner, 2012; Erhardt et al., 2010; Thanassi et al., 2012).

Finally, the type IV pili (related to type IV secretion systems, T4SSs) are present in most bacteria and were derived from a cluster of proteins responsible for the mediation of conjugation (Fronzes et al., 2008). The T4SSs are responsible for translocating DNA and proteins that act as virulence factors into other cells and can be categorized into 3 groups depending on the specific function they exert: 1) conjugation (a mechanism that depends on direct contact and transfers single-stranded DNA across bacteria), 2) effector translocator (capable of sending protein substrates to cells infected in eukaryotes through contact), and 3) uptake or release systems for DNA (similar to conjugation, but this machinery does not involve direct contact between bacterial cells) (Fronzes et al., 2008; Thanassi et al., 2012). Although the T4SSs differ in the function and composition of their subunits, they form channels with similarities in order to transport the virulence factors across the envelope (Thanassi et al., 2012).

1.4 Envelope Stress Response, Two-Component Signal Transduction systems

During the course of colonization and infection, Gram-negative diarrheal pathogens encounter diverse environmental stresses that cause specific disruptions to their cell envelope, affecting periplasmic homeostasis (Leblanc, Oates, & Raivio, 2011; Runkel et al., 2013). Stresses can be characterized into either physical (temperature and osmolarity changes), chemical (pH and

antibiotics administered to treat the host infection) or biological (availability and diverse types of nutrients, components from the host immune system like antimicrobial peptides (AMPs) or metal chelators) groups (Figure 1-2) (Audrain et al., 2013; Bury-Moné et al., 2009; Flores-Kim & Darwin, 2014; Hood & Skaar, 2012).

Bacteria need to sense such pressures from their surroundings, after which they manage to use the information received (ability to transduce the perceived signals) to ultimately mount an adequate response that allows them to cope, adapt and ultimately survive those adverse conditions, specifically through the utilization of complex stress response systems (Bury-Moné et al., 2009; Eguchi & Utsumi, 2008; MacRitchie et al., 2008). In Gram-negatives, such systems are sorted into either extracytoplasmic (responsible for envelope integrity regulation) or cytoplasmic stress responses (Leblanc et al., 2011; MacRitchie et al., 2008). Many pathways that mediate stress responses can be activated by one or more inducers, promoting the incorporation of different mechanisms that work in tandem and regulate a diverse range of adaptations at the same time (Bury-Moné et al., 2009).

1.4.1 General characteristics and mechanism of action

The most prevalent and widespread signaling pathways present in prokaryotes (along with other domains in life including the eukaryotic yeast and plants, but importantly absent in mammals) (Buelow & Raivio, 2010; Yamada & Shiro, 2008) that allow them to respond to diverse microenvironmental stresses and perturbations to the envelope, are represented by TCSTs. These mediate selective changes in the expression of genes as a result of their activation, and comprise approximately 1% of the total encoded proteins (West & Stock, 2001). To date, over 4000 TCSTs have been recognised in 145 genomes in bacteria, thus showing the huge influence that such

mechanisms have on regulating bacterial adaptation to different niches (Beier & Gross, 2006; Eguchi & Utsumi, 2008; Yamada & Shiro, 2008). The specific amount of TCSTs in bacteria is correlated to the size of the genome and the complexity of each specific niche. For instance, the *E. coli* genome encodes 62 TCST proteins that regulate chemotaxis, transport, osmoregulation and metabolism, among other processes (Bretl, Demetriadou, & Zahrt, 2011; West & Stock, 2001).

In general, it can be stated that TCSTs consist of two proteins with multiple domains: 1) a sensor histidine kinase (HK) that can be either periplasmic, inner membrane-anchored, or cytoplasmic; and 2) a cognate response regulator (RR) found in the cytoplasm, however some systems correspondingly involve extra accessory constituents (Figure 1-3) (Bretl et al., 2011; Buelow & Raivio, 2010; Laub, 2011; Wuichet, Cantwell, & Zhulin, 2010). HKs and RRs can be identified by their specific-conserved domain configuration, besides their capacity to modulate events that require signal transduction via phosphorylation steps (Bretl et al., 2011; Yamada & Shiro, 2008).

1.4.1.1 Overview and structural basis of signal transduction in TCSTs

The sensor HK component of any TCSTs is responsible for initiating the response mechanism by sensing either extracellular or intracellular stimuli, and then transmitting such information to the cognate RR in the interior of the cell, via a conserved set of phospho-transfer reactions. Sensor HKs are made up of both the sensor/input domain with limited sequence homology (which is to be expected, since every specific HK has evolved to sense vastly different signals) necessary for signal detection; and the cytoplasmic histidine kinase transmitter domain (divided into catalytic and dimerization domains), identified by a greatly conserved structure and mechanism between distinct TCSTs and needed for information transfer to the RR. In contrast, the

RRs consist of a receiver and a regulatory (also identified as effector or output) domain, working as a homodimer and representing the effector component of the pathway (Buelow & Raivio, 2010; Cheung & Hendrickson, 2008; Mechaly, Sassoon, Betton, & Alzari, 2014; Wuichet et al., 2010; Yamada & Shiro, 2008).

In general, the pathway begins with a HK sensor domain detecting external environmental inducers or internal signals (including ligand molecules), which leads to its dimerization and a histidine amino acid residue (His) within the dimer interface being phosphorylated by the catalytic domain (through ATP usage as a phospho-donor), during a process that is called "autophosphorylation". Afterwards, the phosphate attached to the histidine residue is subsequently transferred to a conserved aspartate amino acid residue (Asp) positioned on the receiver domain of the RR, as a second step in the pathway called "phosphorylation of the RR" (Bretl et al., 2011; Foussard et al., 2001; Kim & Forst, 2001; Yamada & Shiro, 2008). The now phosphorylated RR undergoes a modification in the structural conformation on its regulatory and effector domains, allowing it to act as either a downstream protein activator or as a transcription factor able to bind to specific DNA recognition sites, eliciting transcriptional regulation via expression or repression of downstream genes that set up bacterial adaptation to stress conditions. RRs are responsible for mediating the required cellular response, depending on the specific inducing signal in the environment (Figure 1-3) (Bretl et al., 2011; Cheung & Hendrickson, 2008; Foussard et al., 2001; Wuichet et al., 2010). It is worth mentioning that some HK sensors, in addition to their kinase activity (serving as phospho-donors along the pathway to initiate a response), can function as RR phosphatases too (meaning that they are able to dephosphorylate RRs) to regulate the levels of activation of the system and maintain the pathway in an "off" state, during the absence of inducing cues (Stock, Robinson & Goudreau, 2000; West & Stock, 2001). Since RRs may be

phosphorylated directly in the cytoplasm via alternative small phosphodonor molecules (including acetyl phosphate (Ac~P), imidazole phosphate, carbamoyl phosphate, among others), the dual function of some of the HKs is then used to maintain the response fidelity by the prevention of inappropriate activation of the RR. This ability to dephosphorylate the RR similarly makes possible a rapid attenuation or shutdown of the response, after stresses have been dealt with (Bretl et al., 2011; Stock et al., 2000; Wolfe, 2005, 2010).

The basic chemistry that occurs within the TCSTs described previously can then be summarized by the following sets of phospho-transfer reactions (Stock et al., 2000):

1. HK sensor autophosphorylation: HK-His + ATP ↔ HK-His~P + ADP
2. Phosphorylation of the RR: HK-His~P + RR-Asp ↔ HK-His + RR-Asp~P
3. RR dephosphorylation (HK phosphatase activity): RR-Asp~P + H_2O ↔ RR-Asp + P_i

Moreover, it has been established among recent discoveries that some more sophisticated TCSTs divert from the classical two-component definition of the pathway and can involve two or more phospho-transfer domains that contain histidine or aspartate (multiple sensor or regulatory components), besides multiple accessory intermediate elements that extend the phosphorelays between the HKs and RRs (Wuichet et al., 2010).

1.4.2 Structural characteristics of HKs and RRs present in TCSTs

HKs have been classified into the following classes based on sequence analysis and comparison: class I, hybrid class I and class II types, depending on the composition of each of their domains. As stated previously, the sequences occurring in their sensor components do not display a high degree of similarity between each other. However, within all HKs some common amino

acid motifs have been identified, such being the case of the H, N, G1, G2 and F boxes (Dutta, Qin, & Inouye, 1999; Foussard et al., 2001; Kim & Forst, 2001; Yamada & Shiro, 2008).

Essentially, class I HKs are the most commonly spread across bacteria, and are defined by having an H box (HexxxP) harboring a phosphorylated His amino acid residue in the dimerization domain. The ATP-binding and catalytic regions in the catalytic domain are formed by the N (NLxxxN), G1 (DxGxG), G2 (GxGxGL) and F (FxPF) boxes. This class is exemplified by the *E. coli* osmotic sensor EnvZ (Stock et al., 2000; Yamada & Shiro, 2008). Contrastingly, the HK hybrid class I type can be described as containing multiple phosphodonor and phosphoreceptor sites. These display a histidine kinase domain after which a His-containing phosphotransfer region (HPt) and an Asp-containing acceptor domain are placed in the C- terminal end (such is the case for the *E. coli* ArcB sensor of anoxic redox conditions), so the phosphate group shifts in the His-Asp-His sequence. In comparison, the class II HK chemotaxis (CheA) sensor (solubilized in the cytoplasm) includes five domains on each monomer, and the P1 domain incorporates a phosphorylated His amino acid residue, while the P2 domain recognizes and attaches to RRs, the P3 domain is responsible for dimerization, the P4 domain mediates ATP binding and the P5 domain maintains the regulation of the activity of the kinase. Furthermore, CheA differs from the class I HKs in that the phosphorylated His residue (P1) is situated in another area, as compared to the catalytic site (P4) (Dutta et al., 1999; Foussard et al., 2001; Kato, Mizuno, Shimizu, & Hakoshima, 1997, 1999; Kim & Forst, 2001; Mourey et al., 2001; Stock et al., 2000; West & Stock, 2001; Wuichet et al., 2010; Yamada & Shiro, 2008).

On the other hand, RRs have been catalogued as the terminal component in a TCSTs, working as switches activated by phosphorylation that are able to exert an adaptive and survival response. They oversee the transfer of the phosphate group from the HK to their

regulatory/receiver region, however the majority of the RRs are also capable of catalyzing their own dephosphorylation, to regulate the lifetime of the activated state (Stock et al., 2000). RRs encompass a receiver and an effector domain, as previously stated. The N-terminal receiver domain includes the highly conserved Asp amino acid residue able to accept phosphoryl groups, while the C-terminal effector domain conformation is variable and determines the output specificity (Foussard et al., 2001; Stock et al., 2000).

1.4.2.1 The sensor domain

Sensor domain structures of HKs differ from the dimerization and catalytic regions of the histidine kinase domain, since the conformation is specifically dependent on the particularity of the inducing signals and ligand type (Stock et al., 2000). Sensor domains have been grouped into three main categories depending on the subcellular location of each system and the attributes of the signals detected: periplasmic or extracytoplasmic (the latter which can potentially be displayed extracellularly) surface receptors, transmembrane/membrane-embedded domains (without a distinct periplasmic domain), and cytoplasmic/intracellular receptors (the last two types account for sensing membrane-associated or cytoplasmic inducers, respectively) (Buelow & Raivio, 2010; Cheung & Hendrickson, 2010).

The most common of the of histidine kinase forms is displayed as a protein integrated in the membrane ("membrane-bound") in a homodimeric configuration (Mechaly et al., 2014; West & Stock, 2001). Their specific amino-terminal sensing domain component is periplasmic and is composed of an extracellular loop in the middle of two transmembrane sections. It is coupled with a transmitter region (described as the catalytic core) in the cytoplasm by an adaptor four-helix coiled-coil HAMP ("histidine kinases, adenyl cyclases, methyl-accepting chemotaxis proteins, and

phosphatases") module/linker, right after the final transmembrane portion (Buelow & Raivio, 2010; Mechaly et al., 2014; Stock et al., 2000). Although the role of the linker region within the structure of the HK sensors is not fully understood, several studies have concluded that they are critical for adequate signal transduction (Stock et al., 2000). Chemotaxis sensors also show a comparable topology, however their signaling is mediated through separate proteins of histidine kinase nature and activate flagella instead of genes (Cheung & Hendrickson, 2010; Ferris et al., 2012; Kirby, 2009).

1.4.2.1.1 Periplasmic sensor domains

Structural studies performed over the last 5 years have revealed three conformational categories for periplasmic sensor domains: all-α folds, mixed α+β folds, and sensor domains that have an analogous fold to that of the periplasmic binding proteins. The combined α+β class has been termed the PDC (PhoQ-DcuS-CitA) domain, in allusion to the first three extracytoplasmic sensor regions to whom their structure was initially discovered: PhoQ, DcuS, and CitA (Cheung & Hendrickson, 2008, 2010; Sevvana et al., 2008). These three structures are capable of detecting divalent ions, some C_4-dicarboxylates (like tartrate, malate, fumarate and succinate), and citrate, respectively (Cheung, Bingman, Reyngold, Hendrickson, & Waldburger, 2008; Cheung & Hendrickson, 2008). The PDC sensors seem to be wide-spread and are notable for having a central five-stranded anti-parallel β-sheet structure (that resembles the structural topology of the PAS domains (a structural Per/ARNT/Sim motif associated with interactions of the protein-protein class and ligand binding in multiple proteins (Buelow & Raivio, 2010; Henry & Crosson, 2011), but include a specific set of traits too), surrounded by α-helices on the sides, and start with a lengthy N-terminal helix and in most cases end with a short C-terminal helix. Extracytoplasmic domains

frequently exhibit additional domain insertions described by a second membrane-distal PDC domain that integrates in the middle of the first PDC domain. They form a double-PDC domain with little identity between the sequences of both domains, in spite of the fact that they do show a large structural similarity. The first sensor in which insertion was discovered is the LuxQ quorum sensor, that forges a complex with the LuxP periplasmic accessory protein, and later described in other sensors, like DctB (a detector for C_4-dicarboxylates) (Cheung & Hendrickson, 2008, 2010).

Sensor domains with an all-helical structure are comprised by NarX (that senses nitrite and nitrate by way of direct binding), TorS (HK domain that detects trimethylamine-N-oxide as a consequence of the formation of a complex with the periplasmic protein TorT), and a structure in the PDB with code 3kkb that creates four-helix bundles related to Tar. TorS in turn demonstrates a domain insertion that is similar to those in double-PDC domains, but this one has a "membrane-distal left-handed" set of four helices supported against a "membrane-proximal right-handed four-helix bundle" (Cheung & Hendrickson, 2010).

Finally, the third group of extracellular sensors has been anticipated to have a similar fold to periplasmic binding protein domains, and one example of these is the single structural $HK29_s$ (sensor that is currently unrelated to a specific stimulus). This sensor has an evident absence of flexibility in the pivotal region between both domain lobes. After sequence analysis studies have been performed on such sensor, it has been proved that there are tandem repeat motifs in this conformational group (Cheung & Hendrickson, 2010).

1.4.2.2 The HK dimerization domain

The common structures found in the members in the HK family is the distinctive kinase core formed by the dimerization domain and the catalytic domain (ATP/ADP-binding

phosphotransfer domain) (Stock et al., 2000). HKs generally become a functional dimer once activated, after interaction between the dimerization domain in each monomer occurs. As a specific example, the dimerization domain structure of the EnvZ osmosensor located in *E. coli* was solved by nuclear magnetic resonance (NMR) and X-ray analysis and showed that one subunit displays two long helices (designed as I and II) arranged with the ones from the other subunit, so it can ultimately form a conglomerate consisting of four helices (Dutta et al., 1999; Foussard et al., 2001; Tomomori et al., 1999). The helix I has a more conserved sequence of amino acids in the N-terminal region due to the H box containing the phosphorylated His residue, than that of the helix II. It is important to notice that the H box is located in each subunit, so the four-helix bundle packs two histidine residues able to be phosphorylated. Each specific residue of histidine is oriented so that it can accept phosphate groups from the other monomer within the dimer. This occurs during the autophosphorylation step of the signaling cascade, in addition to transferring the phosphate to the RR afterwards (Foussard et al., 2001; West & Stock, 2001; Yamada & Shiro, 2008).

1.4.2.3 The HK catalytic domain

Many catalytic domain structures of HKs have been solved to date using three-dimensional X-ray crystallography, including EnvZ, CheA, PhoQ (a sensor for detecting Mg^{2+} in *E. coli)*, PrrB in *Mycobacterium tuberculosis*, NtrB (nitrate sensor in *E. coli*), among others. The catalytic domain sequence continues from the dimerization four-helix structural unit and possesses an "α/β sandwich" fold, which means that the three α-helices (α1, α2 and α4) are between the β-sheet. In addition, there is an ATP-lid loop in between the α3 and α4 helices, characterized for its flexibility. The distinctive N, G1, G2 and F conserved boxes of HK are in charge of delimiting the specific

space for binding of ATP, and appear to be amongst residues that show little variation in all sequences (Cheung et al., 2008; Foussard et al., 2001; Yamada & Shiro, 2008).

It is well established that HKs need ATP along with either the Mn^{2+} or Mg^{2+} cations, so that they can carry on with the phosphorylation activity. Structures of the complete aggregate involving a nonhydrolysable ATP and the cation added into the ATP binding site have been described and studied in certain HKs. After the nucleotide binding occurs, the ATP-lid changes into a closed conformation, resulting in the ATP binding site being covered, followed by interactions with the lid and N and G1 boxes that sustain the binding, so the γ-phosphate becomes exposed to the bulk solvent region and accessible to the His residue in specific cases such as CheA (Buelow & Raivio, 2010; West & Stock, 2001; Yamada & Shiro, 2008).

1.4.2.4 The RR receiver (regulatory) domain

RRs receiver domain structures from different TCSTs have been solved, including CheY (this chemotaxis protein with one domain serves as the representative model for regulatory domains), SpoOF, NtrC, CheB, PhoB, KdpE, TorR, PrrA, among others (Stock et al., 2000; Yamada & Shiro, 2008). Receiver domains depend on the phosphorylation state to act as an "on-off" switch for cellular response (Foussard et al., 2001) and share common features: an α/β fold, with central five-stranded parallel β-sheets (β2-β1-β3-β4-β5) surrounded by two (α1, α5) and three (α2, α3, α4) α-helices (Stock et al., 2000; West & Stock, 2001; Yamada & Shiro, 2008). The active site is described as a pocket of predominantly acidic nature, is highly conserved, and is where the aspartate amino acid that is able to be phosphorylated resides. The half-life of RRs once they become activated by phosphorylation can go from seconds to more than an hour, depending on the nature of the cellular response that needs to be accomplished (Buelow & Raivio, 2010).

Descriptions of the receiver domains acting through numerous protein-protein interactions, either in their phosphorylated or dephosphorylated states have been established as well, but its specific significance is still yet to be studied in depth (Foussard et al., 2001).

1.4.2.5 The RR effector domain

Even though effector domains display great diversity in regard to specific DNA sequences recognized, binding site configuration and specific mechanism of mediation of transcription, it can be stated that most RRs work as transcription factors for either negative or positive management of gene expression, and they have been shown to include a typical helix-turn-helix motif as an effector domain that allows DNA binding (Foussard et al., 2001; Yamada & Shiro, 2008). In some RRs, the receiver region and the effector domain demonstrate an interaction which masks the DNA-recognition helix, or α9, in the inactivated shape, also known as the non-phosphorylated state. In other cases, the DNA binding state of the confined effector domain generates a symmetric dimer, followed by a direct interaction of the α9 with the designated DNA. In light of such discoveries and additional biochemical and genetic approaches, it has been proposed that in order for the DNA recognition site to be exposed and to achieve dimer formation, the RR must alter its configuration after it accepts the phosphate group at the conserved Asp residue in the receiver domain (Stock et al., 2000; West & Stock, 2001; Yamada & Shiro, 2008).

1.4.3 Envelope Stress Responses (ESRs)

Currently, *E. coli* has been found to use a minimum of five response mechanisms (including TCSTs) against stress and environmental perturbations to the envelope that enables it to regulate homeostasis (Bury-Moné et al., 2009; Leblanc et al., 2011): The Conjugative plasmid

expression (Cpx) system induced by stressors that generate periplasmic misfolded proteins and trigger envelope disruption, as well as by sensing surface adhesion through the outer membrane new lipoprotein E (NlpE); the σ^E system that detects and reacts principally against inducers affecting the folding and maintenance of the OMPs (Alba & Gross, 2004; MacRitchie et al., 2008; Raivio & Silhavy, 2001); the Phage-shock-Protein (PsP) pathway responsible for adequately controlling the proton motive force (PMF) and the inner membrane structural stability; the Bacterial adaptive response (Bae) needed for the elimination of toxic compounds from the cell (Zhou, Lei, Bochner, & Wanner, 2003); and the Regulator of capsular synthesis (Rcs) pathway believed to intervene in surface structure formation and respond to peptidoglycan that is damaged (Bury-Moné et al., 2009; Imamovic, Martínez-Castillo, Benavides, & Muniesa, 2015; Leblanc et al., 2011; MacRitchie et al., 2008). A newly discovered pathway related to vesicle release is believed to be a general mechanism to alleviate envelope perturbations, working by collecting and then getting rid of misfolded proteins and undesirable molecules, by compartmentalizing them into outer membrane vesicles that can be discharged into the external environment (McBroom & Kuehn, 2007). A more detailed description of two representative examples of these stress responses will be provided in the next subsections.

1.4.3.1 The σ^E envelope stress response

Sigma factors that sense and regulate extracytoplasmic function are derived from σ^{70} and used as a conserved signaling cascade by bacteria as part of mechanisms that aid in the detection and response to the stimuli localized in the environmental context. The σ^E factor, also known as σ^{24}, was initially described by Erickson and Gross in 1989 due to its ability to transcribe a gene that encodes another sigma factor responsible for regulating the heat shock response (*rpoH*) and a

gene (*degP*) which encodes for a periplasmic serine protease with degradation activity (the protease DegP). One of the activators for this response was the heat shock conditions (an increase in temperature beyond 42°C), however such induction constitutes a very general signal that could probably activate many different responses besides σ^E. It was later stated that compounds responsible for the generation of misfolded proteins including ethanol (EtOH), dithiothreitol (DTT) and puromycin, along with the overproduction of PapG (a misfolded P-pilus subunit) increased activity of this signaling pathway. This implied that the specific stress to which σ^E responds to is misfolded proteins in the outer membrane (Danese & Silhavy, 1997; Flores-Kim & Darwin, 2014; MacRitchie et al., 2008).

The σ^E regulon encompasses members involved in different facets of the function of the cell, such as periplasmic protein folding and degradation, building of proteins in the OM, metabolism, transcription, translation, nucleic acid modification and repair, cell structure and division, among others. The principal members of the regulon were identified as *rpoE* and the regulators *rseABC*. σ^E was shown to be auto-regulated, which also occurs in the sigma factors *rpoD* (σ^{70}), the housekeeping factor *rpoH* (σ^H), and the heat shock σ factor, together with other periplasmic chaperones and folding mediators, including DegP (Danese & Silhavy, 1997; MacRitchie et al., 2008).

1.4.3.2 The BaeSR TCST system

The two-component signaling transduction BaeSR response system was originally described in a screen that looked for additional TCSTs in *E. coli*, and later determined to be an envelope stress response by Raffa and Raivio in 2002. It was established that induction of a gene called *"spy"* upon spheroplasting, over-expression of the PapG pili subunit in absence of its

chaperone, and indole exposure were in part due to the activity of the BaeSR cascade. BaeSR is a classical two-component system that is made of the inner membrane-bound sensor histidine kinase BaeS (with an extracellular sensing domain), and a cognate response regulator in the cytoplasm (BaeR). Activation of this RR via phosphorylation allows it to function as a dimer and regulate the BaeR regulon transcription, which consists of the genes *acrD, spy,* and the operon *mdtABCD-baeSR* (Imamovic et al., 2015; Leblanc et al., 2011; Lin, Lin, & Lan, 2015). Altogether, these genes encode MdtABC and AcrD (two "resistance, nodulation and cell division" (RND) multidrug efflux pumps used to export antibiotics and other antibacterial compounds possibly dangerous to the cell), a major facilitator superfamily (MFS) protein (MdtD), BaeR, BaeS, and the Spy chaperone in the periplasm. Other members of the BaeR regulon include *ycaC* that encodes for a cystidine hydrolase enzyme, *tolC* encoding an OM protein commonly used by diverse multidrug efflux pumps, and certain conserved genes that encode proteins whose functions are not yet fully understood, including *yicO, ygcL, yeeN, ynjA* and *ynjB.* Yamaguchi and collaborators found that overexpression of BaeR grants a greater protection against antibiotics, including β-lactams (as a result of *mdtABC* and *acrD* increased expression), condensed tannins, low amounts of sodium dodecyl sulfate (SDS), zinc toxicity, novobiocin and deoxycholate (Bury-Moné et al., 2009; Hirakawa, Nishino, Hirata, & Yamaguchi, 2003; Leblanc et al., 2011; Lin et al., 2015; MacRitchie et al., 2008). Thus, this system plays an important role in coping with potentially dangerous conditions to the bacterial cells.

1.5 The Cpx Envelope Stress Response (ESR)

The Cpx pathway (more specifically referred to as the CpxRA envelope stress response, two-component signal transduction system) was discovered in the late 1970s/early 1980s by the

McEwen and Silverman research group. They conducted experiments in *E. coli* K12 strains that could not conjugate the F-plasmid due to the failure in production of F-pili, instead of from experiments aimed directly at studying responses against insults to the bacterial envelope (MacRitchie et al., 2008; McEwen & Silverman, 1980). The first set of the *cpx* locus mutations generated strains that displayed a wide variety of characteristic phenotypes, including sensitivity to high temperatures resulting in modified protein content in the envelope, isoleucine and valine auxotrophy, decreased conjugation, substrate transport alterations and modified expression of the OM porins and lipoproteins (among others). These results early implied that the genes regulated by this locus could be linked to a response against envelope stress (McEwen & Silverman, 1980, 1982; Raivio, 2014).

1.5.1 Components of the Cpx pathway

The *cpx* locus has been determined to be situated in the chromosome of various Gram-negative gamma proteobacteria, including *E. coli* and *V. cholerae* (Raivio, 2014). The very first experimental results demonstrated that there are two main genes within the locus: first, *cpxA* which encodes the HK sensor CpxA, a transmembrane protein that is homologous to the component of the histidine kinase family EnvZ, (Weber & Silverman, 1988); and second, *cpxR* encoding the cytoplasmic RR CpxR, displaying a structure that in turn is homologous to a subfamily of proteins that bind to DNA, named "OmpR" (Dong, Iuchi, Kwan, Lu, & Lin, 1993).

The specific function of the Cpx system was then researched by means of studying misfolded or mislocalized proteins that were secreted and generated toxicity to the cell. It was concluded that *cpx* mutants that were constitutively active (*cpx** mutants) managed to tolerate increased levels of misfolded proteins in the envelope (Cosma, Danese, Carlson, Silhavy, &

Snyder, 1995). Harmful effects from these proteins included maltose and amikacin sensitivity, as well as outer membrane permeability alterations, thus bacterial cells perished unless they possessed gain-of-function mutations in their *cpx* locus that allowed them to adapt and survive (Cosma et al., 1995). The same research group elucidated that DegP was involved in the endurance of adverse conditions to the cell, by helping with the degradation of toxic proteins in the periplasmic space (protease activity) (Danese, Snyder, Cosma, Davis, & Silhavy, 1995). Additional studies that focused on over-producing the outer membrane lipoprotein NlpE also caused the activation of the Cpx cascade, promoting cell adaptation against toxic conditions (Snyder, Davis, Danese, Cosma, & Silhavy, 1995). Altogether, these findings suggested that the CpxRA TCSTs is importantly involved in dealing with cell damage that arises from the presence of mislocalized or misfolded proteins in the envelope, resulting from harmful conditions in their surroundings (Vogt, Acosta, Wong, Wang, & Raivio, 2012).

While the CpxRA TCSTs was first considered a classical two-component system, it has been more recently discovered that there is an additional constituent of importance for signal transduction in the pathway: CpxP. This new component was described as a small protein in the periplasm, being expressed from *cpxP* after pathway activation. In fact, *cpxP* has been found to be one of the most highly upregulated transcribed genes when the Cpx response is induced (DiGiuseppe & Silhavy, 2003). Subsequent experimental results showed that overproducing CpxP rendered a decrease in gene expression through the signaling cascade (Danese & Silhavy, 1998; Raivio, Popkin, & Silhavy, 1999), and that CpxP attached to the IM did not allow for initiation of the Cpx response (Raivio et al., 2000). Based on the information available from these studies, it was proposed that CpxP is responsible for inhibition of the pathway through a not fully understood

negative-feedback loop mechanism, by means of directly interacting with the periplasmic sensor domain of CpxA ($CpxA_{SD}$) (Raivio et al., 1999).

1.5.2 Structure and characteristics of CpxA, CpxP and NlpE

Both CpxP and NlpE have been proposed to act through not completely understood interactions with the $CpxA_{SD}$, and these interactions could possibly be of the direct-contact type. Novel recent techniques have allowed the solution of the crystal structures of these proteins and revealed the presence of putative ligand-binding domains which may be related to detection of signals by the HK sensor (Raivio, 2014).

1.5.2.1 The CpxA sensor domain

The structure of the soluble periplasmic $CpxA_{SD}$ of *Vibrio parahaemolyticus* (VpCpxA-peri) was solved and published by Kwon and colleagues in 2012, showing that in a comparable way with many other sensor domains, it is formed by a globular PAS domain consisting of a central β-sheet with five strands located in turn in between multiple α helices (potentially important for sensing ligands), and a protruded C-terminal. However, this crystal structure presented some deficits, as one terminus was unstructured and the N- and C-termini were not oriented in a way consistent with them being linked to the transmembrane helices. They were also not able to obtain conclusive results for a possible interaction between the purified $CpxA_{SD}$ and CpxP, leading them to propose that an additional component from membranes was required in their experiments for the binding process (Kwon et al., 2012; Raivio, 2014). More recently, in 2014 the Raivio group solved the crystal structure of the soluble $CpxA_{SD}$ of *E. coli* through a collaborative effort with the Glover group (biochemistry, University of Alberta). It is comprised of 150 amino acid residues

and displays a mixed αβ dimer with predicted interactions between the methionine 48 (M_{48}) residues in the N-terminal α-helices (Figure 1-4a). Unlike the sensor domain described for *V. parahaemolyticus*, the one within *E. coli* was identified to exhibit a PDC fold with certain similarities to the PAS domain, and a more compact structure with the N- and C-termini oriented in a fashion consistent with their connection to the transmembrane α-helices (Margain-Quevedo, Malpica, Thede, Lu, Glover & Raivio, in preparation; Raivio, 2014; Vogt & Raivio, 2012).

An electrostatic surface representation was also retrieved using the PyMOL Molecular Graphics System software (http://www.pymol.org/) (Figure 1-4b), with various surface-exposed charged aggregates of amino acid residues highlighted. Prominent negative patches are labeled in red, perhaps important for contact and interaction with positively charged ligands including CpxP; while blue positive charged patches may be of importance for interacting with the negatively charged IM (Margain-Quevedo et al., in preparation).

Additionally, an alanine-substitution mutagenesis assay of the conserved residues N_{107}, P_{118}, K_{121}, Y_{123} and P_{131} on one of the edges of the PDC β-sheet and adjacent connecting linker and α-helix regions of the dimer was conducted, leading to an activated phenotype even at non-inducing acid pH, as compared to the wild type strain, by means of β-galactosidase assays and employing reporter genes. Activation of the pathway by these mutations may potentially be occurring by alteration of the direct CpxP-mediated inhibition. This effect could lead to either a decreased phosphatase ability under acid pH or increased kinase activity in alkaline conditions for the $CpxA_{SD}$, and multiple amino acid residues may be concomitantly playing a role in signal detection and other interactions (Margain-Quevedo et al., in preparation; Vogt et al., 2012).

1.5.2.2 The CpxA transmitter core

Mechaly and colleagues described in 2014 the complete cytoplasmic region of the CpxA component from *E. coli* ($CpxA_{HDC}$, known as the transmitter core), spanning the HAMP signaling domain, the DHp (dimerization and histidine phosphorylation) and the CA (catalytic and ATP binding) domains, after creating recombinant proteins for structural assays. The $CpxA_{HDC}$ structure is made up of a homodimer, where the HAMP and DHp domains form an elongated central coiled-coil region surrounded by the two CA domains on the sides (Mechaly et al., 2014).

The structures reported in the aforementioned study allowed to have more information about the reaction mechanism of transduction of signals, due to CpxA adopting multiple conformations in an asymmetric manner. The dynamism of the structures shows the changing and extremely asymmetric nature of the active state of CpxA. After research including biochemical, structural and mutagenesis experiments, they could come up with a model based on the fact that propagation of the signal through the HAMP domain regulates the autophosphorylation activity through the induction of segmental motions and flexing of the α-helices at the center of the HK that successively regulate movement of the ATP-binding catalytic domain (Mechaly et al., 2014).

1.5.2.3 CpxP

CpxP is a small accessory inhibitor/chaperone molecule in the periplasm, comprised of 147 amino acid residues and is part of the Cpx signaling system (Thede et al., 2011). Its crystal structure was solved in 2011 by both the Raivio and Hunke research groups, and it was found to form an antiparallel dimer of tangled α-helices with a highly basic concave bowl shape, made from two monomers that comprise a bent structure of resemblance to a hairpin. It is remarkable that the concavity in the bowl's surface is composed by charged patches with predominantly positive

amino acid residues, while the convex surface is negatively charged with a hydrophobic band (Figure 1-5) (Thede et al., 2011; Zhou et al., 2011).

Although the specific molecular nature of the potential ligand or ligands that could be able to interact with the positively charged surface in the CpxP concavity remain uncertain, it has been recently implied that this region could be interacting with a negatively charged partner, including the sensor domain of CpxA exposed to the periplasm and observed to display negative surface charged patches in this area (Figure 1-4b). Misfolded proteins with hydrophobic regions largely exposed to the periplasm could then be responsible for titrating CpxP away from CpxA, by interacting with a hydrophobic stripe on the negatively charged convex surface (Thede et al., 2011; Zhou et al., 2011). However, it is striking that there are not many hydrophobic patches found even on the convexity of CpxP, with only a single stripe showing this characteristic, so the mechanism through which it may directly interact with misfolded proteins is still up for debate (Raivio, 2014). One possibility is that major changes in the structure of CpxP occur for it to work as a chaperone, similarly to what ensues with the chaperone Spy (displaying homology with CpxP) in the presence of misfolded proteins (Merdanovic et al., 2011; Quan et al., 2011).

Another suggestion for CpxP functioning is that an extra third unidentified partner could be mediating an interaction between CpxA and CpxP, since the pathway is closely dependent on local events occurring at the IM, so membranes or parts of them (like phospholipids) could be necessary for the contact. In a less likely explanation, CpxP may be responsible for the detection of some very specific signal that has yet to be described, however no stresses requiring CpxP for initiating a response have been identified to date (DiGiuseppe & Silhavy, 2003; Raivio, 2014)

1.5.2.3.1 Supporting evidence on the $CpxA_{SD}$ direct interaction with CpxP model in *E. coli*

The model for CpxP-mediated inhibition of CpxA through direct interaction emerged from studies that revealed downregulation of the Cpx response when overproducing CpxP tethered to the IM. The excess in CpxP did not allow for complete activation of the response after a major disturbance to the envelope by the presence of spheroplasts (however, the inhibitory effect exerted by CpxP was lost in $CpxA_{SD}$-null strains) (Raivio et al., 1999; Raivio et al., 2000). Additionally, a study that used purified CpxP alongside CpxA in reconstituted proteoliposomes led to the inhibition of the autokinase activity of CpxA, thus preventing pathway initiation (Fleischer et al., 2007).

Buelow and Raivio explored the mechanisms through which CpxP exerts its inhibition, by performing mutagenesis screening assays and identifying many *cpxP* mutants with highly conserved N-terminal domain alterations that were unable to inhibit CpxA. Mutations to *cpxP* also diminished CpxP protein stability, but this trait could be complemented back to normal levels by mutating DegP, thus suggesting that this protease may be related to CpxP stability and the overall Cpx transduction of signals (Buelow & Raivio, 2005).

Tschauner and collaborators recently performed a study using both a bacterial two-hybrid (BACTH) assay and an *in vivo* alternative membrane-Strep-tagged protein interaction experiment (mSpine) that included membrane components, based on previous membrane protein-interaction assays (Karimova, Dautin & Ladant, 2005). They stated that this interaction is dynamic and influenced by high concentrations of salt and the misfolded pilus subunit PapE, required for shifting CpxP away from CpxA (Tschauner, Hörnschemeyer, Muller, & Hunke, 2014).

Moreover, the affinity between CpxA reconstituted in nanodiscs (CpxA-ND) and CpxP has been studied using microscale thermophoresis (MST). The data obtained suggested that the affinity

between these two components was very low. In contrast, the CpxA-ND displayed higher affinity for CpxR. In fact, it is mentioned in the study that even though a critical CpxP concentration close to the one required for precipitation was utilized (deemed as the maximum stock concentration for CpxP), it was not possible to determine the precise point of saturated binding between the CpxA-ND and CpxP. The K_D was mentioned to be over 100μM, confirming an almost undetectable relative affinity between the two. One of the drawbacks with the MST technique however is that measurements are done in aqueous solution, and this does not include the influence of macromolecular crowding into the system, so an even higher molar ratio may be needed for the inhibition provided by CpxP *in vivo* (Hörnschemeyer, Liss, Heermann, Jung, & Hunke, 2016).

1.5.2.4 NlpE

The structure of NlpE that was obtained using crystallography techniques displays a two-domain lipoprotein, with a similar N-terminal β-barrel to that of the lipocalin protein required in lipid-binding in bacteria, linked to a C-terminal β-barrel domain and a fold anticipated to attach oligonucleotide or oligosaccharides. The ligand-binding folds may infer that modifications in the binding of lipids or sugars after cell adherence is involved in propitiating changes in the structure, which are needed for adhesion sensing (Raivio, 2014). A shift in a strand of β-barrels can generate unfolding and orientation modification of the N and C termini, potentially developing a structure able to interact with the $CpxA_{SD}$ at the IM. Rigidity in the loop of a CXXC motif in the N-termus of NlpE can be affected by redox states, creating a disulfide bond in the aforementioned motif. This CXXC domain is encountered in the vicinity of a serine protease inhibitor motif within NlpE, so it is a possibility that redox occurrences in which this cysteine takes part can alter the activity

of the protease inhibitor region, consequently modifying the events in the periplasm of proteolytic nature (Hirano, Hossai, Takeda, Tokuda & Miki, 2007; Raivio, 2014).

1.5.3 Cpx inducing cues

Most of the signals that have been established to induce the Cpx pathway must go first through the sensing domain of CpxA, and then the signal can be passed on to CpxR in the cytoplasm to mediate an adaptive response. However, information is still lacking regarding the nature and molecular particularities of some of these stresses, and furthermore, there are some cytoplasmic activators that can act directly on CpxR without the need for CpxA to sense the signal in the periplasm beforehand (Vogt et al., 2012).

The first activation of the Cpx ESR system was found to occur due to constitutively activated *cpxA** mutants (*cpxA* mutants with decreased phosphatase activity (Raivio & Silhavy, 1997)) that demonstrated the ability to abolish toxic properties from the secretion of mutated misfolded envelope proteins LamBA23D (a variant of an OM porin) and LamB-LacZ-PhoA (a fusion protein) in *E. coli* (Cosma et al., 1995). Overexpression (OX) of the *nlpE* gene resulting in the overproduction of the NlpE lipoprotein was recognised to activate the stress response in a CpxA-dependent manner as well, possibly as a consequence to mislocalized NlpE found in the IM instead of the OM (Snyder et al., 1995; Vogt et al., 2012; Vogt & Raivio, 2012). In later years, additional examples of insults to the cell envelope have been deemed capable of activating the Cpx signaling cascade via the presence of misfolded proteins, including (but not limited to) alkaline pH in the media (Danese & Silhavy, 1998); overexpression of pilus subunits that become misfolded, such as the ones expressed by uropathogenic *E. coli* (UPEC) P or Pap pilus (PapG and PapE in the absence of their PapD chaperone), and the most important subunit of the EPEC type

IV bundle forming pilus called “BfpA” (which does not follow the regular folding pathway for assembly and results in a misfolded variant instead) (Nevesinjac & Raivio, 2005; Vogt et al., 2010; Vogt et al., 2012); adhesion to hydrophobic surfaces through NlpE (Otto & Silhavy, 2002); lipoprotein production distress; spheroplasting; alterations in the composition of the phospholipids located in the inner membrane; antibiotics or antimicrobial peptide compounds; indole; mutation of the multidrug efflux pump component *tolC*; osmolarity changes; metals including copper, iron and zinc; ethylenediaminetetraacetic acid (EDTA); and EtOH, to name a few (Acosta, Pukatzki & Raivio, 2015; Danese & Silhavy, 1998; DiGiuseppe & Silhavy, 2003; Mileykovskaya & Dowhan, 1997; Raivio et al., 2000, Vogt & Raivio, 2012).

An important inducer of Cpx that is worth describing in more detail is elevated pH/alkaline pH, which has been studied in both *E. coli* and *Shigella* species. Bacteria with null mutations in *cpx* genes are less resistant to alkaline pH and undergo growth and survival defects, while expression of genes known to be regulated by the Cpx pathway has been determined to be induced in wild-type strains under such conditions. Even though the specifics on the Cpx induction mediated by the presence of alkaline pH are yet to be fully understood, it has been proposed that the process may involve protein denaturation due to deprotonation of thiol groups present in cysteine amino acid residues and subsequent oxidation of disulfide bonds in strains other than *E. coli* (since there are no cysteines in CpxA or CpxP in *E. coli*) (Danese & Silhavy, 1998; Vogt et al., 2012). In contrast, alkaline pH in *E. coli* could instead have an impact on the total charge of lipopolysaccharides, resulting in an augmented permeability in the OM that disrupts the envelope and then acts as a cue that CpxA can sense to initiate a response (Raetz & Whitfield, 2002).

It is of interest that just as Pap and the type IV bundle forming pilus have an essential part in host cell adherence, NlpE is also implicated in this cellular process. The correlation between the

two was demonstrated by Otto and Silhavy in 2002 through Cpx activation experiments in a manner dependent on NlpE, after detection and attachment to abiotic surfaces. The latter was confirmed in further research that utilized *cpxR* and *nlpE* deletion mutants, both displaying adhesion defects (Otto & Silhavy, 2002; Vogt & Raivio, 2012).

Moreover, modifications to the composition in the membranes that activate the Cpx cascade include the absence of PE (Mileykovskaya & Dowhan, 1997) and the presence of large quantities of an intermediate of enterobacterial common antigen (ECA), commonly resulting in *degP* upregulation to try to alleviate the distress (Danese, Oliver, Barr, Bowman, Rick, & Silhavy, 1998). Although many diverse inducing cues have been demonstrated to activate the Cpx response, further analysis needs to be conducted regarding the exact mechanism by which they are sensed.

1.5.4 Cpx signal transduction

As a summary of information mentioned previously, a total of four major proteins that are found in distinct bacterial cellular locations are responsible for participation in sensing signals and thus regulating the Cpx response cascade: the NlpE lipoprotein in the OM, the transmembrane sensor HK CpxA in the IM, the periplasmic accessory inhibitor and chaperone molecule CpxP, and the RR CpxR located in the cytoplasm (Vogt & Raivio, 2012). Their specific role and characteristics will be described in the following subsections.

1.5.4.1 Cpx inactive state

In the absence of inducers in the environment, it has been proposed that the extracytoplasmic $CpxA_{SD}$ interacts through a not yet fully known mechanism with the periplasmic chaperone CpxP, and such protein-protein $CpxA_{SD}$-CpxP association negatively regulates the

activation of the response, since it inhibits the autokinase-kinase activity of CpxA and causes it to act as a phosphatase instead, able to dephosphorylate CpxR~P and thus maintaining the pathway in an "off" state (Figure 1-6, left portion) (Raivio, 2014; Raivio et al., 1999; Raivio & Silhavy, 1997; Vogt & Raivio, 2012). It is of relevance to highlight that overexpression of *cpxP* cannot entirely shut down the Cpx signaling cascade (there is still a detectable basal low level of activity, specifically in the presence of alkaline pH or pilin subunits) (DiGiuseppe & Silhavy, 2003). On the other hand, when removing the *cpxP* gene there is either an expected noticeable increase in pathway activation in the presence of stress (meaning that CpxP is not responsible for the detection of known specific inducing cues); or only a slight increase under non-inducing conditions (signifying that other inhibitory molecules may be responsible for keeping the pathway "off" in the absence of *cpxP*). This lead to propose that CpxP may be instead playing a part on "fine tuning" the pathway in a sort of a negative loop: in the absence of envelope stress by blocking inadequate or unwanted CpxA activation; or by enabling a fast termination of the response once a stress has been dealt with and keeping it shut down in the case when it is not needed anymore (DiGiuseppe & Silhavy, 2003; Raivio et al., 1999; Vogt & Raivio, 2012).

1.5.4.2 Cpx induction by envelope stress

When one or multiple of the previously mentioned insults to the envelope are encountered, the Cpx two-component system is activated and undergoes a classical mechanism of signal transduction, consisting of reactions that involve transfer of phosphoryl groups between CpxA and CpxR (Fleischer et al., 2007; MacRitchie et al., 2008; Raivio & Silhavy 1997). Inducers allow for the inhibition of CpxA exerted by CpxP to be relieved (DiGiuseppe & Silhavy, 2003), a process believed to be possible through titration alongside misfolded proteins (e.g. pilins) and subsequent

degradation by DegP (suggesting that CpxP becomes a DegP substrate under Cpx-inducing conditions), which in turn allows for the activation of the autokinase activity of CpxA. CpxP may then be acting by means of bringing misfolded proteins to DegP to be degraded concomitantly, or another explanation could be that the conditions that end up creating misfolded proteins may also impact the CpxP structure, causing it to misfold and to be able to get consequently degraded by the protease activity (Buelow & Raivio, 2005; Isaac, Pinkner, Hultgren, & Silhavy, 2005; Vogt & Raivio, 2012). This process results first in the CpxA autophosphorylation at a conserved histidine amino acid residue (autokinase activity), which then can utilize its kinase activity to phosphorylate CpxR by means of transferring the phosphate group to a conserved aspartate amino acid residue in the RR (Figure 1-6, right portion). Since the CpxR conformation is similar to the OmpR subfamily described as "winged-helix-turn-helix DNA binding proteins", phosphorylated CpxR (CpxR~P) can act as a transcription factor (capable of recognizing the specific consensus DNA binding sites 5'-GTAAN$_{(5-7)}$GTAA-3') to regulate the expression or repression of hundreds of downstream genes involved in mechanisms that include protein folding, degradation and transcription regulation processes required for adaptation and survival (Fleischer et al., 2007; MacRitchie et al., 2008; Pogliano, Lynch, Belin, Lin & Beckwith, 1997; Raivio & Silhavy, 1997).

1.5.4.3 Cytoplasmic induction of the pathway (direct CpxR activation)

Discoveries on the activation of the Cpx pathway have also demonstrated that in some specific situations, CpxR can be directly phosphorylated without the need for a previous CpxA phosphorylation in the IM that donates the phosphate group (Vogt et al., 2012). As observed in figure 1-7, CpxR was shown to be phosphorylated in the cytoplasm *in vitro* (Pogliano et al., 1997; Raivio & Silhavy, 1997) and under specific *in vivo* conditions (Klein, Shulla, Reimann, Keating

& Wolfe, 2007; Lima, Lennon, Ross, Gourse & Wolfe, 2016; Wolfe, Parikh, Lima & Zemaitaitis, 2008) by the transfer of a phosphate group from the small molecule Ac~P (the intermediate in the metabolic phosphotransacetylase (Pta)-acetate kinase (AckA) pathway) (Danese et al., 1995; Wolfe, 2010). Another Pta-AckA intermediate, acetyl coenzyme A (Ac~CoA), was found to mediate the acetylation of a specific residue on the alpha C-terminal domain of the RNA polymerase (RNAP), that in turn was linked to *cpxP* induction (Figure 1-7) (Lima et al., 2011; Lima et al., 2016). Gene expression for *cpxP* was also determined to be upregulated by the presence of either pyruvate or glucose in excess in the media, independently of Ac~P and CpxA phosphorylation (De Wulf, Kwon & Lin, 1999; Wolfe et al., 2008).

Finally, stationary growth phase was similarly deemed to be an inducer of the Cpx response downstream of CpxA, since the response was more active during this phase (De Wulf et al., 1999; DiGiuseppe & Silhavy, 2003). Likewise, the *cpxA* and *cpxR* genes were determined to be auto-activated in stationary phase, using *E .coli* K-12 strains, along with the σ^S sigma factor (De Wulf et al., 1999). A possible explanation could be that accumulation of metabolites in such phase require the Cpx pathway for turnover. However, the specifics on how CpxR can sense growth phase or such metabolites are still unknown (Wolfe et al., 2008).

1.5.5 Genes regulated by the Cpx system in *E. coli*

Early analysis of the CpxR regulon determined three principal genes involved in either appropriate protein folding in the envelope or the degradation of misfolded ones, as expected: *dsbA* (encoding for the disulfide oxidoreductase in the periplasm DsbA), *degP* (encoding for the DegP chaperone/protease), and *ppiA* (encoding a periplasmic protein in charge of catalyzing isomerization, the PPIA peptidyl-prolyl *cis/trans* enzyme) (Danese & Silhavy, 1997; Pogliano et

al., 1997). The list of genes influenced by CpxR activation in *E. coli* has been in continuous development, and even though genes linked to monitoring proper protein folding are still the most well characterized target genes regulated, a microarray study discovered that the regulon consists of hundreds of genes (of which approximately 50% were observed to be downregulated) and has a larger effect over the cell maintenance than previously believed. The most recently identified regulon targets are grouped into very different categories depending on their function, among which IM proteins, envelope protein complexes and peptidoglycan metabolic enzymes are found (Price & Raivio, 2009; Raivio, 2014; Raivio, Leblanc & Price, 2013; Vogt & Raivio, 2012).

The first functional subcategory in the regulon consists of genes involved in a direct manner in surveillance of envelope integrity, also known as factors in the periplasm involved in adequate folding and degrading, including some of the afore-mentioned genes: *dsbA, degP, ppiA, psd, secA* and *spy.* The ability for the Cpx system to mediate adaptations is clearly dependent on the presence and adequate action of these members (Danese & Silhavy, 1997; Pogliano et al., 1997).

A second class is formed by regulatory genes that encode Cpx proteins in charge of mediating signal transduction. As an example, autoregulation by CpxA, CpxR and CpxP has been encountered in constitutively activated *cpx** mutants or in the presence of alkaline pH in the form of augmented levels in the three proteins, which is to be expected due to the requirement for a tight regulation of the response while combatting dangerous conditions (Danese & Silhavy, 1998; Raivio et al., 1997).

A third group involves genes that encode proteins in the envelope responsible for transport regulation, like the outer membrane proteins OmpC and OmpF, as well as membrane channels that mediate active efflux and efflux pumps, for example AcrD and MdtABCD. These envelope-

localized complexes are thought to be decreased in expression levels upon Cpx response activation in order to reduce protein conglomeration in areas with a great quantity of proteins or to preserve energy (Batchelor, Walthers, Kenney & Goulian, 2005; MacRitchie et al., 2008).

Finally, a larger number of genes can be classified within a group that comprises elements needed for production and activity of bacterial structures at the exterior of the cell, such as the flagella and pili. These are downregulated when the Cpx response is activated, a process mediated by protein stability after degrading the transcriptional activator for conjugal activity TraJ (through HslVU, a protease regulated by the pathway). Another example of a downregulated gene is the one encoding for the curli fimbriae, by means of repression of the *csgBA* operon in a direct approach, as well as indirectly by inhibition of the *csgDEFG* operon (De Wulf et al., 1999, Vogt & Raivio, 2012).

1.5.6 Cellular roles associated with the Cpx response

Some years after the characterization of the Cpx components, studies regarding the mechanism of action of bactericidal antibiotics towards *E. coli* led to the proposal that all of them killed bacteria in the same fashion, explicitly through the formation of reactive oxygen species (ROS) as a result of the induction of the Cpx signaling cascade (Kohanski, Dwyer & Collins, 2010; Mahoney & Silhavy, 2013). Interestingly, further experiments found instead that the *E. coli cpxA** strain (which was previously shown to constitutively activate the Cpx response) was able to promote antibiotic resistance against aminoglycoside antibiotics (AGAs: amikacin, gentamycin) and small molecules that are toxic to the cells, such as hydroxyurea (HU), via the constant phosphorylation of CpxR, so the system would rather work to shield bacteria in the presence of these harmful substances in the environment (Hirakawa et al., 2003; Mahoney & Silhavy, 2013).

In contrast, this protective effect was not observed when β-lactam antibiotics (ampicillin) or fluoroquinolones (norfloxacin) were present in the media, strongly suggesting that the killing effect of different bactericidal antibiotics may not occur through a unique shared mechanism (Mahoney & Silhavy, 2013).

Although the Cpx pathway is commonly related to genes involved in alleviating envelope stress via correct protein folding and degradation, various other genes with diverse functions are also affected by its regulation. For example, Cpx is involved in pathogenesis by affecting the adhesion process via NlpE and the assembly of pilus and flagella required for attachment, motility and ultimately colonization (Nevesinjac & Raivio, 2005). During pathogenesis of *E. coli,* the Cpx response has been studied by using *ΔcpxR* mutants, triggering a defect in the fabrication of Pap pilus in laboratory strains carrying a plasmid with all of the P pilus genes for construction, thus creating shorter pili. In EPEC, the same null mutation diminished the production of bundle forming pilus and specific adherence, disrupting the first step that EPEC requires for colonization and infection (MacRitchie, Ward, Nevesinjac & Raivio, 2008; Nevesinjac & Raivio, 2005; Vogt et al., 2010).

Additionally, inner membrane transport changes ensued upon Cpx induction in *E. coli cpxA** mutants, resulting in decreased intake of proline and lactose (Raivio, 2014). During response activation, transporters in the envelope were observed to be the most downregulated gene category, likely with the purpose of preserving or rerouting energy toward other cell processes. Another consequence of the Cpx pathway initiation is the reduced transcription of genes encoding for the succinate and NADH dehydrogenases, as well as the cytochrome b_o oxidase of the electron transport chain (ETC) (Raivio et al., 2013). Recent studies in EPEC that specifically focused on the *nuo* and *cyo* operons confirmed the repression of the NADH dehydrogenase I and cytochrome

bo₃ respiratory complexes respectively, after activation of the Cpx response through *nlpE* overexpression (Guest, Wang, Wong & Raivio, 2017). Analyzing all these cellular alterations collectively, it would be predicted that they can lead to decreased respiration. This was also proven to occur in a *cpxA** EPEC strain and surprisingly, even more in a null *cpxRA* strain. Such observation was potentially explained by the need for the presence of CpxRA to mediate proper folding and degradation of already formed aberrant complexes, allowing for respiration to occur normally (Guest, et al., 2017; Raivio, 2014).

1.6 Research objectives

The mechanism by which the $CpxA_{SD}$ in *E. coli* detects and transduces inducing environmental stimuli affecting the bacterial envelope is still not completely understood. Furthermore, it is also unknown whether the recently discovered amino acid residues forming the exposed charged patches at the $CpxA_{SD}$ surface and the M_{48} at the centre of the dimerization interface (Figure 1-4) play a role in the interaction with other charged partners in the pathway (mainly CpxP, Figure 1-5) or in its structural stability, and if so, how important such role may be.

This work sought to expand on the information regarding the $CpxA_{SD}$ and CpxP structural characteristics that potentially allow for them to physically interact and mediate the active/inactive states of the pathway. It is based on the use of specific structure-guided site-directed mutational analysis of select surface-exposed charged amino acid residues. These were previously identified on the $CpxA_{SD}$ and CpxP structures and electrostatic surface representations. Additional phenotypic, biochemical and genetic approaches (using reporter genes) were also used to dissect

Cpx signaling events related to the $CpxA_{SD}$ and its proposed interaction with CpxP, through four main objectives:

1. To determine the phenotypic effect(s), if any, of lysine (negative to positive charge swaps) or alanine (negative to nonpolar hydrophobic swaps) substitutions in the $CpxA_{SD}$ E_{37}, D_{40}, E_{91}, D_{113} and E_{138} (plus M_{48} at the centre of the dimer) amino acid residues under different pH conditions, as well as their response to pathway inhibition or induction after *cpxP* or *nlpE* overexpression, respectively.

2. To determine the correct protein production and stability of the $CpxA_{SD}$ mutated strains compared to the wild-type, *cpxA*-null, *cpxA* complemented and vector control strains, through SDS-PAGE coupled with Western Blot analysis.

3. To determine whether second-site suppressor experiments using glutamate (positive to negative charge swaps) substitutions of the R_{56}, R_{60}, R_{67} and R_{139} residues on the CpxP concave surface can complement lysine substitutions in the $CpxA_{SD}$.

4. Finally, to obtain further evidence on the $CpxA_{SD}$:CpxP protein-protein interaction by means of utilizing a novel UV-induced photo cross-linking *in vivo* assay.

1.7 Figures

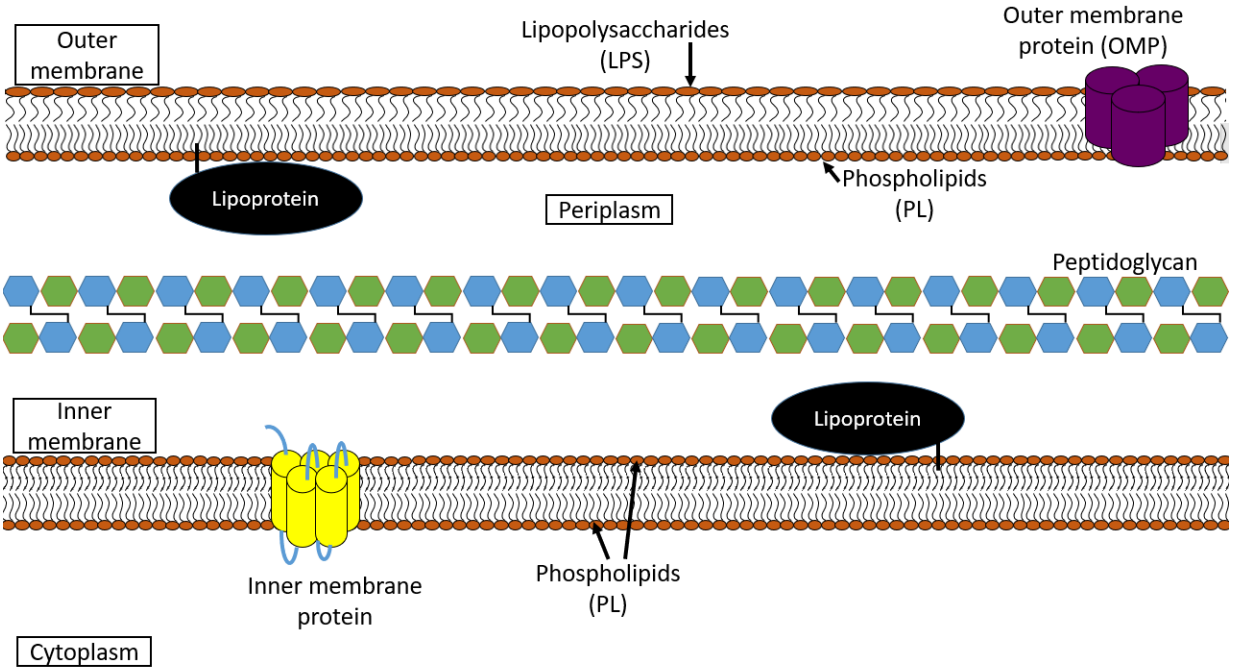

Figure 1-1: **Composition of the Gram-negative cell envelope.** The envelope of Gram-negative bacteria is formed by the externally-located outer membrane (OM), the inner membrane encompassing the cytoplasm (IM, also known as the cytoplasmic membrane), and the periplasmic space (or periplasm, PP) containing a layer of peptidoglycan (PG) localized in between the two mentioned membranes. Figure adapted from Ruiz et al., 2006.

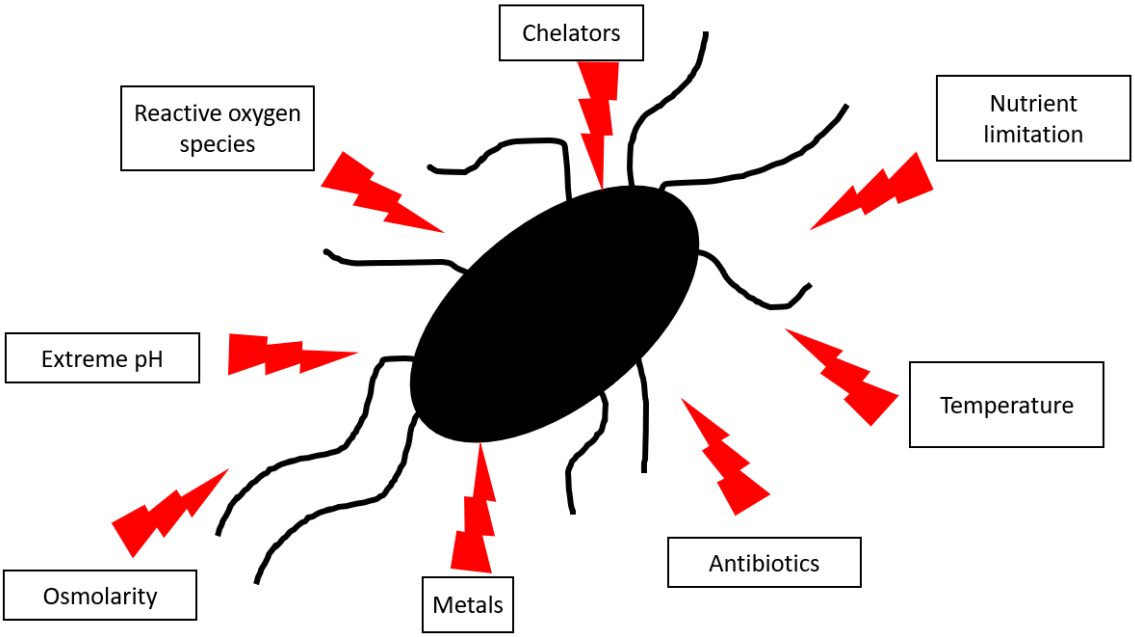

Figure 1-2: **Potential environmental stresses encountered by Gram-negative diarrheal pathogens.** During colonization and infection, Gram-negative diarrheal pathogens may encounter diverse environmental stresses that cause specific disruptions to their cell envelope. These include physical, chemical and biological conditions. Figure adapted from Runkel et al., 2013.

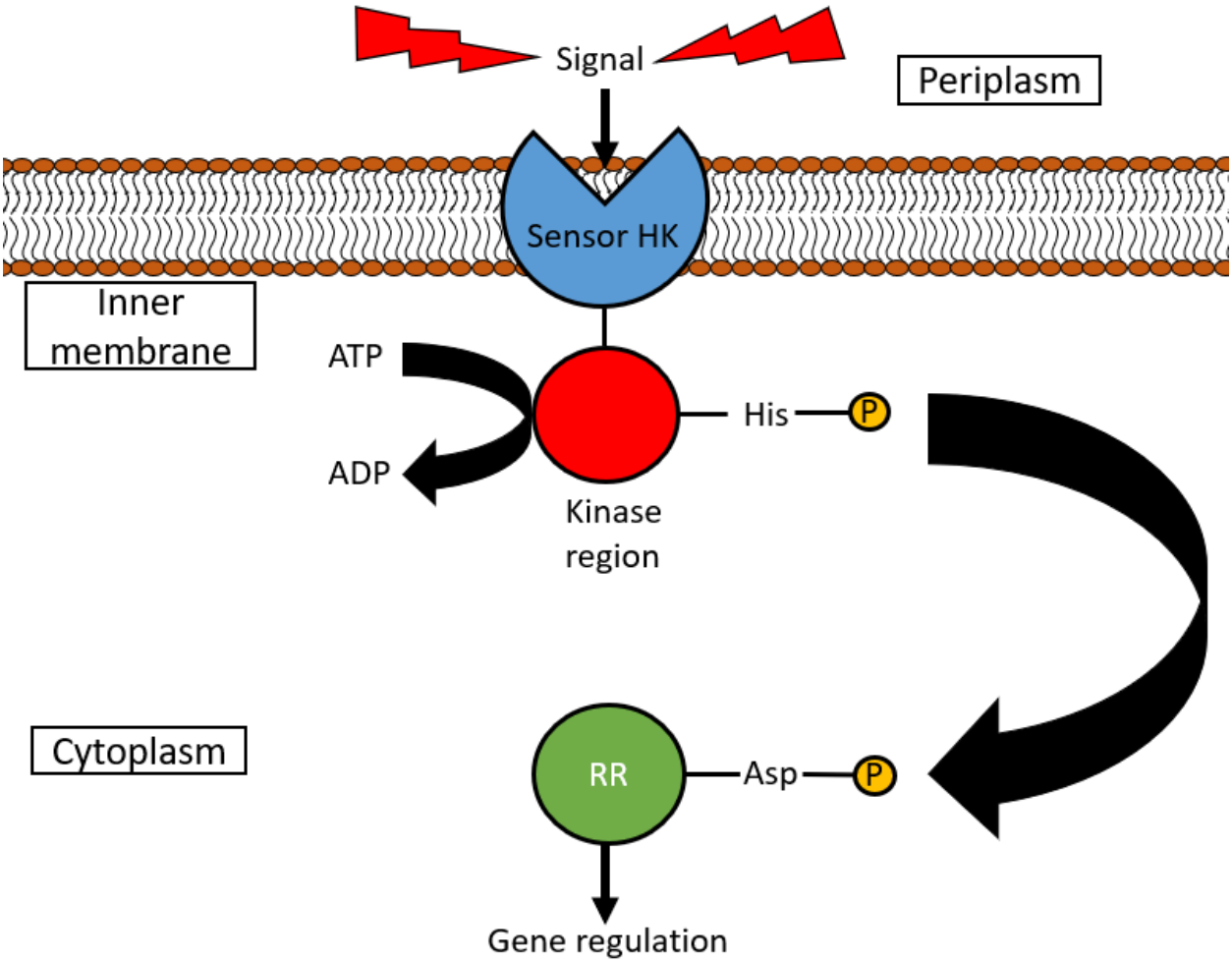

Figure 1-3: Prototypical organization of TCSTs formed by a transmembrane sensor HK and a cytosolic RR. In general, the pathway begins with a HK sensor domain detecting signals. This leads to its dimerization and a histidine amino acid residue (His) within the dimer interface being phosphorylated (autophosphorylation). The phosphate attached to the histidine residue is subsequently transferred to a conserved aspartate amino acid residue (Asp) on the RR, (phosphorylation). The now phosphorylated RR oversees the mounting an adequate response by means of regulation of downstream targets. Figure adapted from Bretl et al., 2011.

A.

B.

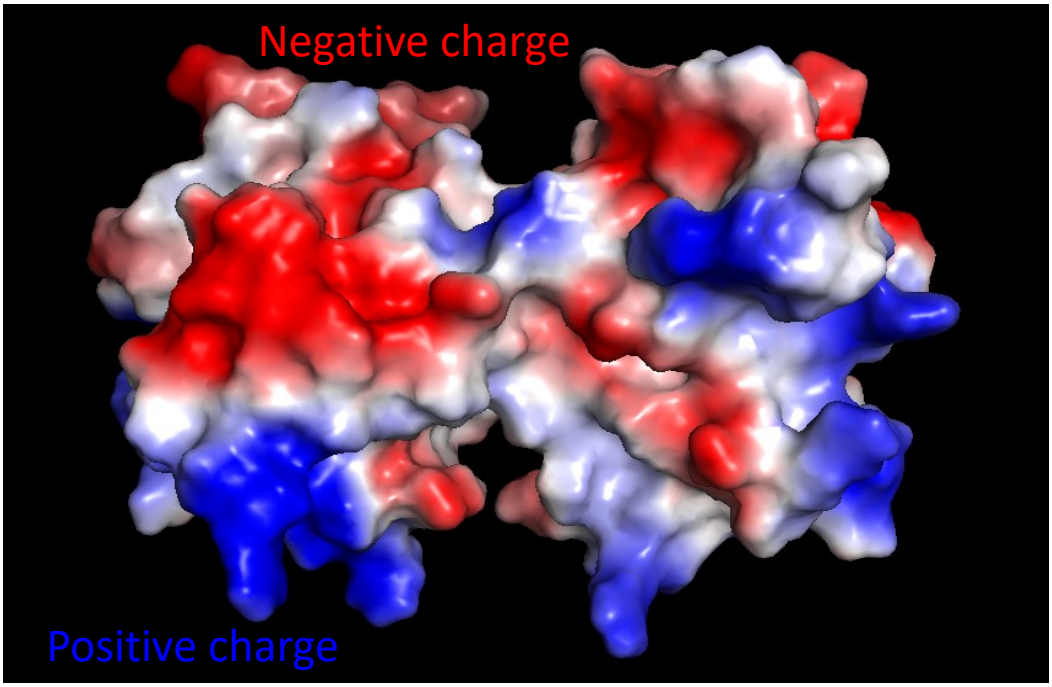

Figure 1-4: (A) Crystal structure and (B) electrostatic surface representation of the soluble $CpxA_{SD}$ of *E. coli*. (A) The $CpxA_{SD}$ of *E. coli* is comprised of 150 amino acid residues and displays a mixed αβ dimer. **(B)** Various surface-exposed charged aggregates of amino acid residues are highlighted.

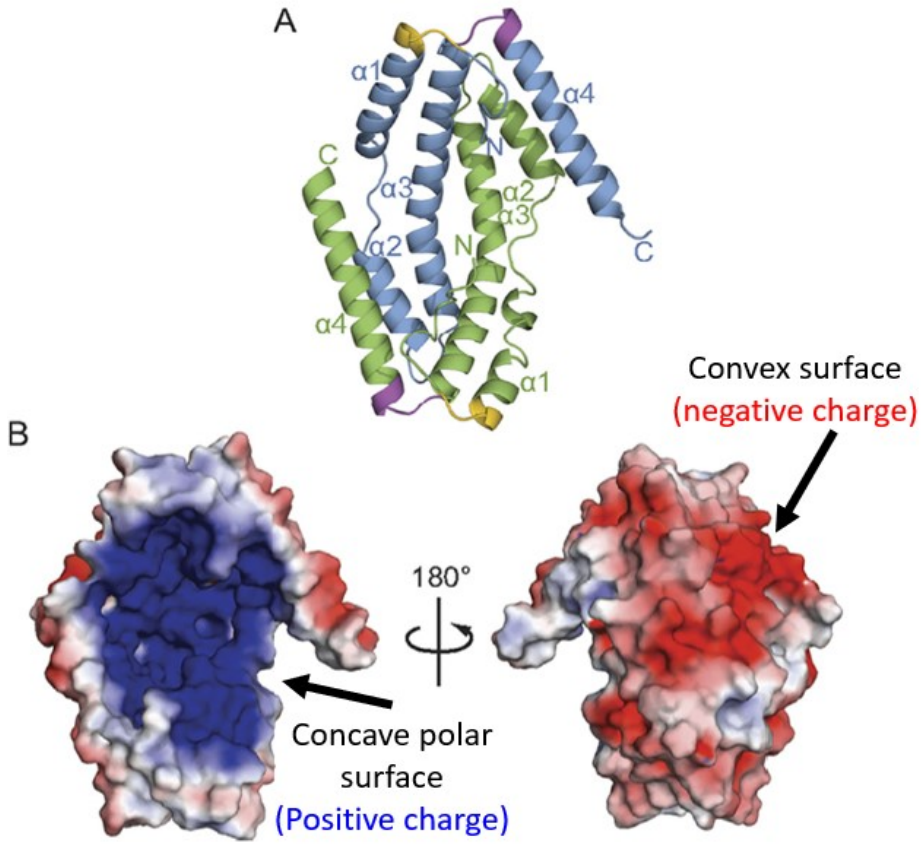

Figure 1-5: (A) Crystal structure and (B) electrostatic surface representation of the CpxP inhibitor in *E. coli*. (A) CpxP is a small accessory inhibitor/chaperone molecule found in the periplasm, comprised of 147 amino acid residues. It forms an antiparallel dimer of tangled α-helices with a highly basic concave bowl shape. **(B)** The concavity in the bowl's surface is composed by charged patches with predominantly positive amino acid residues, while the convex surface is negatively charged with a hydrophobic band Figure adapted from Thede et al., 2011.

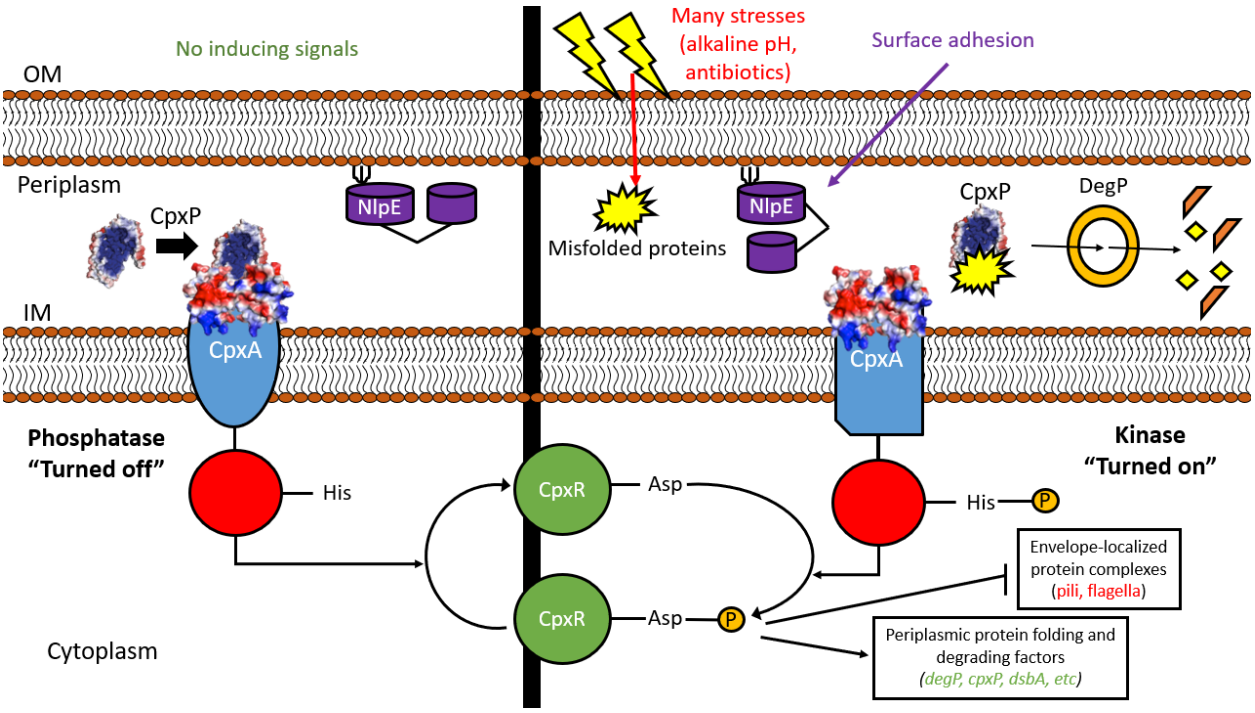

Figure 1-6: Overview of the Cpx ESR TCSTs in *E. coli*. Left side of the diagram displays pathway inactivation in absence of inducers; right side displays pathway activation after inducing signals are detected in the environment. Target genes upregulated by CpxR~P are indicated in green, and the ones downregulated can be observed in red. Figure adapted from Vogt & Raivio, 2012.

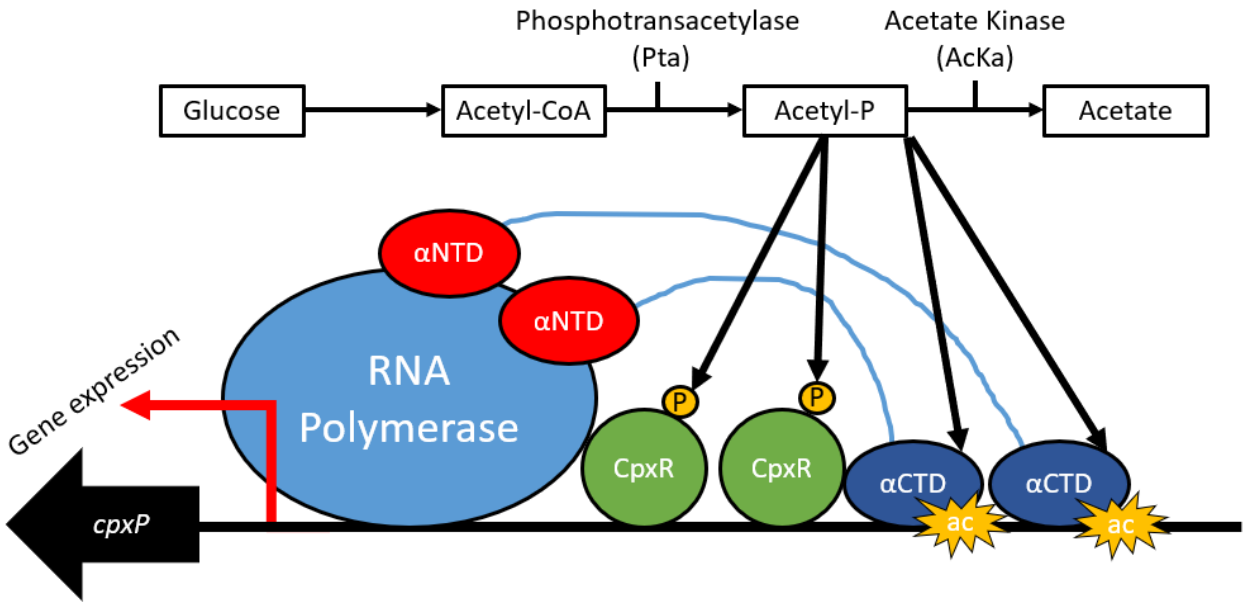

Figure 1-7: Cytoplasmic direct phosphorylation and acetylation of CpxR. In specific situations, CpxR can be directly phosphorylated in the absence of CpxA by the transfer of a phosphate group from the small molecule Ac~P. Alternatively, acetylation of the alpha C-terminal domains on the RNAP was linked to pathway activation and *cpxP* induction. Figure adapted from Lima et al., 2016.

1.8 References

Acosta, N., Pukatzki, S., & Raivio, T. L. (2015). The *Vibrio cholerae* Cpx envelope stress response senses and mediates adaptation to low iron. *Journal of Bacteriology*, *197*(2), 262–276. https://doi.org/10.1128/JB.01957-14

Aggarwal, P., Uppal, B., Ghosh, R., Prakash, S. K., & Rajeshwari, K. (2013). Highly-resistant *E. coli* as a common cause of paediatric diarrhoea in India. *Journal of Health, Population, and Nutrition, 31*(3), 409-412.

Alba, B. M., & Gross, C. A. (2004). Regulation of the *Escherichia coli* sigma-dependent envelope stress response. *Molecular Microbiology*, *52*(3), 613–619. https://doi.org/10.1111/j.1365-2958.2003.03982.x

Allen, W. J., Phan, G., & Waksman, G. (2012). Pilus biogenesis at the outer membrane of Gram-negative bacterial pathogens. *Current Opinion in Structural Biology*, *22*(4), 500–506. https://doi.org/10.1016/j.sbi.2012.02.001

Audrain, B., Ferrières, L., Zairi, A., Soubigou, G., Dobson, C., Coppée, J.-Y., … Ghigo, J.-M. (2013). Induction of the Cpx envelope stress pathway contributes to *Escherichia coli* tolerance to antimicrobial peptides. *Applied and Environmental Microbiology*, *79*(24), 7770–7779. https://doi.org/10.1128/AEM.02593-13

Batchelor, E., Walthers, D., Kenney, L. J., & Goulian, M. (2005). The *Escherichia coli* CpxA-CpxR envelope stress response system regulates expression of the porins ompF and ompC. *Journal of Bacteriology*, *187*(16), 5723–5731. https://doi.org/10.1128/JB.187.16.5723-5731.2005

Beier, D., & Gross, R. (2006). Regulation of bacterial virulence by two-component systems. *Current Opinion in Microbiology, 9*(2), 143-152. doi:10.1016/j.mib.2006.01.005

Bos, M. P., Robert, V., & Tommassen, J. (2007). Biogenesis of the Gram-Negative Bacterial Outer Membrane. *Annual Review of Microbiology*, *61*(1), 191–214. https://doi.org/10.1146/annurev.micro.61.080706.093245

Bretl, D. J., Demetriadou, C., & Zahrt, T. C. (2011). Adaptation to environmental stimuli within the host: two-component signal transduction systems of *Mycobacterium tuberculosis*. *Microbiology and Molecular Biology Reviews : MMBR*, *75*(4), 566–582. https://doi.org/10.1128/MMBR.05004-11

Buelow, D. R., & Raivio, T. L. (2005). Cpx signal transduction is influenced by a conserved N-terminal domain in the novel inhibitor CpxP and the periplasmic protease DegP. *Journal of Bacteriology*, *187*(19), 6622–6630. https://doi.org/10.1128/JB.187.19.6622-6630.2005

Buelow, D. R., & Raivio, T. L. (2010). Three (and more) component regulatory systems – auxiliary regulators of bacterial histidine kinases. *Molecular Microbiology, 75*(3), 547-566. doi:10.1111/j.1365-2958.2009.06982.x

Bury-Moné, S., Nomane, Y., Reymond, N., Barbet, R., Jacquet, E., Imbeaud, S., et al. (2009). Global analysis of extracytoplasmic stress signaling in *Escherichia coli*. *PLoS Genetics, 5*(9), e1000651. doi:10.1371/journal.pgen.1000651

Büttner, D. (2012). Protein export according to schedule: architecture, assembly, and regulation of type III secretion systems from plant- and animal-pathogenic bacteria. *Microbiology and Molecular Biology Reviews: MMBR*, *76*(2), 262–310. https://doi.org/10.1128/MMBR.05017-11

Cheng, A. C., McDonald, J. R., & Thielman, N. M. (2005). Infectious diarrhea in developed and developing countries. *Journal of Clinical Gastroenterology, 39*(9), 757-773. doi:00004836-200510000-00002 [pii]

Cheung, J., & Hendrickson, W. A. (2008). Crystal structures of C4-dicarboxylate ligand complexes with sensor domains of histidine kinases DcuS and DctB. *The Journal of Biological Chemistry*, *283*(44), 30256–30265. https://doi.org/10.1074/jbc.M805253200

Cheung, J., & Hendrickson, W. A. (2010). Sensor domains of two-component regulatory systems. *Current Opinion in Microbiology*, *13*(2), 116–123. https://doi.org/10.1016/j.mib.2010.01.016

Cheung, J., Bingman, C. A., Reyngold, M., Hendrickson, W. A., & Waldburger, C. D. (2008). Crystal structure of a functional dimer of the PhoQ sensor domain. *The Journal of Biological Chemistry*, *283*(20), 13762–13770. https://doi.org/10.1074/jbc.M710592200

Chevance, F. F. V., & Hughes, K. T. (2008). Coordinating assembly of a bacterial macromolecular machine. *Nature Reviews Microbiology*, *6*(6), 455–465. https://doi.org/10.1038/nrmicro1887

Cosma, C. L., Danese, P. N., Carlson, J. H., Silhavy, T. J., & Snyder, W. B. (1995). Mutational activation of the Cpx signal transduction pathway of *Escherichia coli* suppresses the toxicity conferred by certain envelope-associated stresses. *Molecular Microbiology*, *18*(3), 491–505.

Croxen, M. A., & Finlay, B. B. (2010). Molecular mechanisms of *Escherichia coli* pathogenicity. *Nature Reviews Microbiology*, *8*(1), 26–38. https://doi.org/10.1038/nrmicro2265

Dalbey, R. E., Wang, P., & Kuhn, A. (2011). Assembly of Bacterial Inner Membrane Proteins. *Annual Review of Biochemistry*, *80*(1), 161–187. https://doi.org/10.1146/annurev-biochem-060409-092524

Danese, P. N., Oliver, G. R., Barr, K., Bowman, G. D., Rick, P. D., & Silhavy, T. J. (1998). Accumulation of the enterobacterial common antigen lipid II biosynthetic intermediate stimulates *degP* transcription in *Escherichia coli*. *Journal of Bacteriology*, *180*(22), 5875–5884.

Danese, P. N., & Silhavy, T. J. (1997). The sigma(E) and the Cpx signal transduction systems control the synthesis of periplasmic protein-folding enzymes in *Escherichia coli*. *Genes & Development*, *11*(9), 1183–1193.

Danese, P. N., & Silhavy, T. J. (1998). CpxP, a stress-combative member of the Cpx regulon. *Journal of Bacteriology*, *180*(4), 831–839.

Danese, P. N., Snyder, W. B., Cosma, C. L., Davis, L. J., & Silhavy, T. J. (1995). The Cpx two-component signal transduction pathway of *Escherichia coli* regulates transcription of the gene specifying the stress-inducible periplasmic protease, DegP. *Genes & Development*, *9*(4), 387–398.

De Wulf, P., Kwon, O., & Lin, E. C. (1999). The CpxRA signal transduction system of *Escherichia coli*: growth-related autoactivation and control of unanticipated target operons. *Journal of Bacteriology*, *181*(21), 6772–6778.

Debnath, I., Norton, J. P., Barber, A. E., Ott, E. M., Dhakal, B. K., Kulesus, R. R., & Mulvey, M. A. (2013). The Cpx stress response system potentiates the fitness and virulence of uropathogenic *Escherichia coli*. *Infection and Immunity*, *81*(5), 1450–1459. https://doi.org/10.1128/IAI.01213-12

DiGiuseppe, P. A., & Silhavy, T. J. (2003). Signal detection and target gene induction by the CpxRA two-component system. *Journal of Bacteriology*, *185*(8), 2432–2440.

Dong, J., Iuchi, S., Kwan, H. S., Lu, Z., & Lin, E. C. (1993). The deduced amino-acid sequence of the cloned *cpxR* gene suggests the protein is the cognate regulator for the membrane sensor, CpxA, in a two-component signal transduction system of *Escherichia coli*. *Gene*, *136*(1–2), 227–230.

Dutta, R., Qin, L., & Inouye, M. (1999). Histidine kinases: diversity of domain organization. *Molecular Microbiology*, *34*(4), 633–640.

Eguchi, Y., & Utsumi, R. (2008). Introduction to bacterial signal transduction networks. In Utsumi, R. (Ed.), *Bacterial Signal Transduction: Networks and Drug Targets* (pp. 1-6). New York, NY: Springer New York. doi:10.1007/978-0-387-78885-2_1

Ehrmann, M. (2007). The periplasm. *ASM Press*, Washington, D.C., pp. 415.

Erhardt, M., Namba, K., & Hughes, K. T. (2010). Bacterial nanomachines: the flagellum and type III injectisome. *Cold Spring Harbor Perspectives in Biology*, *2*(11), a000299. https://doi.org/10.1101/cshperspect.a000299

Erickson, J. W., & Gross, C. A. (1989). Identification of the sigma E subunit of Escherichia coli RNA polymerase: a second alternate sigma factor involved in high-temperature gene expression. *Genes & Development*, *3*(9), 1462–1471.

Ferris, H. U., Dunin-Horkawicz, S., Hornig, N., Hulko, M., Martin, J., Schultz, J. E., … Coles, M. (2012). Mechanism of Regulation of Receptor Histidine Kinases. *Structure*, *20*(1), 56–66. https://doi.org/10.1016/j.str.2011.11.014

Fleischer, R., Heermann, R., Jung, K., & Hunke, S. (2007). Purification, reconstitution, and characterization of the CpxRAP envelope stress system of E*scherichia coli*. *The Journal of Biological Chemistry, 282*(12), 8583-8593. doi:M605785200 [pii]

Flores-Kim, J., & Darwin, A. J. (2014). Regulation of bacterial virulence gene expression by cell envelope stress responses. *Virulence, 5*(8), 835-851. doi:10.4161/21505594.2014.965580

Foussard, M., Cabantous, S., Pédelacq, J., Guillet, V., Tranier, S., Mourey, L., … Samama, J. (2001). The molecular puzzle of two-component signaling cascades. *Microbes and Infection*, *3*(5), 417–424.

Fronzes, R., Remaut, H., & Waksman, G. (2008). Architectures and biogenesis of non-flagellar protein appendages in Gram-negative bacteria. *The EMBO Journal*, *27*(17), 2271–2280. https://doi.org/10.1038/emboj.2008.155

Giltner, C. L., Nguyen, Y., & Burrows, L. L. (2012). Type IV pilin proteins: versatile molecular modules. *Microbiology and Molecular Biology Reviews: MMBR*, *76*(4), 740–772. https://doi.org/10.1128/MMBR.00035-12

Gotoh, Y., Eguchi, Y., Watanabe, T., Okamoto, S., Doi, A., & Utsumi, R. (2010). Two-component signal transduction as potential drug targets in pathogenic bacteria. *Current Opinion in Microbiology, 13*(2), 232-239. doi:10.1016/j.mib.2010.01.008

Guest, R. L., Wang, J., Wong, J. L., & Raivio, T. L. (2017). A Bacterial Stress Response Regulates Respiratory Protein Complexes To Control Envelope Stress Adaptation. *Journal of Bacteriology*, *199*(20), e00153-17. https://doi.org/10.1128/JB.00153-17

Guttman, J. A., & Finlay, B. B. (2008). Subcellular alterations that lead to diarrhea during bacterial pathogenesis. *Trends in Microbiology, 16*(11), 535-542. doi:10.1016/j.tim.2008.08.004

Henry, J. T., & Crosson, S. (2011). Ligand-binding PAS domains in a genomic, cellular, and structural context. *Annual Review of Microbiology*, *65*(1), 261–286. https://doi.org/10.1146/annurev-micro-121809-151631

Hill, D. R., & Beeching, N. J. (2010). Travelers' diarrhea. *Current Opinion in Infectious Diseases, 23*(5), 481-487. doi:10.1097/QCO.0b013e32833dfca5

Hirakawa, H., Nishino, K., Hirata, T., & Yamaguchi, A. (2003). Comprehensive studies of drug resistance mediated by overexpression of response regulators of two-component signal transduction systems in *Escherichia coli*. *Journal of Bacteriology*, *185*(6), 1851–1856.

Hirano, Y., Hossain, M. M., Takeda, K., Tokuda, H., & Miki, K. (2007). Structural studies of the Cpx pathway activator NlpE on the outer membrane of *Escherichia coli*. *Structure (London, England: 1993)*, *15*(8), 963–976. https://doi.org/10.1016/j.str.2007.06.014

Hodges, K., & Gill, R. (2010). Infectious diarrhea: Cellular and molecular mechanisms. *Gut Microbes, 1*(1), 4-21. doi:10.4161/gmic.1.1.11036

Hood, M. I., & Skaar, E. P. (2012). Nutritional immunity: transition metals at the pathogen–host interface. *Nature Reviews Microbiology*, *10*(8), 525–537. https://doi.org/10.1038/nrmicro2836

Hörnschemeyer, P., Liss, V., Heermann, R., Jung, K., & Hunke, S. (2016). Interaction Analysis of a Two-Component System Using Nanodiscs. *PloS One*, *11*(2), e0149187. https://doi.org/10.1371/journal.pone.0149187

Imamovic, L., Martínez-Castillo, A., Benavides, C., & Muniesa, M. (2015). BaeSR, involved in envelope stress response, protects against lysogenic conversion by Shiga toxin 2-encoding phages. *Infection and Immunity*, *83*(4), 1451–1457. https://doi.org/10.1128/IAI.02916-14

Isaac, D. D., Pinkner, J. S., Hultgren, S. J., & Silhavy, T. J. (2005). The extracytoplasmic adaptor protein CpxP is degraded with substrate by DegP. *Proceedings of the National Academy*

of Sciences of the United States of America, *102*(49), 17775–17779. https://doi.org/10.1073/pnas.0508936102

Ito, K., & Inaba, K. (2008). The disulfide bond formation (Dsb) system. *Current Opinion in Structural Biology*, *18*(4), 450–8. https://doi.org/10.1016/j.sbi.2008.02.002

Kamio, Y., & Nikaido, H. (1976). Outer membrane of *Salmonella typhimurium*: accessibility of phospholipid head groups to phospholipase C and cyanogen bromide activated dextran in the external medium. *Biochemistry,* (15), 2561-2570.

Karimova, G., Dautin, N., & Ladant, D. (2005). Interaction network among *Escherichia coli* membrane proteins involved in cell division as revealed by bacterial two-hybrid analysis. *Journal of Bacteriology*, *187*(7), 2233–2243. https://doi.org/10.1128/JB.187.7.2233-2243.2005

Kato, M., Mizuno, T., Shimizu, T., & Hakoshima, T. (1997). Insights into multistep phosphorelay from the crystal structure of the C-terminal HPt domain of ArcB. *Cell*, *88*(5), 717–723.

Kato, M., Mizuno, T., Shimizu, T., & Hakoshima, T. (1999). Refined structure of the histidine-containing phosphotransfer (HPt) domain of the anaerobic sensor kinase ArcB from *Escherichia coli* at 1.57 A resolution. *Acta Crystallographica. Section D, Biological Crystallography*, *55*(Pt 11), 1842–1849.

Kim, D., & Forst, S. (2001). Genomic analysis of the histidine kinase family in bacteria and archaea. *Microbiology (Reading, England)*, *147*(Pt 5), 1197–1212. https://doi.org/10.1099/00221287-147-5-1197

Kirby, J. R. (2009). Chemotaxis-Like Regulatory Systems: Unique Roles in Diverse Bacteria. *Annual Review of Microbiology*, *63*(1), 45–59. https://doi.org/10.1146/annurev.micro.091208.073221

Klein, A. H., Shulla, A., Reimann, S. A., Keating, D. H., & Wolfe, A. J. (2007). The intracellular concentration of acetyl phosphate in *Escherichia coli* is sufficient for direct phosphorylation of two-component response regulators. *Journal of Bacteriology*, *189*(15), 5574–5581. https://doi.org/10.1128/JB.00564-07

Kohanski, M. A., Dwyer, D. J., & Collins, J. J. (2010). How antibiotics kill bacteria: from targets to networks. *Nature Reviews Microbiology*, *8*(6), 423–435. https://doi.org/10.1038/nrmicro2333

Kosek, M., Bern, C., & Guerrant, R. L. (2003). The global burden of diarrhoeal disease, as estimated from studies published between 1992 and 2000. *Bulletin of the World Health Organization, 81*(3), 197-204. doi:S0042-96862003000300010 [pii]

Kwon, E., Kim, D. Y., Ngo, T. D., Gross, C. A., Gross, J. D., & Kim, K. K. (2012). The crystal structure of the periplasmic domain of *Vibrio parahaemolyticus* CpxA. *Protein Science : A Publication of the Protein Society*, *21*(9), 1334–1343. https://doi.org/10.1002/pro.2120

Laub, M.T. (2011). The Role of Two-Component Signal Transduction Systems in Bacterial Stress Responses p. 45-58. In Storz, G., & Hengge, R. (Ed.), *Bacterial Stress Responses*, 2nd ed. ASM Press, c2011, Washington, DC.

Leblanc, S. K. D., Oates, C. W., & Raivio, T. L. (2011). Characterization of the induction and cellular role of the BaeSR two-component envelope stress response of *Escherichia coli*. *Journal of Bacteriology*, *193*(13), 3367–3375. https://doi.org/10.1128/JB.01534-10

Lima, B. P., Antelmann, H., Gronau, K., Chi, B. K., Becher, D., Brinsmade, S. R., & Wolfe, A. J. (2011). Involvement of protein acetylation in glucose-induced transcription of a stress-responsive promoter. *Molecular Microbiology*, *81*(5), 1190–1204. https://doi.org/10.1111/j.1365-2958.2011.07742.x

Lima, B. P., Lennon, C. W., Ross, W., Gourse, R. L., & Wolfe, A. J. (2016). *In vitro* evidence that RNA Polymerase acetylation and acetyl phosphate-dependent CpxR phosphorylation affect *cpxP* transcription regulation. *FEMS Microbiology Letters*, *363*(5), fnw011. https://doi.org/10.1093/femsle/fnw011

Lin, M.-F., Lin, Y.-Y., & Lan, C.-Y. (2015). The Role of the Two-Component System BaeSR in Disposing Chemicals through Regulating Transporter Systems in *Acinetobacter baumannii*. *PloS One*, *10*(7), e0132843. https://doi.org/10.1371/journal.pone.0132843

Luirink, J., von Heijne, G., Houben, E., & de Gier, J. W. (2005). Biogenesis of inner membrane proteins in *Escherichia coli*. *Annual Review of Microbiology*, *59*, 329–355. https://doi.org/10.1146/annurev.micro.59.030804.121246

MacRitchie, D. M., Acosta, N., & Raivio, T. L. (2012). DegP is involved in Cpx-mediated posttranscriptional regulation of the type III secretion apparatus in enteropathogenic *Escherichia coli*. *Infection and Immunity*, *80*(5), 1766–1772. https://doi.org/10.1128/IAI.05679-11

MacRitchie, D. M., Buelow, D. R., Price, N. L., & Raivio, T. L. (2008). Two-component signaling and Gram negative envelope stress response systems. In Utsumi, R. (Ed.), *Bacterial Signal Transduction: Networks and Drug Targets* (pp. 80-110). New York, NY: Springer New York. doi:10.1007/978-0-387-78885-2_6

MacRitchie, D. M., Ward, J. D., Nevesinjac, A. Z., & Raivio, T. L. (2008). Activation of the Cpx envelope stress response down-regulates expression of several locus of enterocyte effacement-encoded genes in enteropathogenic *Escherichia coli*. *Infection and Immunity*, *76*(4), 1465–1475. https://doi.org/10.1128/IAI.01265-07

Mahoney, T. F., & Silhavy, T. J. (2013). The Cpx Stress Response Confers Resistance to Some, but Not All, Bactericidal Antibiotics. *Journal of Bacteriology*, *195*(9), 1869–1874. https://doi.org/10.1128/JB.02197-12

Margain-Quevedo, R., Malpica, R., Thede, G. L., Lu, J., Glover, J. N. M., & Raivio, T. L. (In preparation). Modulation of the Cpx Envelope Stress Response in *Escherichia coli* by the CpxA Periplasmic Sensing Domain and its Interaction with CpxP. *Manuscript in preparation.*

McBroom, A. J., & Kuehn, M. J. (2007). Release of outer membrane vesicles by Gram-negative bacteria is a novel envelope stress response. *Molecular Microbiology*, 63(2), 545–558. https://doi.org/10.1111/j.1365-2958.2006.05522.x

McEwen, J., & Silverman, P. (1980). Chromosomal mutations of *Escherichia coli* that alter expression of conjugative plasmid functions. *Proceedings of the National Academy of Sciences of the United States of America, 77*(1), 513-517.

McEwen, J., & Silverman, P. M. (1982). Mutations in genes cpxA and cpxB alter the protein composition of *Escherichia coli* inner and outer membranes. *Journal of Bacteriology*, *151*(3), 1553–1559.

Mechaly, A. E., Sassoon, N., Betton, J.-M., & Alzari, P. M. (2014). Segmental helical motions and dynamical asymmetry modulate histidine kinase autophosphorylation. *PLoS Biology*, 12(1), e1001776. https://doi.org/10.1371/journal.pbio.1001776

Merdanovic, M., Clausen, T., Kaiser, M., Huber, R., & Ehrmann, M. (2011). Protein Quality Control in the Bacterial Periplasm. *Annual Review of Microbiology*, *65*(1), 149–168. https://doi.org/10.1146/annurev-micro-090110-102925

Mileykovskaya, E., & Dowhan, W. (1997). The Cpx two-component signal transduction pathway is activated in *Escherichia coli* mutant strains lacking phosphatidylethanolamine. *Journal of Bacteriology*, *179*(4), 1029–1034.

Mourey, L., Da Re, S., Pédelacq, J.-D., Tolstykh, T., Faurie, C., Guillet, V., … Samama, J.-P. (2001). Crystal Structure of the CheA Histidine Phosphotransfer Domain that Mediates Response Regulator Phosphorylation in Bacterial Chemotaxis. *Journal of Biological Chemistry*, *276*(33), 31074–31082. https://doi.org/10.1074/jbc.M101943200

Mullineaux, C. W., Nenninger, A., Ray, N., & Robinson, C. (2006). Diffusion of Green Fluorescent Protein in Three Cell Environments in *Escherichia Coli*. *Journal of Bacteriology*, *188*(10), 3442–3448. https://doi.org/10.1128/JB.188.10.3442-3448.2006

Nevesinjac, A. Z., & Raivio, T. L. (2005). The Cpx envelope stress response affects expression of the type IV bundle-forming pili of enteropathogenic *Escherichia coli*. *Journal of Bacteriology*, *187*(2), 672–686. https://doi.org/10.1128/JB.187.2.672-686.2005

Nguyen, T. V., Le, P. V., Le, C. H., & Weintraub, A. (2005). Antibiotic resistance in diarrheagenic *Escherichia coli* and *Shigella* strains isolated from children in Hanoi, Vietnam. *Antimicrobial Agents and Chemotherapy, 49*(2), 816-819. doi:49/2/816 [pii]

Nikaido, H., & Vaara, M. (1987). Outer membrane. In: Neidhardt FC et al., (Eds), *Escherichia coli and Salmonella: cellular and molecular biology.* ASM Press, Washington, D.C., pp. 7-22.

Notti, R. Q., & Stebbins, C. E. (2016). The Structure and Function of Type III Secretion Systems. *Microbiology Spectrum*, *4*(1). https://doi.org/10.1128/microbiolspec.VMBF-0004-2015

Okuda, S., & Tokuda, H. (2011). Lipoprotein Sorting in Bacteria. *Annual Review of Microbiology*, *65*(1), 239–259. https://doi.org/10.1146/annurev-micro-090110-102859

Otto, K., & Silhavy, T. J. (2002). Surface sensing and adhesion of *Escherichia coli* controlled by the Cpx-signaling pathway. *Proceedings of the National Academy of Sciences of the United States of America*, *99*(4), 2287–2292. https://doi.org/10.1073/pnas.042521699

Pogliano, J., Lynch, A. S., Belin, D., Lin, E. C., & Beckwith, J. (1997). Regulation of *Escherichia coli* cell envelope proteins involved in protein folding and degradation by the Cpx two-component system. *Genes & Development*, *11*(9), 1169–1182.

Price, N. L., & Raivio, T. L. (2009). Characterization of the Cpx regulon in *Escherichia coli* strain MC4100. *Journal of Bacteriology*, *191*(6), 1798–815. https://doi.org/10.1128/JB.00798-08

Quan, S., Koldewey, P., Tapley, T., Kirsch, N., Ruane, K. M., Pfizenmaier, J., … Bardwell, J. C. A. (2011). Genetic selection designed to stabilize proteins uncovers a chaperone called Spy. *Nature Structural & Molecular Biology*, *18*(3), 262–269. https://doi.org/10.1038/nsmb.2016

Raetz, C. R. H., & Dowhan, W. (1990). Biosynthesis and function of phospholipids in *Escherichia coli*. *Journal of Biological Chemistry*, *265*(3), 1235-1238.

Raetz, C. R. H., & Whitfield, C. (2002). Lipopolysaccharide endotoxins. *Annual Review of Biochemistry, 71*, 635-700. doi:10.1146/annurev.biochem.71.110601.135414

Raffa, R. G., & Raivio, T. L. (2002). A third envelope stress signal transduction pathway in *Escherichia coli*. *Molecular Microbiology*, *45*(6), 1599–611. Raivio, T. L., & Silhavy, T. J. (2001). Periplasmic Stress and ECF Sigma Factors. *Annual Review of Microbiology*, *55*(1), 591–624. https://doi.org/10.1146/annurev.micro.55.1.591

Raivio, T. L. (2014). Everything old is new again: an update on current research on the Cpx envelope stress response. *Biochimica et Biophysica Acta*, *1843*(8), 1529–1541. https://doi.org/10.1016/j.bbamcr.2013.10.018

Raivio, T. L., & Silhavy, T. J. (1997). Transduction of envelope stress in *Escherichia coli* by the Cpx two-component system. *Journal of Bacteriology*, *179*(24), 7724–7733. https://doi.org/10.1128/JB.179.24.7724-7733.

Raivio, T. L., Laird, M. W., Joly, J. C., & Silhavy, T. J. (2000). Tethering of CpxP to the inner membrane prevents spheroplast induction of the Cpx envelope stress response. *Molecular Microbiology, 37*(5), 1186-1197. doi:mmi2074 [pii]

Raivio, T. L., Leblanc, S. K. D., & Price, N. L. (2013). The *Escherichia coli* Cpx envelope stress response regulates genes of diverse function that impact antibiotic resistance and membrane integrity. *Journal of Bacteriology*, *195*(12), 2755–2767. https://doi.org/10.1128/JB.00105-13

Raivio, T. L., Popkin, D. L., & Silhavy, T. J. (1999). The Cpx envelope stress response is controlled by amplification and feedback inhibition. *Journal of Bacteriology*, *181*(17), 5263–5272.

Ruiz, N., Kahne, D., & Silhavy, T. J. (2006). Advances in understanding bacterial outer-membrane biogenesis. *Nature Reviews Microbiology, 4*(1), 57-66. doi:nrmicro1322 [pii]

Runkel, S., Wells, H. C., & Rowley, G. (2013). Living with stress: A lesson from the enteric pathogen *Salmonella enterica*. *Advances in Applied Microbiology*, 83, 87-144. https://doi.org/10.1016/B978-0-12-407678-5.00003-9

Schwechheimer, C., & Kuehn, M. J. (2015). Outer-membrane vesicles from gram-negative bacteria: Biogenesis and functions. *Nature Reviews Microbiology, 13*(10), 605-619. doi:10.1038/nrmicro3525

Sevier, C. S., & Kaiser, C. A. (2002). Formation and transfer of disulphide bonds in living cells. *Nature Reviews Molecular Cell Biology*, *3*(11), 836–847. https://doi.org/10.1038/nrm954

Sevvana, M., Vijayan, V., Zweckstetter, M., Reinelt, S., Madden, D. R., Herbst-Irmer, R., … Becker, S. (2008). A ligand-induced switch in the periplasmic domain of sensor histidine kinase CitA. *Journal of Molecular Biology*, *377*(2), 512–23. https://doi.org/10.1016/j.jmb.2008.01.024

Silhavy, T. J., Kahne, D., & Walker, S. (2010). The bacterial cell envelope. *Cold Spring Harbor Perspectives in Biology, 2*(5), a000414. doi:10.1101/cshperspect.a000414

Snyder, W. B., Davis, L. J., Danese, P. N., Cosma, C. L., & Silhavy, T. J. (1995). Overproduction of NlpE, a new outer membrane lipoprotein, suppresses the toxicity of periplasmic LacZ by activation of the Cpx signal transduction pathway. *Journal of Bacteriology*, *177*(15), 4216–4223.

Stephenson, K., & Hoch, J. A. (2002). Two-component and phosphorelay signal-transduction systems as therapeutic targets. *Current Opinion in Pharmacology, 2*(5), 507-512. doi:S1471489202001947 [pii]

Stephenson, K., & Hoch, J. A. (2004). Developing inhibitors to selectively target two-component and phosphorelay signal transduction systems of pathogenic microorganisms. *Current Medicinal Chemistry, 11*(6), 765-773.

Stock, A. M., Robinson, V. L., & Goudreau, P. N. (2000). Two-component signal transduction. *Annual Review of Biochemistry*, *69*(1), 183–215. https://doi.org/10.1146/annurev.biochem.69.1.183

Thanassi, D. G., Bliska, J. B., & Christie, P. J. (2012). Surface organelles assembled by secretion systems of Gram-negative bacteria: diversity in structure and function. *FEMS Microbiology Reviews*, *36*(6), 1046–1082. https://doi.org/10.1111/j.1574-6976.2012.00342.x

Thapar, N., & Sanderson, I. R. (2004). Diarrhoea in children: An interface between developing and developed countries. *Lancet (London, England), 363*(9409), 641-653. doi:10.1016/S0140-6736(04)15599-2

Thede, G. L., Arthur, D. C., Edwards, R. A., Buelow, D. R., Wong, J. L., Raivio, T. L., & Glover, J. N. M. (2011). Structure of the periplasmic stress response protein CpxP. *Journal of Bacteriology, 193*(9), 2149-2157. doi:10.1128/JB.01296-10

Tokuda, H., & Matsuyama, S. I. (2004). Sorting of lipoproteins to the outer membrane in *E. coli*. *Biochimica et Biophysica Acta - Molecular Cell Research*, *1693*(1), 5-13. https://doi.org/10.1016/j.bbamcr.2004.02.005

Tomomori, C., Tanaka, T., Dutta, R., Park, H., Saha, S. K., Zhu, Y., … Ikura, M. (1999). Solution structure of the homodimeric core domain of *Escherichia coli* histidine kinase EnvZ. *Nature Structural Biology*, *6*(8), 729–734. https://doi.org/10.1038/11495

Tschauner, K., Hörnschemeyer, P., Müller, V. S., & Hunke, S. (2014). Dynamic interaction between the CpxA sensor kinase and the periplasmic accessory protein CpxP mediates signal recognition in *E. coli*. *PloS One*, *9*(9), e107383. https://doi.org/10.1371/journal.pone.0107383

Van Dalen, A., & de Kruijff, B. (2004). The role of lipids in membrane insertion and translocation of bacterial proteins. *Biochimica et Biophysica Acta (BBA) - Molecular Cell Research*, *1694*(1–3), 97–109. https://doi.org/10.1016/j.bbamcr.2004.03.007

Van Wielink, J. E., & Duine, J. A. (1990). How big is the periplasmic space? *Trends in Biochemical Sciences*, *15*(4), 136–7.

Viswanathan, V. K., Hodges, K., & Hecht, G. (2009). Enteric infection meets intestinal function: How bacterial pathogens cause diarrhoea. *Nature Reviews Microbiology, 7*(2), 110-119. doi:10.1038/nrmicro2053

Vogt, S. L., & Raivio, T. L. (2012). Just scratching the surface: An expanding view of the cpx envelope stress response. *FEMS Microbiology Letters, 326*(1), 2-11. doi:10.1111/j.1574-6968.2011.02406.x

Vogt, S. L., Nevesinjac, A. Z., Humphries, R. M., Donnenberg, M. S., Armstrong, G. D., & Raivio, T. L. (2010). The Cpx envelope stress response both facilitates and inhibits elaboration of the enteropathogenic *Escherichia coli* bundle-forming pilus. *Molecular Microbiology*, *76*(5), 1095–1110. https://doi.org/10.1111/j.1365-2958.2010.07145.x

Vogt, S., Acosta, N., Wong, J., Wang, J., & Raivio, T. L. (2012). The CpxAR Two-component System Regulates a Complex Envelope Stress Response in Gram-negative Bacteria. In Gross, R., & Beier, D. (Ed.), *Two-Component Systems in Bacteria* (pp. 231–267). UK: Caister Academic Press.

Weber, R. F., & Silverman, P. M. (1988). The Cpx proteins of *Escherichia coli* K12. Structure of the CpxA polypeptide as an inner membrane component. *Journal of Molecular Biology*, *203*(2), 467–478.

West, A. H., & Stock, A. M. (2001). Histidine kinases and response regulator proteins in two-component signaling systems. *Trends in Biochemical Sciences*, *26*(6), 369–76.

Wolfe, A. J. (2005). The acetate switch. *Microbiology and Molecular Biology Reviews: MMBR*, *69*(1), 12–50. https://doi.org/10.1128/MMBR.69.1.12-50.2005

Wolfe, A. J. (2010). Physiologically relevant small phosphodonors link metabolism to signal transduction. *Current Opinion in Microbiology*, *13*(2), 204–209. https://doi.org/10.1016/j.mib.2010.01.002

Wolfe, A. J., Parikh, N., Lima, B. P., & Zemaitaitis, B. (2008). Signal Integration by the Two-Component Signal Transduction Response Regulator CpxR. *Journal of Bacteriology*, *190*(7), 2314–2322. https://doi.org/10.1128/JB.01906-07

Wuichet, K., Cantwell, B. J., & Zhulin, I. B. (2010). Evolution and phyletic distribution of two-component signal transduction systems. *Current Opinion in Microbiology*, *13*(2), 219–225. https://doi.org/10.1016/j.mib.2009.12.011

Xicohtencatl-Cortes, J., Monteiro-Neto, V., Ledesma, M. A., Jordan, D. M., Francetic, O., Kaper, J. B., … Girón, J. A. (2007). Intestinal adherence associated with type IV pili of enterohemorrhagic *Escherichia coli* O157:H7. *Journal of Clinical Investigation*, *117*(11), 3519–3529. https://doi.org/10.1172/JCI30727

Yamada, S., & Shiro, Y. (2008). Structural Basis of the Signal Transduction in the Two-Component System. In Utsumi, R. (Ed.), *Bacterial Signal Transduction: Networks and Drug Targets* (pp. 22–39). New York, NY: Springer New York. https://doi.org/10.1007/978-0-387-78885-2_3

Zhou, L., Lei, X.-H., Bochner, B. R., & Wanner, B. L. (2003). Phenotype microarray analysis of *Escherichia coli* K-12 mutants with deletions of all two-component systems. *Journal of Bacteriology*, *185*(16), 4956–4972.

Zhou, X., Keller, R., Volkmer, R., Krauss, N., Scheerer, P., & Hunke, S. (2011). Structural basis for two-component system inhibition and pilus sensing by the auxiliary CpxP protein. *The Journal of Biological Chemistry, 286*(11), 9805-9814. doi:10.1074/jbc.M110.194092

Chapter 2: Materials and Methods

2.1 Bacterial strains, media and growth conditions

The complete set of bacterial strains and plasmids utilized in the present study are listed in Table 2-1. All the mutated strains and plasmids were constructed through standard genetic approaches and techniques (Lu, Peng, Arutyunov, Frost & Glover, 2012; Sambrook, Fritsch & Maniatis, 1989; Silhavy, Berman & Enquist, 1984). Strains were maintained as 20% glycerol stocks of liquid cultures at -80°C until required for experimentation, at which point they were routinely grown in Luria Bertani broth - Lennox (conveniently referred to simply as "LB" for this study) composed of 1% tryptone (BD Bacto™ Biosciences), 0.5% yeast extract (BD Bacto™ Biosciences), and 0.5% NaCl (Sigma-Aldrich), unless otherwise stated. Liquid cultures were grown in large glass test tubes (16x125mm) under aerobic conditions at 37°C with constant shaking at 225 rpm inside a temperature-controlled shaker. Plated cultures were grown with aeriation inside a static incubator at 37°C, after 1.5% agar dissolved in LB broth was poured into plastic plates and left to solidify overnight at room temperature to prepare LB agar plates (stored in cold room at 4°C until required). Appropriate antibiotics (Sigma-Aldrich) were added to the growth media when needed, in the following concentrations: ampicillin (Amp), 100µg/mL; chloramphenicol (Cam), 25µg/mL; kanamycin (Kan) 50µg/mL.

Isopropyl-β-D-thiogalactopyranoside (IPTG) (Invitrogen) stocks at concentrations of 0.1M and 1M were kept in a -20°C freezer for storage and added into LB growth media to final concentrations of 0.1mM and 1mM (1:1000 dilutions) when needed. Liquid growth media at constant pH values for β-galactosidase assays was prepared by the addition of 1M monobasic (NaH_2PO_4) and/or 1M dibasic (Na_2HPO_4) sterile sodium-phosphate buffers (Sigma-Aldrich) at specific ratios into sterile LB media to a total of 100mL (a final concentration of 100mM): 9.21mL 1M NaH_2PO_4 + 790µL 1M Na_2HPO_4 + 90mL LB broth (pH 5.8); 4.23mL 1M NaH_2PO_4 + 5.77mL

1M Na_2HPO_4 + 90mL LB broth (pH 7.0); and 10mL 1M Na_2HPO_4 + 90mL LB broth (pH 8.0) (Danese & Silhavy, 1998; Raivio et al., 2013). The rest of the chemicals and reagents used for the experimental procedures described in the following subsections were purchased from Sigma-Aldrich, unless otherwise specified.

2.2 Reporter genes

A *cpxP'-lacZ*$^+$ transcriptional fusion was used as the reporter gene in β-galactosidase assays, to indirectly measure Cpx activity (Table 2-1). This gene was present in the chromosome of the *E. coli* laboratory strains utilized throughout this study, in single copy and integrated into the λRS88 site after λ phage recombination, as described elsewhere (Danese et al., 1995; Silhavy, Berman & Enquist, 1984; Simons, Houman & Kleckner, 1987). This transcriptional reporter encompassed DNA from approximately 200bp upstream of the transcription start site to 60bp within *cpxP* (Raivio & Silhavy, 1997).

2.3 Polymerase chain reaction (PCR) conditions

Unless otherwise specifically stated, PCR reactions were conducted using a master mix composed of the following (per 100µL, Invitrogen): 10µL 10X *Pfx* amplification buffer, 10µL 10X PCR_X enhancer solution, 2µL 50mM $MgSO_4$, 1.5µL 10mM dNTP mixture, 1µL (10pg-200ng) template DNA, 2µL 10µM forward primer, 2µL 10µM reverse primer, 1µL Platinum *Pfx* DNA polymerase, and 70.5µL autoclaved Milli-Q H_2O. The protocol consisted of an initial denaturation of 95°C (2 minutes) followed by 25-35 cycles of a 95°C denaturing step (15 seconds), an annealing step of variable temperature (30 seconds), and an extension step of either 68°C, 70°C or 72°C (1 minute per kb). PCR-amplified products were kept at 4°C until retrieved from thermocycler and

either stored at -20°C or purified with the QIAquick PCR purification kit (Qiagen) following manufacturer's instructions and analyzed by 1% agarose gel electrophoresis.

2.4 Plasmid construction and cloning

The *cpxA* gene was sub-cloned from the pCA24N-*cpxA*WT plasmid into two other cloning vectors: 1) the pK184 plasmid (Jobling & Holmes, 1999) (possessing desirable characteristics for subsequent site-directed mutagenesis assays, including: convenient multiple cloning site (MCS), an inducible leaky *lac* promoter, and low copy number) to obtain pK184-*cpxA*WT; and 2) pJ307 (pK184-*traJ*) (Lu, et al., 2012) to generate pJ307-*cpxA*WT and have it as a backup to pK184-*cpxA*WT for *cpxA* mutagenesis assays, in case the leaky lac promoter in pK184 lead to very high *cpxA* expression. Both plasmids were previously digested with *Eco*RI, followed by the addition of the Klenow fragment to change "sticky" ends into "blunt" ends (so that the *Eco*RI site found within *cpxA* was unique in the plasmid once the gene had been introduced and could be used for *cpxA* digestion and further PCR confirmation assays). Primers XA-1 (*cpxA* forward) and XA-2c (*cpxA* reverse) were designed based on the *cpxA*WT sequence and used for *cpxA* amplification and subsequent sub-cloning into the pK184 and pJ307 vectors (all primer sequences used in this study are listed in Table 2-2). pK184-*cpxA*WT was constructed by ligating the 2.4-kb *Bam*HI-*Hind*III fragment of pK184 to the 1.5-kb *Bam*HI-*Hind*III fragment of PCR-amplified DNA (*cpxA*) from pCA24N-*cpxA*WT. Additionally, the 1.5-kb *Bam*HI-*Hind*III fragment of the PCR-amplified *cpxA* from pCA24N-*cpxA*WT was ligated to the 3.2-kb *Bam*HI-*Hind*III fragment of pJ307, resulting in plasmid pJ307-*cpxA*WT (Lu et al., 2012; Sambrook, Fritsch & Maniatis, 1989). Correct *cpxA* insertion was verified by both expected size in agarose gel after restriction analysis and Sanger DNA Sequencing. Restriction enzymes utilized were purchased from Invitrogen.

2.5 Site-directed mutagenesis (overlap extension PCR)

The first three missense substitutions in *cpxA* ($E_{37}K$, $M_{48}K$ and $D_{113}K$) were generated as derivatives of plasmid pK184-*cpxA*WT (also named pCpxA in this study) that constitutively expresses wild-type CpxA close to physiological levels (Figure 3-6 from the Results section). Site-directed mutagenesis through overlap extension PCR was utilized to construct plasmids expressing CpxA-$E_{37}K$, CpxA-$M_{48}K$ and CpxA-$D_{113}K$. Briefly, a first PCR amplification of *cpxA* was conducted in pairs for each desired mutation, using the following primers to introduce point mutations: XA-1+XA-4 and XA-2b+XA-3 for $E_{37}K$ (producing the XA-1-4 and XA-2b-3 fragments), XA-1+XA-6 and XA-2b+XA-5 for $M_{48}K$ (producing the XA-1-6 and XA-2b-5 fragments), XA-1+XA-8 and XA-2b+XA-7 for $D_{113}K$ (producing the XA-1-8 and XA-2b-7 fragments). The cycling conditions were as follows: an initial denaturation of 95°C (2 minutes) followed by 30 cycles of a 95°C denaturing step for 15 seconds, an annealing step at 58°C for 30 seconds, and an extension step of 72°C for 1.5 minutes, then kept at 4°C until retrieved from the thermocycler. Expected band sizes for the amplified DNA were confirmed by 1.5% agarose gel electrophoresis. PCR products were purified after combining the XA-1-4 + XA-2b-3; XA-1-6 + XA-2b-5; and XA-1-8 + XA-2b-7 fragments in single microfuge tubes. A second PCR step was run using these fragments as DNA templates, along with the XA-1 and XA-2b primers, using the same exact cycle conditions as the previous step. The expected bands for all 3 PCR products were detected at 650bp after 1.5% agarose gel electrophoresis. Mutated fragments were purified, digested with *Bam*HI and *Eco*RI restriction endonucleases and ligated into the pK184 vector, resulting in different pCpxA mutant derivatives (Ho, Hunt, Horton, Pullen, & Pease, 1989; Lu et al., 2012)

2.6 Site-directed mutagenesis (New England Biolabs Q5® kit)

The remainder of the missense and nonsense mutations to *cpxA* and *cpxP* were generated as derivatives of plasmids pCpxA and pCpxP (overexpression vector for *cpxP*) (Raivio et al., 1999), respectively. The Q5® site-directed mutagenesis kit (New England Biolabs Inc) was used following the manufacturer's instructions. Primer pairs for each required single substitution were specifically designed through the online NEBaseChanger™ software, by integrating the desired nucleotide change(s) in the middle of the forward primer (including at least 10 complementary nucleotides on the 3' side of the mutation) and the reverse primer designed so that the 5' ends of both primers anneal back-to-back. The mutagenesis consisted of three main phases: 1) an exponential amplification (PCR) in which each single reaction included 12.5µL Q5 Hot Start High-Fidelity 2X Master Mix, 1.25µL 10µM forward primer, 1.25µL 10µM reverse primer, 1µL (1-25ng/µL) template DNA and 9µL nuclease-free H_2O in thin-walled PCR tubes. Cycling conditions were as follows: initial denaturation of 98°C (30 seconds) followed by 25 cycles with a 98°C denaturing step (10 seconds), an annealing step of variable temperature (between 50-72°C depending on each primer pair, for 30 seconds), and an extension step of 72°C (30 seconds per kb; 120 seconds total for pCpxA and pCpxP mutants), after which a final extension of 72°C (2 minutes) concluded the amplification. PCR-amplified products were kept at 4°C until retrieved from the thermocycler and either stored at -20°C or immediately used for the next phase. 2) A kinase, ligase & *Dpn*I (KLD) treatment to get rid of the template DNA and enrich the PCR product DNA, for which each reaction involved 1µL of PCR product, 5µL 2X KLD Reaction Buffer, 1µL 10X KLD Enzyme Mix and 3µL nuclease-free H_2O. KLD reactions were mixed by pipetting and incubated at room temperature for 5 minutes. 3) Transformation in which 5µL of the KLD mix from the previous step were added to a tube of thawed NEB 5-alpha competent *E. coli* cells

(derivatives from DH5α) and carefully flicked to mix, then placed on ice for 30 minutes, heat shocked at 42°C for 30 seconds, and placed back on ice for 5 minutes. Next, 950µL of room temperature Super Optimal broth with Catabolite repression (SOC) were pipetted into the mixture and incubated at 37°C for 60 minutes with constant shaking (225 rpm). After incubation, cells were mixed thoroughly by flicking the tubes and inverting, then 100µL were spread onto LB plates with appropriate antibiotics and incubated overnight at 37°C. The day after transformation, 8 isolated single bacterial colonies (avoiding satellite colonies as best as possible) were identified from each of the overnight plates and struck onto fresh new selective LB agar plates divided into 8 sectors of approximately the same size, then grown overnight at 37°C once again to confirm adequate resistance and isogenic properties for the following experimental procedures.

2.7 Plasmid extraction for stocks

Extraction and isolation of the plasmids used in this study was performed by means of the GenElute^{TM} Plasmid Miniprep Kit purchased from Sigma-Aldrich, according to the instructions published in their included protocol manual. Briefly, 5mL bacterial liquid cultures (LB broth with antibiotics) harbouring the plasmids of interest were grown aerobically overnight at 37°C with constant shaking at 225 rpm in large glass test tubes (16x125mm) and centrifuged for 10 minutes at room temperature (4,000 rpm, 22°C) in an Eppendorf 5810 R centrifuge. The supernatants were discarded, cell pellets resuspended in 200µL of Resuspension Solution containing RNase A and transferred to 1.5 mL Eppendorf plastic microfuge tubes. 200µL of Lysis Solution were now added and the tubes inverted 6-8 times for complete mixing. Then 350µL of Neutralization/Binding Solution were added and mixed by inversion 4-6 times. Cell debris was pelleted by centrifugation at 15,000 rpm for 10 minutes. The binding columns were prepared by adding 500µL of the Column

Preparation Solution and subsequent centrifugation at 15,000 rpm for 1 minute. The clear lysates were transferred to the columns and centrifuged at 15,000 rpm for 1 minute. 750µL of the Wash Solution containing 95% EtOH were added after the flow-through was discarded, followed by centrifugation at 15,000 rpm for 1 minute. Flow-through was discarded once again and the column centrifuged 15,000 rpm for 1 minute to remove leftover Wash Solution. The columns were then transferred to fresh collection tubes and the elution step of the plasmid DNA was carried out by adding 50µL of sterile Milli-Q H_2O (mQ H_2O) and centrifuging at 15,000 rpm for 1 minute, per extraction. Plasmid stocks were kept in the freezer at -20°C until utilized.

2.8 Calcium chloride, heat-shock mediated transformation

Recipient bacteria were cultured overnight in large glass test tubes (16x125mm) at 37°C with constant shaking at 225 rpm and aeriation, by inoculating 5mL of LB broth with single colonies of *E. coli* laboratory strains previously plated on LB agar. Growth media consistently contained either Amp 100µg/mL, Cam 25µg/mL, Kan 50µg/mL, or no antibiotics, depending on each specific case and transformation performed. The following day, desired strains were subcultured in a 1:50 dilution into fresh LB broth containing the appropriate antibiotics if necessary and grown to an optical density at 600 nm (OD_{600}) of between 0.4-0.6 (usually 2.5 - 3 hours growth), for each transformation, under the same growth conditions as the ones utilized for the overnight liquid cultures described above. Liquid cultures were centrifuged at 4,000 rpm for 10 minutes at 4°C, the supernatant discarded and pellet resuspended in 1mL of ice-cold "Magic Formula" (kept inside the refrigerator or on ice at 4°C at all times) containing 0.1M $CaCl_2$ and 0.1M 3-(N-morpholino)propanesulfonic acid (MOPS) pH 6.5 in sterile dH_2O. Resuspended cultures were incubated on ice for 30 minutes and then centrifuged again at 4,000 rpm for 10

minutes at 4°C. Supernatant was removed and the pellets were gently resuspended in fresh 0.2mL cold Magic Formula by pipetting, after which cultures were transferred to small plating glass test tubes (13x100mm). Plasmid DNA (1 - 5μL) was added and cultures were incubated on ice for another 10 minutes. Cultures were subjected to heat-shock using a water bath kept at 42.5°C for exactly 45 seconds and then bacteria were incubated on ice for an additional 2 minutes. 1mL of fresh LB without any antibiotics was added to every tube and strains were incubated at 37°C with constant shaking and aeriation at 225 rpm for 1 hour, to induce phenotypic expression of the antibiotic resistance genes located within the newly acquired plasmids and allow strain recovery from heat-shock. After recovery, 200μL of each culture were plated on selective LB agar media containing antibiotics and incubated overnight at 37°C under aerobic conditions. The day after transformation, 8 isolated single bacterial colonies (avoiding satellite colonies as best as possible) were identified from each of the overnight plates and struck onto fresh new selective LB agar plates divided in 8 spaces of approximately the same size, then grown overnight at 37°C once again to confirm adequate resistance and isogenic properties for the following experimental procedures.

2.9 β-galactosidase assays

β-galactosidase assays were carried out as described previously, with minor pertinent modifications depending on the experiment being performed (Buelow & Raivio, 2005; Slauch & Silhavy, 1991). Isolated single colonies of each *E. coli* strain from freshly streaked-out plates (3 days old or less) were cultured overnight in 2mL of LB broth containing appropriate antibiotics (Amp 100μg/mL, Cam 25μg/mL, Kan 50μg/mL) or without antibiotics on a case-specific basis, in quintuplicates, inside large glass test tubes (16x125mm) at 37°C with constant shaking at 225 rpm

and aeriation. The day after, strains were subcultured by diluting 40µL of each liquid culture into 1.96 mL of fresh LB media (1:50 dilution for each replicate) containing the previously stated concentrations of antibiotics when necessary, in small glass plating tubes (13x100mm) and placed under the same growth conditions as the overnight liquid cultures, for 5 hours in total (mid-log phase). In the cases of pH-dependent experiments, subcultures were centrifuged at 4,000 rpm for 10 minutes at room temperature after 2 hours of incubation and resuspended in sodium-phosphate buffered LB media at pH 5.8, 7.0 or 8.0. Gene expression from pK184-, pTrc99A- and pCA-based plasmids was induced by adding IPTG to a final concentration of either 0.1mM or 1mM at this time point as well, when required. After the addition of buffered LB pH media and/or IPTG, subcultures were returned to incubation for an additional 3 hours (Raivio et al., 2013). The final OD_{600} was between 0.6 and 0.7 for every subculture. Bacterial cells were then pelleted by centrifugation at 4,000 rpm for 10 minutes at 22°C, the supernatant removed, and cells resuspended in 2mL of freshly prepared 1X Z-buffer (0.06M $Na_2HPO_4 \cdot 7H_2O$, 0.04M $NaH_2PO_4 \cdot H_2O$, 0.01M KCl, 0.001M $MgSO_4 \cdot 7H_2O$ and 0.27% β-mercaptoethanol in dH_2O). 250µL from each tube were moved to a clear 96-well plate and the OD_{600} read using a Perkin Elmer Wallac 1420 Victor^2 Multilabel microplate reader. The rest of the cells still in tubes were lysed by the addition of two drops of chloroform (40µL) and one drop of 1% SDS (20µL) and vortexed 15 seconds for each tube, then allowed them to stand for at least 10 minutes to let the chloroform settle. 195µL of 1X Z-buffer was aliquoted into new wells (1 well per tube) of the 96-well plate (or into wells of a new 96-well plate, depending on the size of the experiment) and 5µL of the cell mix (carefully taken from the top of the culture, so there is no chloroform that may degrade the 96-well plate in the following steps) were then added into each respective well. 50µL of 10mg/mL ortho-nitrophenyl-β-D-galactopyranoside (ONPG) was quickly added to each well with a multichannel pipet and the

hydrolysis of ONPG by β-galactosidase was measured using the protocol for absorbance at 420nm (A_{420}, 20 readings with a 45 second interval between each measurement for a total of 30 minutes). β-galactosidase activity was then normalized to growth using the OD_{600} readings, to comprise for slight variations in total cell number between samples and calculated in Miller Units using the following formula:

$$\text{β-galactosidase (}\textit{cpxP'-lacZ}^{+}\text{) activity (Miller Units)} = \frac{A_{420} \text{ x } 600{,}000}{OD_{600}}$$

The average of three biological replicates represent the values for *cpxP'-lacZ*$^{+}$ activity shown in the figures, while the standard deviation between these replicates is depicted as error bars. Every experiment was repeated two more times for confirmation. Representative results from such independent experiments are presented.

2.10 Genetic screen (MacConkey agar plates)

For the first set of pCpxA lysine and alanine substitutions (the latter generated through site-directed mutagenesis Q5® kit) obtained, a genetic screen was performed based on the visualization of color variation in colonies plated on lactose MacConkey agar, using strains that carried the *cpxP'-lacZ*$^{+}$ chromosomal transcriptional fusion as a reporter gene (allowing for an indirect measure of Cpx activity). Since the *cpxP'-lacZ*$^{+}$ reporter exhibits high activity levels once the Cpx pathway is induced, it manifests as bright red/purple colonies on MacConkey plates due to the β-galactosidase produced being able to hydrolyze lactose in the media and lowering its pH, a preliminary comparison can be made with other colonies producing a lighter color (also pink/white colonies) that indicates lower levels of *lacZ* expression, thus lower Cpx activation. Single isolated

colonies of these transformants were streaked onto MacConkey agar plates supplemented with 0.1mM IPTG (final concentration) to induce expression, along with the isogenic vector control strain and the pCpxA complemented strain. After this initial screening, the mutated strains were struck out on LB agar plates and β-galactosidase experiments performed as previously described, to quantify activity levels.

2.11 Whole membrane preparations from cell lysates

Isolated single colonies of each *E. coli* strain were cultured overnight in 5mL of LB broth containing appropriate antibiotics (Amp 100μg/mL, Cam 25μg/mL, Kan 50μg/mL) or without antibiotics on a case-specific basis, inside large glass test tubes (16x125mm) at 37°C with constant shaking at 225 rpm and aerobic conditions. The following day, 1:100 subcultures (50μL of the overnight culture in 5mL total media plus appropriate antibiotics) were made and grown at 37°C with shaking at 225 rpm and aeriation for 4-6 hours until an OD_{600} between 0.6 and 0.7 was reached. Cultures were adjusted to the equivalent of 1mL of the culture displaying the lowest optical density after OD_{600} determination (Buelow & Raivio, 2005). On a case-dependant basis, a final concentration of 0.1mM IPTG was added to cultures for induction, 2 hours after subculture. Centrifugation was carried on for 10 minutes at room temperature and 4,000 rpm in a benchtop centrifuge, and the pellets resuspended in 1mL of 0.1M Tris-HCl adjusted to pH 8.0. Cultures were then sonicated using the micro tip of a Branson 450 Analog Sonifier, doing 30 second pulses for 5 times with 45 seconds cooling intervals between each sonication. Sonicated cultures were transferred to microfuge tubes and centrifuged at 10,000 rpm for 5 minutes at 4°C. 900μL of the supernatants were transferred to new tubes and centrifuged at 15,000 rpm for 5 hours at 4°C (Lobos & Mora, 1991). Supernatants (soluble fractions) were removed and pipetted into separate tubes,

whereas pellets were resuspended in 100µL of 1X Phosphate-buffered saline (PBS: 137mM NaCl, 2.7mM KCl, 10mM Na_2HPO_4 and 1.8mM KH_2PO_4 in dH_2O with pH adjusted to 7.4 by the addition of HCl) and both were either used immediately or stored at a -20°C freezer.

2.12 Total protein determination of membrane extracts and soluble fractions

Total protein concentration was determined with the microplate procedure from the Pierce BCA Protein Assay Kit (Thermo Scientific) following the manufacturers protocol. Briefly, 9 bovine serum albumin (BSA) protein standards at final concentrations of 2000, 1500, 1000, 750, 500, 250, 125, 25 and 0µg/mL were prepared either with 0.1M Tris HCl pH 8.0 for soluble fractions or 1X PBS for crude membrane fractions as diluents. An adequate amount of working reagent (WR) was made according to the number of standards, unknowns and replicates needed by mixing 50 parts of the BCA Reagent A with 1 part of BCA Reagent B (50:1, Reagent A:B). 25µL of each standard or unknown sample replicate were pipetted into microplate wells and 200µL of the WR added to each well, then mixed thoroughly by shaking for 30 seconds. The plate was covered and incubated at 37°C in a standing incubator for 30 minutes. The microplate was cooled to room temperature and absorbance measured at 562nm (A_{562}) in the microplate reader. For calculations, the A_{562} averages from the blank standards were subtracted from the measurements of all other standards and samples, after which a standard curve was prepared by plotting the average blank-corrected A_{562} for every standard vs. its concentration (µg/mL) and used for determination of protein concentration of each sample.

2.13 Sodium dodecyl sulfate – Polyacrylamide gel electrophoresis (SDS-PAGE)

Soluble fractions and resuspended pellets from the whole membrane preparations step were mixed with equal volumes of 2X SDS-PAGE Sample Loading Buffer (0.125M Tris [pH 6.8], 20% glycerol, 10% β-mercaptoethanol, 6% SDS, 0.2% bromophenol blue in dH_2O) to prepare the samples to be analyzed (Raivio et al., 1999; Sambrook et al., 1989), and an adequate amount of frozen 10% ammonium persulfate (APS) tubes were thawed out on ice, according to the total number of gels to be made. Spacer and short glass plates were carefully and thoroughly cleaned by washing with soap, rinsing with tap and distilled water and finally rinsing with 95% EtOH, then left to air dry at room temperature. Plates were placed into gel casting units after aligning and sliding them into green plate holders. Latches on plate holders were closed and double-checked for correct alignment of the plates. Resolving gels (12%) were prepared following the BioRad solutions tables (12% 29:1 acrylamide mix, 0.39M Tris [pH 8.8], 0.1% SDS, 0.1% APS and 0.04% tetramethylethylendiamine (TEMED) in dH_2O). The resolving gel mixture was promptly injected in between the short and spacer plates with a 10mL syringe, leaving approximately 3cm at the top for the stacking gel and completely covering with isopropanol. After solidification occurred, isopropanol was removed, and the top of the gel rinsed with dH_2O, with excess removed using paper towel squares. An adequate number of combs were placed into a weigh boat and soaked in 0.1% SDS. Meanwhile, stacking gels were prepared (4.95% 29:1 acrylamide mix, 0.125M Tris [pH 6.8], 0.1% SDS, 0.1% APS and 0.1% TEMED in dH_2O) and injected into the gel casting unit, filling to the top of the short plate. The combs were slid into the gels and a top up added with extra stacking gel mix. Gels were left to solidify during a 15-minute period and samples were boiled in water bath for 5 minutes. Electrophoresis apparati were assembled by placing gels into plate holders, securing clamps and inserting into chambers. Inner chambers were filled to the top of the

glass plates with 1X Tris-Glycine Buffer (0.302% Tris base, 1.88% glycine and 0.1% SDS in dH_2O) and outer chambers were also filled to approximately 5cm height with the same buffer. 5µL of Broad-Range Ladder were loaded into the first well of each gel and 20µg of total protein for each sample were loaded into different wells (Laemmli, 1970). Gels were run at 100 Volts until dye fronts reached the bottom of the glass plates (1-2 hours) and transferred to nitrocellulose membranes for Western blot analysis.

2.14 Western blot analysis

Filter papers and membranes were cut to the appropriate size for mini blot protein transfers and western blotting to be carried out by the Trans-Blot Semi-Dry electrophoretic transfer cell (BioRad). Acrylamide gels were carefully retrieved from the electrophoresis chambers and equilibrated in Bjerrum and Schafer-Nielsen transfer buffer (48mM Tris, 39mM glycine, 20% methanol (MeOH) and 0.0375% SDS in dH_2O, pH 9.2) for 20-60 minutes, while membranes and filter papers were soaked in the same buffer for 5-10 minutes in open plastic containers under the fume hood, due to MeOH evaporating from the buffer. The safety cover and stainless-steel cathode of the transfer apparatus were removed, after which the gel sandwiches were prepared by placing a pre-wet filter paper, pre-wet membrane, equilibrated gel and another pre-wet filter paper per desired transfer (in order from bottom platinum anode to top cathode) and rolling out air bubbles trapped between layers. The top cathode and safety cover were secured, and blots ran at 15V for 15 minutes (Towbin, Staehelin & Gordon, 1979). Upon completion of each run, the cathode was removed, and the gel-membrane sandwich disassembled. The nitrocellulose membranes were moved to individual clean small Tupperware containers for blocking, covered in 50mL of 2.5% Milk Tris-buffered saline (MTBS: 2.5% skim milk powder and 1X Tris-buffered saline (TBS:

0.9% NaCl & 0.1211% Tris base) in dH_2O) and incubated at room temperature on a rotating platform for at least 1.5 hours or at 4°C overnight. Blocking solution was poured off and 50mL of either primary rabbit α-CpxA-Maltose Binding Protein (MBP), α-CpxP-MBP (Raivio & Silhavy, 1997) or α-OmpA (loading control) antibodies diluted 1:50,000 in 2.5% MTBS were poured onto the membranes and incubated for 1 hour at room temperature with constant rotation. The primary antibody solution was removed (stored at 4°C to be reused in future blots) and the membranes were covered with 50mL of Washing Solution (WS: 1X TBS and 0.05% Tween 20 in dH_2O (TBST)), left at room temperature with constant shaking for four successive 30-minute incubations for each blot, then an extra time overnight to reduce background. The following day the WS was discarded and 50mL of secondary α-rabbit-alkaline phosphatase antibody (Sigma-Aldrich) diluted 1:25,000 in 2.5% MTBS added to the membranes and incubated for 1 hour at room temperature with constant rotation. Secondary antibody solutions were discarded, and the membranes covered in 50mL of WS at room temperature and washes applied as described previously. The day after, the WS was removed and membranes placed on flat pieces of Saran wrap, then 2.5mL of Developer were mixed with 125µL of Enhancer from the BioRad Immun-Star Alkaline Phosphatase Chemiluminescence kit (BioRad) per blot, the mixture dumped onto membranes and the blots were incubated at room temperature for 10 minutes. Excess developer was poured off and membranes wrapped in fresh Saran wrap, then imaged with the BioRad ChemiDoc MP imaging system (Buelow & Raivio, 2005; Raivio et al., 1999). Samples were collected from strains and each Western blot assay done at least twice. A representative blot is presented.

2.15 *In vivo* UV-induced photocrosslinking assay

Single-amino acids were substituted for TAG amber codons in plasmids pCpxA and pCpxP using the Q5® site-directed mutagenesis kit as described previously, to modify specific residues shown to be of importance for interaction and signaling, and others in their close vicinity that protrude toward a potential periplasmic interaction. The plasmid pEVOL-pBpF (containing a tRNA synthetase/tRNA pair for the *in vivo* insertion of an artificial ultraviolet (UV) photocrosslinker, p-benzoyl-l-phenylalanine (*p*BPA), into proteins in *E. coli* at TAG codons) (Chin, Martin, King, Wang & Schultz, 2002) was cotransformed alongside each plasmid encoding the indicated CpxA and CpxP amber mutants into Δ*cpxA* and Δ*cpxP* strains, respectively. For the case of the mutated CpxA strains, the pCpxP overexpression vector was also cotransformed, otherwise the detection of CpxP via Western blot assays is very complicated. Isolated single colonies of each *E. coli* strain were cultured overnight in 5mL of LB broth containing appropriate antibiotics (Amp 100μg/mL, Cam 25μg/mL, Kan 50μg/mL) on a case-specific basis, inside large glass test tubes (16x125mm) at 37°C with constant shaking at 225 rpm and aerobic conditions. The following day, 1:100 subcultures were prepared and grown in LB with 0.16mM *p*BPA (Bachem, solubilized in 1mM NaOH) at 37°C with constant shaking and aeriation for 2 hours, after which they were supplemented with 0.1mM IPTG and 0.02% arabinose to induce expression of the plasmids and grown for 1 more hour until mid-log phase (an OD_{600} of approximately 0.4). Centrifugation was carried on for 10 minutes at room temperature and 4,000 rpm in a benchtop centrifuge, and the pelleted cells were concentrated to an OD_{600} of 10 using ice-cold TBS. 100μL of each cell suspension were transferred to duplicate wells in a clear 96-well plate and subjected to UV irradiation at a wavelength of 365nm for 15 minutes on ice (4°C, 5cm distance of the plate to the UV source (being a handheld UV illuminator), plate enclosed using a cardboard box), after

which they were mixed with 100µL of 2X SDS-PAGE Sample Loading Buffer (Konovalova, Perlman, Cowles, & Silhavy, 2014). Samples were analyzed by SDS-PAGE and Western blotting assays as described before, with a small modification of incubating the blots overnight at 4°C with constant rotation after adding the primary antibodies, instead of incubating for 1 hour at room temperature. The pEVOL-pBpF plasmid was a gift from Peter Schultz (Addgene plasmid # 31190). Each photocrosslinking assay was repeated at least once. A representative blot is presented.

2.16 DNA Sequencing

Verification of the correct mutated genes within plasmids was performed by the University of Alberta Molecular Biology Service Unit (MBSU) through standard Sanger Economy DNA Sequencing on a 3730 Genetic Analyzer. Each reaction required the template and one primer at a time (Forward or Reverse) mixed together in one microfuge tube to a final volume of 10µL. Final concentrations used were as follows: 57.5ng/µL of the plasmid carrying the desired sequence (up to 7.5µL if the plasmid concentration was lower), 2.5µL 0.25µM of the primer, and a top up with Milli-Q H_2O to 10µL (if necessary).

2.17 Sequence alignments

Sequences obtained from MBSU were aligned and compared with the *cpxA* and *cpxP* wildtype sequences from the *E. coli* strain K-12 substrain MC4100 complete genome to confirm single-amino acid substitutions in the correct positions, using the online Molecular Biology Suite tool from the Benchling platform (online software).

2.18 Crystal structure visualization

Crystal structures and electrostatic surface representations for the $CpxA_{SD}$ (PDB file not yet indexed) and CpxP (PDB file 3QZC from Thede et al., 2011) dimers were generated and 3D-visualized via the PyMOL Molecular Graphics System, Version 2.0.1. Images denoting specific amino acids important for the present study are shown.

2.19 Statistics

Statistical analysis was achieved using the GraphPad Prism version 7.04 computational software. The activity of transcriptional fusions working as reporter genes was compared by either one-way or two-way Analysis of Variance (ANOVA) for experiments containing one or two independent variables, respectively, and more than two strains assayed together at the same time. The Sidak's post hoc multiple comparison test was included in the ANOVAs.

Table 2-1 Bacterial strains, plasmids and reporter genes used in this study

Strain or plasmid	Description	Source or reference
Bacterial strains		
MC4100	F$^-$ *araD139*Δ*(argF-lac)* U169 *rpsL*150 (Str^R) *relA1 flhD5301 deoC1 ptsF25 rbsR*	Casadaban, 1976
TR50	MC4100 λRS88[*cpxP'-lacZ*$^+$]; Str^R	Raivio & Silhavy, 1997
RM53	TR50 Δ*cpxA;* Str^R	Roxana Malpica, former post-doctoral fellow
RM55	TR50 Δ*cpxA* (pCA24N-*cpxA*WT); Str^R Cam^R	Roxana Malpica, former post-doctoral fellow
JLW7	TR50 (pCA24N); Str^R Cam^R	Wong, 2015
JSW3	TR50 (pCA-*nlpE*); Str^R Cam^R	Wong, 2015
DB12	TR50 (pTrc99A); Str^R Amp^R	Buelow & Raivio, 2005
DB8	TR50 (pCpxP); Str^R Amp^R	Buelow & Raivio, 2005
JLW392	TR50 Δ*cpxP*; Str^R	Wong, 2015

JLW400	JLW392 (pTrc99A); Str^R Amp^R	Wong, 2015
JLW404	JLW392 (pCpxP); Str^R Amp^R	Wong, 2015
RMQ1	RM53 (pCA24N); Str^R Cam^R	This study
RMQ2	RM53 (pK184-*cpxA*WT); Str^R Kan^R	This study
RMQ3	RM53 (pJ307-*cpxA*WT); Str^R Kan^R	This study
RMQ4	RM53 (pK184-*traJ*); Str^R Kan^R	This study
RMQ5	RM53 (pK184-*cpxA*E_{37}K); Str^R Kan^R	This study
RMQ6	RM53 (pK184-*cpxA*M_{48}K); Str^R Kan^R	This study
RMQ7	RM53 (pK184-*cpxA*D_{113}K); Str^R Kan^R	This study
RMQ8	RM53 (pTrc99A); Str^R Amp^R	This study
RMQ9	RM53 (pCpxP); Str^R Amp^R	This study
RMQ10	RM53 (pK184-*cpxA*WT) (pTrc99A); Str^R Kan^R Amp^R	This study
RMQ11	RM53 (pK184-*cpxA*WT) (pCpxP); Str^R Kan^R Amp^R	This study
RMQ12	RM53 (pK184-*traJ*) (pTrc99A); Str^R Kan^R Amp^R	This study
RMQ13	RM53 (pK184-*traJ*) (pCpxP); Str^R Kan^R Amp^R	This study
RMQ14	RM53 (pK184-*cpxA*E_{37}K) (pTrc99A); Str^R Kan^R Amp^R	This study
RMQ15	RM53 (pK184-*cpxA*E_{37}K) (pCpxP); Str^R Kan^R Amp^R	This study
RMQ16	RM53 (pK184-*cpxA*M_{48}K) (pTrc99A); Str^R Kan^R Amp^R	This study
RMQ17	RM53 (pK184-*cpxA*M_{48}K) (pCpxP); Str^R Kan^R Amp^R	This study
RMQ18	RM53 (pK184-*cpxA*D_{113}K) (pTrc99A); Str^R Kan^R Amp^R	This study
RMQ19	RM53 (pK184-*cpxA*D_{113}K) (pCpxP); Str^R Kan^R Amp^R	This study
RMQ20	RM53 (pCA-*nlpE*); Str^R Cam^R	This study
RMQ21	RM53 (pK184-*cpxA*WT) (pCA24N); Str^R Kan^R Cam^R	This study

RMQ22	RM53 (pK184-*cpxA*WT) (pCA-*nlpE*); Str^R Kan^R Cam^R	This study
RMQ23	RM53 (pK184-*traJ*) (pCA24N); Str^R Kan^R Cam^R	This study
RMQ24	RM53 (pK184-*traJ*) (pCA-*nlpE*); Str^R Kan^R Cam^R	This study
RMQ25	RM53 (pK184-*cpxA*E_{37}K) (pCA24N); Str^R Kan^R Cam^R	This study
RMQ26	RM53 (pK184-*cpxA*E_{37}K) (pCA-*nlpE*); Str^R Kan^R Cam^R	This study
RMQ27	RM53 (pK184-*cpxA*M_{48}K) (pCA24N); Str^R Kan^R Cam^R	This study
RMQ28	RM53 (pK184-*cpxA*M_{48}K) (pCA-*nlpE*); Str^R Kan^R Cam^R	This study
RMQ29	RM53 (pK184-*cpxA*D_{113}K) (pCA24N); Str^R Kan^R Cam^R	This study
RMQ30	RM53 (pK184-*cpxA*D_{113}K) (pCA-*nlpE*); Str^R Kan^R Cam^R	This study
RMQ31	RM53 (pK184-*cpxA*E_{37}A); Str^R Kan^R	This study
RMQ32	RM53 (pK184-*cpxA*D_{40}A); Str^R Kan^R	This study
RMQ33	RM53 (pK184-cpxAM_{48}A); Str^R Kan^R	This study
RMQ34	RM53 (pK184-*cpxA*E_{91}A); Str^R Kan^R	This study
RMQ35	RM53 (pK184-*cpxA*D_{113}A); Str^R Kan^R	This study
RMQ36	RM53 (pK184-*cpxA*E_{37}A) (pTrc99A); Str^R Kan^R Amp^R	This study
RMQ37	RM53 (pK184-*cpxA*E_{37}A) (pCpxP); Str^R Kan^R Amp^R	This study
RMQ38	RM53 (pK184-*cpxA*D_{40}A) (pTrc99A); Str^R Kan^R Amp^R	This study
RMQ39	RM53 (pK184-*cpxA*D_{40}A) (pCpxP); Str^R Kan^R Amp^R	This study
RMQ40	RM53 (pK184-cpxAM_{48}A) (pTrc99A); Str^R Kan^R Amp^R	This study
RMQ41	RM53 (pK184-cpxAM_{48}A) (pCpxP); Str^R Kan^R Amp^R	This study
RMQ42	RM53 (pK184-*cpxA*E_{91}A) (pTrc99A); Str^R Kan^R Amp^R	This study
RMQ43	RM53 (pK184-*cpxA*E_{91}A) (pCpxP); Str^R Kan^R Amp^R	This study
RMQ44	RM53 (pK184-*cpxA*D_{113}A) (pTrc99A); Str^R Kan^R Amp^R	This study

RMQ45	RM53 (pK184-*cpxA*$D_{113}A$) (pCpxP); Str^R Kan^R Amp^R	This study
RMQ46	RM53 (pK184-*cpxA*$E_{37}A$) (pCA24N); Str^R Kan^R Cam^R	This study
RMQ47	RM53 (pK184-*cpxA*$E_{37}A$) (pCA-*nlpE*); Str^R Kan^R Cam^R	This study
RMQ48	RM53 (pK184-*cpxA*$D_{40}A$) (pCA24N); Str^R Kan^R Cam^R	This study
RMQ49	RM53 (pK184-*cpxA*$D_{40}A$) (pCA-*nlpE*); Str^R Kan^R Cam^R	This study
RMQ50	RM53 (pK184-cpxA$M_{48}A$) (pCA24N); Str^R Kan^R Cam^R	This study
RMQ51	RM53 (pK184-cpxA$M_{48}A$) (pCA-*nlpE*); Str^R Kan^R Cam^R	This study
RMQ52	RM53 (pK184-*cpxA*$E_{91}A$) (pCA24N); Str^R Kan^R Cam^R	This study
RMQ53	RM53 (pK184-*cpxA*$E_{91}A$) (pCA-*nlpE*); Str^R Kan^R Cam^R	This study
RMQ54	RM53 (pK184-*cpxA*$D_{113}A$) (pCA24N); Str^R Kan^R Cam^R	This study
RMQ55	RM53 (pK184-*cpxA*$D_{113}A$) (pCA-*nlpE*); Str^R Kan^R Cam^R	This study
RMQ56	RM53 (pK184-*cpxA*$E_{91}K$); Str^R Kan^R	This study
RMQ57	RM53 (pK184-*cpxA*$E_{91}K$+$D_{113}K$); Str^R Kan^R	This study
RMQ58	RM53 (pK184-*cpxA*$E_{138}K$); Str^R Kan^R	This study
RMQ59	RM53 (pK184-*cpxA*$E_{91}A$+$D_{113}A$); Str^R Kan^R	This study
RMQ60	RM53 (pK184-*cpxA*$E_{138}A$); Str^R Kan^R	This study
RMQ61	RM53 (pK184-*cpxA*$E_{91}K$) (pTrc99A); Str^R Kan^R Amp^R	This study
RMQ62	RM53 (pK184-*cpxA*$E_{91}K$) (pCpxP); Str^R Kan^R Amp^R	This study
RMQ63	RM53 (pK184-*cpxA*$E_{91}K$+$D_{113}K$) (pTrc99A); Str^R Kan^R Amp^R	This study
RMQ64	RM53 (pK184-*cpxA*$E_{91}K$+$D_{113}K$) (pCpxP); Str^R Kan^R Amp^R	This study
RMQ65	RM53 (pK184-*cpxA*$E_{138}K$) (pTrc99A); Str^R Kan^R Amp^R	This study
RMQ66	RM53 (pK184-*cpxA*$E_{138}K$) (pCpxP); Str^R Kan^R Amp^R	This study
RMQ67	RM53 (pK184-*cpxA*$E_{91}A$+$D_{113}A$) (pTrc99A); Str^R Kan^R Amp^R	This study

RMQ68	RM53 (pK184-*cpxA*$E_{91}A+D_{113}A$) (pCpxP); Str^R Kan^R Amp^R	This study
RMQ69	RM53 (pK184-*cpxA*$E_{138}A$) (pTrc99A); Str^R Kan^R Amp^R	This study
RMQ70	RM53 (pK184-*cpxA*$E_{138}A$) (pCpxP); Str^R Kan^R Amp^R	This study
RMQ71	RM53 (pK184-*cpxA*$E_{91}K$) (pCA24N); Str^R Kan^R Cam^R	This study
RMQ72	RM53 (pK184-*cpxA*$E_{91}K$) (pCA-*nlpE*); Str^R Kan^R Cam^R	This study
RMQ73	RM53 (pK184-*cpxA*$E_{91}K+D_{113}K$) (pCA24N); Str^R Kan^R Cam^R	This study
RMQ74	RM53 (pK184-*cpxA*$E_{91}K+D_{113}K$) (pCA-*nlpE*); Str^R Kan^R Cam^R	This study
RMQ75	RM53 (pK184-*cpxA*$E_{138}K$) (pCA24N); Str^R Kan^R Cam^R	This study
RMQ76	RM53 (pK184-*cpxA*$E_{138}K$) (pCA-*nlpE*); Str^R Kan^R Cam^R	This study
RMQ77	RM53 (pK184-*cpxA*$E_{91}A+D_{113}A$) (pCA24N); Str^R Kan^R Cam^R	This study
RMQ78	RM53 (pK184-*cpxA*$E_{91}A+D_{113}A$) (pCA-*nlpE*); Str^R Kan^R Cam^R	This study
RMQ79	RM53 (pK184-*cpxA*$E_{138}A$) (pCA24N); Str^R Kan^R Cam^R	This study
RMQ80	RM53 (pK184-*cpxA*$E_{138}A$) (pCA-*nlpE*); Str^R Kan^R Cam^R	This study
RMQ81	TR50 (pCpxP $R_{56}E$); Str^R Amp^R	This study
RMQ82	RM53 (pCpxP $R_{56}E$); Str^R Amp^R	This study
RMQ83	RM53 (pK184-*cpxA*WT) (pCpxP $R_{56}E$); Str^R Kan^R Amp^R	This study
RMQ84	RM53 (pK184-*traJ*) (pCpxP $R_{56}E$); Str^R Kan^R Amp^R	This study
RMQ85	RM53 (pK184-*cpxA*$E_{91}K$) (pCpxP $R_{56}E$); Str^R Kan^R Amp^R	This study
RMQ86	RM53 (pK184-*cpxA*$D_{113}K$) (pCpxP $R_{56}E$); Str^R Kan^R Amp^R	This study
RMQ87	RM53 (pK184-*cpxA*$E_{91}K+D_{113}K$) (pCpxP $R_{56}E$); Str^R Kan^R Amp^R	This study
RMQ88	TR50 (pCpxP $R_{60}E$); Str^R Amp^R	This study
RMQ89	RM53(pCpxP $R_{60}E$); Str^R Amp^R	This study
RMQ90	RM53 (pK184-*cpxA*WT) (pCpxP $R_{60}E$); Str^R Kan^R Amp^R	This study

RMQ91	RM53 (pK184-*traJ*) (pCpxP $R_{60}E$); Str^R Kan^R Amp^R	This study
RMQ92	RM53 (pK184-*cpxA*$E_{91}K$) (pCpxP $R_{60}E$); Str^R Kan^R Amp^R	This study
RMQ93	RM53 (pK184-*cpxA*$D_{113}K$) (pCpxP $R_{60}E$); Str^R Kan^R Amp^R	This study
RMQ94	RM53 (pK184-*cpxA*$E_{91}K+D_{113}K$) (pCpxP $R_{60}E$); Str^R Kan^R Amp^R	This study
RMQ95	TR50 (pCpxP $R_{67}E$); Str^R Amp^R	This study
RMQ96	RM53(pCpxP $R_{67}E$); Str^R Amp^R	This study
RMQ97	RM53 (pK184-*cpxA*WT) (pCpxP $R_{67}E$); Str^R Kan^R Amp^R	This study
RMQ98	RM53 (pK184-*traJ*) (pCpxP $R_{67}E$); Str^R Kan^R Amp^R	This study
RMQ99	RM53 (pK184-*cpxA*$E_{91}K$) (pCpxP $R_{67}E$); Str^R Kan^R Amp^R	This study
RMQ100	RM53 (pK184-*cpxA*$D_{113}K$) (pCpxP $R_{67}E$); Str^R Kan^R Amp^R	This study
RMQ101	RM53 (pK184-*cpxA*$E_{91}K+D_{113}K$) (pCpxP $R_{67}E$); Str^R Kan^R Amp^R	This study
RMQ102	TR50 (pCpxP $R_{139}E$); Str^R Amp^R	This study
RMQ103	RM53 (pCpxP $R_{139}E$); Str^R Amp^R	This study
RMQ104	RM53 (pK184-*cpxA*WT) (pCpxP $R_{139}E$); Str^R Kan^R Amp^R	This study
RMQ105	RM53 (pK184-*traJ*) (pCpxP $R_{139}E$); Str^R Kan^R Amp^R	This study
RMQ106	RM53 (pK184-*cpxA*$E_{91}K$) (pCpxP $R_{139}E$); Str^R Kan^R Amp^R	This study
RMQ107	RM53 (pK184-*cpxA*$D_{113}K$) (pCpxP $R_{139}E$); Str^R Kan^R Amp^R	This study
RMQ108	RM53 (pK184-*cpxA*$E_{91}K+D_{113}K$) (pCpxP $R_{139}E$); Str^R Kan^R Amp^R	This study
RMQ109	TR50 (pCpxP $R_{56}E+R_{60}E$); Str^R Amp^R	This study
RMQ110	RM53 (pCpxP $R_{56}E+R_{60}E$); Str^R Amp^R	This study
RMQ111	RM53 (pK184-*cpxA*WT) (pCpxP $R_{56}E+R_{60}E$); Str^R Kan^R Amp^R	This study
RMQ112	RM53 (pK184-*traJ*) (pCpxP $R_{56}E+R_{60}E$); Str^R Kan^R Amp^R	This study

RMQ113	RM53 (pK184-*cpxA*$E_{91}K$) (pCpxP $R_{56}E+R_{60}E$); Str^R Kan^R Amp^R	This study
RMQ114	RM53 (pK184-*cpxA*$D_{113}K$) (pCpxP $R_{56}E+R_{60}E$); Str^R Kan^R Amp^R	This study
RMQ115	RM53 (pK184-*cpxA*$E_{91}K+D_{113}K$) (pCpxP $R_{56}E+R_{60}E$); Str^R Kan^R Amp^R	This study
RMQ116	TR50 (pCpxP $R_{60}E+R_{67}E$); Str^R Amp^R	This study
RMQ117	RM53 (pCpxP $R_{60}E+R_{67}E$); Str^R Amp^R	This study
RMQ118	RM53 (pK184-*cpxA*WT) (pCpxP $R_{60}E+R_{67}E$); Str^R Kan^R Amp^R	This study
RMQ119	RM53 (pK184-*traJ*) (pCpxP $R_{60}E+R_{67}E$); Str^R Kan^R Amp^R	This study
RMQ120	RM53 (pK184-*cpxA*$E_{91}K$) (pCpxP $R_{60}E+R_{67}E$); Str^R Kan^R Amp^R	This study
RMQ121	RM53 (pK184-*cpxA*$D_{113}K$) (pCpxP $R_{60}E+R_{67}E$); Str^R Kan^R Amp^R	This study
RMQ122	RM53 (pK184-*cpxA*$E_{91}K+D_{113}K$) (pCpxP $R_{60}E+R_{67}E$); Str^R Kan^R Amp^R	This study
RMQ123	RM53 (pK184-*cpxA*WT) (pCpxP) (pEVOL-pBpF); Str^R Kan^R Amp^R Cam^R	This study
RMQ124	RM53 (pK184-*traJ*) (pCpxP) (pEVOL-pBpF); Str^R Kan^R Amp^R Cam^R	This study
RMQ125	RM53 (pK184-*cpxA*$E_{91}A$) (pCpxP) (pEVOL-pBpF); Str^R Kan^R Amp^R Cam^R	This study
RMQ126	RM53 (pK184-*cpxA*$D_{113}A$) (pCpxP) (pEVOL-pBpF); Str^R Kan^R Amp^R Cam^R	This study
RMQ127	RM53 (pK184-*cpxA*T_{89}-TAG) (pCpxP) (pEVOL-pBpF); Str^R Kan^R Amp^R Cam^R	This study

RMQ128	RM53 (pK184-*cpxA*T_{90}-TAG) (pCpxP) (pEVOL-pBpF); Str^R Kan^R Amp^R Cam^R	This study
RMQ129	RM53 (pK184-*cpxA*E_{91}-TAG) (pCpxP) (pEVOL-pBpF); Str^R Kan^R Amp^R Cam^R	This study
RMQ130	RM53 (pK184-*cpxA*G_{92}-TAG) (pCpxP) (pEVOL-pBpF); Str^R Kan^R Amp^R Cam^R	This study
RMQ131	RM53 (pK184-*cpxA*R_{93}-TAG) (pCpxP) (pEVOL-pBpF); Str^R Kan^R Amp^R Cam^R	This study
RMQ132	RM53 (pK184-*cpxA*A_{112}-TAG) (pCpxP) (pEVOL-pBpF); Str^R Kan^R Amp^R Cam^R	This study
RMQ133	RM53 (pK184-*cpxA*D_{113}-TAG) (pCpxP) (pEVOL-pBpF); Str^R Kan^R Amp^R Cam^R	This study
RMQ134	RM53 (pK184-*cpxA*N_{114}-TAG) (pCpxP) (pEVOL-pBpF); Str^R Kan^R Amp^R Cam^R	This study
RMQ135	RM53 (pK184-*cpxA*D_{116}-TAG) (pCpxP) (pEVOL-pBpF); Str^R Kan^R Amp^R Cam^R	This study
RMQ136	RM53 (pK184-*cpxA*H_{117}-TAG) (pCpxP) (pEVOL-pBpF); Str^R Kan^R Amp^R Cam^R	This study
RMQ137	JLW404 (pEVOL-pBpF); Str^R Amp^R Cam^R	This study
RMQ138	JLW400 (pEVOL-pBpF); Str^R Amp^R Cam^R	This study
RMQ139	JLW392 (pCpxP $R_{67}E$) (pEVOL-pBpF); Str^R Amp^R Cam^R	This study
RMQ140	JLW392 (pCpxP $R_{139}E$) (pEVOL-pBpF); Str^R Amp^R Cam^R	This study
RMQ141	JLW392 (pCpxP M_{63}-TAG) (pEVOL-pBpF); Str^R Amp^R Cam^R	This study

RMQ142	JLW392 (pCpxP A_{66}-TAG) (pEVOL-pBpF); Str^R Amp^R Cam^R	This study
RMQ143	JLW392 (pCpxP R_{67}-TAG) (pEVOL-pBpF); Str^R Amp^R Cam^R	This study
RMQ144	JLW392 (pCpxP H_{68}-TAG) (pEVOL-pBpF); Str^R Amp^R Cam^R	This study
RMQ145	JLW392 (pCpxP Q_{70}-TAG) (pEVOL-pBpF); Str^R Amp^R Cam^R	This study
RMQ146	JLW392 (pCpxP H_{136}-TAG) (pEVOL-pBpF); Str^R Amp^R Cam^R	This study
RMQ147	JLW392 (pCpxP Q_{138}-TAG) (pEVOL-pBpF); Str^R Amp^R Cam^R	This study
RMQ148	JLW392 (pCpxP R_{139}-TAG) (pEVOL-pBpF); Str^R Amp^R Cam^R	This study
RMQ149	JLW392 (pCpxP Q_{142}-TAG) (pEVOL-pBpF); Str^R Amp^R Cam^R	This study
RMQ150	JLW392 (pCpxP L_{143}-TAG) (pEVOL-pBpF); Str^R Amp^R Cam^R	This study

Plasmids		
pCA24N	High-copy IPTG-inducible vector control from ASKA library; Cam^R	Kitagawa et al., 2005
pCA-*nlpE*	High-copy, pCA24N-derived, IPTG-inducible *nlpE* overexpression vector from the ASKA library; Cam^R	Kitagawa et al., 2005
pTrc99A	High-copy IPTG-inducible vector control; Amp^R	Pharmacia
pCpxP	High-copy, pTrc99A-derived, IPTG-inducible *cpxP* overexpression vector; Amp^R	Raivio et al., 1999
pK184	Low-copy cloning vector with a p15a replicon, *lacZ-α*, and an IPTG-inducible *lac* promoter; Kan^R	Jobling & Holmes, 1999
pJ307	Low-copy, cloning vector (pK184-derived) with a p15a replicon, *lacZ-α*, and an IPTG-inducible *lac* promoter. The	Lu, et al., 2012

	F plasmid *traJ* was cloned into pK184. Also used as negative vector control; Kan^R	
(pEVOL-pBpF)	High-copy vector with a p15a replicon and an arabinose-inducible *araBAD* promoter. Contains a tRNA synthetase/tRNA pair for the *in vivo* incorporation of the *p*BPA photocrosslinker into proteins in *E. coli* in response to the amber TAG codon; Cam^R	Chin, et al., 2002

Reporter genes		
cpxP'-lacZ$^+$	Chromosomal, single copy *cpxP'-lacZ*$^+$ integrated at λRS88	Raivio & Silhavy, 1997

Table 2-2 Oligonucleotide primers used in this study

Primer name	Sequence* (5' to 3')
pTrc99Aseq-fw	TGCAGGTCGTAAATCACTGC
pTrc99Aseq-rv	CTGGCAGTTCCCTACTCTCG
pCpxAseq-fw	ATGATAGGCAGCTTAACCGCGC
pCpxAseq-rv	GGCAAGGAATTCCTGTGGCCC
XA-1 fw	ATAGGATCCGTGAGGAGGTTCCTATGATAGGC AGCTTAACCGCGC
XA-2b rv	GGCAAGGAATTCCTGTGGCCC

XA-2c rv	TATATAAGCTTCTGCAGTTATGACCGCTTATAC AGCGGCAACCAAATCACC
XA-3 fw	AAGCTTCTGGATAGCGAACAGCGTC
XA-4 rv	GACGCTGTTCGCTATCCAGAAGCTTGGTCATCT GGCGTGAATCGAGC
XA-5 fw	AGATTGAGCAGCATGTCGAAGCG
XA-6 rv	CGCTTCGACATGCTGCTCAATCTTCAGACCCTG ACGCTGTTCGCT
XA-7 fw	AAAAACGCCGATCATCCGCAGAAG
XA-8 rv	CTTCTGCGATGATCGGCGTTTTTGGCCTGACCA ATAAAGTTACGAATGATCTGC
CpxA E_{37}A-fw	CCAGATGACCGCGCTTCTGGATA
CpxA E_{37}A -rv	CGTGAATCGAGCTTGGGTA
CpxA D_{40}A-fw	CGAGCTTCTGGCAAGCGAACAGC
CpxA D_{40}A-rv	GTCATCTGGCGTGAATCG
CpxA M_{48}A-fw	TCAGGGGCTGGCGATTGAGCAGC
CpxA M_{48}A-rv	CGCTGTTCGCTATCCAGA
CpxA E_{91}A-fw	GGTGACCACCGCTGGCCGCGTGA
CpxA E_{91}A-rv	AATAACAAACGCTGTCCTGGC
CpxA D_{113}A-fw	TGGTCAGGCCGCAAACGCCGATC
CpxA D_{113}A-rv	ATAAAGTTACGAATGATCTGCATTTCG
CpxA E_{91}K-fw	GGTGACCACCAAAGGCCGCGTGA
CpxA E_{91}K-rv	AATAACAAACGCTGTCCTGGCGG

CpxA D_{113}A-fw for double mutant	TGGTCAGGCCGCTAACGCCGATC
CpxA D_{113}A-rv for double mutant	ATAAAGTTACGAATGATCTGCATTTCGCTG
CpxP R_{56}E-fw	CGAACATCAGGAACAGCAGATGC
CpxP R_{56}E-rv	GTTAAACTTATGCCGTCG
CpxP R_{60}E-fw	TCAGCAGATGGAAGATCTTATGCAAC
CpxP R_{60}E-rv	CGCTGATGTTCGGTTAAAC
CpxP R_{67}E-fw	GCAACAGGCCGAACACGAACAGC
CpxP R_{67}E-rv	ATAAGATCTCGCATCTGC
CpxP double R_{56}E+R_{60}E-fw	GATGGAAGATCTTATGCAACAGGCC
CpxP double R_{56}E+R_{60}E-rv	TGCTGTTCCTGATGTTCGGTTAAACTTATG
CpxP double R_{60}E+R_{67}E-fw	CAACAGGCCGAACACGAACAGCCTCCTGTT
CpxP double R_{60}E+R_{67}E-rv	CATAAGATCTTCCATCTGCTGACGCTGATG
CpxA E_{138}K-fw	GCGTGATGGCAAAGATAATTACCAACTTTATC
CpxA E_{138}K-rv	ACGGAGAACGGACCGACC
CpxA E_{138}A-fw	GCGTGATGGCGCAGATAATTACCAAC
CpxA E_{138}A-rv	ACGGAGAACGGACCGACC
CpxP R_{139}E-fw	ACATCAACAAGAAATGGAGCAGTTGC
CpxP R_{139}E-rv	TTCTCGTTTAAAACCGCTTG
CpxA T_{89}-TAG-fw	GTTATTGGTGTAGACCGAAGGCCGCGTG
CpxA T_{89}-TAG-rv	AAACGCTGTCCTGGCGGT
CpxA T_{90}-TAG-fw	ATTGGTGACCTAGGAAGGCCGCGTG
CpxA T_{90}-TAG-rv	AACAAACGCTGTCCTGGC
CpxA E_{91}-TAG-fw	GGTGACCACCTAGGGCCGCGTGA

CpxA E_{91}-TAG-rv	AATAACAAACGCTGTCCTGGC
CpxA G_{92}-TAG-fw	GACCACCGAATAGCGCGTGATCG
CpxA G_{92}-TAG-rv	ACCAATAACAAACGCTGTC
CpxA R_{93}-TAG-fw	CACCGAAGGCTAGGTGATCGGCG
CpxA R_{93}-TAG-rv	GTCACCAATAACAAACGC
CpxA A_{112}-TAG-fw	TATTGGTCAGTAGGATAACGCCGATC
CpxA A_{112}-TAG-rv	AAGTTACGAATGATCTGC
CpxA D_{113}-TAG-fw	TGGTCAGGCCTAGAACGCCGATC
CpxA D_{113}-TAG-rv	ATAAAGTTACGAATGATCTGCATTTCG
CpxA N_{114}-TAG-fw	TCAGGCCGATTAGGCCGATCATC
CpxA N_{114}-TAG-rv	CCAATAAAGTTACGAATGATCTG
CpxA D_{116}-TAG-fw	CGATAACGCCTAGCATCCGCAGA
CpxA D_{116}-TAG-rv	GCCTGACCAATAAAGTTACG
CpxA H_{117}-TAG-fw	TAACGCCGATTAGCCGCAGAAGA
CpxA H_{117}-TAG-rv	TCGGCCTGACCAATAAAG
CpxP M_{63}-TAG-fw	GCGAGATCTTTAGCAACAGGCCC
CpxP M_{63}-TAG-rv	ATCTGCTGACGCTGATGTT
CpxP A_{66}-TAG-fw	TATGCAACAGTAGCGGCACGAACAG
CpxP A_{66}-TAG-rv	AGATCTCGCATCTGCTGAC
CpxP R_{67}-TAG-fw	GCAACAGGCCTAGCACGAACAGC
CpxP R_{67}-TAG-rv	ATAAGATCTCGCATCTGCTG
CpxP H_{68}-TAG-fw	ACAGGCCCGGTAGGAACAGCCTC
CpxP H_{68}-TAG-rv	TGCATAAGATCTCGCATCTGCTG

CpxP Q_{70}-TAG-fw	CCGGCACGAATAGCCTCCTGTTA
CpxP Q_{70}-TAG-rv	GCCTGTTGCATAAGATCTCGC
CpxP H_{136}-TAG-fw	AAACGAGAAATAGCAACAACGAATGGAG
CpxP H_{136}-TAG-rv	AAAACCGCTTGCTGCTCC
CpxP Q_{138}-TAG-fw	GAAACATCAATAGCGAATGGAGC
CpxP Q_{138}-TAG-rv	TCGTTTAAAACCGCTTGC
CpxP R_{139}-TAG-fw	ACATCAACAATAGATGGAGCAGTTGCG
CpxP R_{139}-TAG-rv	TTCTCGTTTAAAACCGCTTG
CpxP Q_{142}-TAG-fw	ACGAATGGAGTAGTTGCGTGACG
CpxP Q_{142}-TAG-rv	TGTTGATGTTTCTCGTTTAAAACCG
CpxP L_{143}-TAG-fw	AATGGAGCAGTAGCGTGACGTGA
CpxP L_{143}-TAG-rv	CGTTGTTGATGTTTCTCGTTTAAAACC

* Underlined sequences denote restriction endonucleases cut sites (*Eco*RI: GAATTC, *Bam*HI: GGATCC, *Hind*III: AAGCTT).

2.20 References

Buelow, D. R., & Raivio, T. L. (2005). Cpx signal transduction is influenced by a conserved N-terminal domain in the novel inhibitor CpxP and the periplasmic protease DegP. *Journal of Bacteriology*, *187*(19), 6622–6630. https://doi.org/10.1128/JB.187.19.6622-6630.2005

Casadaban, M. J. (1976). Transposition and fusion of the *lac* genes to selected promoters in *Escherichia coli* using bacteriophage lambda and Mu. *Journal of Molecular Biology*, 104(3), 541–555.

Chin, J. W., Martin, A. B., King, D. S., Wang, L., & Schultz, P. G. (2002). Addition of a photocrosslinking amino acid to the genetic code of *Escherichia coli*. *Proceedings of the National Academy of Sciences of the United States of America*, 99(17), 11020–11024.

Danese, P. N., & Silhavy, T. J. (1998). CpxP, a stress-combative member of the Cpx regulon. *Journal of Bacteriology*, *180*(4), 831–839.

Danese, P. N., Snyder, W. B., Cosma, C. L., Davis, L. J., & Silhavy, T. J. (1995). The Cpx two-component signal transduction pathway of *Escherichia coli* regulates transcription of the gene specifying the stress-inducible periplasmic protease, DegP. *Genes & Development*, *9*(4), 387–398.

Ho, S. N., Hunt, H. D., Horton, R. M., Pullen, J. K., & Pease, L. R. (1989). Site-directed mutagenesis by overlap extension using the polymerase chain reaction. *Gene*, 77(1), 51–59.

Jobling, M. G., & Holmes, R. K. (1990). Construction of vectors with the p15a replicon, kanamycin resistance, inducible *lacZ alpha* and pUC18 or pUC19 multiple cloning sites. *Nucleic Acids Research*, 18(17), 5315–5316.

Kitagawa, M., Ara, T., Arifuzzaman, M., Ioka-Nakamichi, T., Inamoto, E., Toyonaga, H., & Mori, H. (2005). Complete set of ORF clones of *Escherichia coli* ASKA library (A Complete Set of *E. coli* K-12 ORF Archive): Unique Resources for Biological Research. *DNA Research*, 12(5), 291–299.

Konovalova, A., Perlman, D. H., Cowles, C. E., & Silhavy, T. J. (2014). Transmembrane domain of surface-exposed outer membrane lipoprotein RcsF is threaded through the lumen of β-barrel proteins. *Proceedings of the National Academy of Sciences of the United States of America*, 111(41), E4350–E4358.

Laemmli, U. K. (1970). Cleavage of structural proteins during the assembly of the head of bacteriophage T4. *Nature*, 227, 680–685.

Lobos, S. R., & Mora, G. C. (1991). Alteration in the electrophoretic mobility of OmpC due to variations in the ammonium persulfate concentration in sodium dodecyl sulfate-polyacrylamide gel electrophoresis. *Electrophoresis*, 12(6), 448–450.

Lu, J., Peng, Y., Arutyunov, D., Frost, L. S., & Glover, J. N. M. (2012). Error-prone PCR mutagenesis reveals functional domains of a bacterial transcriptional activator, TraJ. *Journal of Bacteriology*, 194(14), 3670–3677.

Raivio, T. L., & Silhavy, T. J. (1997). Transduction of envelope stress in *Escherichia coli* by the Cpx two-component system. *Journal of Bacteriology*, *179*(24), 7724–7733. https://doi.org/10.1128/JB.179.24.7724-7733.

Raivio, T. L., Leblanc, S. K. D., & Price, N. L. (2013). The *Escherichia coli* Cpx envelope stress response regulates genes of diverse function that impact antibiotic resistance and membrane integrity. *Journal of Bacteriology*, *195*(12), 2755–2767. https://doi.org/10.1128/JB.00105-13

Raivio, T. L., Popkin, D. L., & Silhavy, T. J. (1999). The Cpx envelope stress response is controlled by amplification and feedback inhibition. *Journal of Bacteriology*, *181*(17), 5263–5272.

Sambrook, J., Fritsch, E. F., & Maniatis, T. (1989). Molecular cloning: a laboratory manual. 2nd ed. *Cold Spring Harbor Laboratory Press*, Cold Spring Harbor, N.Y.

Silhavy, T. J., Berman, M. L., & Enquist, L. W. (1984). Experiments with gene fusions. *Cold Spring Harbor Laboratory Press*, Cold Spring Harbor, N.Y.

Simons, R. W., Houman, F., & Kleckner, N. (1987). Improved single and multicopy *lac*-based cloning vectors for protein and operon fusions. *Gene*, 53(1), 85–96.

Slauch, J.M., & Silhavy, T.J. (1991). cis-Acting *ompF* mutations that result in OmpR-dependent constitutive expression. *Journal of Bacteriology*, 173, 4039–4048.

The Benchling Enterprise Academic Platform, Molecular Biology Suite tool. *Benchling Inc*. https://benchling.com/enterprise/molecular-biology.

The GraphPad Prism computational software version 7.04. *GraphPad Software.*

The PyMOL Molecular Graphics System, Version 1.2. *Schrödinger, LLC.*

Thede, G. L., Arthur, D. C., Edwards, R. A., Buelow, D. R., Wong, J. L., Raivio, T. L., & Glover, J. N. M. (2011). Structure of the periplasmic stress response protein CpxP. *Journal of Bacteriology, 193*(9), 2149-2157. doi:10.1128/JB.01296-10

Towbin, H., Staehelin, T., & Gordon, J. (1979). Electrophoretic transfer of proteins from polyacrylamide gels to nitrocellulose sheets: procedure and some applications. *Proceedings of the National Academy of Sciences of the United States of America,* 76, 4350–4354.

Wong, J. L. (2015). Cellular role of the inhibitor-chaperone CpxP in *Escherichia coli*. PhD thesis, University of Alberta, Alberta, Canada.

Chapter 3: Results

3.1 Introduction

The crystal structures and electrostatic surface representations for both the soluble *E. coli* $CpxA_{SD}$ (Thede., 2012) and CpxP (Thede et al., 2011) were previously solved in collaboration with Dr. Mark Glover's laboratory research group (Biochemistry Department, University of Alberta) and were established to be dimers of similar size and exhibiting some interesting features regarding their surface and shape. For instance, the CpxP dimer has a striking concave bowl shape lined with highly basic and positively charged amino acid residues, comprising large positive patches, whereas its convex surface on the other side of the bowl is predominantly negative and contains a hydrophobic band (Figure 1-5) (Thede et al., 2011; Zhou et al., 2011). In contrast, the $CpxA_{SD}$ surface displays negative patches of amino acid residues on what could be considered the top of its structure (facing toward the periplasmic space), and positive zones underneath that may be allowing for it to remain in contact with negatively charged molecules in the IM (Figure 1-4) (Margain-Quevedo et al., in preparation). Through the observation of such electrostatic characteristics on the surface of these two Cpx components, I reasoned that the periplasm-exposed negatively charged residues on the $CpxA_{SD}$ may be of importance for allowing its direct protein-protein interaction with positive charges on the surface of other ligands or partners in the periplasm, specifically in the case of the positively-charged concavity located in CpxP. I hypothesized that the surface-exposed amino acid patches of CpxA may form ligand binding sites important for signaling, and specifically for the formation of putative $CpxA_{SD}$-CpxP direct protein-protein interaction, that is believed to regulate the pathway's active and inactive states. To test this hypothesis, I conducted structure-based site-directed mutagenesis assays aimed at individual amino acids that comprise charged regions on both components, and assessed the effect of such substitutions on Cpx pathway activity by means of using a chromosomal *cpxP'-lacZ*$^{+}$ reporter

gene. Additional assays to determine Cpx sensitivity to the inhibitory or inducing ability of *cpxP* or *nlpE* overexpression, respectively, were also performed to determine the extent of the effect of each amino acid substitution, and protein stability determinations were carried out through SDS-PAGE and Western blotting (Raivio et al., 1999). Second-site suppressors in CpxP potentially able to compensate charge-swap effects on CpxA were then tested, and I also attempted to develop a novel $CpxA_{SD}$:CpxP protein-protein interaction assay utilizing UV-induced photocrosslinking in the presence of the artificial amino acid *p*BPA (Konovalova et al., 2014).

3.2 Alkaline pH induces the Cpx response in a Δ*cpxA* (pCA24N-*cpxA*WT) strain, while acid pH hyperactivates the Δ*cpxA* (pCA24N) vector control strain

During the early stages of the research project, I sought to establish the required media conditions in which the Cpx pathway could be induced by alkaline pH 8.0 (Danese & Silhavy, 1998) in a Δ*cpxA* strain complemented with a plasmid carrying the *cpxA* gene, but not in its corresponding vector control strain. Three different IPTG concentrations were used to induce gene expression (0mM, 0.1mM and 1mM IPTG) and results were compared to those obtained under acidic (5.8) and neutral (7.0) pH conditions. The reasoning behind setting up such an experiment was to establish specific conditions that could be applied for screening site-directed mutations in subsequent assays, since complementation analysis has been proven to be a powerful technique when characterizing genes and their products (Jobling & Holmes, 1990). For this, the chloramphenicol-resistant pCA24N plasmid was transformed into a TR50 *cpxA*-null *E. coli* laboratory strain derived from MC4100 (RM53, which will be referred to as "Δ*cpxA*" from this point forward, and that harbors the chromosomal *cpxP'-lacZ*$^{+}$ transcriptional reporter gene that strongly responds to activation of the Cpx signaling cascade (Raivio & Silhavy, 1997)). The Δ*cpxA*

(pCA24N) strain obtained by this transformation was used in this assay as the vector control and would be compared with a *cpxA* complemented strain (RM55 or Δ*cpxA* (pCA24N-*cpxA*WT)), obtained by transforming the pCA24N plasmid containing the wildtype *cpxA* gene into the Δ*cpxA* strain. Both strains were subcultured 1:50 from overnight liquid cultures into LB broth and grown for a total of 5 hours (an OD_{600} of approximately 0.6-0.8), with the addition of the corresponding sodium-phosphate buffered LB media at pH 5.8, 7.0 or 8.0, and either 0.1mM or 1mM IPTG for plasmid induction, both after the first 2 hours of incubation time. Next, the *cpxP'-lacZ*$^{+}$ reporter gene activity of each strain under every IPTG-pH experimental combination was measured by the β-galactosidase assay using a microplate reader (described in section 2.9 of this work).

As observed in Figure 3-1, the Δ*cpxA* vector control strain grown either with or without IPTG at acid pH was found to have highly increased reporter activation, likely due to direct phosphorylation of CpxR in the cytoplasm. In contrast, the Δ*cpxA* (pCA24N-*cpxA*WT) complemented strain showed a 10-fold decrease in Cpx activity as compared to its respective vector control at pH 5.8. Moreover, neutral pH was not a sufficient condition to induce a response from the complemented strains as compared to their respective vector controls and has not been previously reported to activate the pathway.

The condition that better resulted in Cpx activation of the Δ*cpxA* (pCA24N-*cpxA*WT) strain compared to its Δ*cpxA* (pCA24N) control was alkaline pH 8.0 without added IPTG, which suggests that low levels of constitutive expression are still observable even without the addition of the inducer (Figure 3-1). A statistically significant difference was also observed at alkaline pH after the addition of 0.1mM and 1mM IPTG, so it was established that the next experiments for activating the pathway by alkalinized media would be done at pH 8.0 and either without IPTG or with IPTG added to a final concentration of 0.1mM (concentration commonly used for gene

expression, while 1mM is usually added to microarray assays instead) to further induce gene expression. These results are consistent with previous findings demonstrating that a response under alkaline conditions is mounted depending on presence of both the CpxA and CpxR components of the system (Danese & Silhavy, 1998).

3.3 The sub-cloned pK184-*cpxA*WT complements a Δ*cpxA* strain at pH 8.0

I initially planned on utilizing the pCA24N-*cpxA*WT plasmid as template for the upcoming mutagenesis assays to introduce substitutions into *cpxA*, by means of the overlap extension PCR technique in collaboration with Dr. Jun Lu (Department of Biochemistry, Faculty of Medicine and Dentistry). However, it was determined that this *cpxA* expression vector was not completely adequate for this purpose, due to various reasons: it presented compatibility issues with the pCA-*nlpE* overexpression vector (both having chloramphenicol resistance genes) that I planned on using in subsequent experiments, it is a high copy number plasmid and the MCS is not optimal for our approach (Kitagawa et al., 2005).

I then decided to sub-clone *cpxA* into the pK184 plasmid, chosen since it has desired characteristics for site-directed mutagenesis and complementation assays, including: a kanamycin resistance marker; conveniently localized *Bam*HI, *Eco*RI and *Hind*III; an IPTG-inducible and leaky *lac* promoter that expresses low activity levels even without induction (thus can be used to constitutively synthesise proteins for complementation experiments); a *lacZ*-α gene fragment allowing to easily select inserts and control their expression; and low copy number with a p15a origin of replication (Jobling & Holmes, 1990), to obtain pK184-*cpxA*WT (Figure 3-2A). I also sub-cloned *cpxA*WT into the pJ307 vector (which is the same pK184 plasmid but contains a cloned *traJ* gene) to generate pJ307-*cpxA*WT. The *traJ* gene located between the *lac* promoter and the

*cpxA*WT and *lacZ*-α genes in the pJ307 plasmid has a transcriptional terminator able to further attenuate expression of the downstream *cpxA* and *lacZ*-α genes (Lu et al., 2012). This pJ307-*cpxA*WT plasmid was then also available to be used as a backup to pK184-*cpxA*WT for *cpxA* mutagenesis assays, in the potential case of the leaky lac promoter in pK184 leading to very high *cpxA* expression (potentially resulting in the compensation or masking of mutational effects that I was interested in observing).

As presented in Figure 3-2B, the sub-cloning of *cpxA*WT into pK184 was able to return *cpxP'-lacZ*$^{+}$ reporter activity back to WT activity levels when transformed into a *cpxA* null mutant, at alkaline pH. However, this was not the case for the strains carrying pJ307-*cpxA*WT, since the activation levels observed from these colonies were even lower than the activity retrieved from the vector control strain. Intriguingly, the pJ307-*cpxA*WT strains were not able to grow adequately under the same conditions in LB broth as the rest of the strains at 37°C, possibly affecting its ability to activate the Cpx pathway and produce β-galactosidase (observations not shown). Based on these results, I decided to continue the next set of assays with the pK184-*cpxA*WT complemented strain as a positive control (referred to as the pCpxA strain from this point forward) and use this vector as the template to introduce mutations into *cpxA*. I would also be using the pK184-*traJ* (deemed VC) plasmid as the negative vector control, since the *lacZ* expression levels from this vector alone are practically negligible due to the presence of the *traJ* gene, being reported at around only 50 Miller Units (Lu et al., 2012). This VC strain will represent an activity baseline level in further assays to be compared with results from the mutated strains, since its activity is approximately the same to the one observed in the Δ*cpxA* strain (Figure 3-2B).

3.4 The pCpxA-D_{113}K mutant hyperactivates the Cpx response at pH 5.8, 7.0 and 8.0

After finalizing the construction of my vector control and *cpxA*WT complemented strains, I decided that the next step would be to introduce lysine (K) individual substitutions to amino acid residues E_{37} and D_{113}, since they comprise two of the major periplasmic surface-exposed negatively charged patches in the $CpxA_{SD}$ of *E. coli*, to try to observe a dramatic phenotypic effect as compared to my controls, by swapping these residues with the positively charged lysine. The M_{48} residue located at the centre of the dimerization interface between the two $CpxA_{SD}$ monomers would be mutated as well, to test its potential importance in maintaining structural integrity of the dimer, and response ability. The specific location within the $CpxA_{SD}$ dimer for the *cpxA* E_{37}K, M_{48}K and D_{113}K mutations introduced into the pK184 vector can be observed in the crystal representations displayed in Figures 3-2C and 3-2D.

I sought to determine whether there would be any differences in expression levels of the *cpxP'-lacZ*$^+$ reporter gene in these mutants due to differences in the pH of the media. This was done by performing a set of β-galactosidase tests on these strains, using acid (5.8), neutral (7.0) and alkaline (8.0) phosphate-buffered LB media within the same experiment. The reasoning behind this was to investigate whether the individual charge-swap mutations could still activate the Cpx pathway under the alkaline inducing condition (Danese and Silhavy, 1998) as compared to their activity in non-inducing acid and neutral pH media (as well as to the trends observed in the complemented and VC strains), and determine whether there was an impact on CpxA kinase or phosphatase activities (at alkaline and acid pH, respectively).

Both the WT and pCpxA complemented strains responded toward the inducing cue of pH 8.0 with a 7- to 12-fold induction as compared to pH 5.8, reaching over 1,000 MU. However, the pathway was inactive in these two strains at acid and neutral pH, as expected (Figure 3-3A). The

null *cpxA* and VC strains were activated by acid pH, due to consistent cytoplasmic phosphorylation of CpxR in the absence of *cpxA* and had an 8-fold decrease at pH 8.0 as compared to 5.8, confirming my previous results (Figure 3-1). It is of relevance to highlight that all four of these strains had a statistically significant difference (either of increase or decrease, respectively) when comparing activity levels between acid and alkaline pH within each of them (Figure 3-3A).

Mutants $E_{37}K$ and $M_{48}K$ showed similar trends to the ones observed within the complemented and WT strains, in which alkaline pH activity values were higher than their respective acid and neutral pH results. Nevertheless, these two mutated strains exhibited lower activation levels at all three pH conditions when compared to the positive control strains, possibly suggesting their importance in structural stability for the $CpxA_{SD}$ to be able to mount an adequate response to this specific stressor. In addition, $E_{37}K$ results at alkaline pH were statistically different from the empty VC strain, but the $M_{48}K$ mutant did not show a significant difference when compared to the negative control. This could mean that the nature of the two individual residues may be of importance for the structural configuration needed to activate the pathway, and specifically the M_{48} residue in between both monomers may be required (Figure 3-3A).

Finally, the most striking result from these experiments was the hyperactivated "on" signaling phenotype of the Cpx pathway exerted by the $D_{113}K$ mutation at all three pH conditions assayed (Figure 3-3A). The gain-of-function phenotype of approximately 4,000 Miller Units denotes a constitutive upregulation of the *cpxP* promoter fused to the *lacZ* gene from the reporter, by means of CpxR~P acting as a transcription factor and thus regulating the expression of *lacZ* and production of very high amounts of β-galactosidase.

3.5 $CpxA_{SD}$ hyperactivation exerted by $D_{113}K$ presents a blind phenotype toward inhibition by overexpressed *cpxP* and further induction by *nlpE* overexpression

It is of importance to remark that *cpxP* overexpression (OX) has been demonstrated to downregulate the Cpx response in a wildtype background (dependent on CpxA). CpxP is hypothesized to ultimately be able to turn off the pathway when it is no longer required and keep it that way under beneficial environmental conditions (Buelow and Raivio 2005; Raivio et al., 1999). Since the capacity to shut off the pathway was significantly compromised in the pCpxA-$D_{113}K$ variant even under the non-inducing cues of acid and neutral pH, I wanted to know whether such signaling phenotype was related to a desensitization toward CpxP and its ability to inhibit the response. To test this, I transformed the *cpxP* OX plasmid (pCpxP) and its corresponding empty vector (pTrc99A) individually into the same seven strains studied in my previous pH-related assay and conducted a β-galactosidase test under neutral pH. As expected for the WT and pCpxA strains transformed with pCpxP, the activity levels observed were approximately 5-fold lower than those in the same strain but transformed with the parent empty plasmid (Figure 3-3B). This demonstrates the ability of overproduced CpxP to generate a maximum repression level through CpxA at uninduced conditions (Raivio et al., 1999). Meanwhile, both strains lacking *cpxA* (including the double empty vector negative control strain) did not exhibit differences in reporter gene expression after *cpxP* was induced by IPTG, as compared to their pTrc99A results (Figure 3-3B). It can also be observed that the $E_{37}K$ and $M_{48}K$ mutated strains are still sensitive to further inhibition by c*pxP* OX at levels comparable to those from the positive control strains carrying the *cpxA*WT genes, and both showed a significant difference when compared to their pTrc99A control. These results suggest that the phenotypes observed at different pH values in Figure 3-3A for these two mutated strains are not due to a defect in recognition of CpxP. The most outstanding result from this assay

was that the $D_{113}K$ substitution still showed a hyperactivated state of around 12-fold increased as compared to the *cpxA*WT strains. Overexpression from pCpxP was not able to diminish this strain's activity when compared to the same strain carrying the pTrc99A vector instead. This substitution seemingly caused a complete loss in $CpxA_{SD}$ sensitivity to CpxP silencing, presenting now a CpxP-blind phenotype instead (Figure 3-3B).

To further investigate the extent of the effect that these first three lysine substitutions in the $CpxA_{SD}$ had on reporter levels, I decided to utilize *nlpE* OX. This is another well studied inducing signal of the Cpx response, so these new assays would determine if the mutated strains are still sensitive toward such induction. Overproduced NlpE has been previously determined to exert Cpx pathway activation dependent on the presence of a functional CpxA histidine kinase sensor, likely due to the synthesis of misfolded or mislocalized NlpE in the envelope (Snyder et al., 1995; Vogt et al., 2012; Vogt & Raivio, 2012). NlpE has also been shown to activate the Cpx two-component system in relation to adherence to hydrophobic surfaces (Otto & Silhavy, 2002). For these experiments, I transformed the *nlpE* OX vector (pCA-*nlpE*) and its parental empty vector control (pCA24N) into the same set of strains from my assay in Figure 3-3A, and ran a new β-galactosidase assay. As I expected, both strains containing *cpxA*WT were 6-fold induced by overproduction of NlpE as compared to the reporter levels resulting from the same strains containing the pCA24N vector (Figure 3-3C). In contrast, the null *cpxA* strain and the one with the vector control for *cpxA* were not significantly induced by *nlpE* overexpressed from its multicopy plasmid, thus confirming previously published results and highlighting the need for CpxA to recognize this cue and initiate a response (Otto & Silhavy, 2002; Snyder et al., 1995; Vogt et al., 2012; Vogt & Raivio, 2012). The strains containing pCpxA-$E_{37}K$ and $M_{48}K$ substitutions were still induced by this stimulus to an extent, as the results are statistically significant when compared

to the control strains harboring the pCA24N plasmid. As per Figure 3-C, the $E_{37}K$ strain presents a response phenotype almost identical to the WT, however $M_{48}K$ resulted in a loss of sensitivity of 2-fold when compared to the same control strain. This is similar to what was observed for this second mutation when induced by alkaline pH in Figure 3-A but to a more minor extent, suggesting a potential stimulus-specific effect for this mutant and potentially a defective recognition to adhesion. Once again, the striking result from this graph is that even though the $D_{113}K$ substitution was able to be further induced by *nlpE* OX to a minor degree, the fold change for this induction was only 1.2 and it is still hyperactivated, reaching about 3,000 MU even when only harboring the vector control. This phenotype can be described as a partially-blind signaling phenotype toward NlpE induction of the Cpx response (Figure 3-3C).

3.6 The $E_{91}A$ and $D_{113}A$ substitutions result in hyperactivation under alkaline pH only, with $E_{91}A$ displaying higher activity levels between these two

After analyzing the results obtained after performing charge-swap single mutations to amino acid residues E_{37}, M_{48} and D_{113}, I wanted to determine if the signaling phenotypes observed in Figures 3-3A to 3-3C were a result of this charge modification from negative to positive or just an effect of modifying these residues. To test this, I created a new set of mutated strains harboring the pCpxA plasmid with alanine substitutions to amino acid residues E_{37}, M_{48} and D_{113}, and now included D_{40} and E_{91} as well (two additional residues comprising negatively charged regions of the $CpxA_{SD}$). I decided to modify the residues to alanine as these new substitutions might help prevent any potential large structural changes that could occur as result of making charge swap changes. Alanine was also chosen to further observe signaling effects and functional role of amino acid residues, since it no longer possesses a side chain beyond the β carbon and does not significantly

modify the configuration of the main chain (Lefèvre, Rémy & Masson., 1997). The specific location within the $CpxA_{SD}$ dimer for the $E_{37}A$, $D_{40}A$, $M_{48}A$, $E_{91}A$ and $D_{113}A$ mutations introduced into the pCpxA vector can be observed in the structure representations displayed in Figures 3-4A and 3-4B.

I again sought to determine first whether there would be any differences in expression levels of the reporter gene in the *ΔcpxA* mutant complemented with the alanine substitution mutants due to differences in the pH of the media, and as compared to my previous lysine substitution assay. As anticipated, the WT and pCpxA complemented strains responded to the inducing cue of alkaline pH, with a 7- to 12-fold induction as compared to acid or neutral pH of the growth media, while the *ΔcpxA* and VC strains were activated at pH 5.8 (Figure 3-4C), confirming my previous results from Figure 3-3A. Alanine substitutions to all five amino acids resulted in similar trends in regard to only resulting in activation under alkaline pH condition in a statistically significant manner as compared to acid pH, with milder phenotypes than the ones observed when the same residues were substituted by lysine. The $E_{37}A$, $D_{40}A$ and $M_{48}A$ mutants displayed 1.2- to 1.8-fold lower activity levels as compared to the pCpxA strain at pH 8.0, in similarity to the results described for the $E_{37}K$ and $M_{48}K$ strains in section 3.5. However, reporter gene activity levels of the strains carrying the alanine mutants were considerably higher in alkaline conditions when compared to the results obtained for the VC strain under the same condition (Figure 3-4C).

Interestingly, the $E_{91}A$ mutant resulted in the highest expression of the reporter gene, reaching up to almost 4,000 Miller Units and a hyperactivated state, but only in alkaline pH, unlike the previous $D_{113}K$ mutant which displayed these same activity levels but irrespective of media pH (Figure 3-3A). Even though activity levels for this $E_{91}A$ strain were higher at acid and neutral

pH than the ones displayed by pCpxA and WT strains, they did not reach the same activation levels resulting from alkaline pH induction (Figure 3-4C). Notably and a bit unexpectedly, the alanine substitution to D_{113} completely modifies the signaling phenotype observed in Figure 3-3A for this same residue when substituted with lysine. Alanine at the 113th position of the $CpxA_{SD}$ results in trends and activity values similar to the positive control strains, in the sense that activation is now only observed at the inducing pH 8.0 condition and not at pH 5.8 or 7.0. Activity levels do not reach anywhere close to the previously observed 4,000 Miller Units, suggesting an important role for signaling dependent on the charge of the amino acid at this position (Figure 3-4C).

3.7 The E_{91}A mutant is not sensitive to inhibition by *cpxP* OX but can be further induced by *nlpE* OX, while D_{113}A responds to both OX conditions

Even though the ability to shut down the response at non-inducing conditions was not extremely impaired in the pCpxA-E_{91}A mutant and especially not in the D_{113}A mutated strain, activity levels at all three pH values assayed were higher for the E_{91}A strain as compared to the levels observed in each of these conditions for the WT strain (Figure 3-4C). I was interested in determining if these higher than usual activation results would correlate to loss in sensitivity toward either inhibition by *cpxP* OX or further induction by *nlpE* OX, and how these results would compare to the observations made from my previous lysine substitution analysis from Figures 3-3B and C.

To start to investigate this, pCpxP and pTrc99A were co-transformed into the *cpxA* null strain carrying the individual pCpxA plasmids with the five alanine substitutions, and β-galactosidase activity as a result of the reporter gene was measured. The results for the WT and pCpxA strains were once again verified, with *cpxP* OX able to reduce the reporter activity levels

by 3-fold as compared to the vector control pTrc99A (Raivio et al., 1999), while the null *cpxA* and VC strains were not sensitive to this inhibition, since CpxA is not present in them (Figure 3-4D). In comparison, the strains with *cpxA* alleles carrying $E_{37}A$ and $D_{40}A$ substitutions displayed comparable sensitivity levels and inhibition rendered by pCpxP to those observed for the positive control strains. CpxA carrying the $M_{48}A$ substitution located at the center of both CpxA monomers exhibited similar sensitivity, with reporter gene activity levels that were lower than the ones obtained for the WT strains, revealing an importance of this residue for proper Cpx activation by the $CpxA_{SD}$ and potential interaction with partner proteins. The higher activity levels obtained in the presence of the $E_{91}A$ substituted CpxA were not decreased in a statistically significant manner by pCpxP, depicting a loss in sensitivity to CpxP inhibition. This potentially due to an interaction site being compromised by this substitution of E_{91}, even though it was only an alanine mutant and not a charge-swap. It is also very relevant to note that the D_{113} residue in CpxA was still able to be inhibited by *cpxP* OX when mutated to alanine (Figure 3-4D), even though activity levels observed in the pCpxA-$D_{113}A$ (pTrc99A) strain were a bit higher than the WT ones. This was not the case for the $D_{113}K$ strain (Figure 3-3B), possibly suggesting that the specific negative charge from this residue (which comprises a major negative patch on the structure's surface) could be an interaction or docking site for CpxP.

In regard to the induction effect that *nlpE* OX had on the alanine substituted strains, both the WT and pCpxA strains were susceptible to pathway activation by this signal, but no significant increase in reporter levels was observed in the *ΔcpxA* and VC strains, as predicted and observed previously for these controls (Figures 3-3C and 3-4E). I now saw an interesting phenotype regarding the $E_{37}A$ mutant, since this strain did not show increased activation levels under alkaline pH, however it responded more drastically to *nlpE* overexpression, increasing its activity by 10-

fold compared to the pCA24N empty plasmid (Figure 3-4E). The $D_{40}A$ and $M_{48}A$ mutants were still activated by overproduction of NlpE, to a similar degree by which the positive control pCpxA and WT strains were induced, and this time the $M_{48}A$ substitution did not have an effect of displaying lower capacity for this activation. Meanwhile, reporter gene activity in the strain carrying the $D_{113}A$ *cpxA* allele was further induced by 2-fold when compared to the WT strains, but it did not reach a hyperactivated state either. Yet again, the $E_{91}A$ mutant was the one that resulted in the highest induction of all of the strains in this assay, reaching over 2,000 MU. This was observed as a statistically significant increase of 1.5-fold from the result obtained in this same strain containing pCA24N, and demonstrated that the hyperactivated Cpx response in this mutant was still sensitive to further induction by *nlpE* OX (Figure 3-4E).

3.8 The $D_{113}K$ and $E_{91}K+D_{113}K$ mutations share the common phenotype of hyperactivation regardless of pH, while the $E_{91}K$, $E_{91}A$ and $E_{91}A+D_{113}A$ substitutions result in hyperactivation at pH 8.0 only

Mutation of charged, surface-exposed, negative amino acids (plus the buried M_{48} residue) in the $CpxA_{SD}$ identified two specific amino acids that exhibited extremely interesting signaling phenotypes when mutated. These resulted in either hyperactivation of the Cpx pathway at all pH values assayed and desensitization to both pCpxP inhibition and pNlpE further induction ($D_{113}K$), or a milder hyperactivation more evident at alkaline pH while still not responding to *cpxP* or *nlpE* OX ($E_{91}A$). These observations were similar to the results obtained years ago while analyzing the constitutively activated *cpxA** strains (Raivio & Silhavy, 1997; Raivio et al., 1999). The E_{91} and D_{113} residues have in common that they are located protruding externally of the structure and likely facing the periplasmic space, as per our crystal representation from Figure 3-5A and 3-5B. In order

to directly compare the lysine and alanine substitutions for these two residues, I compared their impact on reporter gene expression in the same experiment. I also examined the effect of mutating both these residues to either lysine or alanine at the same time, and additionally examined another charged residue on the surface of CpxA not previously investigated (E_{138}).

It can be observed in Figure 3-5C that the $E_{91}K$ mutant presented the same trend as when it was mutated to alanine ($E_{91}A$), as these strains were not hyperactivated at all pH conditions assayed, but instead were most highly induced at alkaline pH, even though acid and neutral pH results were also higher than the ones obtained in a WT strain. The lysine substitution for this residue resulted in higher activation than the corresponding E_{91} alanine mutation, which was expected to only show milder phenotypes due to the nature of the swap. In comparison, the strain carrying the *cpxA* allele with the double $E_{91}K+D_{113}K$ mutations showed a more similar phenotype to the single $D_{113}K$ substitution instead (hyperactivation at pH 5.8, 7.0 and 8.0 in levels 3-fold higher than the WT strain). However, the double mutant resulted in even higher reporter gene activity than the $D_{113}K$ strain, implying a possible additive effect between $E_{91}K$ and $D_{113}K$ mutations (Figure 3-5C). On the other hand, strains carrying the *cpxA* allele containing the double $E_{91}A+D_{113}A$ mutations displayed reporter gene activity comparable to the $E_{91}A$ strain in terms of total Miller units and a greater activation under alkaline pH. It can then be stated that a different additive effect from the one previously described for the CpxA $E_{91}K+D_{113}K$ strain was observed, since here the effect from $E_{91}A$ has more weight on the result of the double alanine mutant, while $D_{113}A$ is not hyperactivated even at pH 8.0. Neither the $E_{138}K$ nor the $E_{138}A$ new substitutions studied in this experiment were hyperactivated at any pH condition (Figure 3-5C).

3.9 The $E_{91}K$, $D_{113}K$, $E_{91}K+D_{113}K$, $E_{91}A$ and $E_{91}A+D_{113}A$ mutants are not inhibited by *cpxP* OX, while of these only $E_{91}A$ is significantly induced by *nlpE* OX

After studying how these mutations from Figure 3-5C would impact inhibition by *cpxP* OX or induction by *nlpE* OX, it can be observed in Figure 3-5D that none of the hyperactivated states obtained from either of the $E_{91}K$, $D_{113}K$, $E_{91}K+D_{113}K$, $E_{91}A$ or $E_{91}A+D_{113}A$ mutated strains were able to be suppressed by overproduction of CpxP. Only the strains containing *cpxA* alleles with the $E_{138}K$, $D_{113}A$ and $E_{138}A$ mutations displayed sensitivity toward *cpxP* OX inhibition in a statistically significant manner.

Regarding figure 3-5E, even though seemingly the $E_{91}K$, $D_{113}K$ and $E_{91}A+D_{113}A$ CpxA mutant strains displayed a statistically significant difference in reporter gene expression response to *nlpE* OX of either $P \leq 0.01$ for the first two or $P \leq 0.001$ (for the $E_{91}A+D_{113}A$ strain), they did not result in a fold increase of more than 1.5 when compared to the vector control for pNlpE. These strains were still further induced by *nlpE* OX but such recognition was now faulty, almost as affected as the results obtained for the ones carrying the *cpxA* alleles with the $E_{91}K+D_{113}K$ mutations. Reporter gene expression was only significantly induced by overexpression of *nlpE* in strains carrying *cpxA* alleles with the mutations $E_{138}K$, $E_{91}A$, $D_{113}A$ and $E_{138}A$ (Figure 3-5E). The most striking result from these two graphs when comparing results between both was that the $E_{91}A$ mutant could not be inhibited by pCpxP but could be further induced by pNlpE in a significant form.

3.10 CpxA protein levels of all the lysine and alanine mutants is not compromised by these substitutions

The next logical step to my investigation was that I needed to determine whether all of the mutational effects of the $CpxA_{SD}$ exerted on signaling phenotypes by the lysine and alanine substitutions were not due to differences in protein levels. Membrane preparations were made for each of these mutated strains and assayed by SDS-PAGE 12% gels followed by protein detection by semi-dry Western blotting, using an α-CpxA-MBP anti-rabbit primary antibody for CpxA detection, and an α-OmpA anti-rabbit primary antibody utilized for detecting the loading control, OmpA. Such loading control was selected since it was easy to detect and is an outer membrane protein that was not altered or deleted in my previous assays, so this would serve to confirm that the same amount of total protein was loaded into the gel even in the strains lacking *cpxA*.

All the pCpxA-$E_{37}K$, $M_{48}K$, $E_{91}K$, $D_{113}K$, $E_{91}K+D_{113}K$ and $E_{138}K$ lysine substitutions were indeed expressed, localized to the membrane and their protein levels were not affected as a result of the mutagenesis. These results are observable in Figure 3-6, displaying bands at approximately the size of CpxA (51.6 kDa) only on the blot obtained from the membrane preparations, but not in the one from the soluble fractions (Figure 3-6). The size and intensity of these bands were comparable to the results obtained for the positive control pCpxA and seem to be even more stable or expressed than the CpxA from the WT strain. This result may be due to the expression of CpxA from a multicopy plasmid instead of chromosomally, as is the case for the TR50 WT strain. Such observations were confirmed by comparing the results obtained for the null *cpxA* and VC strains, in which no band was detected for CpxA, however all the strains displayed a band in a separate blot corresponding to the OmpA loading control at 37 kDa. This confirmed that the same amount

of protein was loaded for every strain used in this experiment, even the ones lacking CpxA (Figure 3-6).

Similarly, all the pCpxA-$E_{37}A$, $D_{40}A$, $M_{48}A$, $E_{91}A$, $D_{113}A$, $E_{91}A$+$D_{113}A$ and $E_{138}A$ alanine substitutions did not exhibit signs of protein instability, since they all showed bands at approximately the expected size of 51.6 kDa for CpxA in the blot resulting from the membrane preparations only (Figure 3-7). Interestingly, it would seem as if the $M_{48}A$ and $D_{113}A$ expression levels were lower than those of the other alanine mutants, however all these strains displayed a similar band for the OmpA loading control (Figure 3-7), so this apparent difference might have occurred due to a random error while loading this specific gel. It was later confirmed on a repeat gel that all these alanine mutants exhibited a band of the correct size with similar intensity (Figure 3-7).

3.11 The $R_{139}E$ mutation in pCpxP partially complements the hyperactivation exerted by the $D_{113}K$ charge swap mutation in pCpxA

My previously described data indicated that the most dramatic hyperactivated signaling phenotypes obtained were caused by the swapping of negatively charged residues comprising surface-exposed negative patches in the $CpxA_{SD}$ to the positive residue lysine, and specifically were observed with the $E_{91}K$, $D_{113}K$ and double $E_{91}K$+$D_{113}K$ mutated strains (Figures 3-3A and 3-5C). In collaboration with Dr. Mark Glover, a potential docking model for the $CpxA_{SD}$-CpxP predicted interaction utilizing the available crystal structures of each of these components was developed using PyMOL (Figure 3-8). In this representation, two dimers of CpxP are configured in a manner for them to be interacting with each single monomer of the $CpxA_{SD.}$ Remarkably, some of the positive residues that comprise major patches in the positively charged polar concavity

of the CpxP bowl including R_{56}, R_{60}, R_{67} and R_{139} would seem to be located in close proximity of the E_{91} and D_{113} residues that I found to be of interest from the $CpxA_{SD}$ and protruding externally toward the periplasm, which could allow for specific docking sites that would facilitate this protein-protein interaction to happen (Figure 3-8). Additionally, it has been previously reported that CpxP substitutions $R_{56}Q$, $R_{60}Q$ and $R_{67}Q$ generated stable CpxP variants that are unable to exert their proper inhibitory capacity (Buelow & Raivio, 2005; Thede., 2012; Thede et al., 2011; Zhou et al., 2011). Taking this information into consideration, I designed a second-site suppressor experiment to test whether the $CpxA_{SD}$ hyperactivation exerted by the $E_{91}K$, $D_{113}K$ and $E_{91}K+D_{113}K$ mutants could be complemented back to WT levels by an opposite charge swap in the R_{56}, R_{60}, R_{67} and R_{139} residues (from positively arginine to negatively charged glutamate), which in such case could potentially indicate interaction sites between the two proteins. For this purpose, the pCpxP plasmid was mutated at the proposed four residues plus two double mutants were constructed ($R_{56}E+R_{60}E$ and $R_{60}E+ R_{67}E$). These plasmids were individually co-transformed into the $CpxA_{SD}$-substituted $E_{91}K$, $D_{113}K$ and $E_{91}K+D_{113}K$ strains, as well as the WT, pCpxA, *ΔcpxA* and VC strains. The expression of the Cpx-regulated *cpxP-lacZ* reporter gene was then compared to that of the pTrc99A vector control in a new set of β-galactosidase assays (Figure 3-9A to F).

The first important observation from these graphs was that the pCpxP glutamate substitutions do not modify activity of the reporter gene in the *cpxA* negative control strains, however they seem to impair the ability of overproduced mutated CpxP to inhibit the WT and pCpxA controls. Specifically, in strains carrying CpxP mutants $R_{56}E$, $R_{60}E$, $R_{56}E+R_{60}E$ and $R_{60}E+ R_{67}E$, the statistical significance of reporter gene inhibition was lower as compared to that exerted by the pCpxP WT plasmid (Figure 3-9A to F). Unfortunately, for the cases of pCpxP $R_{56}E$, $R_{60}E$,

$R_{67}E$ and $R_{56}E+R_{60}E$ strains, no statistically significant inhibitory effect was observed toward any of the $E_{91}K$, $D_{113}K$ and double $E_{91}K+D_{113}K$ hyperactivated mutated pCpxA strains (Figures 3-9A, B, C and E).

Despite the majority of these negative data obtained, a very interesting result was shown in Figure 3-9D, since these results showed a potential partial complementation of the hyperactivated states in the strains carrying pCpxA $E_{91}K$ and $D_{113}K$ individual substitutions when in the presence of the pCpxP $R_{139}E$ mutant. pCpxA $E_{91}K$ was very minimally inhibited by pCpxP $R_{139}E$ and its activity decreased only by 1.2-fold, while activity of the reporter gene in the strain carrying the pCpxA $D_{113}K$ mutation was further reduced by this same CpxP mutant by 1.7-fold, when compared to strains harboring the parental pTrc99A vector control (Figure 3-9D). In a similar fashion, Figure 3-9F revealed only a partial complementation of the pCpxA $E_{91}K+D_{113}K$ double mutant by the pCpxP double $R_{60}E+R_{67}E$ substitution, where reporter gene activity was decreased by approximately 1.3-fold.

A further confirmatory β-gal experiment of these striking results was performed and is represented in Figure 3-10. Here, reporter gene activity was measured in the pCpxA WT, $E_{91}K$, $D_{113}K$ and $E_{91}K+D_{113}K$ strains co-transformed with the pCpxP mutants that previously showed any suggestion of being able to inhibit these CpxA mutants (from Figures 3-9A to 3-9F). In this new graph, it can be seen that pCpxP WT was able to normally inhibit pCpxA WT (as compared to the pTrc99A VC) and resulted in a reduction of reporter gene levels by 4.6-fold. In comparison, the pCpxP $R_{139}E$ mutant exhibited diminished inhibitory capacity, and both the pCpxP $R_{56}E+R_{60}E$ and $R_{60}E+R_{67}E$ double mutants resulted in a complete loss of inhibition of pCpxA WT, potentially due to structural modification of CpxP by these charge-swap mutations (Figure 3-10). Moreover, the only specific combination of pCpxA and pCpxP amino acid substitutions that was confirmed

to have a partial, statistically significant inhibitory effect were the pCpxA $D_{113}K$ and pCpxP $R_{139}E$ mutants (Figure 3-10). This might signify a direct contact point between these two residues that plays a role in a direct protein-protein interaction of the $CpxA_{SD}$ with CpxP.

3.12 Figures

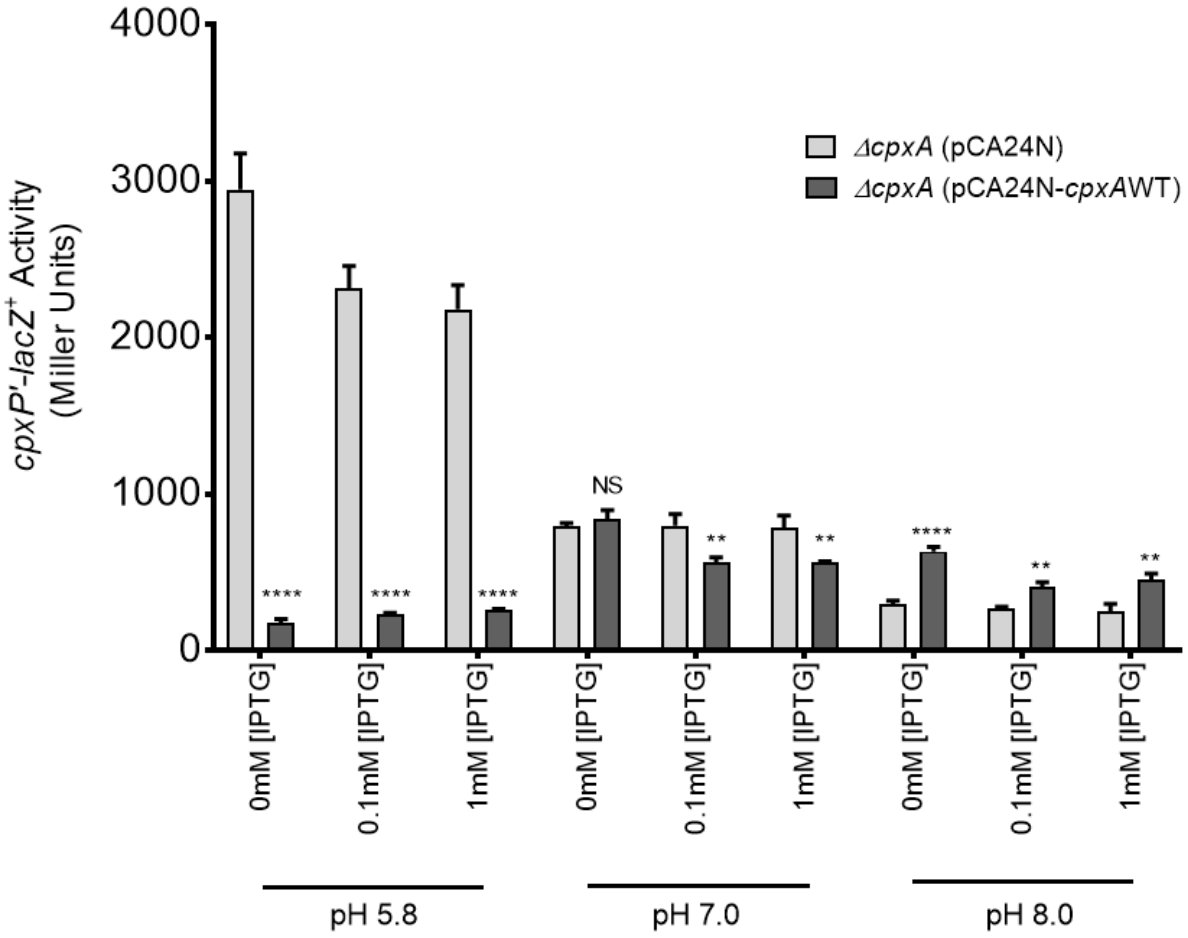

Figure 3-1: Alkaline pH activates a complemented Δ*cpxA* (pCA24N-*cpxA*WT) strain. A β-galactosidase assay for complementation was performed on *E. coli* MC4100 *cpxA*-null strains containing a chromosomal *cpxP'-lacZ*$^+$ reporter and harboring either the pCA24N vector control (RMQ1) or the pCA24N-*cpxA*WT plasmid (RM55). Overnight liquid cultures were subcultured 1:50 into fresh LB and grown for 2 hours at 37°C. Cells were pelleted by centrifugation, resuspended in sodium-phosphate buffered LB media at pH 5.8, 7.0 or 8.0, and *cpxA* transcription induced by the addition of either 0.1mM or 1mM IPTG. The cultures carrying the empty vector control also received IPTG. Bacteria were grown for 3 more hours and resuspended in 1X Z-buffer, after which the OD_{600} was read. Cells were lysed with chloroform and SDS. β-galactosidase activity was recorded for each sample and standardized to their OD_{600}. Data represent the mean and standard deviation of three replicate cultures. Results represent three independent experiments. Asterisks indicate statistically significant difference from the vector control strain (** $P \leq 0.01$, **** $P \leq 0.0001$; two-way ANOVA with Sidak's post hoc multiple comparison test). NS denotes no statistically significant difference in reporter activity.

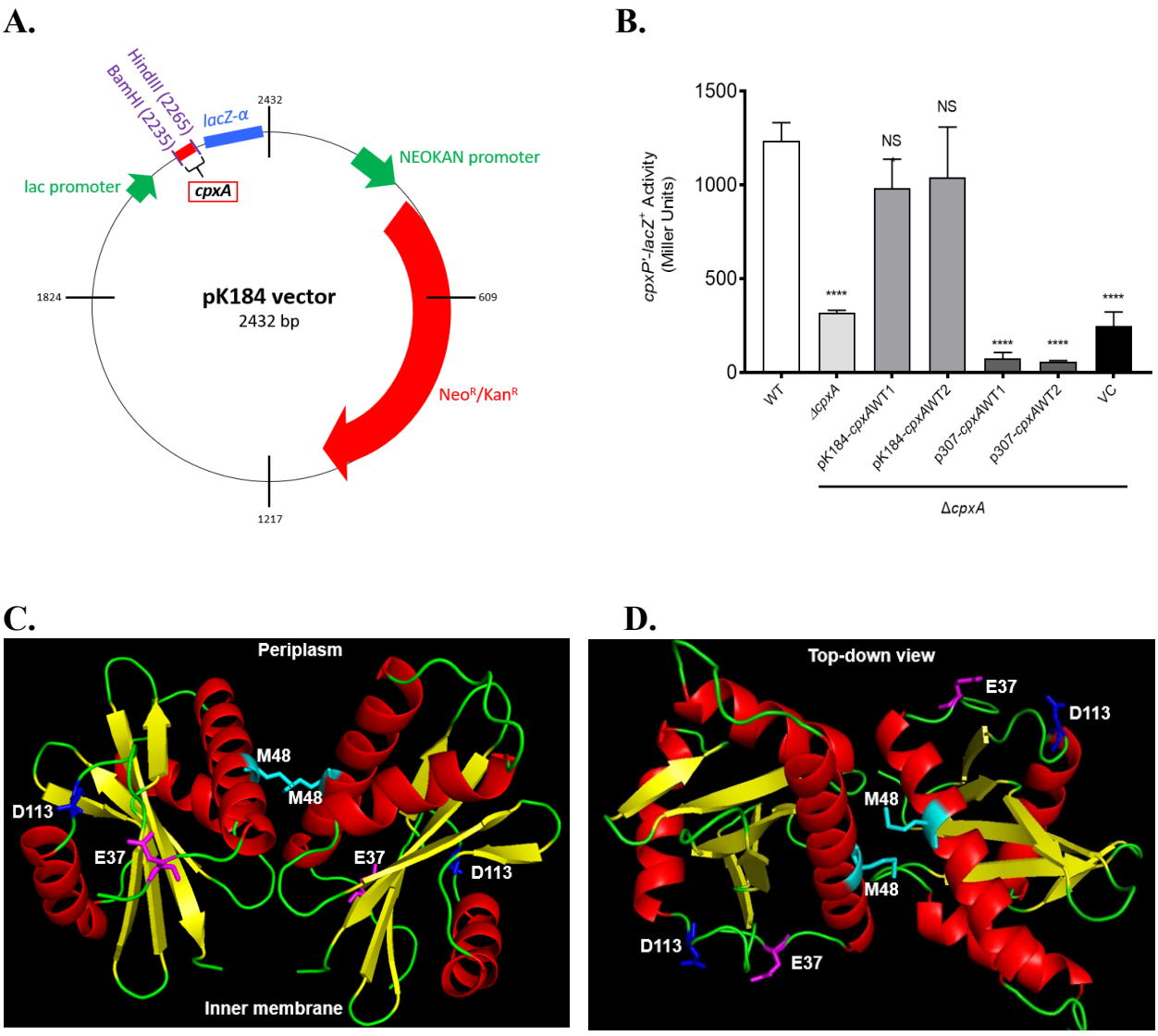

Figure 3-2: Sub-cloning of *cpxA*WT into pK184 complements a Δ*cpxA* strain. (A) Specific location of the sub-cloned *cpxA* in between *Bam*HI and *Hind*III restriction sites within the pK184 plasmid (from -23 nucleotides 5' of the ATG start codon to +17 nucleotides 3' of the TAA stop codon in *cpxA*). Figure adapted from https://www.addgene.org/vector-database/3301/. **(B)** *E. coli* WT (TR50), Δ*cpxA* (RM53), and the transformed Δ*cpxA* strains harboring either the pK184-*cpxA*WT (RMQ2), pJ307-*cpxA*WT (RMQ3) or the VC (RMQ4) plasmids, were cultured overnight, subcultured 1:50 into fresh LB and grown for 2 hours at 37°C. Cells were centrifuged and resuspended in sodium-phosphate buffered LB media pH 8.0, and 0.1mM IPTG added for *cpxA* induction. Bacteria were grown for another 3 hours, resuspended in 1X Z-buffer and the OD_{600} was read. Cells were then lysed with chloroform and SDS. β-galactosidase activity was recorded for each sample and standardized to their OD_{600}. Data represent the mean and standard deviation of three replicate cultures. Results represent three independent experiments. Asterisks indicate statistically

significant difference from the WT strain (**** $P \leq 0.0001$; one-way ANOVA with Sidak's post hoc multiple comparison test). NS denotes no statistically significant difference in reporter activity. **(C)** $CpxA_{SD}$ crystal representation generated in PyMOL. The E_{37}, M_{48} and D_{113} residues substituted for lysine are labeled. **(D)** Top-down view of the same $CpxA_{SD}$ crystal structure and labeled residues.

A.

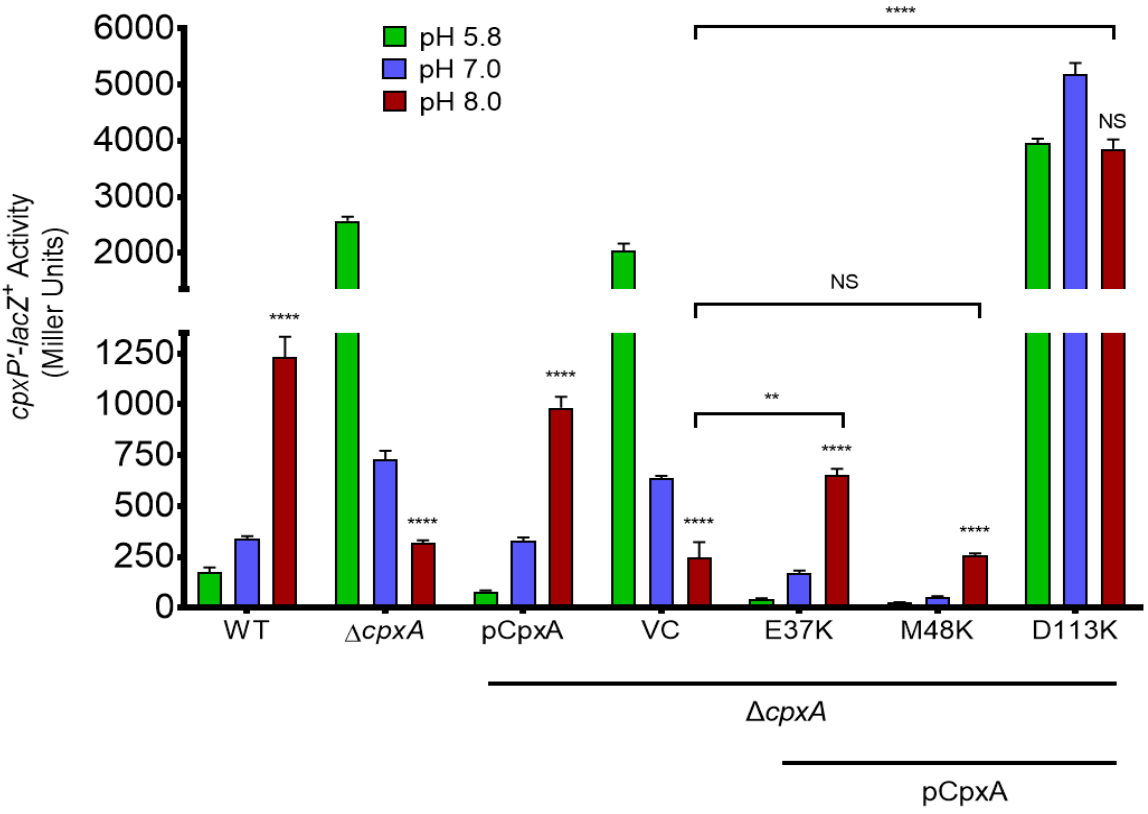
pH 5.8
pH 7.0
pH 8.0
cpxP'-lacZ+ Activity (Miller Units)
6000
5000
4000
3000
2000
1250
1000
750
500
250
0
****
**
NS
WT
ΔcpxA
pCpxA
VC
E37K
M48K
D113K
ΔcpxA
pCpxA

B.

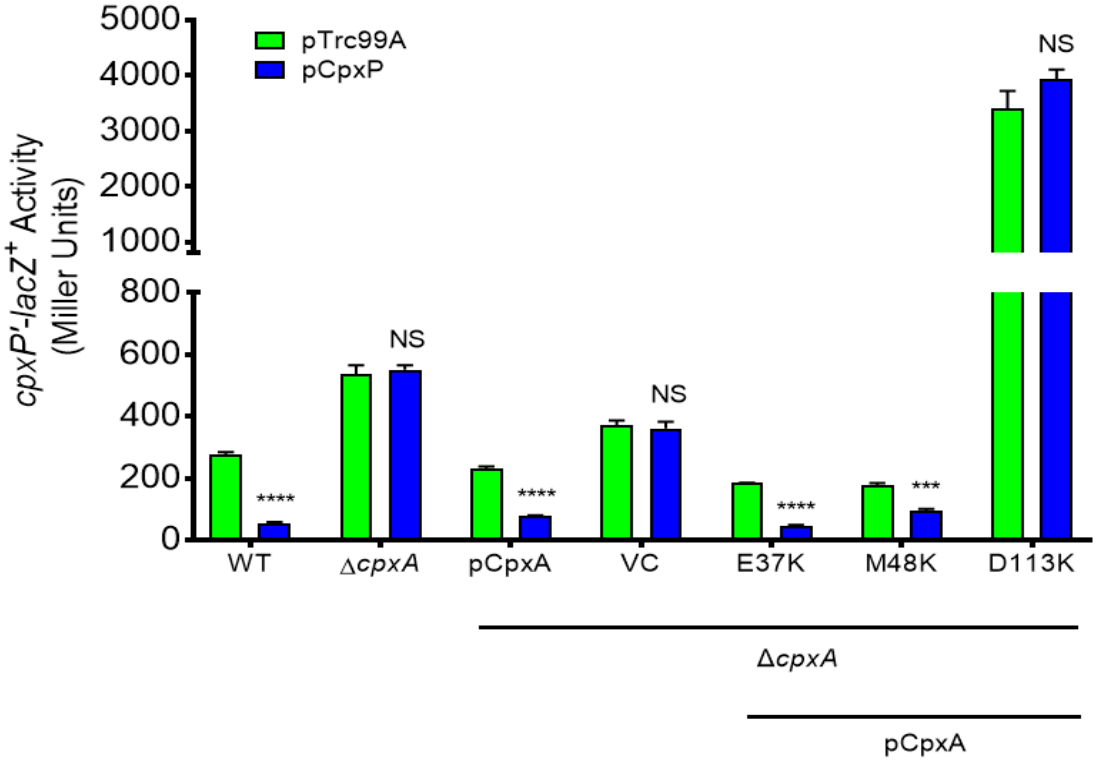
pTrc99A
pCpxP
cpxP'-lacZ+ Activity (Miller Units)
5000
4000
3000
2000
1000
800
600
400
200
0
****
***
NS
WT
ΔcpxA
pCpxA
VC
E37K
M48K
D113K
ΔcpxA
pCpxA

C.

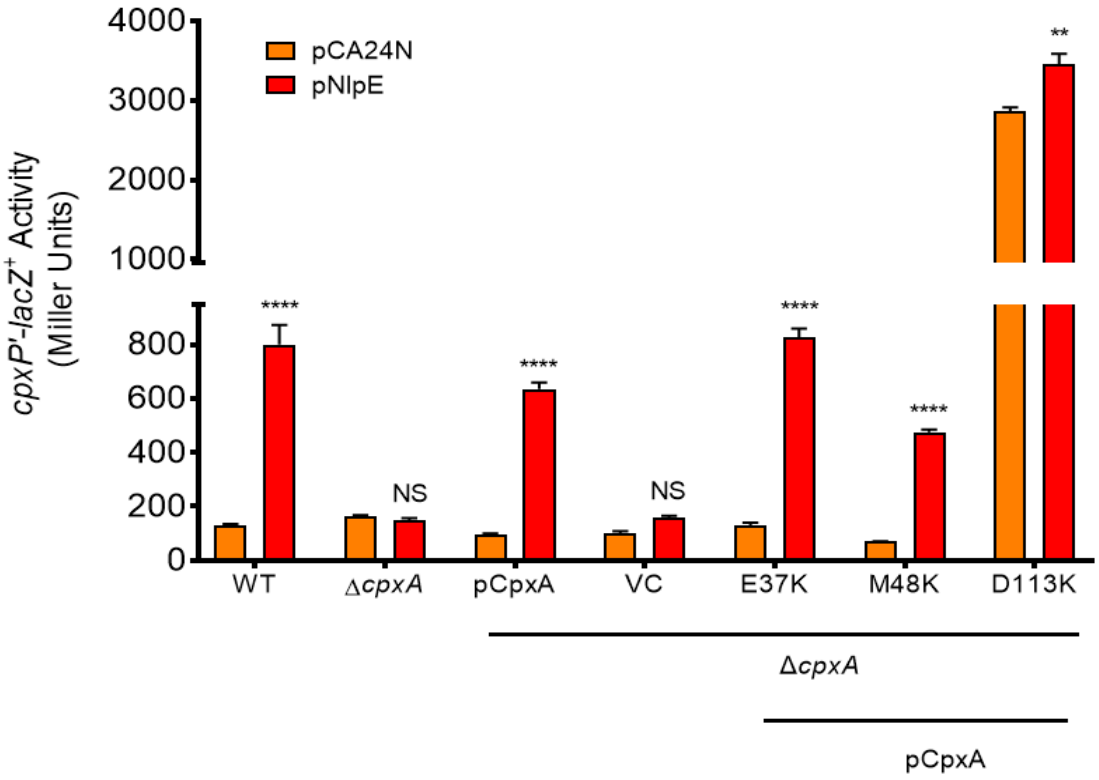

Figure 3-3: Signaling phenotypes displayed by the pCpxA-E_{37}K, M_{48}K and D_{113}K lysine substitutions in the $CpxA_{SD}$. (A) The pCpxA-D_{113}K mutation results in Cpx response hyperactivation irrespective of media pH. Single isolated colonies of *E. coli* WT (TR50), Δ*cpxA* (RM53), and the transformed *ΔcpxA* strains harboring either the pCpxA (RMQ2), VC (RMQ4), pCpxA-E_{37}K (RMQ5), pCpxA-M_{48}K (RMQ6) or pCpxA-D_{113}K (RMQ7) plasmids were cultured overnight, subcultured 1:50 into fresh LB and grown for 2 hours at 37°C. Cells were centrifuged and resuspended in sodium-phosphate buffered LB media at pH 5.8, 7.0 & 8.0, and 0.1mM IPTG added for *cpxA* induction. Bacteria were grown for an additional 3 hours, resuspended in 1X Z-buffer and the OD_{600} was read. Cells were lysed by the addition of chloroform and SDS. β-galactosidase activity was recorded for each sample and standardized to their OD_{600}. Data represent the mean and standard deviation of three replicate cultures. Results represent three independent experiments. Asterisks indicate statistically significant difference at pH 8.0 either from their respective pH 5.8 result, or as compared to the empty VC strain (** $P \leq 0.01$, **** $P \leq 0.0001$; one-way ANOVA with Sidak's post hoc multiple comparison test). NS denotes no statistically significant difference in reporter activity. **(B)** The $CpxA_{SD}$ becomes insensitive to inhibition by overexpressed (OX) *cpxP* and **(C)** further induction by overexpression of *nlpE* in the pCpxA-D_{113}K strain. Single isolated colonies of *E. coli* WT (TR50), Δ*cpxA* (RM53), and the transformed *ΔcpxA* strains harboring either the pCpxA, VC, pCpxA-E_{37}K,

pCpxA-M_{48}K or pCpxA-D_{113}K plasmids were individually co-transformed with the pTrc99A, pCpxP, pCA24N and pCA-*nlpE* plasmids (the strains shown in bars in (B) are DB12, DB8, RMQ8, RMQ9, RMQ10, RMQ11, RMQ12, RMQ13, RMQ14, RMQ15, RMQ16, RMQ17, RMQ18 and RMQ19; in (C) the strains are JLW7, JSW3, RMQ1, RMQ20, RMQ21, RMQ22, RMQ23, RMQ24, RMQ25, RMQ26, RMQ27, RMQ28, RMQ29 and RMQ30. in order from left to right). Strains were cultured overnight, subcultured 1:50 into fresh LB and grown for 2 hours at 37°C. 0.1mM IPTG was added for *cpxA*, *cpxP* and *nlpE* induction. Bacteria were grown for an additional 3 hours, resuspended in 1X Z-buffer and the OD_{600} was read. Cells were lysed by the addition of chloroform and SDS. β-galactosidase activity was recorded for each sample and standardized to their OD_{600}. Data represent the mean and standard deviation of three replicate cultures. Results represent three independent experiments. Asterisks indicate statistically significant difference within the same strain harboring the overexpression plasmid or its parental vector (**$P \leq 0.01$, *** $P \leq 0.001$, **** $P \leq 0.0001$; one-way ANOVA with Sidak's post hoc multiple comparison test). NS denotes no statistically significant difference in reporter activity.

A.

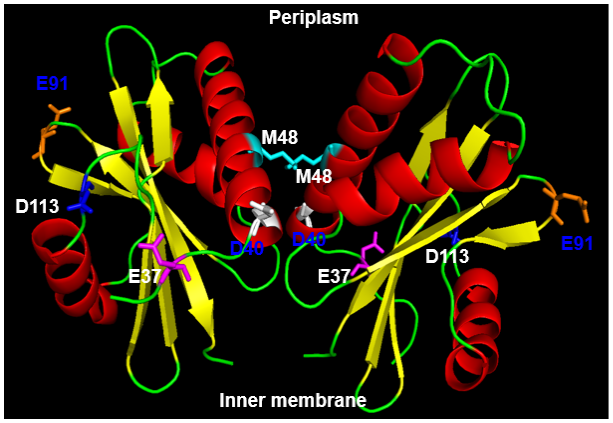
Periplasm
E91
M48
M48
D113
D40
D40
E37
E37
D113
E91
Inner membrane

B.

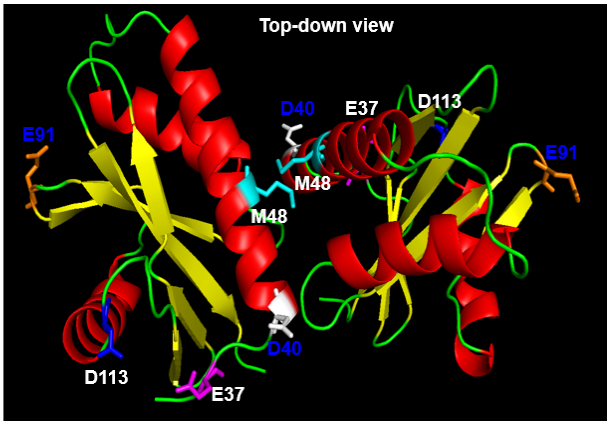
Top-down view
D40
E37
D113
E91
M48
M48
E91
D40
D113
E37

C.

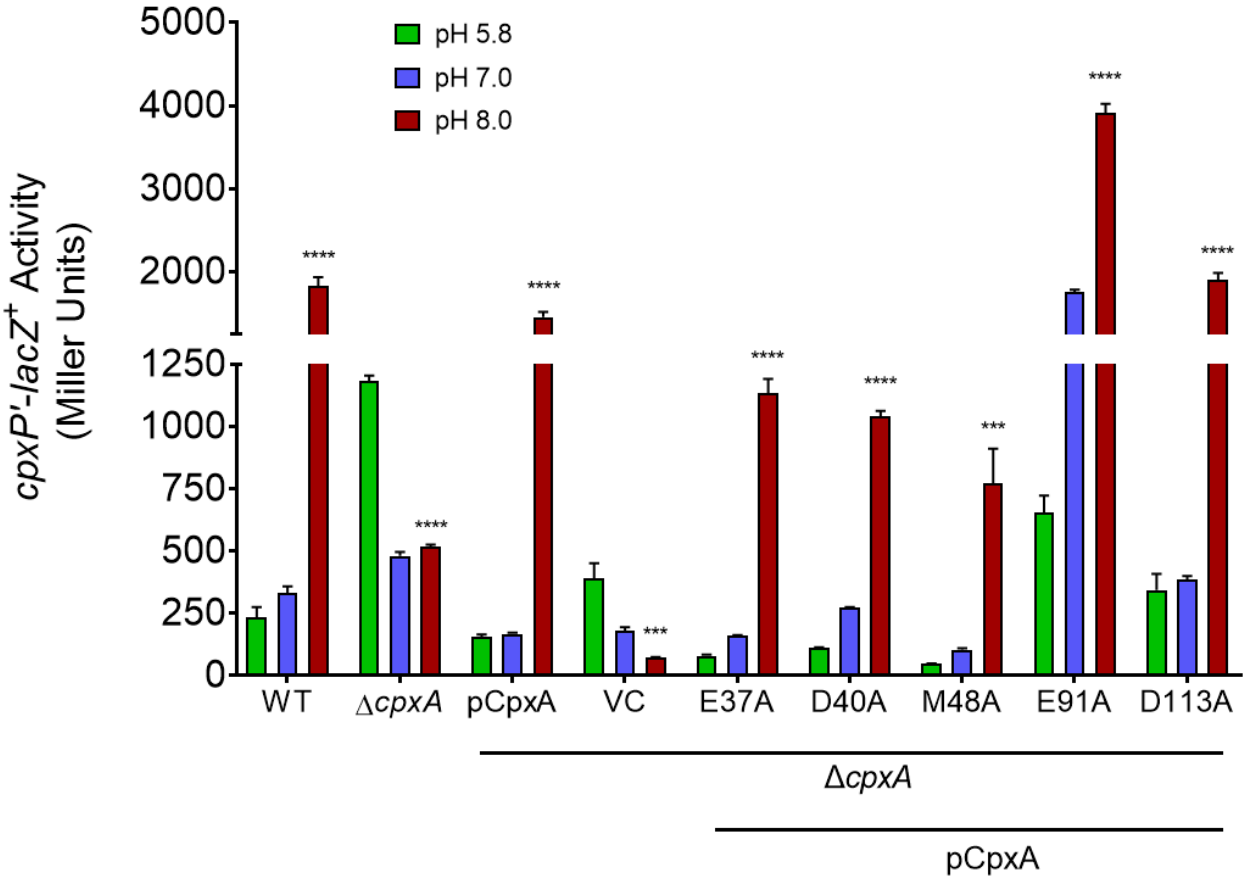
cpxP'-lacZ+ Activity (Miller Units)
5000
4000
3000
2000
1250
1000
750
500
250
0
pH 5.8
pH 7.0
pH 8.0
****
****
****
****
***
****
****
***
****
****
WT
ΔcpxA
pCpxA
VC
E37A
D40A
M48A
E91A
D113A
ΔcpxA
pCpxA

D.

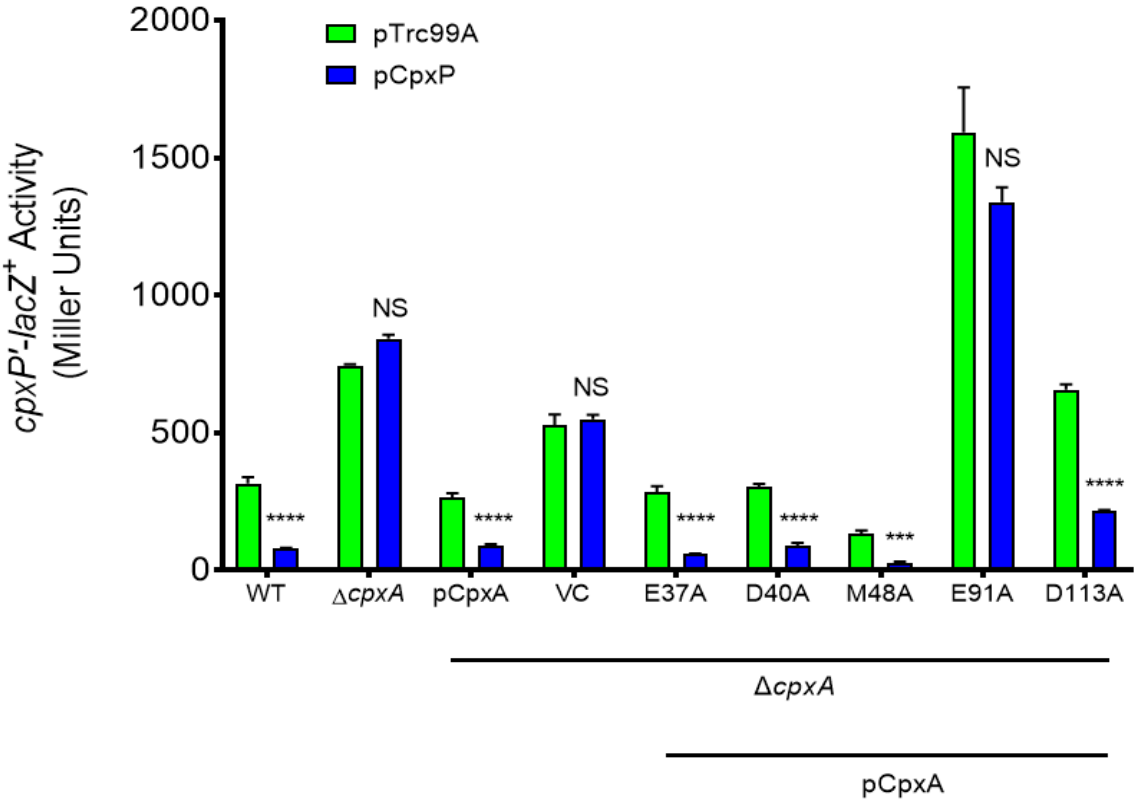
2000
1500
1000
500
0
pTrc99A
pCpxP
cpxP'-lacZ+ Activity
(Miller Units)
NS
NS
NS
****
****
****
****
****
***
****
WT
ΔcpxA
pCpxA
VC
E37A
D40A
M48A
E91A
D113A
ΔcpxA
pCpxA

E.

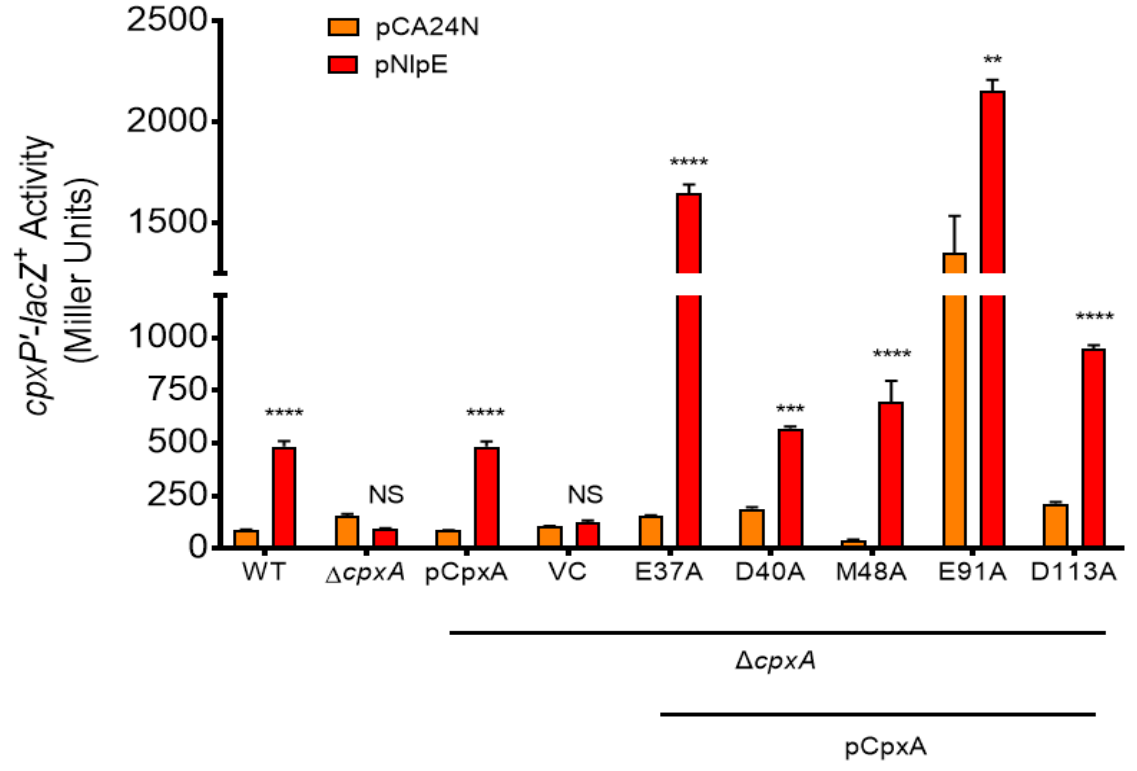
2500
2000
1500
1000
750
500
250
0
pCA24N
pNlpE
cpxP'-lacZ+ Activity
(Miller Units)
****
NS
****
NS
****
**
***
****
****
WT
ΔcpxA
pCpxA
VC
E37A
D40A
M48A
E91A
D113A
ΔcpxA
pCpxA

Figure 3-4: Signaling phenotypes displayed by the pCpxA-E_{37}A, D_{40}A, M_{48}A, E_{91}A and D_{113}A alanine substitutions in the $CpxA_{SD}$. (A) $CpxA_{SD}$ crystal representation generated in PyMOL. The E_{37}, D_{40}, M_{48}, E_{91} and D_{113} residues substituted for alanine are labeled. **(B)** Top-down view of the same $CpxA_{SD}$ crystal structure and labeled residues. **(C)** The pCpxA-E_{91}A mutation results in Cpx response hyperactivation at alkaline pH only, while pCpxA-D_{113}A has lost the hyperactivated phenotype observed with the lysine substitution. Single isolated colonies of *E. coli* WT (TR50), Δ*cpxA* (RM53), and the transformed *ΔcpxA* strains harboring either the pCpxA (RMQ2), VC (RMQ4), pCpxA-E_{37}A (RMQ31), pCpxA-D_{40}A (RMQ32), pCpxA-M_{48}A (RMQ33), pCpxA-E_{91}A (RMQ34) or pCpxA-D_{113}A (RMQ35) plasmids were cultured overnight, subcultured 1:50 into fresh LB and grown for 2 hours at 37°C. Cells were centrifuged and resuspended in sodium-phosphate buffered LB media at pH 5.8, 7.0 & 8.0, and 0.1mM IPTG added for *cpxA* induction. Bacteria were grown for an additional 3 hours, resuspended in 1X Z-buffer and the OD_{600} was read. Cells were lysed by the addition of chloroform and SDS. β-galactosidase activity was recorded for each sample and standardized to their OD_{600}. Data represent the mean and standard deviation of three replicate cultures. Results represent three independent experiments. Asterisks indicate statistically significant difference at pH 8.0 from their respective pH 5.8 result (*** $P \leq 0.001$, **** $P \leq 0.0001$; one-way ANOVA with Sidak's post hoc multiple comparison test). NS denotes no statistically significant difference in reporter activity. **(D)** The $CpxA_{SD}$ becomes insensitive to inhibition by OX *cpxP*, **(E)** but not to further induction by OX *nlpE* in the pCpxA-E_{91}A strain. Single isolated colonies of *E. coli* WT (TR50), Δ*cpxA* (RM53), and the transformed *ΔcpxA* strains harboring either the pCpxA, VC, pCpxA-E_{37}A, pCpxA-D_{40}A, pCpxA-M_{48}A, pCpxA-E_{91}A or pCpxA-D_{113}A plasmids were individually co-transformed with the pTrc99A, pCpxP, pCA24N and pCA-*nlpE* plasmids (the strains shown in bars in (D) are DB12, DB8, RMQ8, RMQ9, RMQ10, RMQ11, RMQ12, RMQ13, RMQ36, RMQ37, RMQ38, RMQ39, RMQ40, RMQ41, RMQ42, RMQ43, RMQ44 and RMQ45; in (E) the strains are JLW7, JSW3, RMQ1, RMQ20, RMQ21, RMQ22, RMQ23, RMQ24, RMQ46, RMQ47, RMQ48, RMQ49, RMQ50, RMQ51, RMQ52, RMQ53, RMQ54 and RMQ55, in order from left to right). Strains were cultured overnight, subcultured 1:50 into fresh LB and grown for 2 hours at 37°C. 0.1mM IPTG was added for *cpxA*, *cpxP* and *nlpE* induction. Bacteria were grown for an additional 3 hours, resuspended in 1X Z-buffer and the OD_{600} was read. Cells were lysed by the addition of chloroform and SDS. β-galactosidase activity was recorded for each sample and standardized to their OD_{600}. Data represent the mean and standard deviation of three replicate cultures. Results represent three independent experiments. Asterisks indicate statistically significant difference within the same strain harboring the overexpression plasmid or its parental vector (** $P \leq 0.01$, *** $P \leq 0.001$, **** $P \leq 0.0001$; one-way ANOVA with Sidak's post hoc multiple comparison test). NS denotes no statistically significant difference in reporter activity.

A.

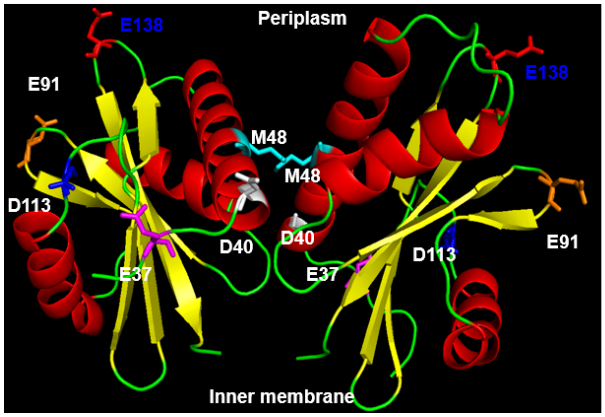
Periplasm
E138
E91
E138
M48
M48
D113
D40
D40
E37
E37
D113
E91
Inner membrane

B.

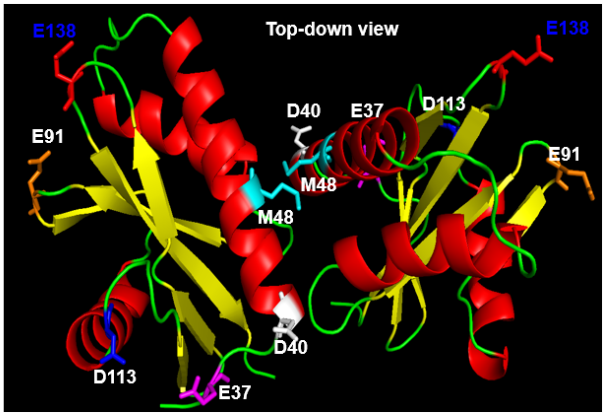
Top-down view
E138
E138
D40
E37
D113
E91
E91
M48
M48
D40
D113
E37

C.

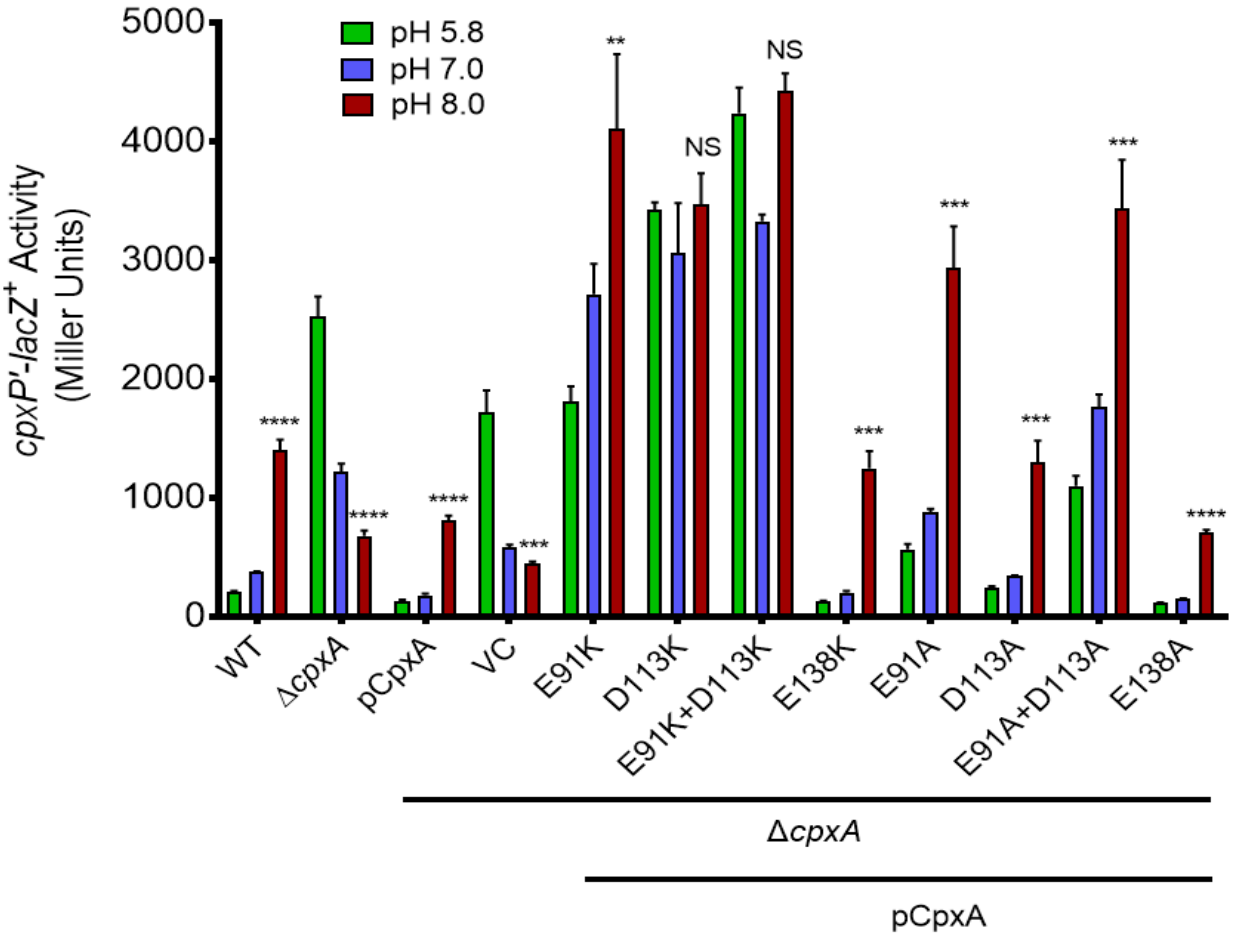
pH 5.8
pH 7.0
pH 8.0
cpxP'-lacZ+ Activity (Miller Units)
5000
4000
3000
2000
1000
0
****
****
****
****
***
**
NS
NS
***
***
***
***
****
WT
ΔcpxA
pCpxA
VC
E91K
D113K
E91K+D113K
E138K
E91A
D113A
E91A+D113A
E138A
ΔcpxA
pCpxA

D.

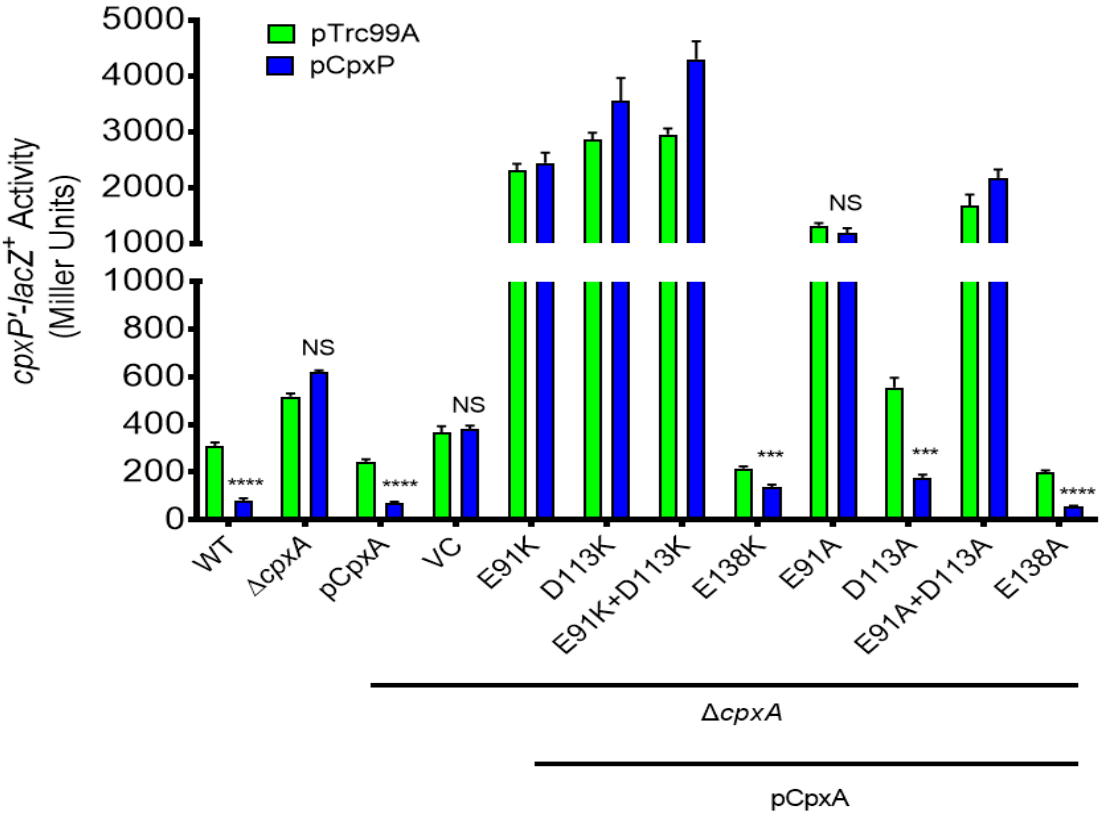
pTrc99A
pCpxP
cpxP'-lacZ+ Activity (Miller Units)
5000
4000
3000
2000
1000
1000
800
600
400
200
0
NS
NS
NS
****
****
****
***
***
***
****
WT
ΔcpxA
pCpxA
VC
E91K
D113K
E91K+D113K
E138K
E91A
D113A
E91A+D113A
E138A
ΔcpxA
pCpxA

E.

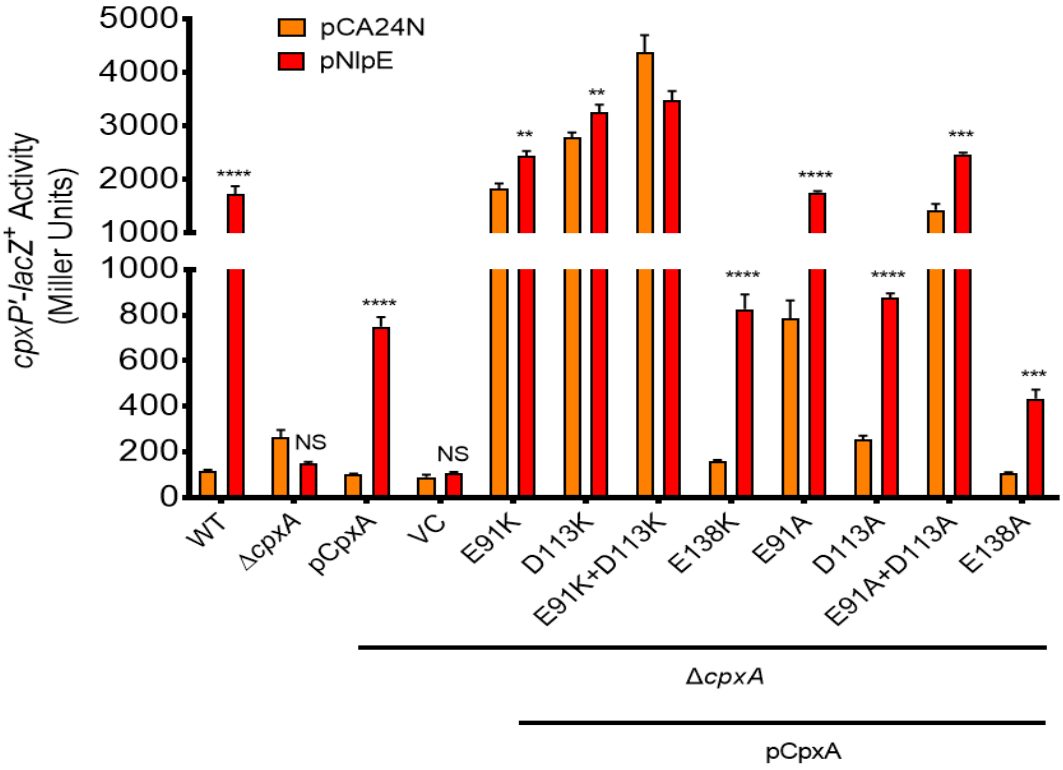
pCA24N
pNlpE
cpxP'-lacZ+ Activity (Miller Units)
5000
4000
3000
2000
1000
1000
800
600
400
200
0
NS
NS
****
****
**
**
****
****
***
***
WT
ΔcpxA
pCpxA
VC
E91K
D113K
E91K+D113K
E138K
E91A
D113A
E91A+D113A
E138A
ΔcpxA
pCpxA

Figure 3-5: Signaling phenotypes displayed by the pCpxA-$E_{91}K$, $D_{113}K$, $E_{91}K+D_{113}K$, $E_{138}K$, $E_{91}A$, $D_{113}A$, $E_{91}A+D_{113}A$ and $E_{138}A$ single and double lysine or alanine substitutions in the $CpxA_{SD}$. (A) $CpxA_{SD}$ crystal representation generated in PyMOL. The E_{91}, D_{113} and E_{138} residues substituted for either lysine or alanine are labeled. **(B)** Top-down view of the same $CpxA_{SD}$ crystal structure and labeled residues. **(C)** The pCpxA-$D_{113}K$ and double $E_{91}K+D_{113}K$ mutations result in Cpx response hyperactivation at all pH assayed, while pCpxA-$E_{91}K$, $E_{91}A$ and $E_{91}A+D_{113}A$ hyperactivate the pathway only at pH 8.0. Single isolated colonies of *E. coli* WT (TR50), Δ*cpxA* (RM53), and the transformed *ΔcpxA* strains harboring either the pCpxA (RMQ2), VC (RMQ4), pCpxA-$E_{91}K$ (RMQ56), pCpxA-$D_{113}K$ (RMQ7), pCpxA-$E_{91}K+D_{113}K$ (RMQ57), pCpxA-$E_{138}K$ (RMQ58), pCpxA-$E_{91}A$ (RMQ34), pCpxA-$D_{113}A$ (RMQ35), pCpxA-$E_{91}A+D_{113}A$ (RMQ59) or pCpxA-$E_{138}A$ (RMQ60) plasmids were cultured overnight, subcultured 1:50 into fresh LB and grown for 2 hours at 37°C. Cells were centrifuged and resuspended in sodium-phosphate buffered LB media at pH 5.8, 7.0 & 8.0, and 0.1mM IPTG added for *cpxA* induction. Bacteria were grown for an additional 3 hours, resuspended in 1X Z-buffer and the OD_{600} was read. Cells were lysed by the addition of chloroform and SDS. β-galactosidase activity was recorded for each sample and standardized to their OD_{600}. Data represent the mean and standard deviation of three replicate cultures. Results represent three independent experiments. Asterisks indicate statistically significant difference at pH 8.0 from their respective pH 5.8 result (** $P \leq 0.01$, *** $P \leq 0.001$, **** $P \leq 0.0001$; one-way ANOVA with Sidak's post hoc multiple comparison test). NS denotes no statistically significant difference in reporter activity. **(D)** The pCpxA-$E_{91}K$, $D_{113}K$, $E_{91}K+D_{113}K$, $E_{91}A$ and $E_{91}A+D_{113}A$ mutations are not inhibited by OX *cpxP*, **(E)** however only the $E_{91}K+D_{113}K$ activity is not further induced by OX *nlpE*. Single isolated colonies of *E. coli* WT (TR50), Δ*cpxA* (RM53), and the transformed *ΔcpxA* strains harboring either the pCpxA, VC, pCpxA-$E_{91}K$, pCpxA-$D_{113}K$, pCpxA-$E_{91}K+D_{113}K$, pCpxA-$E_{138}K$, pCpxA-$E_{91}A$, pCpxA-$D_{113}A$, pCpxA-$E_{91}A+D_{113}A$ or pCpxA-$E_{138}A$ plasmids were individually co-transformed with the pTrc99A, pCpxP, pCA24N and pCA-*nlpE* plasmids (the strains shown in bars in (D) are DB12, DB8, RMQ8, RMQ9, RMQ10, RMQ11, RMQ12, RMQ13, RMQ61, RMQ62, RMQ18, RMQ19, RMQ63, RMQ64, RMQ65, RMQ66, RMQ42, RMQ43, RMQ44, RMQ45, RMQ67, RMQ68, RMQ69 and RMQ70; in (E) the strains are JLW7, JSW3, RMQ1, RMQ20, RMQ21, RMQ22, RMQ23, RMQ24, RMQ71, RMQ72, RMQ29, RMQ30, RMQ73, RMQ74, RMQ75, RMQ76, RMQ52, RMQ53, RMQ54, RMQ55, RMQ77, RMQ78, RMQ79 and RMQ80, in order from left to right). Strains were cultured overnight, subcultured 1:50 into fresh LB and grown for 2 hours at 37°C. 0.1mM IPTG was added for *cpxA*, *cpxP* and *nlpE* induction. Bacteria were grown for an additional 3 hours, resuspended in 1X Z-buffer and the OD_{600} was read. Cells were lysed by the addition of chloroform and SDS. β-galactosidase activity was recorded for each sample and standardized to their OD_{600}. Data represent the mean and standard deviation of three replicate cultures. Results represent three independent experiments. Asterisks indicate statistically significant difference

within the same strain harboring the overexpression plasmid or its parental vector (**$P \leq 0.01$, *** $P \leq 0.001$, **** $P \leq 0.0001$; one-way ANOVA with Sidak's post hoc multiple comparison test). NS denotes no statistically significant difference in reporter activity.

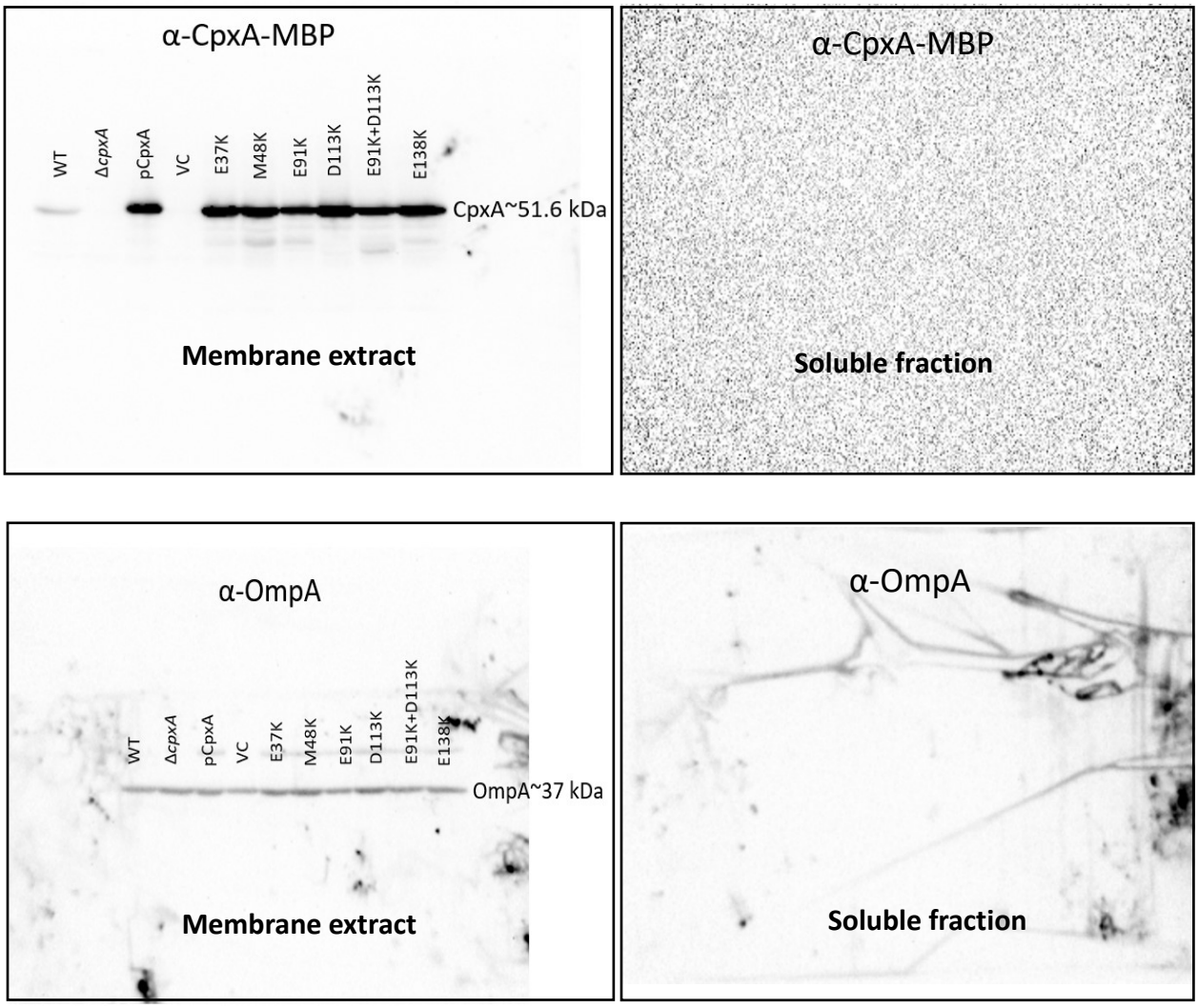

Figure 3-6: The pCpxA-E_{37}K, M_{48}K, E_{91}K, D_{113}K, E_{91}K+D_{113}K and E_{138}K lysine substitutions do not affect CpxA protein stability. Western blotting results displaying the $CpxA_{SD}$ protein expression levels in total membrane preparations from *E. coli* WT (TR50), Δ*cpxA* (RM53), and the transformed *ΔcpxA* strains harboring either the pCpxA (RMQ2), VC (RMQ4), pCpxA-E_{37}K (RMQ5), pCpxA-M_{48}K (RMQ6), pCpxA-E_{91}K (RMQ56), pCpxA-D_{113}K (RMQ7), pCpxA-E_{91}K+D_{113}K (RMQ57) or pCpxA-E_{138}K (RMQ58) plasmids. Bacterial strains were cultured overnight, subcultured 1:100 into fresh LB, grown for 4-6 hours until an OD_{600} of 0.6-0.7 was reached and then adjusted to the equivalent of 1mL of the culture displaying the lowest OD_{600}. 0.1mM IPTG (final concentration) was added for *cpxA* induction 2 hours after subculture. Cells were centrifuged, resuspended in 1mL of 0.1M Tris-HCl pH 8.0 and lysed by sonication. Lysates were centrifuged at 10,000 rpm for 5 minutes at 4°C to remove debris. 900µL of the supernatants were transferred to new microfuge tubes and centrifuged at 15,000 rpm for 5 hours at 4°C to pellet the

membranes. Supernatants (soluble fractions) were removed and pipetted into separate tubes, whereas pellets were resuspended in 100μL of 1X PBS. Total protein concentrations of membrane preparations and soluble fractions were obtained by means of the Pierce BCA Protein Assay Kit, then mixed with equal volumes of 2X SDS-PAGE Sample Loading Buffer. 20μg of total protein for each sample were run in 12% SDS-PAGE gels and subsequent western blotting performed using the α-CpxA-MBP antibody. OmpA was detected and used as loading control in a separate blot using α-OmpA antibody. Results represent two independent experiments.

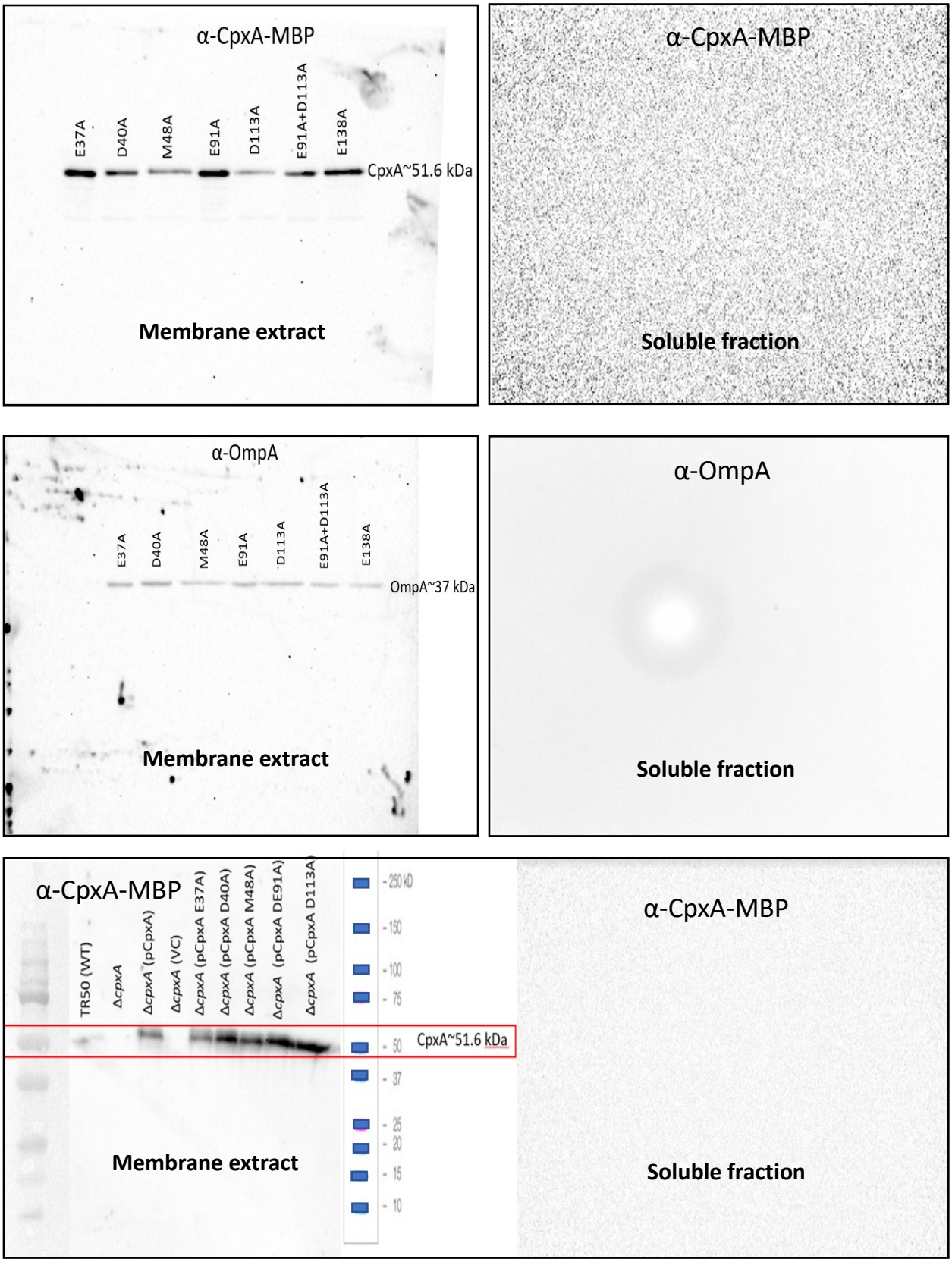
α-CpxA-MBP
E37A
D40A
M48A
E91A
D113A
E91A+D113A
E138A
CpxA~51.6 kDa
Membrane extract
α-CpxA-MBP
Soluble fraction
α-OmpA
E37A
D40A
M48A
E91A
D113A
E91A+D113A
E138A
OmpA~37 kDa
Membrane extract
α-OmpA
Soluble fraction
α-CpxA-MBP
TR50 (WT)
ΔcpxA
ΔcpxA (pCpxA)
ΔcpxA (VC)
ΔcpxA (pCpxA E37A)
ΔcpxA (pCpxA D40A)
ΔcpxA (pCpxA M48A)
ΔcpxA (pCpxA DE91A)
ΔcpxA (pCpxA D113A)
250 kD
150
100
75
50
37
25
20
15
10
CpxA~51.6 kDa
Membrane extract
α-CpxA-MBP
Soluble fraction

Figure 3-7: The pCpxA-E_{37}A, D_{40}A, M_{48}A, E_{91}A, D_{113}A, E_{91}A+D_{113}A and E_{138}A alanine substitutions do not affect CpxA protein stability. Western blotting results displaying the $CpxA_{SD}$ protein expression levels in total membrane preparations from *E. coli* transformed *ΔcpxA* strains harboring either pCpxA-E_{37}A (RMQ31), pCpxA-D_{40}A (RMQ32), pCpxA-M_{48}A (RMQ33), pCpxA-E_{91}A (RMQ34), pCpxA-D_{113}A (RMQ35), pCpxA-E_{91}A+D_{113}A (RMQ59) or pCpxA-E_{138}A (RMQ60) plasmids. Bacterial strains were cultured overnight, subcultured 1:100 into fresh LB, grown for 4-6 hours until an OD_{600} of 0.6-0.7 was reached and then adjusted to the equivalent of 1mL of the culture displaying the lowest OD_{600}. 0.1mM IPTG (final concentration) was added for *cpxA* induction 2 hours after subculture. Cells were centrifuged, resuspended in 1mL of 0.1M Tris-HCl pH 8.0 and lysed by sonication. Lysates were centrifuged at 10,000 rpm for 5 minutes at 4°C to remove debris. 900µL of the supernatants were transferred to new microfuge tubes and centrifuged at 15,000 rpm for 5 hours at 4°C to pellet the membranes. Supernatants (soluble fractions) were removed and pipetted into separate tubes, whereas pellets were resuspended in 100µL of 1X PBS. Total protein concentrations of membrane preparations and soluble fractions were obtained by means of the Pierce BCA Protein Assay Kit, then mixed with equal volumes of 2X SDS-PAGE Sample Loading Buffer. 20µg of total protein for each sample were run in 12% SDS-PAGE gels and subsequent western blotting performed using the α-CpxA-MBP antibody. OmpA was detected and used as loading control in a separate blot using α-OmpA antibody. Results represent two independent experiments.

A.

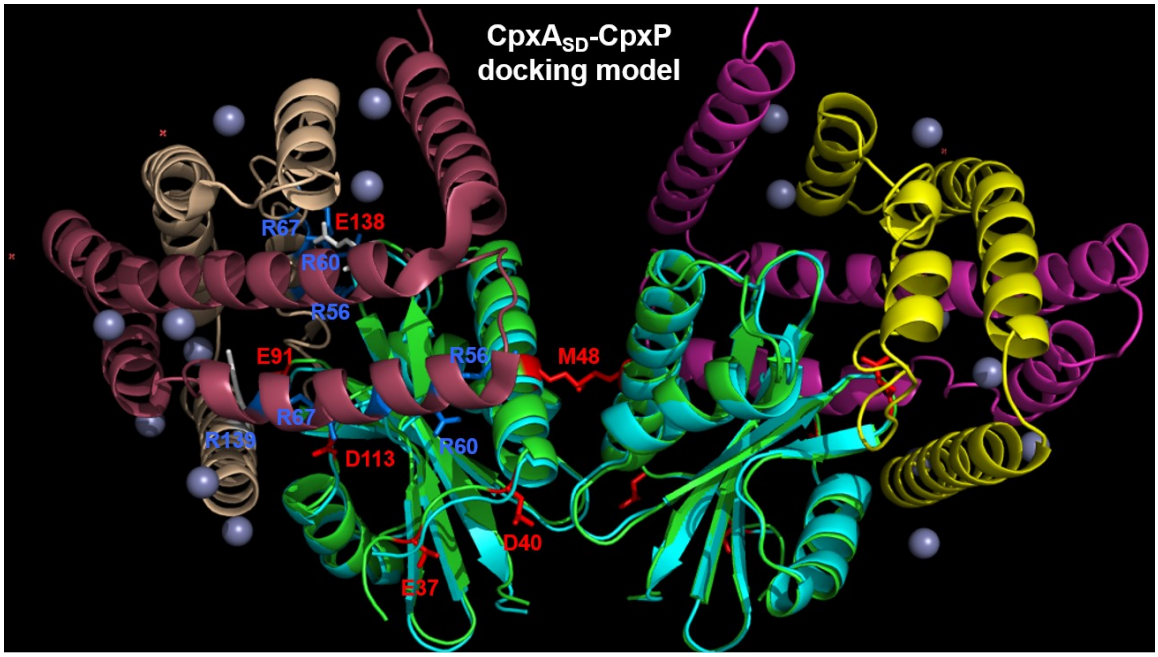

B.

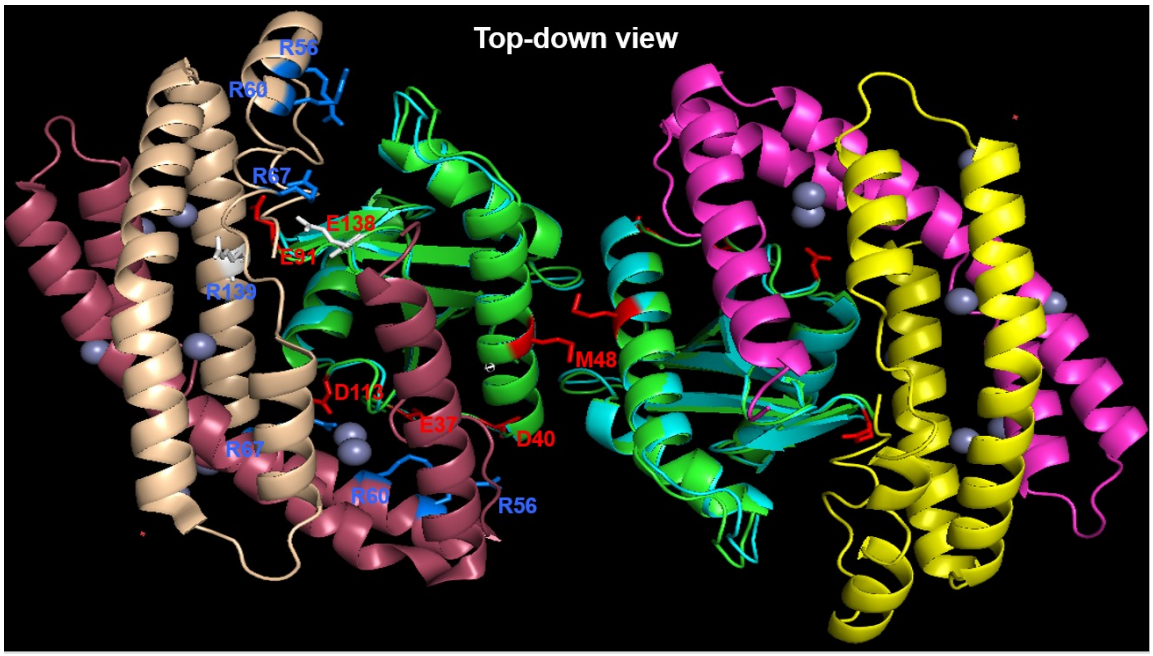

Figure 3-8: Crystal representation of a CpxA$_{SD}$-CpxP potential interaction/docking model. (A) Docking model representing the CpxA$_{SD}$-CpxP potential protein-protein interaction (generated in PyMOL). The E_{37}, D_{40}, M_{48}, E_{91}, D_{113} and E_{138} residues from one monomer of the CpxA$_{SD}$ (written in red) and the R_{56}, R_{60}, R_{67} and R_{139} residues from two monomers comprising a single CpxP dimer (written in blue) utilized in the mutagenesis assays in this study are labeled. **(B)** Top-down view of the same docking model and labeled

red and blue residues as per (A). In this possible representation of the interaction, two dimers of CpxP are configured in a manner for them to be in close proximity and contact with each single monomer of the $CpxA_{SD}$ in *E. coli*. Note that the green and blue overlaid structure observed in the $CpxA_{SD}$ is an artifact of the software utilized, and this figure represents one $CpxA_{SD}$ dimer only.

A.

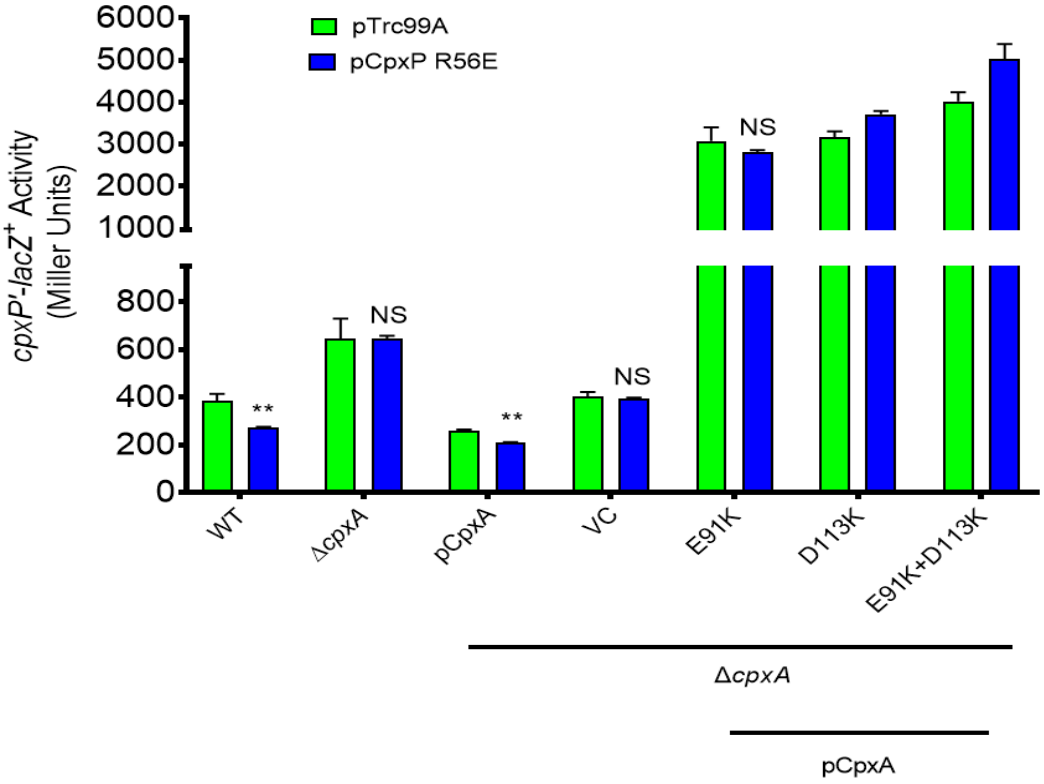
pTrc99A
pCpxP R56E
cpxP'-lacZ+ Activity (Miller Units)
6000
5000
4000
3000
2000
1000
800
600
400
200
0
**
NS
**
NS
NS
WT
ΔcpxA
pCpxA
VC
E91K
D113K
E91K+D113K
ΔcpxA
pCpxA

B.

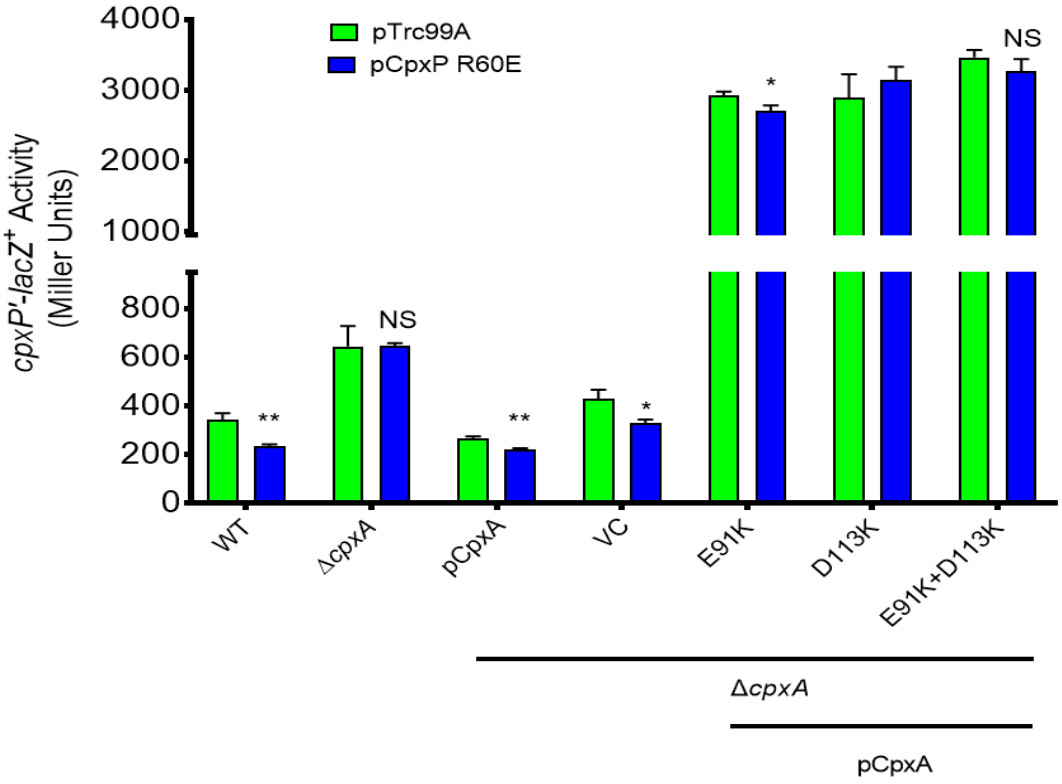
pTrc99A
pCpxP R60E
cpxP'-lacZ+ Activity (Miller Units)
4000
3000
2000
1000
800
600
400
200
0
**
NS
**
*
*
NS
WT
ΔcpxA
pCpxA
VC
E91K
D113K
E91K+D113K
ΔcpxA
pCpxA

C.

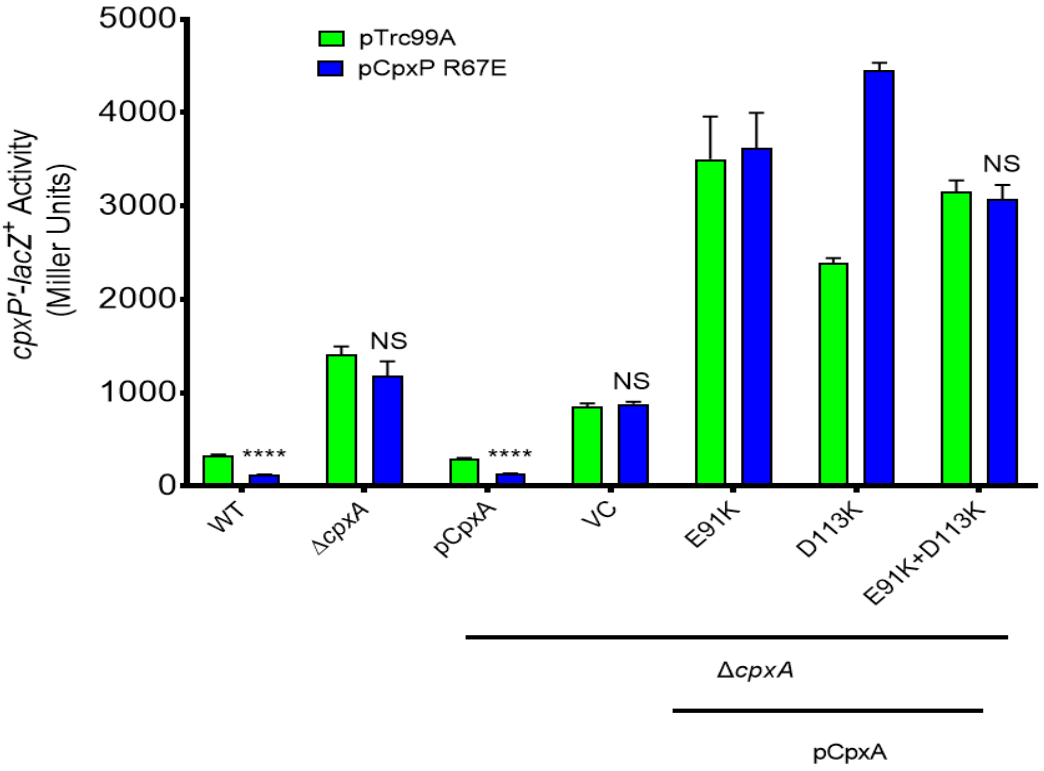
pTrc99A
pCpxP R67E
cpxP'-lacZ+ Activity (Miller Units)
5000
4000
3000
2000
1000
0
****
NS
****
NS
NS
WT
ΔcpxA
pCpxA
VC
E91K
D113K
E91K+D113K
ΔcpxA
pCpxA

D.

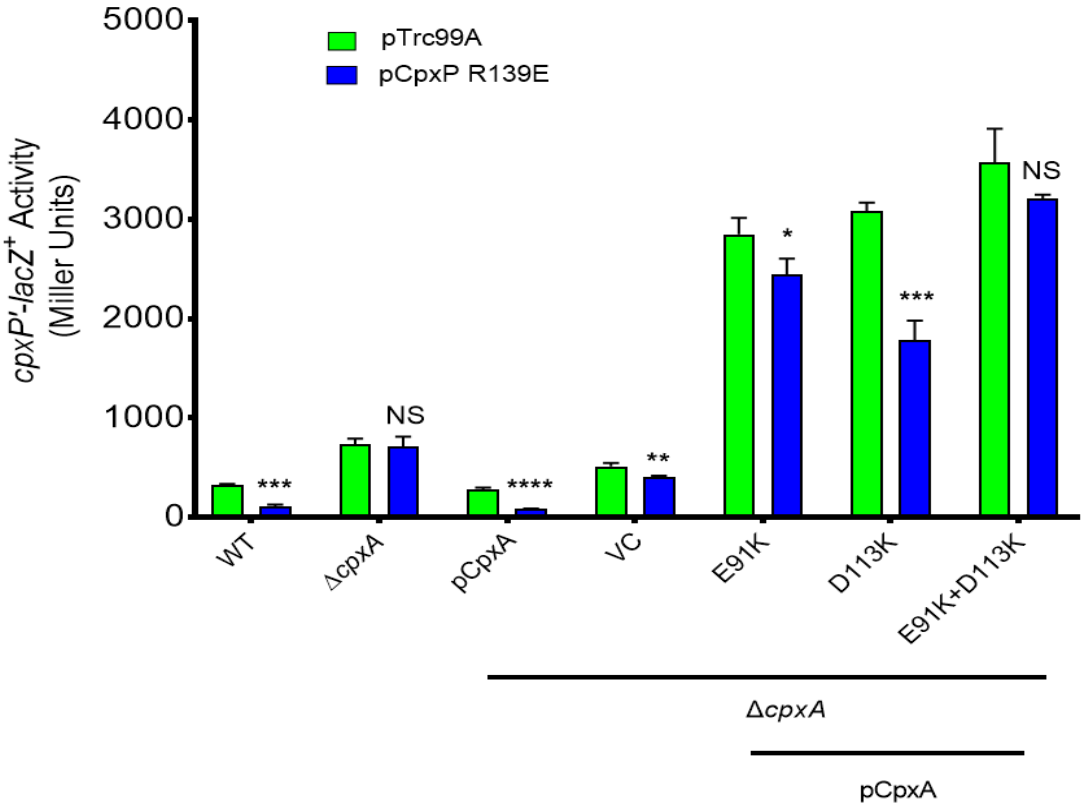
pTrc99A
pCpxP R139E
cpxP'-lacZ+ Activity (Miller Units)
5000
4000
3000
2000
1000
0
***
NS
****
**
*
***
NS
WT
ΔcpxA
pCpxA
VC
E91K
D113K
E91K+D113K
ΔcpxA
pCpxA

E.

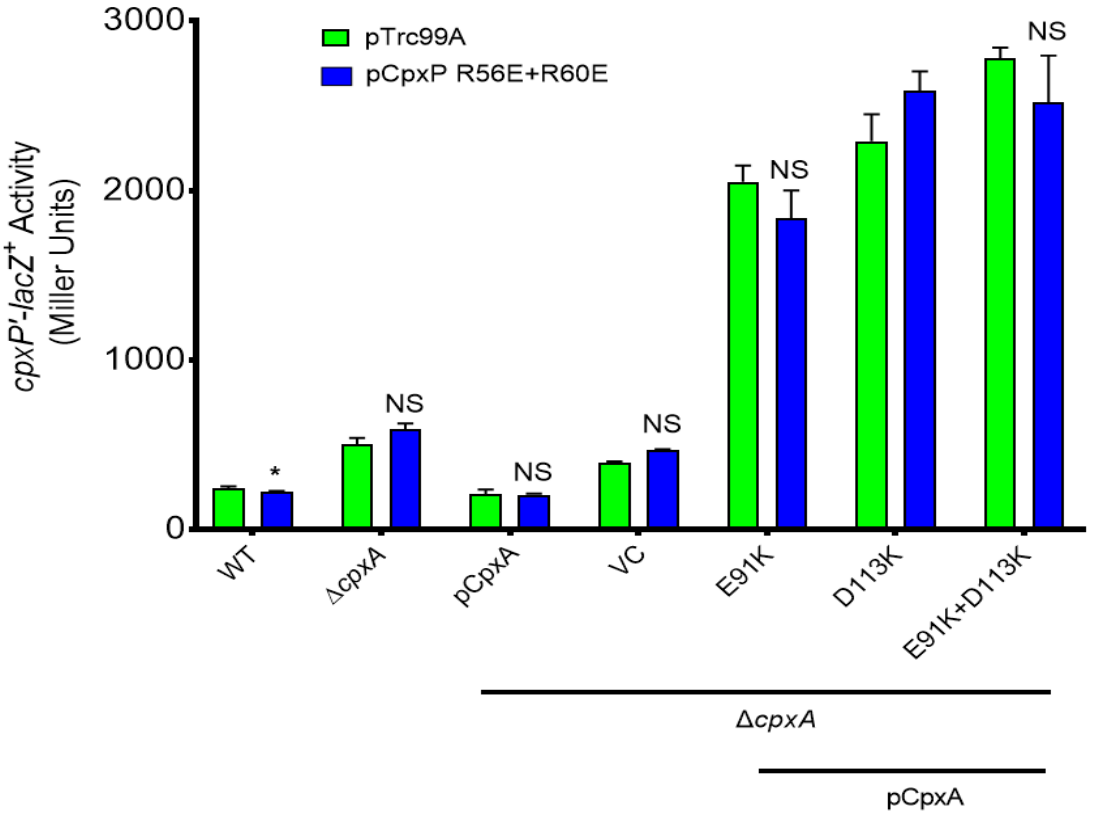
pTrc99A
pCpxP R56E+R60E
cpxP'-lacZ+ Activity (Miller Units)
3000
2000
1000
0
*
NS
NS
NS
NS
NS
WT
ΔcpxA
pCpxA
VC
E91K
D113K
E91K+D113K
ΔcpxA
pCpxA

F.

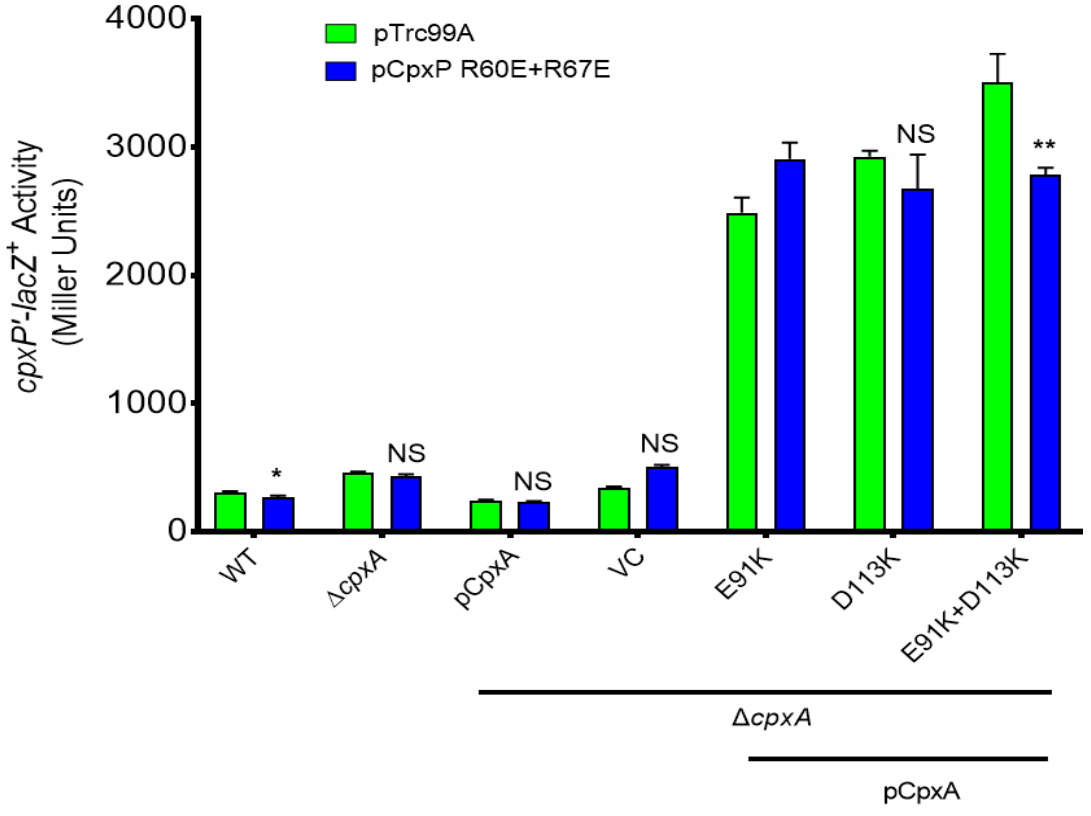
pTrc99A
pCpxP R60E+R67E
cpxP'-lacZ+ Activity (Miller Units)
4000
3000
2000
1000
0
*
NS
NS
NS
NS
**
WT
ΔcpxA
pCpxA
VC
E91K
D113K
E91K+D113K
ΔcpxA
pCpxA

Figure 3-9: Second-site suppressor assays of hyperactivated pCpxA lysine mutated strains by aspartate substitutions in pCpxP arginine residues comprising surface-exposed positively charged patches. Single isolated colonies of *E. coli* WT (TR50), Δ*cpxA* (RM53), and the transformed *ΔcpxA* strains harboring either the pCpxA, VC, pCpxA-$E_{91}K$, pCpxA-$D_{113}K$ or pCpxA-$E_{91}K$+$D_{113}K$ plasmids were individually co-transformed with the pTrc99A, pCpxP-$R_{56}E$, pCpxP-$R_{60}E$, pCpxP-$R_{67}E$, pCpxP-$R_{139}E$, pCpxP-$R_{56}E$+$R_{60}E$ or pCpxP-$R_{60}E$+$R_{67}E$ plasmids. Specific strains depicted from left to right in each graph are as follows: **(A)** DB12, RMQ81, RMQ8, RMQ82, RMQ10, RMQ83, RMQ12, RMQ84, RMQ61, RMQ85, RMQ18, RMQ86, RMQ63 and RMQ87; **(B)** DB12, RMQ88, RMQ8, RMQ89, RMQ10, RMQ90, RMQ12, RMQ91, RMQ61, RMQ92, RMQ18, RMQ93, RMQ63 and RMQ94; **(C)** DB12, RMQ95, RMQ8, RMQ96, RMQ10, RMQ97, RMQ12, RMQ98, RMQ61, RMQ99, RMQ18, RMQ100, RMQ63 and RMQ101; **(D)** DB12, RMQ102, RMQ8, RMQ103, RMQ10, RMQ104, RMQ12, RMQ105, RMQ61, RMQ106, RMQ18, RMQ107, RMQ63 and RMQ108; **(E)** DB12, RMQ109, RMQ8, RMQ110, RMQ10, RMQ111, RMQ12, RMQ112, RMQ61, RMQ113, RMQ18, RMQ114, RMQ63 and RMQ115; **(F)** DB12, RMQ116, RMQ8, RMQ117, RMQ10, RMQ118, RMQ12, RMQ119, RMQ61, RMQ120, RMQ18, RMQ121, RMQ63 and RMQ122. Strains were cultured overnight, subcultured 1:50 into fresh LB and grown for 2 hours at 37°C. 0.1mM IPTG was added for *cpxA* and *cpxP* induction. Bacteria were grown for an additional 3 hours, resuspended in 1X Z-buffer and the OD_{600} was read. Cells were lysed by the addition of chloroform and SDS. β-galactosidase activity was recorded for each sample and standardized to their OD_{600}. Data represent the mean and standard deviation of three replicate cultures. Results represent three independent experiments. Asterisks indicate statistically significant difference within the same strain harboring the overexpression plasmid or its parental vector (*$P \leq 0.05$, **$P \leq 0.01$, *** $P \leq 0.001$, **** $P \leq 0.0001$; one-way ANOVA with Sidak's post hoc multiple comparison test). NS denotes no statistically significant difference in reporter activity.

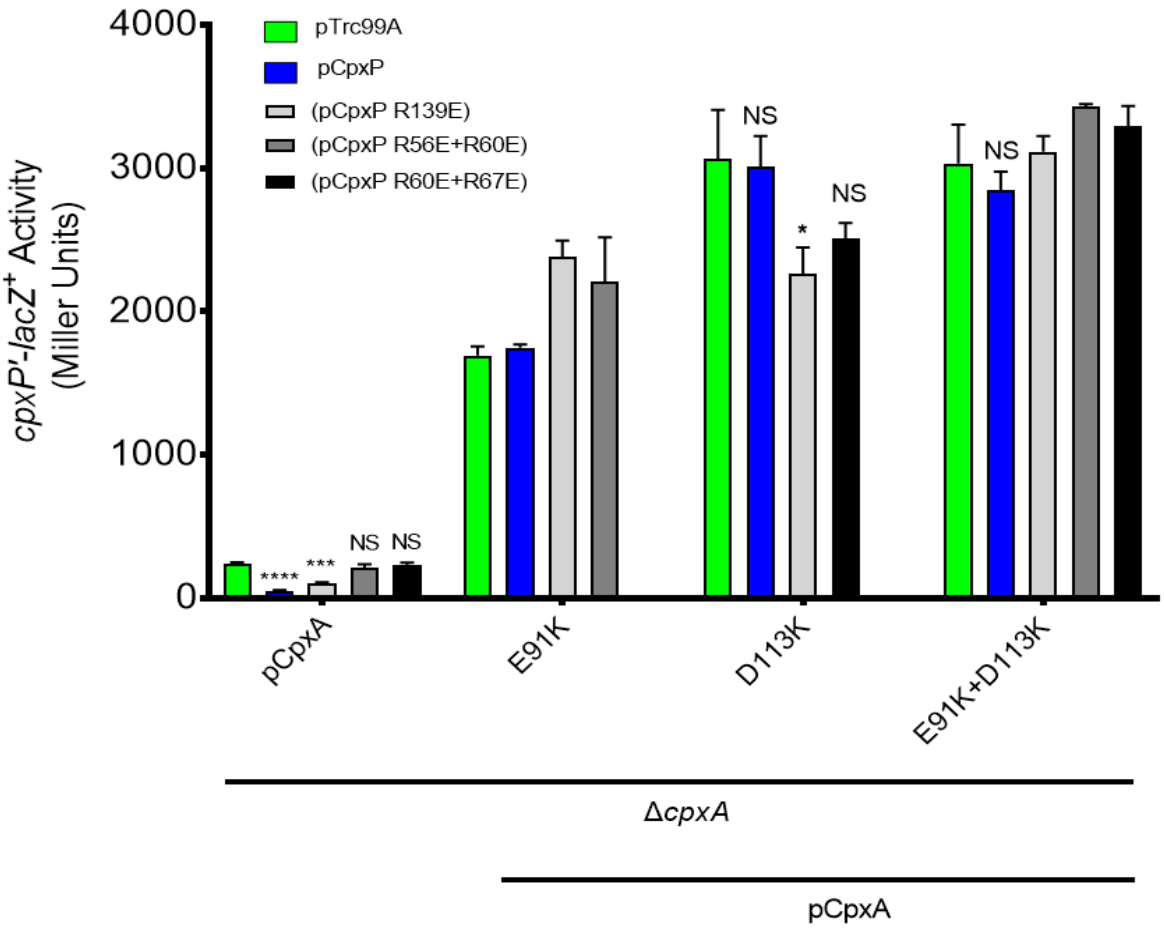

Figure 3-10: The pCpxP-R_{139}E mutation partially complements the pCpxA-D_{113}K hyperactivation. Single isolated colonies of transformed *E. coli ΔcpxA* strains harboring either the pCpxA, pCpxA-E_{91}K, pCpxA-D_{113}K or pCpxA-E_{91}K+D_{113}K plasmids were individually co-transformed with the pTrc99A, pCpxP, pCpxP-R_{139}E, pCpxP-R_{56}E+R_{60}E or pCpxP-R_{60}E+R_{67}E plasmids. Specific strains depicted from left to right are as follows: RMQ10, RMQ11, RMQ104, RMQ111, RMQ118; RMQ61, RMQ62, RMQ106, RMQ113; RMQ18, RMQ19, RMQ114, RMQ121; RMQ63, RMQ64, RMQ108, RMQ115 and RMQ122. Strains were cultured overnight, subcultured 1:50 into fresh LB and grown for 2 hours at 37°C. 0.1mM IPTG was added for *cpxA* and *cpxP* induction. Bacteria were grown for an additional 3 hours, resuspended in 1X Z-buffer and the OD_{600} was read. Cells were lysed by the addition of chloroform and SDS. β-galactosidase activity was recorded for each sample and standardized to their OD_{600}. Data represent the mean and standard deviation of three replicate cultures. Results represent three independent experiments. Asterisks indicate statistically significant difference within the same strain harboring the overexpression plasmid or its parental vector (*$P \leq 0.05$, **$P \leq 0.01$, *** $P \leq 0.001$, **** $P \leq 0.0001$; one-way ANOVA with Sidak's post hoc multiple comparison test). NS denotes no statistically significant difference in reporter activity.

3.13 References

Buelow, D. R., & Raivio, T. L. (2005). Cpx signal transduction is influenced by a conserved N-terminal domain in the novel inhibitor CpxP and the periplasmic protease DegP. *Journal of Bacteriology*, *187*(19), 6622–6630. https://doi.org/10.1128/JB.187.19.6622-6630.2005

Cosma, C. L., Danese, P. N., Carlson, J. H., Silhavy, T. J., & Snyder, W. B. (1995). Mutational activation of the Cpx signal transduction pathway of *Escherichia coli* suppresses the toxicity conferred by certain envelope-associated stresses. *Molecular Microbiology*, *18*(3), 491–505.

Danese, P. N., & Silhavy, T. J. (1998). CpxP, a stress-combative member of the Cpx regulon. *Journal of Bacteriology*, *180*(4), 831–839.

Gross, R., & Beier, D. (Ed.), *Two-Component Systems in Bacteria* (pp. 231–267). UK: Caister Academic Press.

Jobling, M. G., & Holmes, R. K. (1990). Construction of vectors with the p15a replicon, kanamycin resistance, inducible *lacZ alpha* and pUC18 or pUC19 multiple cloning sites. *Nucleic Acids Research*, 18(17), 5315–5316.

Kitagawa, M., Ara, T., Arifuzzaman, M., Ioka-Nakamichi, T., Inamoto, E., Toyonaga, H., & Mori, H. (2005). Complete set of ORF clones of *Escherichia coli* ASKA library (A Complete

Set of *E. coli* K-12 ORF Archive): Unique Resources for Biological Research. *DNA Research*, 12(5), 291–299.

Konovalova, A., Perlman, D. H., Cowles, C. E., & Silhavy, T. J. (2014). Transmembrane domain of surface-exposed outer membrane lipoprotein RcsF is threaded through the lumen of β-barrel proteins. *Proceedings of the National Academy of Sciences of the United States of America*, 111(41), E4350–E4358.

Lefèvre, F., Rémy, M.-H., & Masson, J.-M. (1997). Alanine-stretch scanning mutagenesis: a simple and efficient method to probe protein structure and function. *Nucleic Acids Research*, 25(2), 447–448.

Lu, J., Peng, Y., Arutyunov, D., Frost, L. S., & Glover, J. N. M. (2012). Error-prone PCR mutagenesis reveals functional domains of a bacterial transcriptional activator, TraJ. *Journal of Bacteriology*, 194(14), 3670–3677.

Otto, K., & Silhavy, T. J. (2002). Surface sensing and adhesion of *Escherichia coli* controlled by the Cpx-signaling pathway. *Proceedings of the National Academy of Sciences of the United States of America*, *99*(4), 2287–2292. https://doi.org/10.1073/pnas.042521699

Raivio, T. L., & Silhavy, T. J. (1997). Transduction of envelope stress in *Escherichia coli* by the Cpx two-component system. *Journal of Bacteriology*, *179*(24), 7724–7733. https://doi.org/10.1128/JB.179.24.7724-7733

Raivio, T. L., Popkin, D. L., & Silhavy, T. J. (1999). The Cpx envelope stress response is controlled by amplification and feedback inhibition. *Journal of Bacteriology*, *181*(17), 5263–5272.

Snyder, W. B., Davis, L. J., Danese, P. N., Cosma, C. L., & Silhavy, T. J. (1995). Overproduction of NlpE, a new outer membrane lipoprotein, suppresses the toxicity of periplasmic LacZ by activation of the Cpx signal transduction pathway. *Journal of Bacteriology*, *177*(15), 4216–4223.

The Addgene nonprofit plasmid repository. *Addgene*. https://www.addgene.org/vector-database/3301/

The PyMOL Molecular Graphics System, Version 1.2. *Schrödinger, LLC.*

Thede, G. L. (2012). Biochemical and structural investigation of CpxP and CpxA, key components of an envelope stress response in *Escherichia coli*. PhD thesis, University of Alberta, Alberta, Canada.

Thede, G. L., Arthur, D. C., Edwards, R. A., Buelow, D. R., Wong, J. L., Raivio, T. L., & Glover, J. N. M. (2011). Structure of the periplasmic stress response protein CpxP. *Journal of Bacteriology, 193*(9), 2149-2157. doi:10.1128/JB.01296-10

Vogt, S. L., & Raivio, T. L. (2012). Just scratching the surface: An expanding view of the cpx envelope stress response. *FEMS Microbiology Letters, 326*(1), 2-11. doi:10.1111/j.1574-6968.2011.02406.x

Vogt, S., Acosta, N., Wong, J., Wang, J., & Raivio, T. L. (2012). The CpxAR Two-component System Regulates a Complex Envelope Stress Response in Gram-negative Bacteria. In Gross, R., & Beier, D. (Ed.), *Two-Component Systems in Bacteria* (pp. 231–267). UK: Caister Academic Press.

Zhou, X., Keller, R., Volkmer, R., Krauss, N., Scheerer, P., & Hunke, S. (2011). Structural basis for two-component system inhibition and pilus sensing by the auxiliary CpxP protein. *The Journal of Biological Chemistry, 286*(11), 9805-9814. doi:10.1074/jbc.M110.194092

Chapter 4: Discussion

The ability of *Escherichia coli* and other pathogenic Gram-negative bacteria to adapt to a plethora of changes in their environment is of vital importance for them to successfully colonize and survive within a host organism (Buelow & Raivio, 2010). They are able to achieve this objective by utilizing widely conserved Two-Component Signal Transduction systems (TCSTs), which allow for selective gene modulation that results in differential protein production, depending on the circumstance encountered (Buelow & Raivio, 2010; Bury-Moné et al., 2009; MacRitchie et al., 2008).

My study focused on the Cpx envelope stress response TCST system of *E. coli*, a pathway necessary to deal with periplasmic misfolded proteins that could negatively impact the integrity of the envelope (MacRitchie et al., 2008; McEwen & Silverman, 1980; Vogt & Raivio, 2012). Even though recent experimental contributions have provided new insights into our understanding on the structural configuration and function of the $CpxA_{SD}$, the specifics on how this HK sensor detects and transduces signals are still not completely clear (Keller, Havemann & Hunke, 2011). Additional studies over the last 20 years have resulted in further evidence that support a model with a likely ocurring direct protein-protein interaction between the $CpxA_{SD}$ and CpxP during the inactive state of the Cpx pathway (Buelow & Raivio, 2005; Fleischer et al., 2007; Hörnschemeyer et al., 2016; Raivio et al., 1999; Raivio et al., 2000; Raivio & Silhavy, 1997; Tschauner et al., 2014). However, the specific direct contact between both components of the Cpx pathway has yet to be demonstrated adequately, as well as the molecular and structural characteristics that allow for this interaction to occur *in vivo*.

In this work, I sought to increase the knowledge on whether some of the recently identified surface-exposed amino acid residues comprising large negatively charged patches in the $CpxA_{SD}$ of *E. coli* are important for pathway activation, interaction with charged partners (specifically

CpxP) and stability of the protein levels produced. Experimental analyses were performed by following a site-directed specific mutational approach, based on structural and electrostatic analysis of the $CpxA_{SD}$, and several particular signaling phenotypes were retrieved. I also investigated the potential for specific positively charged residues in CpxP to be direct contact sites of the previosuly characterized negatively charged residues in $CpxA_{SD}$, using complementary charge mutations. Results from these second-site supressor assays identified a possible specific interaction point between both Cpx components.

4.1 Cpx pathway activation was confirmed to occur under alkaline pH dependant on CpxA, as well as at acid pH in the absence of CpxA

The experimental approach that I followed consisted of assessing Cpx activity levels that resulted from site-directed substitutions of surface-exposed negatively charged residues located on the $CpxA_{SD}$. Using the chromosomal *cpxP'-lacZ*$^+$ reporter gene present in TR50 (an MC4100-derived *E. coli* laboratory strain) allowed me to indirectly measure Cpx activation, based on the amount of β-galactosidase produced when this reporter gene is expressed. This enzyme is produced since the induction of the Cpx response results in phosphorylation of CpxR. CpxR~P then acts as a regulator of gene transcription that binds to specific recognition motifs on the *cpxP* promoter. This binding mediates the expression of its *lacZ* transcriptionally-fused gene, and finally results in the production of β-galactosidase (Fleischer et al., 2007; MacRitchie et al., 2008; Raivio & Silhavy, 1997). This enzyme is able to cleave the colorless ONPG (a lactose analog) into galactose and the yellow o-nitrophenol (ONP) compound (Kennedy & Scarborough, 1967). ONP possesses a maximum absorbance value at a wavelength of 420nm, so its increasing production can be measured through spectrophotometry. The *cpxP'-lacZ*$^+$ reporter gene has been widely utilized in

previous published experiments, since *cpxP* was demonstrated to be one of the most highly upregulated genes when the pathway is activated, and both its expression and regulation are strictly dependent on CpxR~P (Danese et al., 1998; DiGiuseppe & Silhavy, 2003).

It can be consistently observed throughout figures 3-3A, 3-4C and 3-5C (which represent the results from β-galactosidase assays during my study of the numerous *cpxA* mutated alleles under fixed acid, neutral and alkaline media conditions) that both the Δ*cpxA* and vector control strains were found to have highly increased reporter activation at pH 5.8. This is explained since the response regulator CpxR can be constitutively phosphorylated in an alternative manner directly in the cytoplasm (instead of by CpxA, which is not present in these null strains). Such phosphorylation has been previously reported to occur by the transfer of a phosphoryl group from small phosphodonor molecules (including Ac~P and other PtA-AckA pathway intermediates) under acid pH conditions (Danese et al., 1995; Klein et al., 2007; Lima et al., 2016; Raivio & Silhavy, 1997; Wolfe, 2010; Wolfe et al., 2008). Moreover, acetyl phosphate is reported to possess greater stability under acidic conditions in between the pH values of 5 and 6 (Lipmann & Tuttle, 1944), which supports the explanation for its availability only at my studied condition of pH 5.8 to be able to transfer a phosphate molecule to CpxR. In fact, this form of cytoplasmic CpxR phosphorylation allows for its binding to promoters of downstream targets with higher affinity (Raivio & Silhavy, 1997). Even though acid pH is not reported as an inducer of the Cpx response, the pathway is kept "turned on" in this specific scenario, since CpxA is absent from this strain and the CpxR~P produced in excess is not being dephosphorylated and accumulates over time. In contrast, the WT and pCpxA complemented strains showed no activation of the Cpx response at pH 5.8, when compared to the high activity levels of the vector control strain at this same condition. Although CpxR may still be directly phosphorylated in the cytoplasm under this non-inducing

acidic condition, CpxA is able to maintain the pathway in an "off" state by acting as a phosphatase to turn any CpxR~P potentially being produced into CpxR in this new scenario.

Here I have also obtained results regarding the activation of the Cpx pathway in strains carrying the *cpxA* WT gene under extracellular alkaline pH conditions. This activation occurred specifically at pH 8.0 and for the cases of the WT and complemented pCpxA strains in my study (Figures 3-3A, 3-4C and 3-5C). Alkaline pH was reported to induce the Cpx response in WT *E. coli* strains in 1998 by Danese and Silhavy. Such inducer drastically increased the transcription levels for the *cpxP* and *cpxP-lacZ* genes when comparing these levels at acid pH (5.3) against alkaline pH (8.4), and my WT results were in line with these previously reported findings. To the contrary, the Cpx response was not activated at pH 8.0 in the *cpxA* null and vector control strains, since in this case the lack of CpxA results in CpxR not being phosphorylated (not even by Ac~P since it is unstable under alkaline pH (Lipmann & Tuttle, 1944)). These results are yet again consistent with no transcriptional induction of *cpxP* occurring in a null *cpxA::cam* strain (Danese & Silhavy, 1998). Taken together, these observations confirm that the phenotype of alkaline activation of the Cpx pathway relies on the presence of CpxA.

4.2 Strains harboring the $D_{113}K$ or $E_{91}K+D_{113}K$ *cpxA* alleles displayed a *cpx**-like constitutively hyperactivated signaling phenotype, blind to *nlpE* OX

Availability of the recently solved and yet to be published *E. coli* $CpxA_{SD}$ crystal structure and electrostatic surface representation (Margain-Quevedo et al., in preparation) allowed me to design a novel structure-based site-directed mutagenesis assay. For this purpose, the identification of amino acid residues exposed on the $CpxA_{SD}$ surface that comprise major negatively charged patches was conducted, and residues E_{37}, D_{40}, E_{91}, D_{113} and E_{138} (plus M_{48} at the centre of the

dimer) were selected. The reasoning behind choosing these amino acid residues was that the major negative regions that they comprise may play a role in the formation of potential binding sites with positively charged surfaces in ligands, as well as in mediating the $CpxA_{SD}$-CpxP direct contact and interaction. A structure-based approach based on substitution of specific surface charges on the $CpxA_{SD}$ of *E. coli* has not been tried previously to study their possible importance for signaling and interaction. The effects of the $CpxA_{SD}$ missense mutations on activation of the Cpx response in *E. coli* strains containing these extrachromosomal *cpxA* alleles were then evaluated through the *cpxP'-lacZ*$^+$ reporter gene in β-galactosidase assays. Activity that resulted from these variants was established after induction with either alkaline pH (8.0) (Danese & Silhavy, 1998) or *nlpE* overexpression (Snyder et al., 1995) (both well known activators of the Cpx pathway); or inhibition by *cpxP* overexpression (Buelow & Raivio, 2005; Raivio et al., 1999). The purpose for these assays was to determine whether or not the mutated alleles impacted CpxA phosphatase activity at acid pH and/or autokinase/kinase function under alkaline pH induction. Both functions of CpxA are of importance to establish its activity and ability to sense and transduce signals.

Some of the most striking results from my work originated from the pH β-galactosidase experiments in figures 3-3A and 3-5C (depicting *cpxA* alleles carrying lysine substitutions), and in specific, from the single $D_{113}K$ and double $E_{91}K+D_{113}K$ *cpxA* mutants. Their activation values of approximately 4,000 Miller Units (irrespective of media pH condition) are comparable to the ones displayed over 20 years ago by the constitutively activated *cpxA** strain named TR10 (*E. coli* MC4100 *cpxA24*, a deletion of 32 residues between R_{93} and G_{124} in the center of the periplasmic region) (Cosma et al., 1995; Raivio & Silhavy, 1997; Raivio et al., 1999). TR10 was the strongest allele isolated in 1995 by Cosma and collaborators, alongside several other gain-of-function *cpx** mutants. It was then better characterized when utilized again two years later for additional in-depth

studies of Cpx signal transduction, however it was incorrectly referenced as TR20 in these experiments (Raivio & Silhavy, 1997). Such *cpx** activated strains were also distinctive in the fact that they displayed between 3- to 10-fold expression induction of downstream genes regulated by the Cpx response, including *degP*; while null *cpxA* mutated strains lowered its transcription (Danese et al., 1995). Further, both the $D_{113}K$ and $E_{91}K+D_{113}K$ mutated strains from my work stayed locked in the hyperactivated state at either the acid, neutral or basic pH values studied (Figure 3-5C). This result is remarkable, since in these strains the Cpx response was mounted at very high levels even without the presence of an environmental inducer at pH 5.8. This could be due to a faulty recognition of the inhibitor CpxP, which could have favored the autokinase/kinase activities of CpxA and resulted in the default induction of the pathway. This possibility seems more likely according to the *cpxP* OX results that will be addressed in the following subsections. Another possible explanation could be that these specific charge-swap substitutions may have caused a conformational change that inhibited the ability for CpxA to dephosphorylate CpxR at non-inducing conditions. The mutated CpxA in these cases would not possess an adequate phosphatase activity, so CpxR would be consistently phosphorylated in the cytoplasm causing response initiation (Klein et al., 2007; Lima et al., 2016; Wolfe, 2010; Wolfe et al., 2008). To further test the second supposition, future experiments could take advantage of the phenotype observed at acid pH in a single deleted *cpxA* strain compared to a double null *cpxA* plus *ptA-ackA* strain (Wolfe et al., 2008). For the single mutant, the previously described hyperactivated state would be expected, due to the lack of phosphatase activity since no CpxA is present. To the contrary, in the double mutant there would be no induction of the Cpx pathway at acid pH. This since the CpxR phosphorylation would not occur, as there would not be either CpxA or small phosphodonor intermediates from the PtA-AckA pathway to carry this function. These controls

could then be used to compare to strains harboring my CpxA substituted alleles, both with and without the genes required for the PtA-AckA pathway. It would then be expected that if the phosphatase activity is not impaired due to the mutations, then no difference would be observed with or without *ptA-ackA* (no activation at acid pH, similar to a WT strain). If phosphatase function is indeed affected, then similar results to the null strains would be obtained (activation of the response only in the presence of PtA-AckA at acid pH conditions).

When an MC4100 *cpxA24* strain containing the chromosomal *cpxP-lacZ* reporter gene (referenced as the TR34 strain) was assayed by the Raivio and Silhavy group, it exhibited between 5,000 and 6,000 MU (pathway hyperactivation) and proved to be refractive (signal blind) to further induction by overproduction of NlpE (Raivio & Silhavy, 1997). These results are similar when compared with the phenotypes observed from the strains harboring the *cpxA* mutated $D_{113}K$ and $E_{91}K+D_{113}K$ alleles. These two mutated strains were not susceptible to a significant further induction by pNlpE when compared to their respective pCA24N vector control (Figure 3-5E). Altogether, these results suggest that the specific nature and location of the E_{91} and D_{113} amino acid residues on the $CpxA_{SD}$ surface may indeed be playing an important role that allows for regulation of the pathway and mediation of signaling detection and transduction. The hyperactivated state observed under two different inducing conditions and even at a non-inducing environment may support the idea of a common mechanism for sensing diverse stimuli by the Cpx response in these two mutants.

4.3 The $E_{91}K$, $E_{91}A$ and $E_{91}A+D_{113}A$ *cpxA* mutants displayed a different type of hyperactivated phenotype, reaching its highest levels at alkaline pH

Another interesting Cpx signaling phenotype (different from the constitutive hyperactivation described in section 4.2 for strains harboring the *cpxA* alleles $D_{113}K$ and $E_{91}K+D_{113}K$) was observed for the $E_{91}K$, $E_{91}A$ and $E_{91}A+D_{113}A$ mutants. For these *cpxA* mutated alleles, the highest hyperactivation of the Cpx response occurred under alkaline pH 8.0 inducing conditions. The $E_{91}K$ mutant resulted in over 4,000 MU in this pH value, while the pathway was still activated under acid and neutral media but did not reach those hyperactivated levels (Figure 3-5C). This lysine substitution of the E_{91} residue has actually been described before as TR11 (*E. coli* MC4100 *cpxA102*, a different Cpx* mutation than *cpxA24*) (Cosma et al., 1995; Price & Raivio, 2009) and incorrectly described in previous publications as "$E_{92}K$" (Keller et al., 2011; Raivio & Silhavy, 1997; Raivio et al., 1999). During my current work, both the *E. coli* periplasmic $CpxA_{SD}$ crystal structure and sequencing results (data not shown) confirmed that the correct position for this glutamate is 91 instead of 92, which contributes to the knowledge regarding this specific allele and may allow for a better characterization in the future. Even though the CpxA102 protein had been shown to lead to induction of genes in the Cpx regulon (Cosma et al., 1995), it resulted in a small reduction of CpxA and CpxR phosphorylation instead of augmented levels, during *in vitro* studies that incorporated the mutant into reconstituted proteoliposomes (Keller et al., 2011). Such seemingly conflicting result suggests that the gene induction phenotype observed for *cpxA102* was not directly caused by changes in the autokinase/kinase/phosphatase activities of CpxA102. Furthermore, overexpression of *cpxP* could not decrease the *cpxP-lacZ* reporter gene expression in the TR36 (MC4100 [*cpxP-lacZ*] *cpxA102*) strain of over 4,000 MU, resulting in it being insensitive toward inhibition by pCpxP OX (Raivio et al., 1999). In line with these

observations, my $E_{91}K$ substitution appeared to disturb CpxA interaction with CpxP, since *cpxP* OX was not able to inhibit its hyperactivation (Figure 3-5D). Together, these results confirm that the hyperactivated state of the pCpxA-$E_{91}K$ strain at alkaline pH was due to an improper recognition or interaction with CpxP in the periplasm. In similar fashion, the $E_{91}A$ and $E_{91}A$+$D_{113}A$ substitutions were more active under alkaline pH as well, however their obtained values did not reach 4,000 MU (Figure 3-5C). Intriguingly, single alanine substitution of the D_{113} residue completely took away the hyperactivated phenotype (Figures 3-4C and 3-5C) previously observed in the $D_{113}K$ strain results (Figure 3-3A). These data together support the idea that a charge-swap from negative to positive generates a more drastic and potential bigger structural effect in these residues, compared to a modification for alanine. It also further highlights the importance for the presence of these specific negative surface charges in the $CpxA_{SD}$ comprised by E_{91} and D_{113}, as modification may also alter their ability to maintain important partner interactions.

Unfortunately, the strains containing the $E_{37}K$, $M_{48}K$, $E_{138}K$, $E_{37}A$, $D_{40}A$, $M_{48}A$, and $E_{138}A$ *cpxA* mutated alleles (Figures 3-3A, 3-4C and 3-5C) did not display hyperactivated signaling phenotypes as the ones previously described. Instead, their phenotypes under the different pH media conditions studied resembled the trends observed in the WT and pCpxA complemented strains (only being somewhat activated under alkaline pH in levels comparable to the WT) (Figures 3-3A and 3-5C). These observations suggest that either these residues are not as important for regulating the CpxA phosphatase activity, mediating interactions with nearby proteins and signal detection, or that they might be exerting their function only in combination between each other or with different residues yet to be studied. However, M_{48} remains a residue of interest, since it is localized at the center of the dimer interface (Figure 3-2C). It also appears to have at least a degree of influence on the overall maintenance of the structure and intramolecular interactions, since the

$M_{48}K$ mutant was less activated under alkaline pH and pNlpE OX conditions as compared to the WT and pCpxA strains (Figures 3-3A and C).

4.4 Strains harboring gain-of-function lysine and alanine *cpxA* mutated alleles lost sensitivity toward *cpxP* overexpression

Overproduction of the regulon member CpxP has been clearly demonstrated to inhibit activation of the Cpx response, in a manner dependent on the presence of wildtype *cpxA*. (Buelow and Raivio 2005; Raivio et al., 1999). A small but noticeable decrease was also observed in *cpxP-lacZ* activity in a CpxA101 Cpx* mutant (in which T_{252} located in the cytoplasm and close to the putative autophosphorylation location has been modified to proline). This cytoplasmic mutation also disrupted CpxA phosphatase activity toward phosphorylated CpxR (Raivio et al., 1999). Notably however, CpxP was not able to diminish the hyperactivated state of the CpxA102 gain-of-function strain (containing a lysine substitution to the periplasmic E_{91} amino acid residue that makes it irresponsive to inducers), also harboring a Cpx-mediated *cpxP-lacZ* reporter gene. These results lead to the conclusion that the ability of CpxP OX to repress response activity occurs through the $CpxA_{SD,}$ and modification of specific residues in it may lead to such repression not being able to take place (Keller et al., 2011; Raivio et al., 1999). Since inhibition was significantly compromised at non-inducing conditions for the hyperactivated strains carrying the periplasmic mutated alleles $E_{91}K$, $D_{113}K$, $E_{91}K+D_{113}K$, $E_{91}A$ and $E_{91}A+D_{113}A$ (Figure 3-5D), I then wanted to determine the extent of a possible effect of these $CpxA_{SD}$ modifications on CpxP-mediated inhibition. Interestingly, all five of these mutated strains are either individual or combination of the E_{91} and D_{113} negatively-charged residues on the $CpxA_{SD}$ surface. This trend appears to further confirm the nature and position of these two residues as very important determinants for

recognition of the inhibitor CpxP and its ability to diminish Cpx response activation. This evidence is in support of the idea that modification of these two residues (especially when it is a charge-swap) may lead to changes in the $CpxA_{SD}$ configuration and a faulty recognition or interaction with CpxP in the periplasm. Such structural modifications may later affect the nature of the signal normally propagated into the cytoplasmic transmitter core ($CpxA_{HDC}$), formed by 1) the HAMP linker, 2) the enzymatic dimerization and histidine phosphorylation (DHp) domain, and 3) the catalytic ATP-binding (CA) domain (Mechaly et al., 2014). Thus, the ability for CpxA to autophosphorylate and then phosphorylate CpxR may not be regulated in these two mutants, locking the CpxA conformation into constant autokinase/kinase activities and hyperactivating the response. This effect was not observed in the rest of the mutants assayed, as they showed decrease of activity levels in the presence of CpxP OX. The latter observation could signify that their role is not as important for CpxP recognition, or that they act as a combination with other residues. Whether a specific component of the CpxA transmitter core or a combination of the three is affected, as well as the potential abnormal structural conformation that CpxA may take in the presence of the $E_{91}K$ and $D_{113}K$ mutants, remain to be determined.

Lastly, it was confirmed that the CpxA protein levels for all of the strains containing the lysine and alanine mutated alleles were maintained almost statically throughout assays involving SDS-PAGE coupled with Western blotting. This signifies that the *cpxA* was being expressed at approximately the same levels and practically unaltered, also suggesting that they possessed similar stability compared to the wildtype (Figures 3-6 and 3-7). It also adds to the conclusion that the signaling phenotypes retrieved from the various β-galactosidase assays are in fact due to the mutations introduced and did not occur because of a significant difference in the levels of mutated CpxA proteins produced.

4.5 A potential interaction site is located between the CpxA D_{113} and CpxP R_{139} amino acid residues

Various studies have resulted in compelling experimental evidence that convincingly propose a direct protein-protein interaction between the wildtype CpxA and CpxP proteins *in vivo*. The first observations that pointed toward this model described a set of Cpx* constitutively activated mutants that generated signal-blind phenotypes and increased kinase activity and regulated gene transcription. These mutant's sequences and phenotypes suggested that wildtype CpxA could then interact with CpxP in the periplasm under non-stressful conditions, which would then favor its phosphatase activity (Raivio & Silhavy, 1997). Additional studies discovered that excess CpxP anchored to the inner membrane did not allow for a complete activation of the Cpx response by spheroplasting induction (Raivio et al., 2000). Moreover, the addition of purified CpxP to proteoliposomes containing CpxA resulted in the inability for CpxA autophosphorylation and subsequent obstruction of pathway initiation as well (Fleischer et al., 2007). To the contrary, inhibition of CpxA by CpxP was not observed in either strains lacking a functional $CpxA_{SD}$ or strains with CpxP mutations in the conserved N-terminus (Buelow & Raivio, 2005; Raivio et al., 2000). A recent peptide screening experiment showed that two cellulose-bound peptides from the C-terminus and one from the α1 helix in CpxP were potentially interacting with acidic amino acid residues in the purified soluble $CpxA_{SD}$. A complete modification of the $CpxA_{SD}$ C-terminus in this same study did not identify residues of importance for binding CpxP, but introduction of additional negative residues in this structure did improve binding (Zhou et al., 2011). More recently, another experiment determined that affinity between CpxA reconstituted in nanodiscs (CpxA-ND) and CpxP is very low. Interestingly, CpxA-ND displayed higher affinity for CpxR than for CpxP in such study. Observations for the affinity between CpxA-ND and CpxP required

an extremely high CpxP concentration, close to the amount needed for precipitation (supersaturated solution), and the relative affinity between both was practically undetectable (Hörnschemeyer et al., 2016). This last piece of evidence still supports a direct interaction between both components but may point to a transient or weak state, which could partially explain why the study and observation of this contact is still a difficult task to accomplish.

Even though we possess all of the previously mentioned evidence for direct contact between the $CpxA_{SD}$ and CpxP, specific contact points between the $CpxA_{SD}$ negatively charged surface-exposed residues and the CpxP positively charged residues in its concave surface that mediate their direct interaction in the absence of stressors have not been determined to date. Parting from my previously discussed results, I decided to try a second site suppressor assay in which I would mutate some of the main positively charged solvent-exposed residues contributing to the positive polar concavity in CpxP (R_{56}, R_{60} and R_{67}) into negative glutamates (Buelow & Raivio, 2005; Thede et al., 2011; Zhou et al., 2011). These three residues in CpxP have been reported to lose their capacity of inhibiting normal Cpx activation when mutated to glutamine (Q) (Buelow & Raivio, 2005; Zhou et al., 2011). In addition, the CpxP R_{139} residue would also be substituted for glutamate, since it can be observed in our *in-silico* docking model that it might contact a distinct negative surface in the $CpxA_{SD}$ (Figure 3-8). These positive to negative mutations would potentially complement the hyperactivated states observed for the $CpxA_{SD}$ strains carrying the mutated $E_{91}K$, $D_{113}K$ and $E_{91}K+D_{113}K$ (negative to positive charge swap). This in turn would signify a specific point of contact for direct interaction between $CpxA_{SD}$ and CpxP *in vivo*.

Results obtained in Figures 3-9A to F displayed a loss-of-function phenotype in the single and double substitutions made to the arginine residues in CpxP, in line with the observations reported by Buelow & Raivio, as well as Zhou and collaborators. These mutations were impaired

in their inhibitory capacity of a WT strain, as compared to the inhibition by WT pCpxP. Such phenotypes of the mutated strains were more apparent in the double mutants, confirming that these residues might in fact be important for interaction with CpxA, and that they exert this function through multiple amino acid residues at the same time. Unfortunately, none of the R_{56}, R_{60} and R_{67} mutants were able to complement hyperactivation from my CpxA lysine substituted strains, not even when in R_{56}+R_{60} or R_{60}+R_{67} combination. This could mean that there is a requirement for additional or different CpxP residues to interact with CpxA, or simply that they might be interacting with different CpxA residues not explored in this study. Another possibility is that the $CpxA_{SD}$-CpxP interaction could be very weak, transient, or occur with very low affinity (Hörnschemeyer et al., 2016). This could make the sensitive detection of the interaction a difficult task for these types of enzymatic assays.

Strikingly, a specific CpxP-CpxA *in vivo* interaction point not previously described was found in this work, while complementing the pCpxA-D_{113}K strain with the pCpxP-R_{139}E strain. Even though only a partial complementation could be retrieved and the pCpxP substitution was not able to return the pCpxA mutant back to wildtype levels (Figure 3-9D and 4-2), this result was reproducible and confirmed in a subsequent assay (Figure 3-10). This genetic data proposes a new and different interaction domain in CpxP for contact with CpxA than the ones referenced before, localized in either the C-terminus or the α1 helix (Zhou et al., 2011), since the R_{139} residue is located in the α4 helix of the CpxP dimer instead. No specific $CpxA_{SD}$ residues with potential importance for this interaction have been described previously either, until the D_{113} result from the structure-guided site-directed mutagenesis and complementation assays. This interaction can be visualized in our predicted docking model (Figure 3-8), in which the D_{113} residue in the left

monomer of CpxA (residue labelled in red) is located in close proximity to the R_{139} residue in the crimson CpxP dimer (residue labelled in blue).

4.6 Final model, concluding remarks and suggested future directions

The experimental results depicted in this study were obtained based on a novel structure-guided site-directed mutagenesis approach. They established that the identity and position of the E_{91} and D_{113} surface-exposed amino acid residues comprising large surface-exposed negatively charged patches in the $CpxA_{SD}$ of *E. coli* are important for mediation of the direct $CpxA_{SD}$-CpxP interaction. The *cpxA* strains harboring the $E_{91}K$, $D_{113}K$ or $E_{91}K+D_{113}K$ mutated alleles lost sensitivity toward overproduction of CpxP (which in turn is no longer able to inhibit activation of the response). Such mutated strains also displayed pathway hyperactivation comparable to *cpx** strains previously characterized. Therefore, the lysine substitutions may have generated structural modifications on CpxA, with the consequence of faulty recognition of CpxP. This may have then affected signaling transduction and locked the CpxA structure into constitutive autophosphorylation/CpxR-phosphorylation activities (Figure 4-1). For the specific case of $E_{91}K$, further conformational studies might be required to determine the exact cause for pathway hyperactivation, as published data reported that its enzymatic activities were not compromised (Keller et al., 2011). Likewise, it is yet to be determined whether CpxA phosphatase activity has been compromised by these substitutions as well.

Furthermore, a new proposed specific direct-contact interaction site between the D_{113} amino acid residue in the $CpxA_{SD}$ and the R_{139} residue in CpxP was described (Figures 4-2 and 4-3). This observation arose from the fact that an $R_{139}E$ substitution in CpxP was able to partially complement the hyperactivated state of the $D_{113}K$ mutant in CpxA (Figure 4-2). It still remains

unclear whether other residues could be concomitantly aiding in this interaction point, and which residues these might be. This is a relevant result since it describes an interaction site in a different region of the proteins from the ones proposed in past published results (Zhou et al., 2011), adding to our knowledge on the $CpxA_{SD}$-CpxP protein-protein interaction that allows for regulation of the Cpx pathway activity.

Future directions to have a better understanding on the results presented in this work might include moving the mutations assayed into the chromosome through lambda-red mediated recombination and check whether the signalling phenotypes are still maintained; trying different combination of mutations to the residues to look for potential additional additive effects on the interaction; performing phosphorylation assays to determine the exact extent of the mutation effects toward phosphotransfer ability and CpxA enzymatic activities; and doing pulse-chase experiments to confirm protein stability with a higher degree of confidence.

Finally, the significance of this research for increasing our understanding on how the $CpxA_{SD}$ can sense environmental stimuli and interact with partner proteins like CpxP, lies on the fact that they have been considered potential targets for therapeutic treatment alternatives for diseases caused by pathogenic bacteria (Buelow & Raivio, 2010; Gotoh et al., 2010; Stephenson & Hoch, 2002, 2004). The Cpx envelope stress response plays a role in regulating bacterial virulence factors when activated by inducers. Synthesis of molecules that could mimic the CpxP-$CpxA_{SD}$ interaction or recognize the $CpxA_{SD}$ to interact with it (in a similar fashion in which CpxP does) could lead to targeted inhibition of the pathway and better control of virulence. This would present a viable alternative or complementary treatment to the current antibiotic therapies in the future, an era in which multi-drug resistance in bacteria is increasingly becoming a major concern for public health.

4.7 Figures

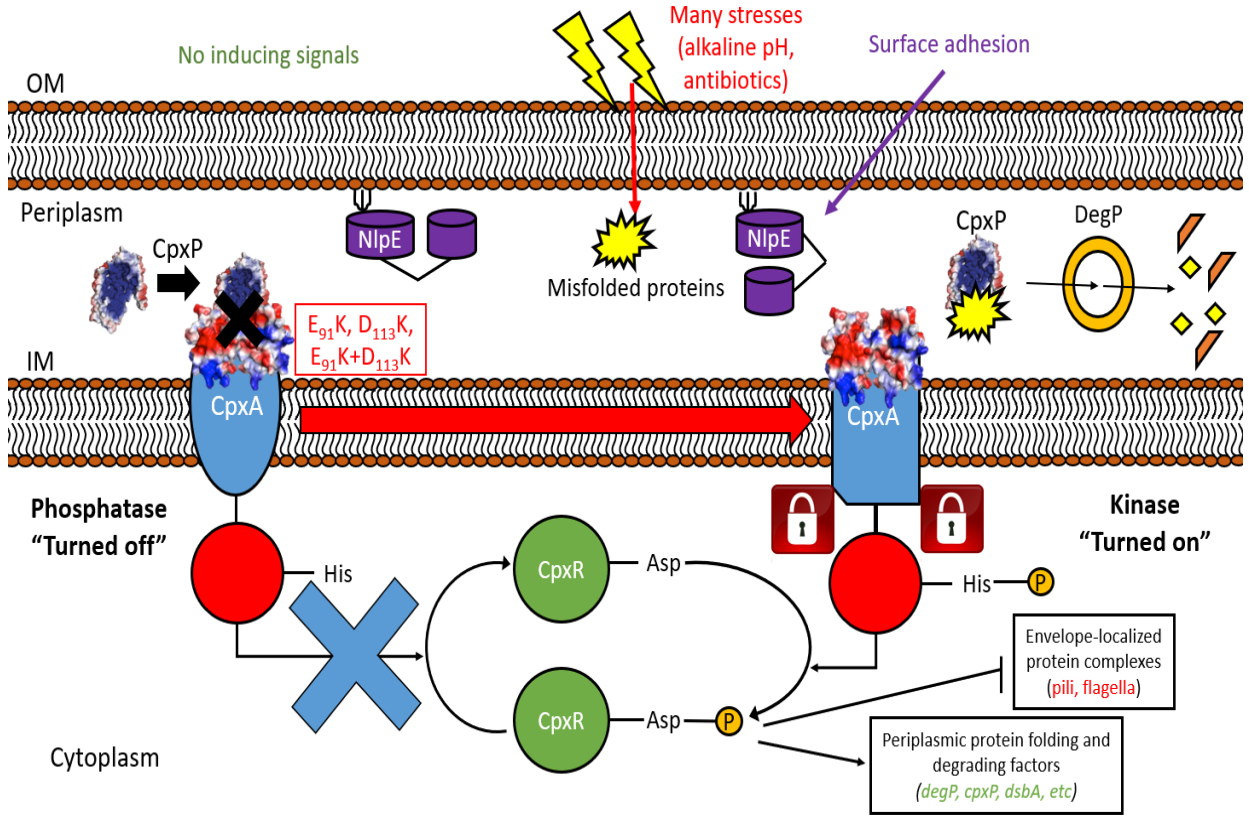

Figure 4-1: The *cpxA* strains harboring the $E_{91}K$, $D_{113}K$ or $E_{91}K+D_{113}K$ mutated alleles displayed sensitivity loss toward CpxP that resulted in Cpx pathway hyperactivation. Lysine substitution of residues E_{91}, D_{113} or the double $E_{91}+D_{113}$ in the $CpxA_{SD}$ likely generate conformational modifications that result in the inability for inhibition by CpxP. The autokinase/kinase activities of CpxA are favored over the phosphatase activity in this scenario, even under non-inducong conditions. This locks CpxA in a constant "turned on" phenotype, resulting in hyperactivated activity levels (similar to the levels described for *cpx** TR10 and TR11strains) under different pH conditions and even after overexpression of *nlpE* or *cpxP*.

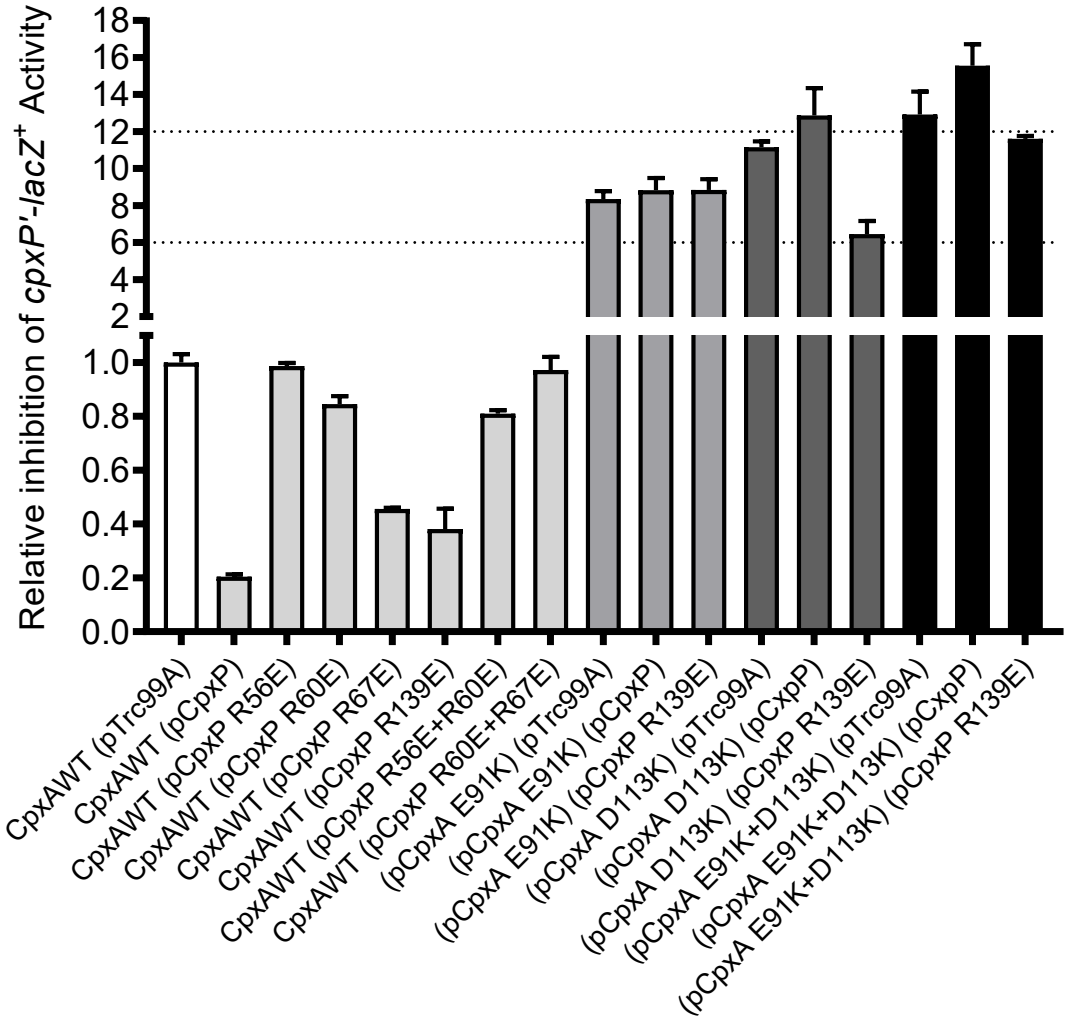

Figure 4-2: Summary for data depicting evidence for the allele-specific suppression of the $CpxA_{SD}$ $D_{113}K$ hyperactivated mutant by the CpxP $R_{139}E$ substitution. Individual point mutants (glutamate substitutions) in pCpxP resulted in differential decrease for CpxAWT inhibition, as compared to wildtype pCpxP. Second-site suppressor assays showed that the $R_{139}E$ substitution in CpxP was only able to partially complement the hyperactivated state of the $D_{113}K$ mutant in the $CpxA_{SD}$, but failed to supress hyperactivation exerted by the $E_{91}K$ and $E_{91}K+D_{113}K$ substitutions. The relative inhibition values of β-galactosidase activity (*cpxP'-lacZ*$^+$ reporter gene activity) were standardized considering a CpxAWT (pTrc99A) activity level equal to "1".

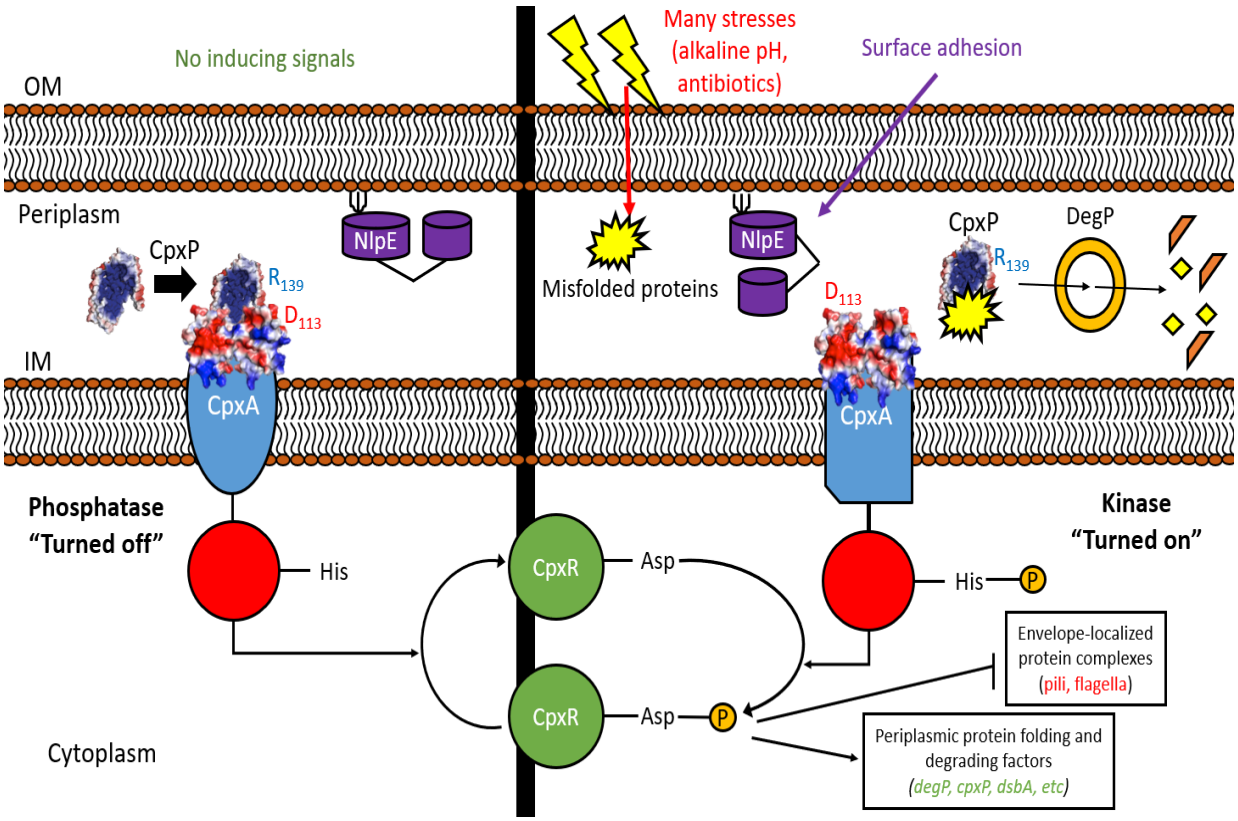

Figure 4-3: The D_{113} negatively charged surface-exposed residue in the $CpxA_{SD}$ is very likely a contact point for direct interaction with the positively charged R_{139} residue in the CpxP concavity. Second-site suppressor assays demonstrated that the $R_{139}E$ substitution in CpxP was able to partially complement the hyperactivated state of the $D_{113}K$ mutant in CpxA. This suggests a very likely interaction point between the D_{113} residue (labelled in red) comprising an important negative patch on the $CpxA_{SD}$ surface, and the R_{139} residue (labelled in blue) located in the concave positive polar region in CpxP.

4.8 References

Buelow, D. R., & Raivio, T. L. (2005). Cpx signal transduction is influenced by a conserved N-terminal domain in the novel inhibitor CpxP and the periplasmic protease DegP. *Journal of Bacteriology*, *187*(19), 6622–6630. https://doi.org/10.1128/JB.187.19.6622-6630.2005

Buelow, D. R., & Raivio, T. L. (2010). Three (and more) component regulatory systems – auxiliary regulators of bacterial histidine kinases. *Molecular Microbiology, 75*(3), 547-566. doi:10.1111/j.1365-2958.2009.06982.x

Bury-Moné, S., Nomane, Y., Reymond, N., Barbet, R., Jacquet, E., Imbeaud, S., et al. (2009). Global analysis of extracytoplasmic stress signaling in *Escherichia coli*. *PLoS Genetics, 5*(9), e1000651. doi:10.1371/journal.pgen.1000651

Cosma, C. L., Danese, P. N., Carlson, J. H., Silhavy, T. J., & Snyder, W. B. (1995). Mutational activation of the Cpx signal transduction pathway of *Escherichia coli* suppresses the toxicity conferred by certain envelope-associated stresses. *Molecular Microbiology*, *18*(3), 491–505.

Danese, P. N., Oliver, G. R., Barr, K., Bowman, G. D., Rick, P. D., & Silhavy, T. J. (1998). Accumulation of the enterobacterial common antigen lipid II biosynthetic intermediate stimulates *degP* transcription in *Escherichia coli*. *Journal of Bacteriology*, *180*(22), 5875–5884.

Danese, P. N., & Silhavy, T. J. (1998). CpxP, a stress-combative member of the Cpx regulon. *Journal of Bacteriology*, *180*(4), 831–839.

Danese, P. N., Snyder, W. B., Cosma, C. L., Davis, L. J., & Silhavy, T. J. (1995). The Cpx two-component signal transduction pathway of *Escherichia coli* regulates transcription of the gene specifying the stress-inducible periplasmic protease, DegP. *Genes & Development*, *9*(4), 387–398.

DiGiuseppe, P. A., & Silhavy, T. J. (2003). Signal detection and target gene induction by the CpxRA two-component system. *Journal of Bacteriology*, *185*(8), 2432–2440.

Fleischer, R., Heermann, R., Jung, K., & Hunke, S. (2007). Purification, reconstitution, and characterization of the CpxRAP envelope stress system of E*scherichia coli*. *The Journal of Biological Chemistry, 282*(12), 8583-8593. doi:M605785200 [pii]

Gotoh, Y., Eguchi, Y., Watanabe, T., Okamoto, S., Doi, A., & Utsumi, R. (2010). Two-component signal transduction as potential drug targets in pathogenic bacteria. *Current Opinion in Microbiology, 13*(2), 232-239. doi:10.1016/j.mib.2010.01.008

Hörnschemeyer, P., Liss, V., Heermann, R., Jung, K., & Hunke, S. (2016). Interaction Analysis of a Two-Component System Using Nanodiscs. *PloS One*, *11*(2), e0149187. https://doi.org/10.1371/journal.pone.0149187

Keller, R., Havemann, J., & Hunke, S. (2011). Different regulatory regions are located on the sensor domain of CpxA to fine-tune signal transduction. *Research in Microbiology*, 162(4), 405–409.

Kennedy, E. P., & Scarborough, G. A. (1967). Mechanism of Hydrolysis of O-Nitrophenyl-β -Galactoside in *Staphylococcus aureus* and its Significance for Theories of Sugar Transport. *Proceedings of the National Academy of Sciences of the United States of America,* 58(1), 225-228.

Klein, A. H., Shulla, A., Reimann, S. A., Keating, D. H., & Wolfe, A. J. (2007). The intracellular concentration of acetyl phosphate in *Escherichia coli* is sufficient for direct phosphorylation of two-component response regulators. *Journal of Bacteriology*, *189*(15), 5574–5581. https://doi.org/10.1128/JB.00564-07

Lima, B. P., Lennon, C. W., Ross, W., Gourse, R. L., & Wolfe, A. J. (2016). *In vitro* evidence that RNA Polymerase acetylation and acetyl phosphate-dependent CpxR phosphorylation affect *cpxP* transcription regulation. *FEMS Microbiology Letters*, *363*(5), fnw011. https://doi.org/10.1093/femsle/fnw011

Lipmann, F., & Tuttle, L. C. (1944). Acetyl phosphate: chemistry, determination, and synthesis. *Journal of Biological Chemistry*, 153, 571-582.

MacRitchie, D. M., Buelow, D. R., Price, N. L., & Raivio, T. L. (2008). Two-component signaling and Gram negative envelope stress response systems. In Utsumi, R. (Ed.), *Bacterial*

Signal Transduction: Networks and Drug Targets (pp. 80-110). New York, NY: Springer New York. doi:10.1007/978-0-387-78885-2_6

Margain-Quevedo, R., Malpica, R., Thede, G. L., Lu, J., Glover, J. N. M., & Raivio, T. L. (In preparation). Modulation of the Cpx Envelope Stress Response in *Escherichia coli* by the CpxA Periplasmic Sensing Domain and its Interaction with CpxP. *Manuscript in preparation.*

McEwen, J., & Silverman, P. (1980). Chromosomal mutations of *Escherichia coli* that alter expression of conjugative plasmid functions. *Proceedings of the National Academy of Sciences of the United States of America, 77*(1), 513-517.

Mechaly, A. E., Sassoon, N., Betton, J.-M., & Alzari, P. M. (2014). Segmental helical motions and dynamical asymmetry modulate histidine kinase autophosphorylation. *PLoS Biology*, 12(1), e1001776. https://doi.org/10.1371/journal.pbio.1001776

Price, N. L., & Raivio, T. L. (2009). Characterization of the Cpx regulon in *Escherichia coli* strain MC4100. *Journal of Bacteriology*, *191*(6), 1798–815. https://doi.org/10.1128/JB.00798-08

Raivio, T. L., & Silhavy, T. J. (1997). Transduction of envelope stress in *Escherichia coli* by the Cpx two-component system. *Journal of Bacteriology*, *179*(24), 7724–7733. https://doi.org/10.1128/JB.179.24.7724-7733

Raivio, T. L., Laird, M. W., Joly, J. C., & Silhavy, T. J. (2000). Tethering of CpxP to the inner membrane prevents spheroplast induction of the Cpx envelope stress response. *Molecular Microbiology, 37*(5), 1186-1197. doi:mmi2074 [pii]

Raivio, T. L., Popkin, D. L., & Silhavy, T. J. (1999). The Cpx envelope stress response is controlled by amplification and feedback inhibition. *Journal of Bacteriology*, *181*(17), 5263–5272.

Snyder, W. B., Davis, L. J., Danese, P. N., Cosma, C. L., & Silhavy, T. J. (1995). Overproduction of NlpE, a new outer membrane lipoprotein, suppresses the toxicity of periplasmic LacZ by activation of the Cpx signal transduction pathway. *Journal of Bacteriology*, *177*(15), 4216–4223.

Stephenson, K., & Hoch, J. A. (2002). Two-component and phosphorelay signal-transduction systems as therapeutic targets. *Current Opinion in Pharmacology, 2*(5), 507-512. doi:S1471489202001947 [pii]

Stephenson, K., & Hoch, J. A. (2004). Developing inhibitors to selectively target two-component and phosphorelay signal transduction systems of pathogenic microorganisms. *Current Medicinal Chemistry, 11*(6), 765-773.

Thede, G. L., Arthur, D. C., Edwards, R. A., Buelow, D. R., Wong, J. L., Raivio, T. L., & Glover, J. N. M. (2011). Structure of the periplasmic stress response protein CpxP. *Journal of Bacteriology, 193*(9), 2149-2157. doi:10.1128/JB.01296-10

Tschauner, K., Hörnschemeyer, P., Müller, V. S., & Hunke, S. (2014). Dynamic interaction between the CpxA sensor kinase and the periplasmic accessory protein CpxP mediates signal recognition in *E. coli*. *PloS One*, *9*(9), e107383. https://doi.org/10.1371/journal.pone.0107383

Vogt, S. L., & Raivio, T. L. (2012). Just scratching the surface: An expanding view of the cpx envelope stress response. *FEMS Microbiology Letters, 326*(1), 2-11. doi:10.1111/j.1574-6968.2011.02406.x

Wolfe, A. J. (2010). Physiologically relevant small phosphodonors link metabolism to signal transduction. *Current Opinion in Microbiology*, *13*(2), 204–209. https://doi.org/10.1016/j.mib.2010.01.002

Wolfe, A. J., Parikh, N., Lima, B. P., & Zemaitaitis, B. (2008). Signal Integration by the Two-Component Signal Transduction Response Regulator CpxR. *Journal of Bacteriology*, *190*(7), 2314–2322. https://doi.org/10.1128/JB.01906-07

Zhou, X., Keller, R., Volkmer, R., Krauss, N., Scheerer, P., & Hunke, S. (2011). Structural basis for two-component system inhibition and pilus sensing by the auxiliary CpxP protein. *The Journal of Biological Chemistry, 286*(11), 9805-9814. doi:10.1074/jbc.M110.194092

Bibliography

Acosta, N., Pukatzki, S., & Raivio, T. L. (2015). The *Vibrio cholerae* Cpx envelope stress response senses and mediates adaptation to low iron. *Journal of Bacteriology*, *197*(2), 262–276. https://doi.org/10.1128/JB.01957-14

Aggarwal, P., Uppal, B., Ghosh, R., Prakash, S. K., & Rajeshwari, K. (2013). Highly-resistant *E. coli* as a common cause of paediatric diarrhoea in India. *Journal of Health, Population, and Nutrition, 31*(3), 409-412.

Alba, B. M., & Gross, C. A. (2004). Regulation of the *Escherichia coli* sigma-dependent envelope stress response. *Molecular Microbiology*, *52*(3), 613–619. https://doi.org/10.1111/j.1365-2958.2003.03982.x

Allen, W. J., Phan, G., & Waksman, G. (2012). Pilus biogenesis at the outer membrane of Gram-negative bacterial pathogens. *Current Opinion in Structural Biology*, *22*(4), 500–506. https://doi.org/10.1016/j.sbi.2012.02.001

Audrain, B., Ferrières, L., Zairi, A., Soubigou, G., Dobson, C., Coppée, J.-Y., … Ghigo, J.-M. (2013). Induction of the Cpx envelope stress pathway contributes to *Escherichia coli* tolerance to antimicrobial peptides. *Applied and Environmental Microbiology*, *79*(24), 7770–7779. https://doi.org/10.1128/AEM.02593-13

Batchelor, E., Walthers, D., Kenney, L. J., & Goulian, M. (2005). The *Escherichia coli* CpxA-CpxR envelope stress response system regulates expression of the porins ompF and ompC. *Journal of Bacteriology*, *187*(16), 5723–5731. https://doi.org/10.1128/JB.187.16.5723-5731.2005

Beier, D., & Gross, R. (2006). Regulation of bacterial virulence by two-component systems. *Current Opinion in Microbiology, 9*(2), 143-152. doi:10.1016/j.mib.2006.01.005

Bos, M. P., Robert, V., & Tommassen, J. (2007). Biogenesis of the Gram-Negative Bacterial Outer Membrane. *Annual Review of Microbiology*, *61*(1), 191–214. https://doi.org/10.1146/annurev.micro.61.080706.093245

Bretl, D. J., Demetriadou, C., & Zahrt, T. C. (2011). Adaptation to environmental stimuli within the host: two-component signal transduction systems of *Mycobacterium tuberculosis*. *Microbiology and Molecular Biology Reviews: MMBR*, *75*(4), 566–582. https://doi.org/10.1128/MMBR.05004-11

Buelow, D. R., & Raivio, T. L. (2005). Cpx signal transduction is influenced by a conserved N-terminal domain in the novel inhibitor CpxP and the periplasmic protease DegP. *Journal of Bacteriology*, *187*(19), 6622–6630. https://doi.org/10.1128/JB.187.19.6622-6630.2005

Buelow, D. R., & Raivio, T. L. (2010). Three (and more) component regulatory systems – auxiliary regulators of bacterial histidine kinases. *Molecular Microbiology, 75*(3), 547-566. doi:10.1111/j.1365-2958.2009.06982.x

Bury-Moné, S., Nomane, Y., Reymond, N., Barbet, R., Jacquet, E., Imbeaud, S., et al. (2009). Global analysis of extracytoplasmic stress signaling in *Escherichia coli*. *PLoS Genetics, 5*(9), e1000651. doi:10.1371/journal.pgen.1000651

Büttner, D. (2012). Protein export according to schedule: architecture, assembly, and regulation of type III secretion systems from plant- and animal-pathogenic bacteria. *Microbiology and Molecular Biology Reviews: MMBR*, *76*(2), 262–310. https://doi.org/10.1128/MMBR.05017-11

Casadaban, M. J. (1976). Transposition and fusion of the *lac* genes to selected promoters in *Escherichia coli* using bacteriophage lambda and Mu. *Journal of Molecular Biology*, 104(3), 541–555.

Cheng, A. C., McDonald, J. R., & Thielman, N. M. (2005). Infectious diarrhea in developed and developing countries. *Journal of Clinical Gastroenterology, 39*(9), 757-773. doi:00004836-200510000-00002 [pii]

Cheung, J., & Hendrickson, W. A. (2008). Crystal structures of C4-dicarboxylate ligand complexes with sensor domains of histidine kinases DcuS and DctB. *The Journal of Biological Chemistry*, *283*(44), 30256–30265. https://doi.org/10.1074/jbc.M805253200

Cheung, J., & Hendrickson, W. A. (2010). Sensor domains of two-component regulatory systems. *Current Opinion in Microbiology*, *13*(2), 116–123. https://doi.org/10.1016/j.mib.2010.01.016

Cheung, J., Bingman, C. A., Reyngold, M., Hendrickson, W. A., & Waldburger, C. D. (2008). Crystal structure of a functional dimer of the PhoQ sensor domain. *The Journal of Biological Chemistry*, *283*(20), 13762–13770. https://doi.org/10.1074/jbc.M710592200

Chevance, F. F. V., & Hughes, K. T. (2008). Coordinating assembly of a bacterial macromolecular machine. *Nature Reviews Microbiology*, *6*(6), 455–465. https://doi.org/10.1038/nrmicro1887

Chin, J. W., Martin, A. B., King, D. S., Wang, L., & Schultz, P. G. (2002). Addition of a photocrosslinking amino acid to the genetic code of *Escherichia coli*. *Proceedings of the National Academy of Sciences of the United States of America*, 99(17), 11020–11024.

Cosma, C. L., Danese, P. N., Carlson, J. H., Silhavy, T. J., & Snyder, W. B. (1995). Mutational activation of the Cpx signal transduction pathway of *Escherichia coli* suppresses the toxicity conferred by certain envelope-associated stresses. *Molecular Microbiology*, *18*(3), 491–505.

Croxen, M. A., & Finlay, B. B. (2010). Molecular mechanisms of *Escherichia coli* pathogenicity. *Nature Reviews Microbiology*, *8*(1), 26–38. https://doi.org/10.1038/nrmicro2265

Dalbey, R. E., Wang, P., & Kuhn, A. (2011). Assembly of Bacterial Inner Membrane Proteins. *Annual Review of Biochemistry*, *80*(1), 161–187. https://doi.org/10.1146/annurev-biochem-060409-092524

Danese, P. N., & Silhavy, T. J. (1997). The sigma(E) and the Cpx signal transduction systems control the synthesis of periplasmic protein-folding enzymes in *Escherichia coli*. *Genes & Development*, *11*(9), 1183–1193.

Danese, P. N., & Silhavy, T. J. (1998). CpxP, a stress-combative member of the Cpx regulon. *Journal of Bacteriology*, *180*(4), 831–839.

Danese, P. N., Oliver, G. R., Barr, K., Bowman, G. D., Rick, P. D., & Silhavy, T. J. (1998). Accumulation of the enterobacterial common antigen lipid II biosynthetic intermediate stimulates *degP* transcription in *Escherichia coli*. *Journal of Bacteriology*, *180*(22), 5875–5884.

Danese, P. N., Snyder, W. B., Cosma, C. L., Davis, L. J., & Silhavy, T. J. (1995). The Cpx two-component signal transduction pathway of *Escherichia coli* regulates transcription of the gene specifying the stress-inducible periplasmic protease, DegP. *Genes & Development*, *9*(4), 387–398.

De Wulf, P., Kwon, O., & Lin, E. C. (1999). The CpxRA signal transduction system of *Escherichia coli*: growth-related autoactivation and control of unanticipated target operons. *Journal of Bacteriology*, *181*(21), 6772–6778.

Debnath, I., Norton, J. P., Barber, A. E., Ott, E. M., Dhakal, B. K., Kulesus, R. R., & Mulvey, M. A. (2013). The Cpx stress response system potentiates the fitness and virulence of uropathogenic *Escherichia coli*. *Infection and Immunity*, *81*(5), 1450–1459. https://doi.org/10.1128/IAI.01213-12

DiGiuseppe, P. A., & Silhavy, T. J. (2003). Signal detection and target gene induction by the CpxRA two-component system. *Journal of Bacteriology*, *185*(8), 2432–2440.

Dong, J., Iuchi, S., Kwan, H. S., Lu, Z., & Lin, E. C. (1993). The deduced amino-acid sequence of the cloned *cpxR* gene suggests the protein is the cognate regulator for the membrane sensor, CpxA, in a two-component signal transduction system of *Escherichia coli*. *Gene*, *136*(1–2), 227–230.

Dutta, R., Qin, L., & Inouye, M. (1999). Histidine kinases: diversity of domain organization. *Molecular Microbiology*, *34*(4), 633–640.

Eguchi, Y., & Utsumi, R. (2008). Introduction to bacterial signal transduction networks. In Utsumi, R. (Ed.), *Bacterial Signal Transduction: Networks and Drug Targets* (pp. 1-6). New York, NY: Springer New York. doi:10.1007/978-0-387-78885-2_1

Ehrmann, M. (2007). The periplasm. *ASM Press*, Washington, D.C., pp. 415.

Erhardt, M., Namba, K., & Hughes, K. T. (2010). Bacterial nanomachines: the flagellum and type III injectisome. *Cold Spring Harbor Perspectives in Biology*, *2*(11), a000299. https://doi.org/10.1101/cshperspect.a000299

Erickson, J. W., & Gross, C. A. (1989). Identification of the sigma E subunit of Escherichia coli RNA polymerase: a second alternate sigma factor involved in high-temperature gene expression. *Genes & Development*, *3*(9), 1462–1471.

Ferris, H. U., Dunin-Horkawicz, S., Hornig, N., Hulko, M., Martin, J., Schultz, J. E., … Coles, M. (2012). Mechanism of Regulation of Receptor Histidine Kinases. *Structure*, *20*(1), 56–66. https://doi.org/10.1016/j.str.2011.11.014

Fleischer, R., Heermann, R., Jung, K., & Hunke, S. (2007). Purification, reconstitution, and characterization of the CpxRAP envelope stress system of E*scherichia coli*. *The Journal of Biological Chemistry, 282*(12), 8583-8593. doi:M605785200 [pii]

Flores-Kim, J., & Darwin, A. J. (2014). Regulation of bacterial virulence gene expression by cell envelope stress responses. *Virulence, 5*(8), 835-851. doi:10.4161/21505594.2014.965580

Foussard, M., Cabantous, S., Pédelacq, J., Guillet, V., Tranier, S., Mourey, L., … Samama, J. (2001). The molecular puzzle of two-component signaling cascades. *Microbes and Infection*, *3*(5), 417–424.

Fronzes, R., Remaut, H., & Waksman, G. (2008). Architectures and biogenesis of non-flagellar protein appendages in Gram-negative bacteria. *The EMBO Journal*, *27*(17), 2271–2280. https://doi.org/10.1038/emboj.2008.155

Giltner, C. L., Nguyen, Y., & Burrows, L. L. (2012). Type IV pilin proteins: versatile molecular modules. *Microbiology and Molecular Biology Reviews: MMBR*, *76*(4), 740–772. https://doi.org/10.1128/MMBR.00035-12

Gotoh, Y., Eguchi, Y., Watanabe, T., Okamoto, S., Doi, A., & Utsumi, R. (2010). Two-component signal transduction as potential drug targets in pathogenic bacteria. *Current Opinion in Microbiology, 13*(2), 232-239. doi:10.1016/j.mib.2010.01.008

Gross, R., & Beier, D. (Ed.), *Two-Component Systems in Bacteria* (pp. 231–267). UK: Caister Academic Press.

Guest, R. L., Wang, J., Wong, J. L., & Raivio, T. L. (2017). A Bacterial Stress Response Regulates Respiratory Protein Complexes To Control Envelope Stress Adaptation. *Journal of Bacteriology*, *199*(20), e00153-17. https://doi.org/10.1128/JB.00153-17

Guttman, J. A., & Finlay, B. B. (2008). Subcellular alterations that lead to diarrhea during bacterial pathogenesis. *Trends in Microbiology, 16*(11), 535-542. doi:10.1016/j.tim.2008.08.004

Henry, J. T., & Crosson, S. (2011). Ligand-binding PAS domains in a genomic, cellular, and structural context. *Annual Review of Microbiology*, *65*(1), 261–286. https://doi.org/10.1146/annurev-micro-121809-151631

Hill, D. R., & Beeching, N. J. (2010). Travelers' diarrhea. *Current Opinion in Infectious Diseases, 23*(5), 481-487. doi:10.1097/QCO.0b013e32833dfca5

Hirakawa, H., Nishino, K., Hirata, T., & Yamaguchi, A. (2003). Comprehensive studies of drug resistance mediated by overexpression of response regulators of two-component signal transduction systems in *Escherichia coli*. *Journal of Bacteriology*, *185*(6), 1851–1856.

Hirano, Y., Hossain, M. M., Takeda, K., Tokuda, H., & Miki, K. (2007). Structural studies of the Cpx pathway activator NlpE on the outer membrane of *Escherichia coli*. *Structure (London, England: 1993)*, *15*(8), 963–976. https://doi.org/10.1016/j.str.2007.06.014

Ho, S. N., Hunt, H. D., Horton, R. M., Pullen, J. K., & Pease, L. R. (1989). Site-directed mutagenesis by overlap extension using the polymerase chain reaction. *Gene*, 77(1), 51–59.

Hodges, K., & Gill, R. (2010). Infectious diarrhea: Cellular and molecular mechanisms. *Gut Microbes, 1*(1), 4-21. doi:10.4161/gmic.1.1.11036

Hood, M. I., & Skaar, E. P. (2012). Nutritional immunity: transition metals at the pathogen–host interface. *Nature Reviews Microbiology*, *10*(8), 525–537. https://doi.org/10.1038/nrmicro2836

Hörnschemeyer, P., Liss, V., Heermann, R., Jung, K., & Hunke, S. (2016). Interaction Analysis of a Two-Component System Using Nanodiscs. *PloS One*, *11*(2), e0149187. https://doi.org/10.1371/journal.pone.0149187

Imamovic, L., Martínez-Castillo, A., Benavides, C., & Muniesa, M. (2015). BaeSR, involved in envelope stress response, protects against lysogenic conversion by Shiga toxin 2-encoding phages. *Infection and Immunity*, *83*(4), 1451–1457. https://doi.org/10.1128/IAI.02916-14

Isaac, D. D., Pinkner, J. S., Hultgren, S. J., & Silhavy, T. J. (2005). The extracytoplasmic adaptor protein CpxP is degraded with substrate by DegP. *Proceedings of the National Academy of Sciences of the United States of America*, *102*(49), 17775–17779. https://doi.org/10.1073/pnas.0508936102

Ito, K., & Inaba, K. (2008). The disulfide bond formation (Dsb) system. *Current Opinion in Structural Biology*, *18*(4), 450–8. https://doi.org/10.1016/j.sbi.2008.02.002

Jobling, M. G., & Holmes, R. K. (1990). Construction of vectors with the p15a replicon, kanamycin resistance, inducible *lacZ alpha* and pUC18 or pUC19 multiple cloning sites. *Nucleic Acids Research*, 18(17), 5315–5316.

Kamio, Y., & Nikaido, H. (1976). Outer membrane of *Salmonella typhimurium*: accessibility of phospholipid head groups to phospholipase C and cyanogen bromide activated dextran in the external medium. *Biochemistry,* (15), 2561-2570.

Karimova, G., Dautin, N., & Ladant, D. (2005). Interaction network among *Escherichia coli* membrane proteins involved in cell division as revealed by bacterial two-hybrid analysis. *Journal of Bacteriology*, *187*(7), 2233–2243. https://doi.org/10.1128/JB.187.7.2233-2243.2005

Kato, M., Mizuno, T., Shimizu, T., & Hakoshima, T. (1997). Insights into multistep phosphorelay from the crystal structure of the C-terminal HPt domain of ArcB. *Cell*, *88*(5), 717–723.

Kato, M., Mizuno, T., Shimizu, T., & Hakoshima, T. (1999). Refined structure of the histidine-containing phosphotransfer (HPt) domain of the anaerobic sensor kinase ArcB from *Escherichia coli* at 1.57 A resolution. *Acta Crystallographica. Section D, Biological Crystallography*, *55*(Pt 11), 1842–1849.

Keller, R., Havemann, J., & Hunke, S. (2011). Different regulatory regions are located on the sensor domain of CpxA to fine-tune signal transduction. *Research in Microbiology*, 162(4), 405–409.

Kennedy, E. P., & Scarborough, G. A. (1967). Mechanism of Hydrolysis of O-Nitrophenyl-β -Galactoside in *Staphylococcus aureus* and its Significance for Theories of Sugar Transport. *Proceedings of the National Academy of Sciences of the United States of America,* 58(1), 225-228.

Kim, D., & Forst, S. (2001). Genomic analysis of the histidine kinase family in bacteria and archaea. *Microbiology (Reading, England)*, *147*(Pt 5), 1197–1212. https://doi.org/10.1099/00221287-147-5-1197

Kirby, J. R. (2009). Chemotaxis-Like Regulatory Systems: Unique Roles in Diverse Bacteria. *Annual Review of Microbiology*, *63*(1), 45–59. https://doi.org/10.1146/annurev.micro.091208.073221

Kitagawa, M., Ara, T., Arifuzzaman, M., Ioka-Nakamichi, T., Inamoto, E., Toyonaga, H., & Mori, H. (2005). Complete set of ORF clones of *Escherichia coli* ASKA library (A Complete Set of *E. coli* K-12 ORF Archive): Unique Resources for Biological Research. *DNA Research*, 12(5), 291–299.

Klein, A. H., Shulla, A., Reimann, S. A., Keating, D. H., & Wolfe, A. J. (2007). The intracellular concentration of acetyl phosphate in *Escherichia coli* is sufficient for direct phosphorylation of two-component response regulators. *Journal of Bacteriology*, *189*(15), 5574–5581. https://doi.org/10.1128/JB.00564-07

Kohanski, M. A., Dwyer, D. J., & Collins, J. J. (2010). How antibiotics kill bacteria: from targets to networks. *Nature Reviews Microbiology*, *8*(6), 423–435. https://doi.org/10.1038/nrmicro2333

Konovalova, A., Perlman, D. H., Cowles, C. E., & Silhavy, T. J. (2014). Transmembrane domain of surface-exposed outer membrane lipoprotein RcsF is threaded through the lumen of β-barrel proteins. *Proceedings of the National Academy of Sciences of the United States of America*, 111(41), E4350–E4358.

Kosek, M., Bern, C., & Guerrant, R. L. (2003). The global burden of diarrhoeal disease, as estimated from studies published between 1992 and 2000. *Bulletin of the World Health Organization, 81*(3), 197-204. doi:S0042-96862003000300010 [pii]

Kwon, E., Kim, D. Y., Ngo, T. D., Gross, C. A., Gross, J. D., & Kim, K. K. (2012). The crystal structure of the periplasmic domain of *Vibrio parahaemolyticus* CpxA. *Protein Science : A Publication of the Protein Society*, *21*(9), 1334–1343. https://doi.org/10.1002/pro.2120

Laemmli, U. K. (1970). Cleavage of structural proteins during the assembly of the head of bacteriophage T4. *Nature*, 227, 680–685.

Laub, M.T. (2011). The Role of Two-Component Signal Transduction Systems in Bacterial Stress Responses p. 45-58. In Storz, G., & Hengge, R. (Ed.), *Bacterial Stress Responses*, 2nd ed. ASM Press, c2011, Washington, DC.

Leblanc, S. K. D., Oates, C. W., & Raivio, T. L. (2011). Characterization of the induction and cellular role of the BaeSR two-component envelope stress response of *Escherichia coli*. *Journal of Bacteriology*, *193*(13), 3367–3375. https://doi.org/10.1128/JB.01534-10

Lefèvre, F., Rémy, M.-H., & Masson, J.-M. (1997). Alanine-stretch scanning mutagenesis: a simple and efficient method to probe protein structure and function. *Nucleic Acids Research*, 25(2), 447–448.

Lima, B. P., Antelmann, H., Gronau, K., Chi, B. K., Becher, D., Brinsmade, S. R., & Wolfe, A. J. (2011). Involvement of protein acetylation in glucose-induced transcription of a stress-responsive promoter. *Molecular Microbiology*, *81*(5), 1190–1204. https://doi.org/10.1111/j.1365-2958.2011.07742.x

Lima, B. P., Lennon, C. W., Ross, W., Gourse, R. L., & Wolfe, A. J. (2016). *In vitro* evidence that RNA Polymerase acetylation and acetyl phosphate-dependent CpxR phosphorylation affect *cpxP* transcription regulation. *FEMS Microbiology Letters*, *363*(5), fnw011. https://doi.org/10.1093/femsle/fnw011

Lin, M.-F., Lin, Y.-Y., & Lan, C.-Y. (2015). The Role of the Two-Component System BaeSR in Disposing Chemicals through Regulating Transporter Systems in *Acinetobacter baumannii*. *PloS One*, *10*(7), e0132843. https://doi.org/10.1371/journal.pone.0132843

Lipmann, F., & Tuttle, L. C. (1944). Acetyl phosphate: chemistry, determination, and synthesis. *Journal of Biological Chemistry*, 153, 571-582.

Lobos, S. R., & Mora, G. C. (1991). Alteration in the electrophoretic mobility of OmpC due to variations in the ammonium persulfate concentration in sodium dodecyl sulfate-polyacrylamide gel electrophoresis. *Electrophoresis*, 12(6), 448–450.

Lu, J., Peng, Y., Arutyunov, D., Frost, L. S., & Glover, J. N. M. (2012). Error-prone PCR mutagenesis reveals functional domains of a bacterial transcriptional activator, TraJ. *Journal of Bacteriology*, 194(14), 3670–3677.

Luirink, J., von Heijne, G., Houben, E., & de Gier, J. W. (2005). Biogenesis of inner membrane proteins in *Escherichia coli*. *Annual Review of Microbiology*, *59*, 329–355. https://doi.org/10.1146/annurev.micro.59.030804.121246

MacRitchie, D. M., Acosta, N., & Raivio, T. L. (2012). DegP is involved in Cpx-mediated posttranscriptional regulation of the type III secretion apparatus in enteropathogenic *Escherichia coli*. *Infection and Immunity*, *80*(5), 1766–1772. https://doi.org/10.1128/IAI.05679-11

MacRitchie, D. M., Buelow, D. R., Price, N. L., & Raivio, T. L. (2008). Two-component signaling and Gram negative envelope stress response systems. In Utsumi, R. (Ed.), *Bacterial Signal Transduction: Networks and Drug Targets* (pp. 80-110). New York, NY: Springer New York. doi:10.1007/978-0-387-78885-2_6

MacRitchie, D. M., Ward, J. D., Nevesinjac, A. Z., & Raivio, T. L. (2008). Activation of the Cpx envelope stress response down-regulates expression of several locus of enterocyte

effacement-encoded genes in enteropathogenic *Escherichia coli*. *Infection and Immunity*, *76*(4), 1465–1475. https://doi.org/10.1128/IAI.01265-07

Mahoney, T. F., & Silhavy, T. J. (2013). The Cpx Stress Response Confers Resistance to Some, but Not All, Bactericidal Antibiotics. *Journal of Bacteriology*, *195*(9), 1869–1874. https://doi.org/10.1128/JB.02197-12

Margain-Quevedo, R., Malpica, R., Thede, G. L., Lu, J., Glover, J. N. M., & Raivio, T. L. (In preparation). Modulation of the Cpx Envelope Stress Response in *Escherichia coli* by the CpxA Periplasmic Sensing Domain and its Interaction with CpxP. *Manuscript in preparation.*

McBroom, A. J., & Kuehn, M. J. (2007). Release of outer membrane vesicles by Gram-negative bacteria is a novel envelope stress response. *Molecular Microbiology*, 63(2), 545–558. https://doi.org/10.1111/j.1365-2958.2006.05522.x

McEwen, J., & Silverman, P. (1980). Chromosomal mutations of *Escherichia coli* that alter expression of conjugative plasmid functions. *Proceedings of the National Academy of Sciences of the United States of America, 77*(1), 513-517.

McEwen, J., & Silverman, P. M. (1982). Mutations in genes cpxA and cpxB alter the protein composition of *Escherichia coli* inner and outer membranes. *Journal of Bacteriology*, *151*(3), 1553–1559.

Mechaly, A. E., Sassoon, N., Betton, J.-M., & Alzari, P. M. (2014). Segmental helical motions and dynamical asymmetry modulate histidine kinase autophosphorylation. *PLoS Biology*, 12(1), e1001776. https://doi.org/10.1371/journal.pbio.1001776

Merdanovic, M., Clausen, T., Kaiser, M., Huber, R., & Ehrmann, M. (2011). Protein Quality Control in the Bacterial Periplasm. *Annual Review of Microbiology*, *65*(1), 149–168. https://doi.org/10.1146/annurev-micro-090110-102925

Mileykovskaya, E., & Dowhan, W. (1997). The Cpx two-component signal transduction pathway is activated in *Escherichia coli* mutant strains lacking phosphatidylethanolamine. *Journal of Bacteriology*, *179*(4), 1029–1034.

Mourey, L., Da Re, S., Pédelacq, J.-D., Tolstykh, T., Faurie, C., Guillet, V., … Samama, J.-P. (2001). Crystal Structure of the CheA Histidine Phosphotransfer Domain that Mediates Response Regulator Phosphorylation in Bacterial Chemotaxis. *Journal of Biological Chemistry*, *276*(33), 31074–31082. https://doi.org/10.1074/jbc.M101943200

Mullineaux, C. W., Nenninger, A., Ray, N., & Robinson, C. (2006). Diffusion of Green Fluorescent Protein in Three Cell Environments in *Escherichia Coli*. *Journal of Bacteriology*, *188*(10), 3442–3448. https://doi.org/10.1128/JB.188.10.3442-3448.2006

Nevesinjac, A. Z., & Raivio, T. L. (2005). The Cpx envelope stress response affects expression of the type IV bundle-forming pili of enteropathogenic *Escherichia coli*. *Journal of Bacteriology*, *187*(2), 672–686. https://doi.org/10.1128/JB.187.2.672-686.2005

Nguyen, T. V., Le, P. V., Le, C. H., & Weintraub, A. (2005). Antibiotic resistance in diarrheagenic *Escherichia coli* and *Shigella* strains isolated from children in Hanoi, Vietnam. *Antimicrobial Agents and Chemotherapy, 49*(2), 816-819. doi:49/2/816 [pii]

Nikaido, H., & Vaara, M. (1987). Outer membrane. In: Neidhardt FC et al., (Eds), *Escherichia coli and Salmonella: cellular and molecular biology.* ASM Press, Washington, D.C., pp. 7-22.

Notti, R. Q., & Stebbins, C. E. (2016). The Structure and Function of Type III Secretion Systems. *Microbiology Spectrum*, *4*(1). https://doi.org/10.1128/microbiolspec.VMBF-0004-2015

Okuda, S., & Tokuda, H. (2011). Lipoprotein Sorting in Bacteria. *Annual Review of Microbiology*, *65*(1), 239–259. https://doi.org/10.1146/annurev-micro-090110-102859

Otto, K., & Silhavy, T. J. (2002). Surface sensing and adhesion of *Escherichia coli* controlled by the Cpx-signaling pathway. *Proceedings of the National Academy of Sciences of the United States of America*, *99*(4), 2287–2292. https://doi.org/10.1073/pnas.042521699

Pogliano, J., Lynch, A. S., Belin, D., Lin, E. C., & Beckwith, J. (1997). Regulation of *Escherichia coli* cell envelope proteins involved in protein folding and degradation by the Cpx two-component system. *Genes & Development*, *11*(9), 1169–1182.

Price, N. L., & Raivio, T. L. (2009). Characterization of the Cpx regulon in *Escherichia coli* strain MC4100. *Journal of Bacteriology*, *191*(6), 1798–815. https://doi.org/10.1128/JB.00798-08

Quan, S., Koldewey, P., Tapley, T., Kirsch, N., Ruane, K. M., Pfizenmaier, J., … Bardwell, J. C. A. (2011). Genetic selection designed to stabilize proteins uncovers a chaperone called Spy. *Nature Structural & Molecular Biology*, *18*(3), 262–269. https://doi.org/10.1038/nsmb.2016

Raetz, C. R. H., & Dowhan, W. (1990). Biosynthesis and function of phospholipids in *Escherichia coli*. *Journal of Biological Chemistry*, *265*(3), 1235-1238.

Raetz, C. R. H., & Whitfield, C. (2002). Lipopolysaccharide endotoxins. *Annual Review of Biochemistry, 71*, 635-700. doi:10.1146/annurev.biochem.71.110601.135414

Raffa, R. G., & Raivio, T. L. (2002). A third envelope stress signal transduction pathway in *Escherichia coli*. *Molecular Microbiology*, *45*(6), 1599–611. Raivio, T. L., & Silhavy, T. J. (2001). Periplasmic Stress and ECF Sigma Factors. *Annual Review of Microbiology*, *55*(1), 591–624. https://doi.org/10.1146/annurev.micro.55.1.591

Raivio, T. L. (2014). Everything old is new again: an update on current research on the Cpx envelope stress response. *Biochimica et Biophysica Acta*, *1843*(8), 1529–1541. https://doi.org/10.1016/j.bbamcr.2013.10.018

Raivio, T. L., & Silhavy, T. J. (1997). Transduction of envelope stress in *Escherichia coli* by the Cpx two-component system. *Journal of Bacteriology*, *179*(24), 7724–7733. https://doi.org/10.1128/JB.179.24.7724-7733.

Raivio, T. L., Laird, M. W., Joly, J. C., & Silhavy, T. J. (2000). Tethering of CpxP to the inner membrane prevents spheroplast induction of the Cpx envelope stress response. *Molecular Microbiology, 37*(5), 1186-1197. doi:mmi2074 [pii]

Raivio, T. L., Leblanc, S. K. D., & Price, N. L. (2013). The *Escherichia coli* Cpx envelope stress response regulates genes of diverse function that impact antibiotic resistance and membrane integrity. *Journal of Bacteriology*, *195*(12), 2755–2767. https://doi.org/10.1128/JB.00105-13

Raivio, T. L., Popkin, D. L., & Silhavy, T. J. (1999). The Cpx envelope stress response is controlled by amplification and feedback inhibition. *Journal of Bacteriology*, *181*(17), 5263–5272.

Ruiz, N., Kahne, D., & Silhavy, T. J. (2006). Advances in understanding bacterial outer-membrane biogenesis. *Nature Reviews Microbiology, 4*(1), 57-66. doi:nrmicro1322 [pii]

Runkel, S., Wells, H. C., & Rowley, G. (2013). Living with stress: A lesson from the enteric pathogen *Salmonella enterica*. *Advances in Applied Microbiology*, 83, 87-144. https://doi.org/10.1016/B978-0-12-407678-5.00003-9

Sambrook, J., Fritsch, E. F., & Maniatis, T. (1989). Molecular cloning: a laboratory manual. 2nd ed. *Cold Spring Harbor Laboratory Press*, Cold Spring Harbor, N.Y.

Schwechheimer, C., & Kuehn, M. J. (2015). Outer-membrane vesicles from gram-negative bacteria: Biogenesis and functions. *Nature Reviews Microbiology, 13*(10), 605-619. doi:10.1038/nrmicro3525

Sevier, C. S., & Kaiser, C. A. (2002). Formation and transfer of disulphide bonds in living cells. *Nature Reviews Molecular Cell Biology*, *3*(11), 836–847. https://doi.org/10.1038/nrm954

Sevvana, M., Vijayan, V., Zweckstetter, M., Reinelt, S., Madden, D. R., Herbst-Irmer, R., … Becker, S. (2008). A ligand-induced switch in the periplasmic domain of sensor histidine kinase CitA. *Journal of Molecular Biology*, *377*(2), 512–23. https://doi.org/10.1016/j.jmb.2008.01.024

Silhavy, T. J., Berman, M. L., & Enquist, L. W. (1984). Experiments with gene fusions. *Cold Spring Harbor Laboratory Press*, Cold Spring Harbor, N.Y.

Silhavy, T. J., Kahne, D., & Walker, S. (2010). The bacterial cell envelope. *Cold Spring Harbor Perspectives in Biology, 2*(5), a000414. doi:10.1101/cshperspect.a000414

Simons, R. W., Houman, F., & Kleckner, N. (1987). Improved single and multicopy *lac*-based cloning vectors for protein and operon fusions. *Gene*, 53(1), 85–96.

Simpson, B. W., Owens, T. W., Orabella, M. J., Davis, R. M., May, J. M., Trauger, S. A., … Ruiz, N. (2016). Identification of Residues in the Lipopolysaccharide ABC Transporter That Coordinate ATPase Activity with Extractor Function. *mBio*, 7(5), 1-10. https://doi.org/10.1128/mBio.01729-16

Slauch, J.M., & Silhavy, T.J. (1991). cis-Acting *ompF* mutations that result in OmpR-dependent constitutive expression. *Journal of Bacteriology*, 173, 4039–4048.

Snyder, W. B., Davis, L. J., Danese, P. N., Cosma, C. L., & Silhavy, T. J. (1995). Overproduction of NlpE, a new outer membrane lipoprotein, suppresses the toxicity of periplasmic LacZ by activation of the Cpx signal transduction pathway. *Journal of Bacteriology*, *177*(15), 4216–4223.

Stephenson, K., & Hoch, J. A. (2002). Two-component and phosphorelay signal-transduction systems as therapeutic targets. *Current Opinion in Pharmacology, 2*(5), 507-512. doi:S1471489202001947 [pii]

Stephenson, K., & Hoch, J. A. (2004). Developing inhibitors to selectively target two-component and phosphorelay signal transduction systems of pathogenic microorganisms. *Current Medicinal Chemistry, 11*(6), 765-773.

Stock, A. M., Robinson, V. L., & Goudreau, P. N. (2000). Two-component signal transduction. *Annual Review of Biochemistry*, *69*(1), 183–215. https://doi.org/10.1146/annurev.biochem.69.1.183

Thanassi, D. G., Bliska, J. B., & Christie, P. J. (2012). Surface organelles assembled by secretion systems of Gram-negative bacteria: diversity in structure and function. *FEMS Microbiology Reviews*, *36*(6), 1046–1082. https://doi.org/10.1111/j.1574-6976.2012.00342.x

Thapar, N., & Sanderson, I. R. (2004). Diarrhoea in children: An interface between developing and developed countries. *Lancet (London, England), 363*(9409), 641-653. doi:10.1016/S0140-6736(04)15599-2

The Addgene nonprofit plasmid repository. *Addgene*. https://www.addgene.org/vector-database/3301/

The Benchling Enterprise Academic Platform, Molecular Biology Suite tool. *Benchling Inc*. https://benchling.com/enterprise/molecular-biology

The GraphPad Prism computational software version 7.04. *GraphPad Software.*

The PyMOL Molecular Graphics System, Version 1.2. *Schrödinger, LLC.*

Thede, G. L. (2012). Biochemical and structural investigation of CpxP and CpxA, key components of an envelope stress response in *Escherichia coli*. PhD thesis, University of Alberta, Alberta, Canada.

Thede, G. L., Arthur, D. C., Edwards, R. A., Buelow, D. R., Wong, J. L., Raivio, T. L., & Glover, J. N. M. (2011). Structure of the periplasmic stress response protein CpxP. *Journal of Bacteriology, 193*(9), 2149-2157. doi:10.1128/JB.01296-10

Tokuda, H., & Matsuyama, S. I. (2004). Sorting of lipoproteins to the outer membrane in *E. coli*. *Biochimica et Biophysica Acta - Molecular Cell Research*, *1693*(1), 5-13. https://doi.org/10.1016/j.bbamcr.2004.02.005

Tomomori, C., Tanaka, T., Dutta, R., Park, H., Saha, S. K., Zhu, Y., … Ikura, M. (1999). Solution structure of the homodimeric core domain of *Escherichia coli* histidine kinase EnvZ. *Nature Structural Biology*, *6*(8), 729–734. https://doi.org/10.1038/11495

Towbin, H., Staehelin, T., & Gordon, J. (1979). Electrophoretic transfer of proteins from polyacrylamide gels to nitrocellulose sheets: procedure and some applications. *Proceedings of the National Academy of Sciences of the United States of America,* 76, 4350–4354.

Tschauner, K., Hörnschemeyer, P., Müller, V. S., & Hunke, S. (2014). Dynamic interaction between the CpxA sensor kinase and the periplasmic accessory protein CpxP mediates signal recognition in *E. coli*. *PloS One*, *9*(9), e107383. https://doi.org/10.1371/journal.pone.0107383

Van Dalen, A., & de Kruijff, B. (2004). The role of lipids in membrane insertion and translocation of bacterial proteins. *Biochimica et Biophysica Acta (BBA) - Molecular Cell Research*, *1694*(1–3), 97–109. https://doi.org/10.1016/j.bbamcr.2004.03.007

Van Wielink, J. E., & Duine, J. A. (1990). How big is the periplasmic space? *Trends in Biochemical Sciences*, *15*(4), 136–7.

Viswanathan, V. K., Hodges, K., & Hecht, G. (2009). Enteric infection meets intestinal function: How bacterial pathogens cause diarrhoea. *Nature Reviews Microbiology, 7*(2), 110-119. doi:10.1038/nrmicro2053

Vogt, S. L., & Raivio, T. L. (2012). Just scratching the surface: An expanding view of the cpx envelope stress response. *FEMS Microbiology Letters, 326*(1), 2-11. doi:10.1111/j.1574-6968.2011.02406.x

Vogt, S. L., Nevesinjac, A. Z., Humphries, R. M., Donnenberg, M. S., Armstrong, G. D., & Raivio, T. L. (2010). The Cpx envelope stress response both facilitates and inhibits elaboration of the enteropathogenic *Escherichia coli* bundle-forming pilus. *Molecular Microbiology*, *76*(5), 1095–1110. https://doi.org/10.1111/j.1365-2958.2010.07145.x

Vogt, S., Acosta, N., Wong, J., Wang, J., & Raivio, T. L. (2012). The CpxAR Two-component System Regulates a Complex Envelope Stress Response in Gram-negative Bacteria. In Gross, R., & Beier, D. (Ed.), *Two-Component Systems in Bacteria* (pp. 231–267). UK: Caister Academic Press.

Weber, R. F., & Silverman, P. M. (1988). The Cpx proteins of *Escherichia coli* K12. Structure of the CpxA polypeptide as an inner membrane component. *Journal of Molecular Biology*, *203*(2), 467–478.

West, A. H., & Stock, A. M. (2001). Histidine kinases and response regulator proteins in two-component signaling systems. *Trends in Biochemical Sciences*, *26*(6), 369–76.

Wolfe, A. J. (2005). The acetate switch. *Microbiology and Molecular Biology Reviews: MMBR*, *69*(1), 12–50. https://doi.org/10.1128/MMBR.69.1.12-50.2005

Wolfe, A. J. (2010). Physiologically relevant small phosphodonors link metabolism to signal transduction. *Current Opinion in Microbiology*, *13*(2), 204–209. https://doi.org/10.1016/j.mib.2010.01.002

Wolfe, A. J., Parikh, N., Lima, B. P., & Zemaitaitis, B. (2008). Signal Integration by the Two-Component Signal Transduction Response Regulator CpxR. *Journal of Bacteriology*, *190*(7), 2314–2322. https://doi.org/10.1128/JB.01906-07

Wong, J. L. (2015). Cellular role of the inhibitor-chaperone CpxP in *Escherichia coli*. PhD thesis, University of Alberta, Alberta, Canada.

Wuichet, K., Cantwell, B. J., & Zhulin, I. B. (2010). Evolution and phyletic distribution of two-component signal transduction systems. *Current Opinion in Microbiology*, *13*(2), 219–225. https://doi.org/10.1016/j.mib.2009.12.011

Xicohtencatl-Cortes, J., Monteiro-Neto, V., Ledesma, M. A., Jordan, D. M., Francetic, O., Kaper, J. B., … Girón, J. A. (2007). Intestinal adherence associated with type IV pili of enterohemorrhagic *Escherichia coli* O157:H7. *Journal of Clinical Investigation*, *117*(11), 3519–3529. https://doi.org/10.1172/JCI30727

Yamada, S., & Shiro, Y. (2008). Structural Basis of the Signal Transduction in the Two-Component System. In Utsumi, R. (Ed.), *Bacterial Signal Transduction: Networks and Drug Targets* (pp. 22–39). New York, NY: Springer New York. https://doi.org/10.1007/978-0-387-78885-2_3

Zhou, L., Lei, X.-H., Bochner, B. R., & Wanner, B. L. (2003). Phenotype microarray analysis of *Escherichia coli* K-12 mutants with deletions of all two-component systems. *Journal of Bacteriology*, *185*(16), 4956–4972.

Zhou, X., Keller, R., Volkmer, R., Krauss, N., Scheerer, P., & Hunke, S. (2011). Structural basis for two-component system inhibition and pilus sensing by the auxiliary CpxP protein. *The Journal of Biological Chemistry, 286*(11), 9805-9814. doi:10.1074/jbc.M110.194092

Appendices

Appendix I - Preliminary results for the UV-induced photo cross-linking assay of TAG substitutions in pCpxA and pCpxP believed to play a role in their interaction

After possessing the information and data obtained from all the mutagenesis analysis of surface-exposed charged residues in both the $CpxA_{SD}$ and CpxP believed to play a role in electrostatic interactions that allow a direct interaction (described in this work), I tried to develop a novel experimental procedure to visualize such interaction. The reasoning for designing this experiment was that the previous attempts to characterize this interaction have been through either overproduced pCpxP tethered to the inner membrane (which prevented the Cpx response induction by spheroplasting) (Raivio et al., 2000); inhibition of CpxA kinase activity when reconstituted alongside CpxP in proteoliposomes (Fleischer et al., 2007); indirect mutagenesis results (Buelow & Raivio, 2005), or have required the use of a saturated concentration for CpxP close to where it precipitates, to only observe a very low affinity between this component and CpxA reconstituted in nanodiscs (Hörnschemeyer et al., 2016). Overall, these results through the years have indicated that the CpxA-CpxP direct protein-protein interaction, although described multiple times and used for our current model of the Cpx response regulation and activity, is very difficult to be detected in *in vivo* assays. A potential explanation for this may be that such direct interaction is very transient and context specific that occurs under non-inducing conditions only, and even minor alterations on the pathway could modify it.

This novel assay was based on the work of Konovalova and collaborators from 2014, in which they studied the RcsF (regulator of capsule synthesis sensor) interaction with OmpA, OmpC and BamA. This assay required that single amino acid residues of interest were substituted for the TAG codon, and then a plasmid encoding a tRNA synthetase/tRNA pair is added for the *in vivo* insertion of the artificial p-benzoil-l-phenylalanine (*p*BPA) photocrosslinker amino acid at the

TAG mutants. This *p*BPA can then be cross-linked to nearby proteins by irradiating with UV light, and the interaction can be detected by a regular SDS-PAGE + Western Blot assay, observed as a higher molecular weight protein complex than the one it would be expected for the individual proteins (Konovalova et al., 2014).

For my study, I substituted residues E_{91} and D_{113} in pCpxA to the TAG codon, as well as four amino acid residues (for each) in their vicinity, that are located protruding outside the structure and toward the periplasmic space (T_{89}, T_{90}, G_{92}, R_{93}, A_{112}, N_{114}, D_{116} and H_{117}, observed in Figure S1A and S1B, respectively) where a potential interaction with CpxP would occur (since the direct mutation to the specific E_{91} and D_{113} residues could result in destruction of an interaction with CpxP). Null *ΔcpxA* strains harboring pCpxA, VC, E_{91}A and D_{113}A were the controls, and an α-CpxA-MBP anti-rabbit primary antibody was used for CpxA detection (Figure S1C). An α-CpxP anti-rabbit primary antibody was used instead for detecting CpxP and as a loading control when observing mutated pCpxA strain results (as CpxP levels are not modified in these strains) (Figure S1D). It is important to highlight that all of these 14 strains contained both the pEVOL-pBpF (responsible for the insertion of *p*BPA in the TAG sites) and the pCpxP plasmids co-transformed into them. The pCpxP plasmid is present to overexpress *cpxP* and have a better chance of detecting an interaction (and also, unless *cpxP* is overexpressed, it has been established in unpublished observations that detection of CpxP WT levels is very difficult through Western blotting in WT strains, unless it is overproduced). Unfortunately, only the band corresponding to the detection of CpxA at 51.6 kDa was observed for all strains (including the positive controls) in blot shown on Figure S1C, while only the CpxP band at 18.97 kDa was detected on the blot in figure S1D for all of the strains at about the same intensity (confirming that the same amount of total protein was

loaded into each well). No band of higher molecular weight that could suggest an interaction at any of the mutated residues was obtained in any of the two blots.

Similarly, I substituted residues R_{67} and R_{139} in the pCpxP overexpression vector for the TAG codon, as well as four amino acid residues (for each) in their vicinity, that are located protruding outside the structure concavity and toward the periplasmic space (M_{63}, A_{66}, H_{68}, Q_{70}, H_{136}, Q_{138}, Q_{142} and L_{143}, observed in Figure S2A and S2B, respectively). Strains *ΔcpxP* harboring the pCpxP, pTrc99A, R_{67}E and R_{139}E plasmids were used as controls, and an α-CpxA-MBP anti-rabbit primary antibody for CpxA detection (Figure SC) and used as a loading control when observing mutated pCpxP strain results, while an α-CpxP anti-rabbit primary antibody was used for detecting CpxP (Figure S1D). All of these strains also contained the pEVOL-pBpF plasmid co-transformed into them. Once again, only the band corresponding to the detection of CpxA at 51.6 kDa was observed for all strains in blot shown on Figure S2C (loading control), while only the CpxP band at 18.97 kDa was detected on the blot in figure S2D for all of the strains (but with a different intensity, likely due to an issue with the α-CpxP antibody) except for Q_{138}TAG, intriguingly. No band of higher molecular weight that could suggest an interaction at any of the mutated residues was obtained in any of these two new blots.

I still believe that this is a potentially useful assay for studying this interaction in the near future, and one of the flaws that could have occurred is that it needs further standardization regarding the specifics on the UV induction step, including the exact handheld lamp that would need to be utilized, and the distance between this UV source and the samples. These details have been recently proposed to have an extensive effect on whether the assay works and renders appropriate results or not (Simpson et al., 2016), so it potentially can still be used in the future as another tool to observe the $CpxA_{SD}$-CpxP direct interaction.

Appendix Figures

A.

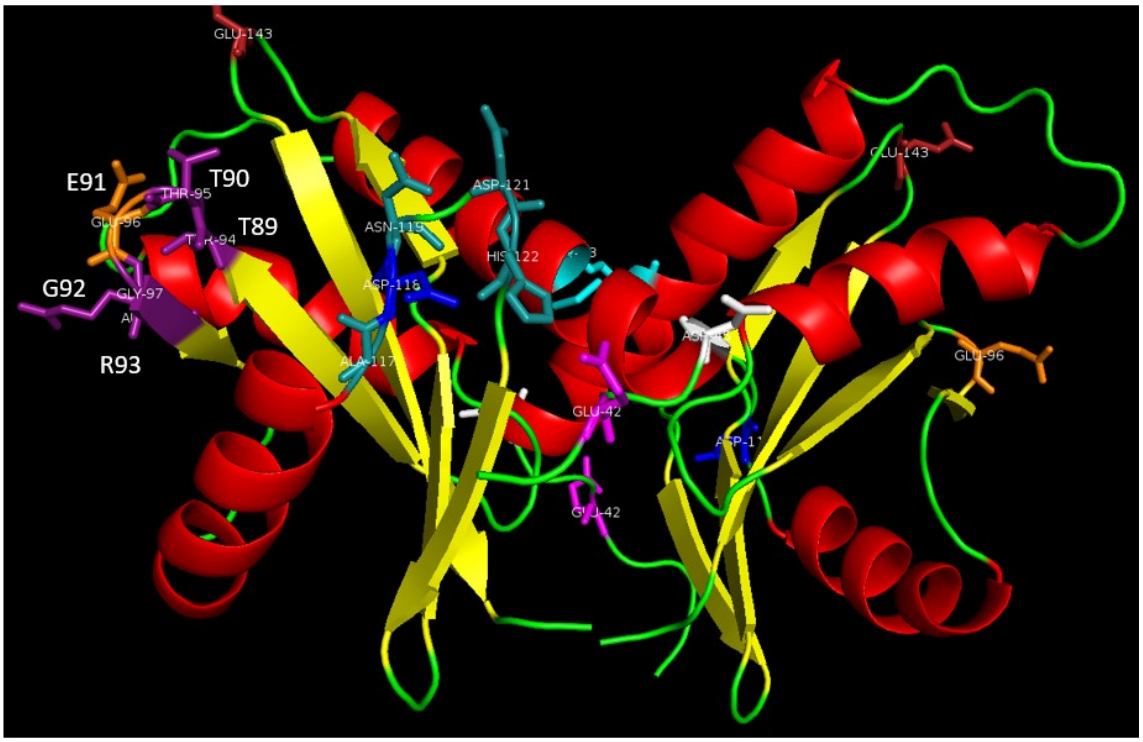

B.

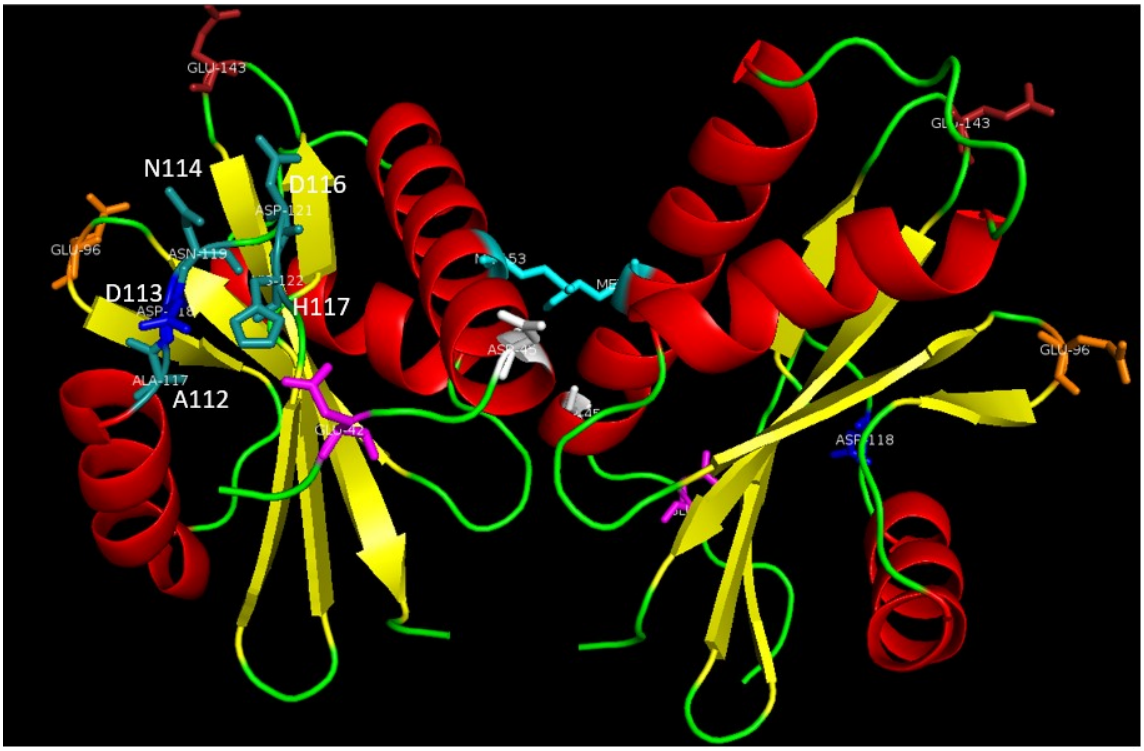

C.

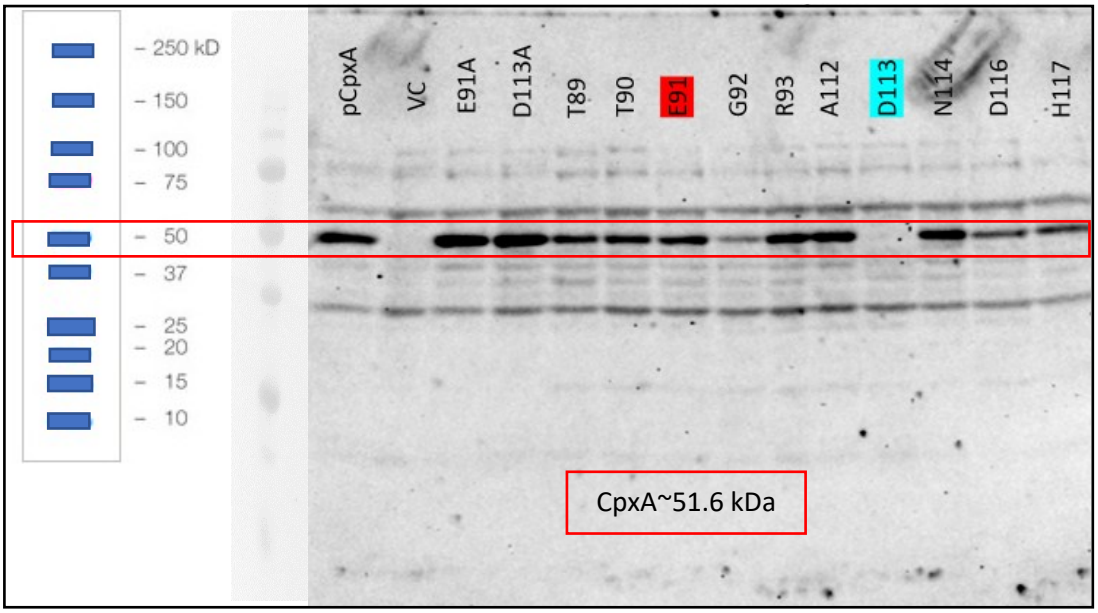

D.

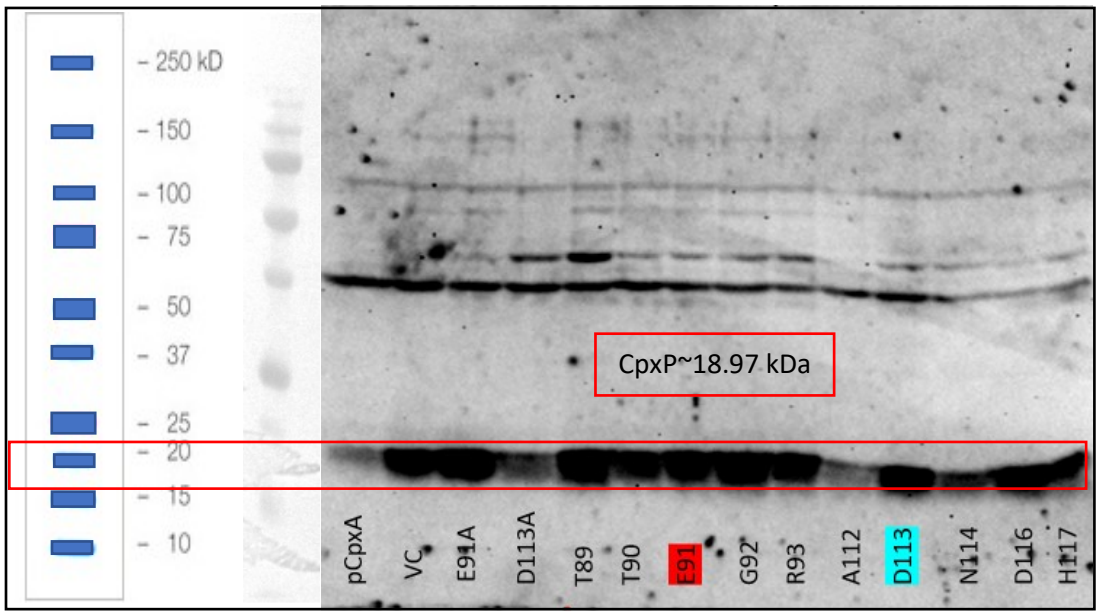

Figure S1: Preliminary results for the UV-induced photo cross-linking assay of TAG substitutions in residues T_{89}, T_{90}, G_{92}, R_{93}, A_{112}, N_{114}, D_{116} and H_{117} surrounding E_{91} and D_{113} within pCpxA. (A) $CpxA_{SD}$ crystal representation generated in PyMOL. The T_{89}, T_{90}, E_{91}, G_{92}, R_{93} (all in purple), and **(B)** A_{112}, D_{113}, N_{114}, D_{116} and H_{117} (all in green) residues substituted for the TAG amber codon are labeled. **(C)** Western blotting using either the α-CpxA-MBP or **(D)** α-CpxP-MBP primary antibodies for detection. Results display the protein expression levels in total membrane preparations from *E. coli* transformed *ΔcpxA* strains harboring both the pCpxP + pEVOL-pBpF plasmids, and one of the pCpxA (RMQ123), VC (RMQ124)

pCpxA-E_{91}A (RMQ125), pCpxA-D_{113}A (RMQ126), pCpxA-T_{89}TAG (RMQ127), pCpxA-T_{90}TAG (RMQ128), pCpxA-E_{91}TAG (RMQ129), pCpxA-G_{92}TAG (RMQ130), pCpxA-R_{93}TAG (RMQ131), pCpxA-A_{112}TAG (RMQ132), pCpxA-D_{113}TAG (RMQ133), pCpxA-N_{114}TAG (RMQ134), pCpxA-D_{116}TAG (RMQ135) or pCpxA-H_{117}TAG (RMQ136) plasmids. Bacterial strains were cultured overnight, subcultured 1:100 into fresh LB containing 0.16mM *p*BPA (final concentration) for 2 hours. 0.1mM IPTG and 0.02% arabinose (final concentration) were added for expression induction at this timepoint, and cells grown for 1 more hour until an OD_{600}~0.4. Bacteria were centrifuged and concentrated to an OD_{600}=10 in ice-cold TBS. 100µL of each cell suspension were transferred to duplicate wells in a clear 96-well plate and subjected to UV irradiation (365 nm, 15 minutes, 4°C) and then mixed with 100µL of 2X SDS-PAGE Sample Loading Buffer. 20µg of total protein for each sample were run in 12% SDS-PAGE gels and subsequent western blotting performed as previously described in sections 2.14 and 2.15. Results represent two independent experiments.

A.

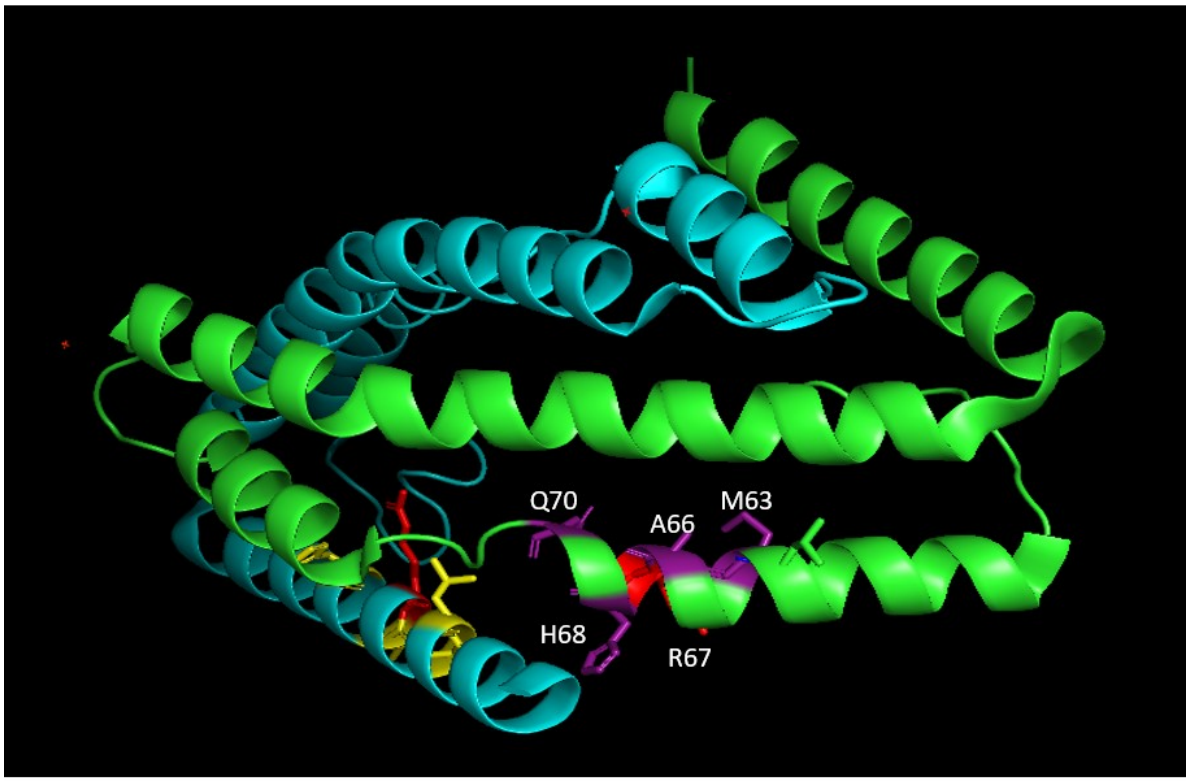

B.

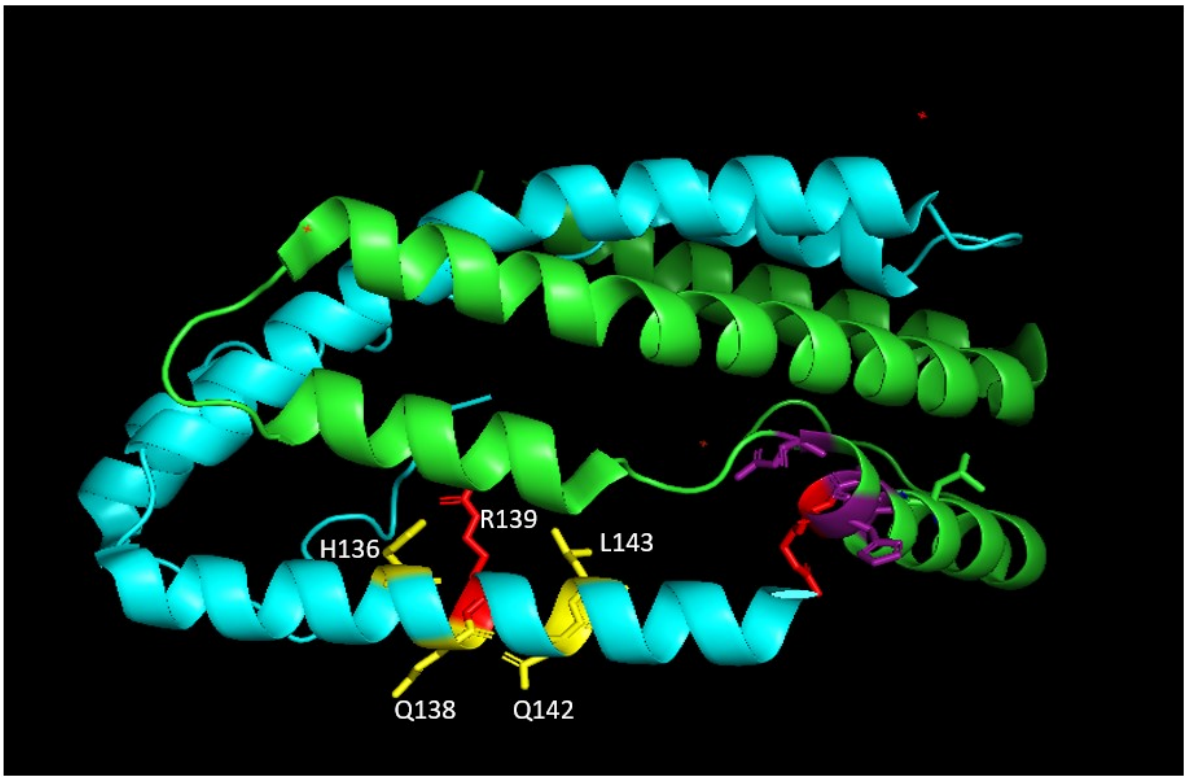

C.

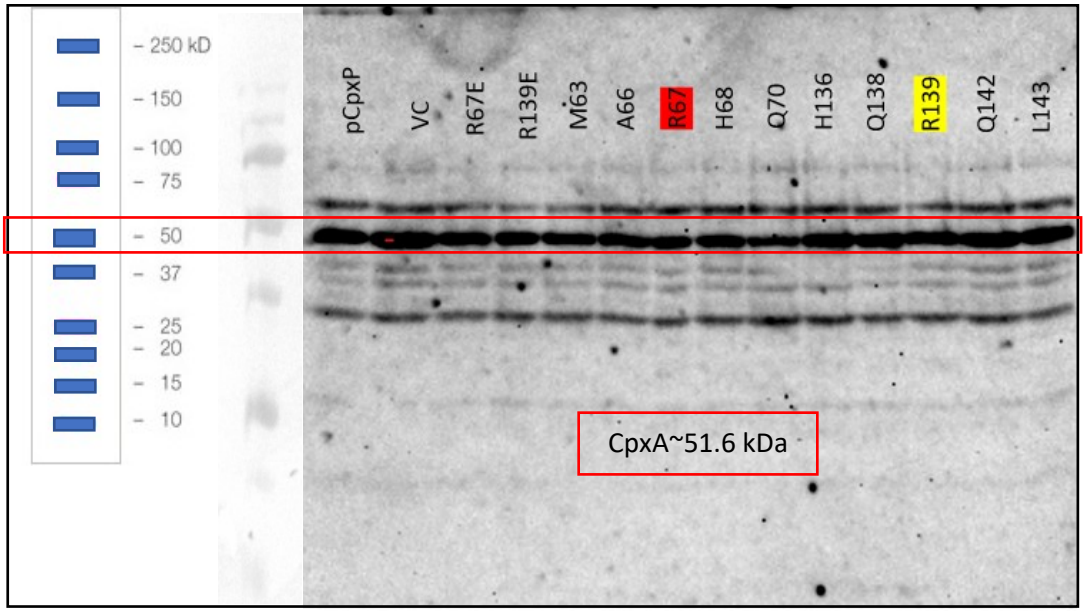

D.

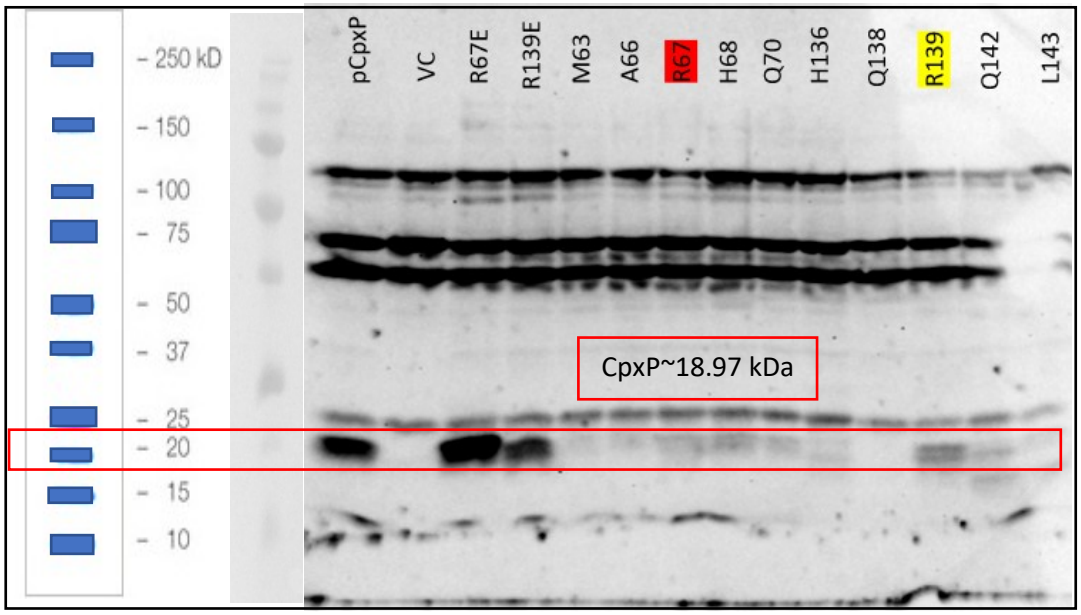

Figure S2: Preliminary results for the UV-induced photo cross-linking assay of TAG substitutions in residues M_{63}, A_{66}, H_{68}, Q_{70}, H_{136}, Q_{138}, Q_{142} and L_{143} surrounding R_{67} and R_{139} within pCpxP. (A) CpxP crystal representation generated in PyMOL. The M_{63}, A_{66}, R_{67}, H_{68} and Q_{70} (all in purple), and **(B)** H_{136}, Q_{138}, R_{139}, Q_{142} and L_{143} (all in yellow) residues substituted for the TAG amber codon are labeled. **(C)** Western blotting using either the α-CpxA-MBP or **(D)** α-CpxP-MBP primary antibodies for detection. Results display the protein expression levels in total membrane preparations from *E. coli* transformed *ΔcpxP* strains harboring the pEVOL-pBpF plasmid and one of the pCpxP (RMQ137), pTrc99A VC

(RMQ138) pCpxP-$R_{67}E$ (RMQ139), pCpxP-$R_{139}E$ (RMQ140), pCpxP-$M_{63}TAG$ (RMQ141), pCpxP-$A_{66}TAG$ (RMQ142), pCpxP-$R_{67}TAG$ (RMQ143), pCpxP-$H_{68}TAG$ (RMQ144), pCpxP-$Q_{70}TAG$ (RMQ145), pCpxP-$H_{136}TAG$ (RMQ146), pCpxP-$Q_{138}TAG$ (RMQ147), pCpxP-$R_{139}TAG$ (RMQ148), pCpxP-$Q_{142}TAG$ (RMQ149) or pCpxP-$L_{143}TAG$ (RMQ150) plasmids. Bacterial strains were cultured overnight, subcultured 1:100 into fresh LB containing 0.16mM *p*BPA (final concentration) for 2 hours. 0.1mM IPTG and 0.02% arabinose (final concentration) were added for expression induction at this timepoint, and cells grown for 1 more hour until an OD_{600}~0.4. Bacteria were centrifuged and concentrated to an OD_{600}=10 in ice-cold TBS. 100µL of each cell suspension were transferred to duplicate wells in a clear 96-well plate and subjected to UV irradiation (365 nm, 15 minutes, 4°C) and then mixed with 100µL of 2X SDS-PAGE Sample Loading Buffer. 20µg of total protein for each sample were run in 12% SDS-PAGE gels and subsequent western blotting performed as previously described in sections 2.14 and 2.15. Results represent two independent experiments.

Appendix references

Buelow, D. R., & Raivio, T. L. (2005). Cpx signal transduction is influenced by a conserved N-terminal domain in the novel inhibitor CpxP and the periplasmic protease DegP. *Journal of Bacteriology*, *187*(19), 6622–6630. https://doi.org/10.1128/JB.187.19.6622-6630.2005

Fleischer, R., Heermann, R., Jung, K., & Hunke, S. (2007). Purification, reconstitution, and characterization of the CpxRAP envelope stress system of E*scherichia coli*. *The Journal of Biological Chemistry, 282*(12), 8583-8593. doi:M605785200 [pii]

Hörnschemeyer, P., Liss, V., Heermann, R., Jung, K., & Hunke, S. (2016). Interaction Analysis of a Two-Component System Using Nanodiscs. *PloS One*, *11*(2), e0149187. https://doi.org/10.1371/journal.pone.0149187

Konovalova, A., Perlman, D. H., Cowles, C. E., & Silhavy, T. J. (2014). Transmembrane domain of surface-exposed outer membrane lipoprotein RcsF is threaded through the lumen of β-barrel proteins. *Proceedings of the National Academy of Sciences of the United States of America*, 111(41), E4350–E4358.

Raivio, T. L., Laird, M. W., Joly, J. C., & Silhavy, T. J. (2000). Tethering of CpxP to the inner membrane prevents spheroplast induction of the Cpx envelope stress response. *Molecular Microbiology, 37*(5), 1186-1197. doi:mmi2074 [pii]

Simpson, B. W., Owens, T. W., Orabella, M. J., Davis, R. M., May, J. M., Trauger, S. A., … Ruiz, N. (2016). Identification of Residues in the Lipopolysaccharide ABC Transporter That Coordinate ATPase Activity with Extractor Function. *mBio*, 7(5), 1-10. https://doi.org/10.1128/mBio.01729-16